INTEGRATION OF STATIC AND DYNAMIC RESERVOIR PROPERTIES FOR SCREENING OIL-RIM DEVELOPMENT

A thesis presented to the Department of Petroleum Engineering

African University of Science and Technology

In partial fulfilment of the requirements for the degree of

MASTER OF SCIENCE IN PETROLEUM ENGINEERING

By

IDOKO JOB JOHN

Supervised by

Dr Saka Matemilola

African University of Science and Technology
www.aust.edu.ng
P.M.B 681, Garki, Abuja F.C.T
Nigeria

December 2017

CERTIFICATION

This is to certify that the thesis titled "**Integration of Static and Dynamic Reservoir Properties for Screening Oil-rim Development**" submitted to the school of postgraduate studies, African University of Science and Technology (AUST), Abuja Nigeria, in partial fulfilment of the requirements for the award of a Master's degree in Petroleum Engineering, is a record of original research carried out by Idoko Job John in the Department of Petroleum Engineering.

INTEGRATION OF STATIC AND DYNAMIC RESERVOIR PROPERTIES FOR SCREENING OIL-RIM DEVELOPMENT

By

Idoko Job John

A THESIS APPROVED BY THE PETROLEUM ENGINEERING DEPARTMENT

RECOMMENDED: ----------

Dr Saka Matemilola
Supervisor

Dr Kazeem Lawal
Co-supervisor

Head, Department of Petroleum Engineering

APPROVED: ----------

Chief Academic Officer

December, 2017

Date

ABSTRACT

This work adds to the current body of knowledge on the characterization and flow behaviours of oil-rim reservoirs. It presents the workflow and results of investigations conducted on the effect of some static and dynamic properties on the performance of oil-rim reservoirs under three development options: sequential oil-then-gas development (OTG), concurrent oil-and-gas development (COG) and gas-only development (GOD). The findings provide operators with insights on the parameters with the most influence on oil/gas recovery and hence, assistance on what development options to adopt depending on the dominant properties of their subsurface assets. That way, computationally expensive reservoir simulation studies, which are conducted even at the preliminary stages of oil-rim reservoirs maturation, can potentially be minimized.

A range of eight different static and dynamic reservoir properties was selected. A two-level factorial design was then used to create 17 experiments, including the combination of factors that maximize and minimize oil recovery factor (RF). A generic dynamic reservoir box model was developed and used to conduct a total of 51 experiments, including some in-fill tests. The responses were populated in the designs which were analyzed to generate surrogate models for predicting the RF and screened to identify the most significant factors among the properties investigated.

For the specific box model studied and the parameter space covered, it was found that the major RF-impacting variables are oil API, vertical anisotropy, oil relative permeability, liquid offtake rate and interaction of oil API and vertical anisotropy. The COG case reported oil API, vertical anisotropy, liquid offtake rate and oil relative permeability as the most influential factors on oil recovery, while the GOD option returned oil-rim thickness, relative permeabilities and gas offtake rate as the key drivers of reservoir performance.

Performance comparison of the three development options examined reveals that when reservoir properties are promising, the sequential oil-then-gas option is the preferred oil-rim development option. Because the GOD yields far less barrel-of-equivalent (BOE) than others, the OTG and COG options are generally more promising, relatively, to develop oil-rim reservoirs. Finally, it was observed that the GOD option performs better than the others only when the combination of reservoir properties is highly unfavourable.

ACKNOWLEDGEMENT

Immense gratitude goes to the personnel of the Nelson Mandela Institute and The African University of Science and Technology (AUST) Abuja for providing sponsorship for this Master of Science Program. I extend my gratitude to all who provided financial support during my stay at AUST. In this regard, those who regularly came to mind include my lovely parents, Mr and Mrs John Idoko and uncle, Mr Patrick Idoko.

The majority of the credit for the success of this work goes to Dr Kazeem Lawal of First Exploration and Petroleum Development Company Limited (FIRST E&P), Nigeria. There is hardly any section of the work in which his technical endowments were not employed to authenticate, embellish, scrutinize and perfect. Much technical guidance was also sought from Dr Saka Matemilola, who supervised this work; Engr. Yetunde Aladeitan, Dr Akeem Arinkoola, Engr. Mariam Abdulkarim, Engr. Mike Adejare, Engr. Ikpeka Princewill, Engr. Jemima-Sandra Samuel and my colleagues at AUST.

Many thanks to my friends who made the rigour of this intensive program a lot of fun. Bishop never relented in prayers for us. He motivated me in ways he does not even know; Jonah was always the brother from another mother; Isah is a born-leader and true philanthropist; there was never a dull moment with Christian.

Above all, I give all thanks to God. He is ever faithful.

DEDICATION

To Bishop, Jonah, Isah and Christian.

TABLE OF CONTENTS

LIST OF FIGURES

LIST OF TABLES

NOMENCLATURE

3D:	Three dimensions (i.e. featuring the x, y, and z orthogonal planes)
ANOVA:	Analysis of Variance
API:	American Petroleum Institute
Aqfac:	Aquifer factor
BBD:	Box-Behnken design
BSW:	Basic Sediments and Water
COG:	Concurrent oil and gas
COGR1:	Run number 1 or Model Number 1 of the Concurrent Oil and Gas Case
ED:	Experimental Design
FDP:	Field Development Plan
FFM:	Full Field Model
GOC:	Gas-Oil-Contact
GOD:	Gas-Only Development
GODR1:	Run number 1 or Model Number 1 of the Gas-Only Development Case
GOR:	Gas-Oil-Ratio
HGOC:	Height between GOC and completion (ft.)
H_o:	Oil-rim thickness (ft.)
HWL:	Horizontal well length (ft.)

K_h:	Horizontal permeability (mD)
K_{rg}:	Relative Permeability to Gas (fraction)
K_{ro}:	Relative Permeability to Oil (fraction)
Kr_w:	Relative permeability to water (fraction)
K_v/K_h:	Ratio of vertical to horizontal permeability (anisotropy)
Mfac:	Ratio of gas cap volume to oil column volume
OTG:	Oil-then-Gas
OTGR1:	Model number 1 or Run number 1 of the Oil-then-Gas Development Case
OWC:	Oil-Water-Contact
PVT:	Pressure-Volume-Temperature
P_{wh}:	Wellhead Pressure (psia)
Q:	Oil rate in Stock Tank Barrel per Day (stb/d)
RF:	Recovery Factor (%)
RSM:	Response Surface Model
SCAL:	Special Core Analysis
scf:	Standard Cubic Feet
S_{orw}:	Residual oil saturation to water (fraction)
STB:	Stock tank barrel

WOR: Water-oil-ratio

CHAPTER ONE

INTRODUCTION

1.0 BACKGROUND OF STUDY

1.01 Overview of Oil-Rim Reservoirs

An oil-rim reservoir is a saturated hydrocarbon reservoir with an oil column of limited thickness (20 - 60 ft.) overlain by a gas cap and underlain by an aquifer. Maximizing oil recovery in this reservoir type is very challenging (Razak et al. 2010, Yeoh 2014, Shrivastava et al. 1998). Masoudi (2011) mentioned water/gas coning and breakthrough, spread out resources, complicated production mechanisms, presence of transition and invasion zones, oil smearing, and a low recovery factor of less than 18% as common technical challenges of oil-rim reservoirs. Good knowledge of this reservoir type is essential to combat these technical challenges.

Another challenge often associated with oil-rim reservoirs is the difficulty with the making of an early decision on the optimum development strategy between oil and the gas cap (Lawal et al. 2010, Uwaga and Lawal 2006). Considering that both oil and gas are potential sources of revenue, it is usually not straightforward deciding on the best development strategy that will maximize value for all stakeholders. Specific to the exploitation of oil-rim reservoirs, it is not unusual for decision-makers to be faced with selecting between the following mutually exclusive options:

- Develop oil first, and the gas later.
- Develop only the gas, largely neglecting the oil.
- Develop both oil and gas simultaneously.

Therefore, the primary objective of the proposed research is to formulate simple guidelines for addressing the previous decision questions, especially during the early stages of field studies and development planning.

1.1 STATEMENT OF PROBLEM

Numerous production challenges are associated with the management of thin oil columns. These challenges stem from the fact that the oil accumulation is often spread out in thin layers with small initial mobile thickness, sandwiched between huge overlying gas cap and varying strength of underlying water. One of the key challenges facing the evaluation of this class of reservoirs is the considerable manpower, and computational costs often incurred in screening the possible development options at the initial stages. Usually, detailed and computationally expensive reservoir simulation studies are conducted, even at the preliminary stages of opportunity maturation.

1.2 RESEARCH OBJECTIVES

As an improvement over the existing practice, this research seeks to develop a simple, yet robust method for evaluating the feasibility of developing oil-rim reservoirs. In particular, as an improvement over current screening techniques, this work will integrate both static and dynamic reservoir properties, hence facilitating a holistic screening.

The following are the main objectives of this research:

I. Understand the main subsurface properties that influence the performance of oil-rim reservoirs.
II. Gain insights into how combinations of static and dynamic reservoir properties affect the ultimate recovery of thin oil reservoirs.
III. Provide guidelines on the best high-level development strategy for oil-rim reservoirs. This will address the optimum strategy in terms of (i) oil-then-gas development; (ii) gas-only development; and (iii) simultaneous oil and gas development.

1.3 SIGNIFICANCE OF STUDY

This research improves the current understanding of the main static and dynamic reservoir properties that control the development and performance of oil-rim reservoirs. In essence, it contributes to the library of guidelines for (i) screening and ranking candidate oil-rim reservoirs for possible development; and (ii) identifying optimum development strategy for oil-rim reservoirs.

1.4 SCOPE AND LIMITATIONS

The range of investigation for this research is limited to model oil-rim reservoirs. Detailed reservoir simulations were performed with the aid of a commercial simulation package. Using representative data of some oil-rim reservoirs in the Niger Delta, credible and robust generic simulation models were constructed to gain insights into the dynamics of oil-rim reservoirs and the influence of key static and dynamic reservoir properties on their lifecycle performances.

CHAPTER TWO

LITERATURE REVIEW

2.0 OIL-RIM OPTIMIZATION STRATEGIES AND DEVELOPMENT CHALLENGES

Many oil reservoirs have a gas cap and/or water support. The structure of such reservoirs may be dome-shaped with the oil sandwiched between the gas cap and the bottom water, sloping with the edge water or in a linear geometry (Silva and Dawe 2010). In general, the configuration of oil-rim reservoirs in terms of the gas cap to the oil column is either pancake or doughnut (Lawal et al. 2010). In the pancake configuration, a plan view of the reservoir would reveal the oil zone enclosing the gas zone as concentric circles (or other geometries as applicable). Conversely, a doughnut configuration has the gas cap sitting roughly on the oil column, with the GOC not quite visible from a plan view (Fig. 2.1).

2.01 HISTORIC OIL-RIM DEVELOPMENT AND OPTIMIZATION APPROACHES

Various research has been conducted in an attempt to improve oil recovery from thin oil columns sandwiched between a bottom aquifer and a very large gas cap. In most cases, the decisions typically focus on optimizing the timing for oil and gas development driven by the primary objectives of maximizing hydrocarbon recovery and project economics.

According to Masoudi (2011), thin oil column development and depletion strategies include gas cap blowdown, sequential development, concurrent development, and swing-gas development. He also noted that the eventual field development plan (FDP), well design and philosophy as well as the reservoir management plan (RMP) are highly dependent on the selected development strategy in terms of the relative timing of oil and gas developments. It is important to re-emphasize that the main differentiating philosophy among these proven strategies for exploiting oil-rim reservoirs is the relative timing of oil and gas development.

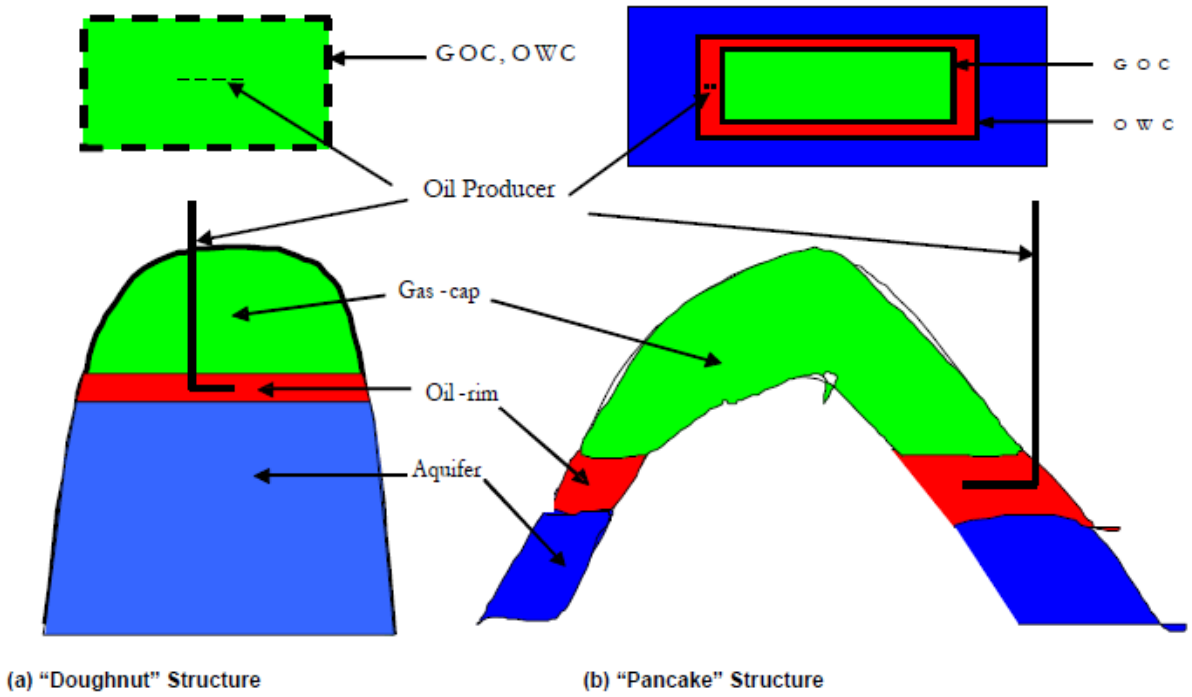

Fig. 2.1: Simple configurations of oil-rim reservoirs in plan and cross-section (Lawal et al., 2010)

1. **Sequential Development – Oil-then-Gas**

Considering the higher market value of a unit volume of oil in comparison to its equivalent gas counterpart, this is the conventional development strategy for oil-rim reservoirs. This development concept initially drills and completes production wells in the oil zone and attempts to manage the offtake (by balancing gas cap expansion and aquifer encroachment) to minimize movement of the rim. Oil recovery and production performance depend, to a large degree, on the balance of water drive and gas cap drive.

The conservation of gas cap energy will generally lead to higher oil recoveries. Production rates are controlled to manage coning and cusping effects, hence mitigating excessive gas production. After the oil-rim has become economically exhausted, the second phase is to develop the gas cap. This explains the idea of the sequential development of oil first, then gas later.

In a publication by Kabir et al. (2008), this depletion strategy was investigated to improve the recovery of the remaining oil. In their first stage, a conventional horizontal well was completed below the gas-oil contact (GOC) to drain the oil accumulation. Once the well waters out, the well is recompleted in the gas zone. Completion occurs either at the crest for a small gas cap reservoir or at the GOC, inducing reverse cone, for a reservoir with thick-gas columns.

Putten and VNaus (2008) also carried out a study on this conventional strategy of oil-rim development. The development of the reservoir studied consisted of an oil development phase with two dedicated oil wells, followed by a gas development phase with two dedicated gas wells (i.e., a total of four development wells, with four drainage points). In principle, this phased production strategy aims at limiting the pressure decline in the reservoir by constraining wells and thereby minimizing the movement of the oil-rim.

2. Gas Cap Blow Down

In this approach, oil production is initially ignored while the gas cap is depleted. The oil recovery factor associated with this approach is usually low (Masoudi, 2011). This relatively low oil recovery factor is traceable to the energy loss associated with the early gas cap production. However, Behrenbruch and Mason (1993) showed that oil recovery could be maximized from an oil-rim reservoir with a small gas cap ($m<0.2$) by blowing down the gas cap during the initial production phase, provided a strong aquifer exists. Where the aquifer is strong, the essence of this strategy is to develop the gas cap first and then allow the oil-rim to move to the crest of the reservoir that will be produced by the same crestal gas cap well rather than attempting to control offtake and manage coning and cusping effects. Re-saturation losses will occur. However, depending on the geometry of the reservoir, the remaining oil at abandonment should be less in this case than in the conventional oil-then-gas (sequential development) scenario described earlier.

3. Concurrent Development of the Oil and Gas Zones

Behrenbruch and Mason (1993) discussed the methods used to evaluate the sensitivity of oil-rim recovery to reservoir uncertainties and development strategy. This was accomplished using an idealized box model, preconditioned to match historical production in reservoirs, to guide development plans which were later validated in full three-dimensional (3D) reservoir simulation models. With the simulations, they were able to show that simultaneous depletion of the oil zone and the gas cap from oil-rim reservoirs can be achieved while optimizing oil recovery from the rims. Their goal was to manage gas offtake between reservoirs to secure optimal hydrocarbon recovery from the oil-rims under concurrent production of both gas cap gas and oil from the oil-rim. Material balance modelling was used for most of the reservoirs to ascertain possible aquifer characteristics and to determine the fraction of cumulative underground withdrawal due to various reservoir drive mechanisms.

The authors employed idealized box models to guide oil-rim development under concurrent oil and gas production. History matched, dynamic full-field models (FFM) were subsequently used to confirm preferred future drilling locations. Several model sensitivities were used to assess the production performances of new horizontal oil-rim wells. It was relevant to establish which parameters (reservoir or operational) affected oil recovery under planned concurrent oil and gas production. Sensitivities were run on the effects of landing depth inside an oil-rim, well spacing and horizontal well length, producing gas-oil ratio (GOR) control, the timing of gas cap offtake, the rate of gas cap offtake and timing of gas compression on the performance of the production strategy under investigation.

For the example case studied, Cosmo and Fatoke (2004) discovered that under concurrent production of the gas cap and oil-rim, it was best to land the horizontal well midway in the oil column. Sensitivity analysis on the effect of well spacing and depth on recovery revealed that well interference reduces with increasing well spacing. Therefore, individual wells

access larger oil volumes but were discovered to have lower volumetric sweep compared to higher well density. Interference between wells in a denser drilling pattern resulted in less ultimate recovery per well but gave more uniform drainage of the oil-rim. In summary, it was concluded that a denser drilling pattern with longer horizontals would optimize recovery within economic constraints.

Sensitivity test on permeability reveals its high influence on recovery considering that an example of permeability variation between 750 and 3000md caused recovery to vary by more than ±25% on the base permeability of 1500md (Cosmo and Fatoke, 2004). However, uncertainty in the ratio of vertical to horizontal permeability (K_v/K_h) tested for values of 0.01, 0.1 and 1 showed much less impact (±5%) on recovery relative to the base case K_v/K_h of 0.1.

Sensitivity analysis on producing GOR indicated that there are some benefits of not constraining the producing GOR too tightly. It was also reported that oil recovery did not increase significantly with the reduction in gas cap offtake rate.

4. Gas-only Development

This development strategy focuses entirely on the gas cap and does not attempt oil-rim development. This is generally applied when the oil-rim is considered to be uneconomical to develop at prevailing technical and commercial conditions. The gas recovery factor strongly depends on the aquifer size/support, residual gas saturation and availability of compression (either surface or subsurface). For depletion systems with little or no aquifer support, gas recovery can be up to 80-90% with compression in late life. The presence of a strong aquifer or lack of compression limits the extent of pressure decline and generally results in lower gas recovery in the range of 50-70%.

The encroachment of an aquifer can result in large amounts of gas being trapped at high pressure as well as bypassing large areas of gas if water breaks through to the wells preferentially through high permeability zones. If a strong aquifer is suspected, it is recommended to produce the gas as quickly as possible to out-run aquifer encroachment, thereby resulting in trapping gas at a lower pressure and maximizing gas recovery. Another possible gas-only production strategy, in the case of a strong aquifer, is to drill dedicated producer wells into the aquifer to pump off the aquifer water. However, this option might only be practical and economical if the aquifer size is relatively small to moderate and there is an acceptable sink for the produced water.

2.02 TECHNICAL CHALLENGES OF THIN OIL-RIMS

I. High GOR and water cut

The production of thin oil columns is often associated with high GOR and water cut. Several studies have been conducted to mitigate these challenges. Shrivastava et al. (1998) examined the strategy for alleviating the excessive production of gas and water by controlling the movement of fluid interfaces. This was accomplished by withdrawing gas cap gas and aquifer water by separate horizontal completions, one each in the gas cap and the aquifer, which are parallel and aligned with the oil zone completion. The gas cap gas, oil from the oil zone and water from the aquifer were therefore produced through separate strings. Simulation of the proposed system indicated a 25 - 50% increase in oil recovery over conventional horizontal wells for different ratios of vertical to horizontal permeability over 5 years. Advantages of this proposed system included: relatively easier effluent handling and sustained production of normal GOR plus low water cut oil for a longer duration. They highlighted proper well steering, completion and its maintenance as keys to the economic success of this production strategy.

II. Water/Gas Coning

Shrivastava et al. (1998) noted that the problem of water and gas coning in oil-rim exploitation is so severe that the use of vertical wells for production is essentially unattractive. Since the early 1980s, horizontal wells have been used in such situations to defer water and gas ingress and thus prolong the life of the field. As a result of this, many otherwise marginal and uneconomical pools have become exploitable. Their study covered oil-rims of thickness range 0 - 26 m.

According to Silva and Dawe (2010), coning occurs particularly at high production rates where gravity effects are too small to counteract the effects of viscosity ratio. In other words, water or gas coning will occur when the viscous force induced by pressure drawdown in the near-wellbore area exceeds the gravitational force holding the fluid in place in the original order. The cone height increases with increase in the flow rate until a critical flow rate is reached when the cone becomes unstable and water or gas is drawn into the wellbore above the oil-water contact (OWC) or below the GOC.

Coning is a problem because of the increase in GOR and/or water-oil ratio (WOR) as the case may be. Also, if the produced water contains salts such as sodium chloride, production facilities such as separators and connecting pipework will be susceptible to corrosion. An additional cost of separating the produced fluid before it meets market specifications is incurred. The reduction in oil production and increased operating expenses all lead to reduced net profit.

III. Difficulty in Locating the Well due to Complicated Production Mechanism

Knowledge of the depths of the fluid contacts is essential for proper horizontal well placement. Conventionally, landing of the well at the desired depth is achieved using any combination of the following techniques (Vo et al. 2004):

1. Drilling a vertical pilot hole to locate the GOC and the OWC. Once these depths are known, the well is sidetracked and positioned at the required depth.
2. Intentional drilling at the OWC and then changing the well trajectory upwards into the oil-rim at the required depth.
3. Drilling into the target area with a trajectory already near horizontal. Once the GOC is located, the horizontal section of the well is drilled but maintaining a certain distance from the GOC.

In addition to the earlier mentioned problems, Masoudi (2011) identified oil smearing above the GOC and below the OWC as well as relatively low recovery factors (<18%) as additional challenges of developing and managing oil-rim reservoirs.

2.2 SOME EXISTING SCREENING GUIDELINES FOR OIL-RIMS

Sensitivity studies on the effect of different parameters on recovery factors from oil-rim reservoirs have been used in the past to generate models that predict the performance of oil-rim reservoirs under varying combinations of operating and reservoir parameters. Reservoirs with parameters that yielded higher recovery factors were ranked higher. Table 2.1 provides a good summary of some available literature materials on the current subject.

Table 2.1: Preliminary Summary of Previous Works

Paper	Summary	Limitation(s)
Cosmo and Fatoke (2004). "Challenges of Gas Development: Soku Field Oil-Rim	A sensitivity study on the parameters affecting oil recovery from thin oil-rim reservoirs was used to propose an optimal horizontal well	Sensitivities performed, considered only one of the oil-rim reservoir development scenarios: concurrent production of both gas cap and oil-rims.

Reservoirs," SPE Paper 88894.	placement in Soku Field under concurrent oil and gas development.	Reservoir modelling did not account for transition zones. Key findings are specific to the field worked on and may not apply to other fields with different reservoir properties and operating philosophy.
Obah et al. (2012). "Simplified Models for Forecasting Oil Production: Niger Delta Oil-Rim Reservoirs Case," ISSN 1595-9104.	Models were developed for forecasting oil production using the least-square regression method. Also, three production forecast models for oil-rim reservoirs were obtained using Monte-Carlo simulation approach.	Models were based solely on simulation data. There was no validation with production data. Reservoir modelling did not account for transition zones, the impact of well trajectory and perforation efficiencies. Models applicability is limited to the range of data source and two horizontal wells.
Olamigoke et al. (2009), "First-Pass Screening of Reservoirs with Large Gas Caps for Oil-Rim Development," SPE Paper 128603	An assessment of actual oil-rim performance and a generic oil-rim simulation study was used to establish oil recovery trends that can be used for screening of oil-rim reservoirs.	Simulation studies were constrained to a minimum oil recovery volume of 1 MMSTB per drainage point and favourable geological conditions: limited geological complexity, low oil viscosity, and strong aquifer.
Lawal et al. (2010), "Preliminary Assessment of Oil-	The authors reviewed five common models for preliminary screening of oil-	The scope of applicability of the research findings is limited to only gas cap drive systems.

Rim Reservoirs: A Review of Current Practices and Formulation of New Concepts", SPE Paper 136955	rim reservoirs. The models were found to be generally inconsistent, inherently limited in the scope of applicability and capable of giving non-practical results. Energy balance approach was then used by the authors to derive an expression for the hydrocarbon recovery limit of a system under gas cap drive.	Model formulation method did not take cognizance of changes in reservoir energy with production, development patterns and production policy.
Vo et al. (2004), "Look back on Performance of 50 Horizontal Wells Targeting Thin Oil Columns, Mahakam Delta, East Kalimantan"; SPE Paper 64385	An analysis of the performance of 50 horizontal wells was carried out to use lessons learned from actual well performance data to improve future well planning as horizontal wells continue to be used in the fields.	The paper did not account for any relationship between Recovery Efficiency (RE) and m-factor and fluid properties such as oil formation volume factor and viscosity. Also, there was no consideration for development pattern, production policy, and abandonment condition, e.g., Wellhead pressure.

Omeke et al. (2010), "A proposed cone breakthrough time model for horizontal wells in thin oil-rim reservoirs" SPE Paper 140743.	A combination of Placket Burman design technique, material balance approach and numerical reservoir simulation was used to formulate a model for predicting cone breakthrough time in oil-rim reservoirs.	Reservoir modelling did not account for transition zones, the impact of well trajectory and perforation efficiencies. Models applicability is limited to two horizontal wells. Simulation study did not consider different oil-rim development approaches.
Abdulkarim (2014), Development of Coning Correlations for Oil-Rim Reservoirs Using Experimental Design and Response Surface Methodology.	The effect of reservoir and fluid properties on coning tendencies of thin oil column reservoirs was studied. Models for predicting oil recovery and water breakthrough time for oil-rim reservoirs were proposed.	This study did not consider different oil-rim development approaches. Findings are, therefore, only applicable to the oil-then-gas development scenario as the simulation model consists of only one well producing from the oil column.

2.3 CONCEPT AND APPLICATION OF EXPERIMENTAL DESIGN, PARAMETER SCREENING, AND RESPONSE SURFACE METHODOLOGY

Experimental design (ED) and parameter screening are tools for estimating the degree to which a set of parameters or independent variables affect a response (dependent variable). Design of experiment allows the study of the effect of the possible different combinations of the variables on the response while parameter screening can be used to evaluate the extent of the significance of each parameter and different interactions of parameters, thereby

allowing us to identify the most important parameters and the effect of their interactions on the response. Damsleth et al. (1992) demonstrated that information can be maximized from a minimum number of simulation runs through a "recipe" of combining parameter settings. They also verified the possibility of substituting a response surface for reservoir simulation in a probabilistic Monte-Carlo analysis (Quinao and Zarrouk (2014), Abdulkarim (2015)). The response surface is a polynomial describing the relationship between the simulation output and the investigated parameters (Hoang et al., 2005). It can also be described as regression equations relating the response variable and the independent variables (Olatunde 2015).

Quinao and Zarrouk (2014) provided a preliminary understanding of the potential strengths and weaknesses of the ED and RSM methodologies as applied to geothermal resource assessment by applying them to a simple geothermal process model and using them to estimate the amount of electrical generating capacity from a synthetic geothermal system. A response variable (electrical generating capacity), as a function of the main uncertain parameters, was then derived from the simulation runs. The authors reiterated that the response function serves as the proxy model in Monte-Carlo probabilistic analysis. The probabilistic results from the proxy model were compared with the probabilistic results from the mass in-place volumetric reserves method of estimating geothermal resources.

ED, parameter screening and response surface methodology (RSM) have enjoyed vast applications in the Oil and Gas Industry. Olatunde et al. (2015) presented an approach for quantifying uncertainties in petroleum production forecast by incorporating uncertainty inherent in structural maps with the ED technique in the reservoir modelling and simulation studies. They developed three static models - a low, mid and high case, history matched them using conventional techniques and used the simulation for the production forecast. After performing an analysis of variance on the input variables and simulation results, the

significant parameters were used to formulate the response surfaces which are the regression equations relating ultimate recovery and the independent variables.

Yao et al. (2013) used ED and RSM techniques to study horizontal well performance, under different values and the effect of the interaction of 13 different dimensionless variables that affect horizontal well performance. In their work, the authors, firstly, introduced 13 dimensionless variables to describe the factors that influence horizontal well performance in bottom water reservoirs and calculated the range of all the variables from a statistic of the actual field data of 23 horizontal wells. The oil recovery model was then generated with RSM using 3 level-13 variables Box-Behnken design (BBD). Based on the evaluation model, single factor sensitivity and interaction analyses between any two factors were carried out. The research indicated that the values calculated by the new evaluation model fit the actual field data and proved that the evaluation model could provide criteria for the design or optimization of horizontal well development in a bottom water reservoir.

In this work, ED was used to create 16 different experiments, with 2-level factorial design, for a study of the effect of 7 independent variables on the performance of oil-rim reservoirs. Parameter screening was then used to identify the most significant variables.

After conducting the experiments through dynamic reservoir simulation, the responses (RF) were populated in the design which was analyzed to generate surrogate models for predicting the response (recovery factor). The analysis was used to identify the most significant factors and heavy hitters among the variables by comparing the relative contribution of each variable and their aliases to recovery factor or oil-rim reservoir performance. These experiments were carried out for three different development approaches for thin oil reservoirs with large gas cap and active aquifer of varying strength and size.

CHAPTER THREE

METHODOLOGY

3.0 DESIGN OF THE EXPERIMENTS

The static and dynamic reservoir parameters investigated in this work are oil-rim thickness (H_o), Oil API, vertical anisotropy, rock relative permeabilities, horizontal well landing depth, and liquid/gas withdrawal rates. The range of parameters used in the models is presented in Table 3.1.

Table 3.1: Range of Parameters

VARIABLE	LOW	MEDIUM	HIGH
***H_o* (ft.)**	20	40	60
Oil API	24	32	40
K_v/K_h	0.01	0.1	0.5
K_{rg}	0.7	0.85	1
K_{rw}	0.3	0.5	0.7
K_{ro}	0.5	0.7	0.9
HGOC (ft.)	0.5 from GOC (i.e. 50% of oil-rim)		
	10	20	30
K_h (md)	500		
HWL (ft.)	2000		
Q_{liquid} (%STOIIP per annum)	5		
Q_{gas} (% FGIIP) per annum	5		

3.01 PARAMETER SCREENING

The effect of the variables in Table 3.1 on oil recovery in oil-rim reservoirs was investigated using Design Expert®, MS Excel®, and Minitab®, for the three development scenarios considered in this work. To accomplish this, a 2-level factorial design was created as shown in Table 3.2. A total of 51 experiments, including the low, median and high cases, for the three development options, were conducted using Schlumberger Eclipse 100® (black oil) dynamic reservoir simulator

Table 3.2: Design of Experiment

RUN	Ho (ft.)	Oil API	Kv/Kh (fraction)	Krg (fraction)	Krw (fraction)	Kro (fraction)	Ql (5% STOIIP/yr) (STB/d)	FGIIP (BSCF)	STOIP (MMSTB)
1	20	40	0.5	0.7	0.3	0.9	442	43.90	3.23
2	60	24	0.5	0.7	0.7	0.5	1654	48.77	12.07
3	60	40	0.01	1	0.3	0.5	1328	52.11	9.70
4	20	24	0.5	1	0.3	0.5	551	42.79	4.02
5	20	24	0.01	1	0.7	0.9	551	42.79	4.02
6	20	40	0.01	0.7	0.7	0.5	442	43.90	3.23
7	60	24	0.01	0.7	0.3	0.9	1654	48.77	12.07
8	20	24	0.01	0.7	0.3	0.5	551	42.79	4.02
9	40	32	0.1	0.85	0.5	0.7	1007	46.97	7.35
10	60	40	0.5	1	0.7	0.9	1328	52.12	9.70
11	60	24	0.5	0.7	0.3	0.9	1654	48.77	12.07
12	60	24	0.01	0.7	0.7	0.5	1654	48.77	12.07
13	20	24	0.5	0.7	0.7	0.9	551	42.79	4.02
14	20	24	0.5	1	0.7	0.5	551	42.79	4.02
15	60	24	0.01	1	0.7	0.9	1654	48.77	12.07
16	20	40	0.5	1	0.3	0.9	442	43.90	3.23
17	60	40	0.01	0.7	0.3	0.9	1328	52.12	9.70

3.1 GENERIC MODEL DESCRIPTION

3.11 GRID STRUCTURE

The 20 x 20 x 50 grid cells generic box model, shown in Figure 3.1, consists of parameters from the mid-case (run 9) in Table 3.2. The model has areal dimensions of 2500ft by 2500ft and a total thickness of 320ft, 340ft, and 360ft for the lowest, median and highest oil-rim thicknesses, respectively. A 2000ft horizontal well was used in all models for all scenarios. The reference reservoir pressure and temperature are 4573psia and 183^{o}F at a reference depth of 10180ft, respectively. Average reservoir porosity was set to 25%, and the model top is at a depth of 10080ft, while the horizontal oil producers were all landed at the middle of the oil-rim as indicated in Table 3.1.

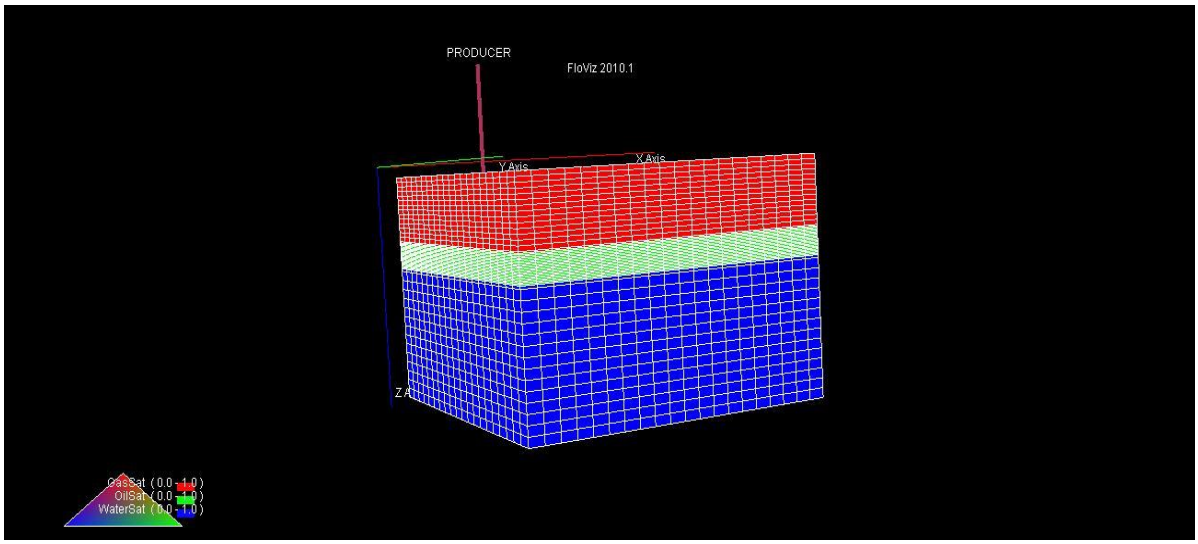

Figure 3.1: Generic model grid block (Oil-then-Gas Development Scenario).

3.12 SCAL

Reservoir relative permeability and capillary pressure properties were modelled using Corey correlations, among the SCAL options available in the Eclipse ® software. Table 3.3 gives the variables used in the correlation while Figures 3.2 and 3.3 present the relative permeability curves for the median case (run 9 in Table 3.2). To generate relative permeability functions for the other experiments, the variables in Table 3.3 were adjusted following their values in Table 3.2.

Table 3.3: Parameters for SCAL Modeling (Mid-Case Model/Run 9)

PARAMETER	VALUE	UNIT
S_{wcr}	0.2	Fraction
S_{orw}	0.2	Fraction
S_{org}	0.1	Fraction
S_{gcr}	0.05	Fraction
n_w	3	Dimensionless
n_g	2	Dimensionless
n_{ow}	2.5	Dimensionless
n_{og}	2.5	Dimensionless
$(Krg)_{sorg}$	0.85	Fraction
$(Krw)_{Sorw}$	0.5	Fraction
$(Kro)_{Swmin}$	0.7	Fraction
$(Krg)_{Sgmax}$	1	Fraction
$(Krw)_{Swmax}$	1	Fraction

	$(Kro)_{Sgmin}$	1	Fraction

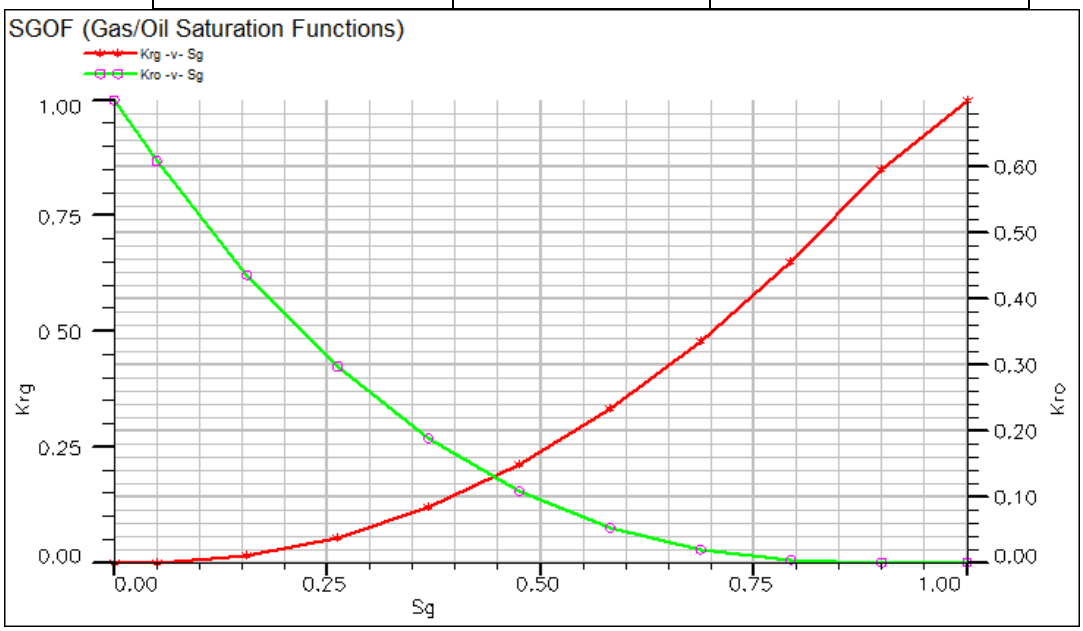

Figure 3.2: Generic model gas/oil relative permeability curves (mid-case)

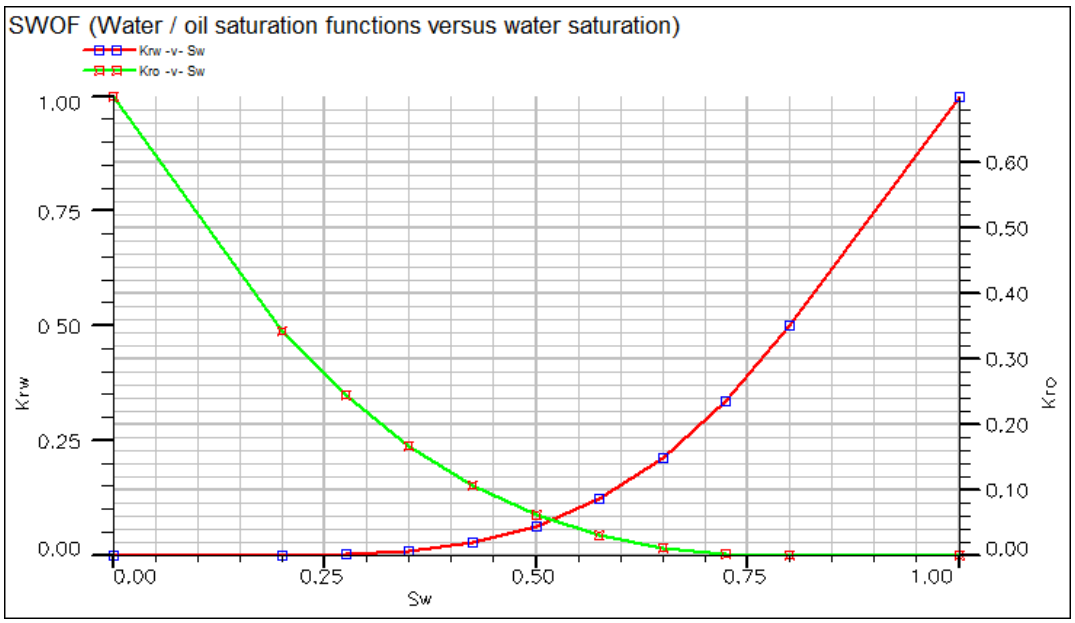

Figure 3.3: Generic model water/oil relative permeability curves (mid-case)

3.13 PVT Model

Fluid properties (PVT models) were estimated using correlations in Eclipse Office®. The parameters used for the PVT modelling of the mid-case run are given in Table 3.4, while the resulting fluid properties as functions of pressure are presented in Figures 3.4 and 3.5 for the

median run. For the other experiments, the variables in Table 3.4 were adjusted by the corresponding values specified in Table 3.2.

Table 3.4: Data used for PVT modelling

SURFACE PROPERTIES			
S/N	**Parameter**	**Value**	**Unit**
1	Oil API	32	deg. API
2	Gas gravity	0.65	Dimensionless
3	GOR	800	scf/stb
4	Salinity	0	fraction
SURFACE CONDITIONS			
5	Standard Temp.	60	deg F.
6	Standard Press.	14.7	psia
7	Separator Temp.	60	deg F.
8	Separator Press.	14.7	psia
RESERVOIR CONDITIONS			
9	Res. Temp	183	deg. F @ 10180 ftss
10	Reference Pressure	4573	psia
11	Porosity	0.25	Fraction
12	Rock type	Consolidated sandstone	
NON-HYDROCARBON COMPONENTS			
13	Fraction of H_2S	0	Mol. fraction
14	Fraction of CO_2	0.5	Mol. fraction
15	Fraction of N_2	0.8	Mol. fraction

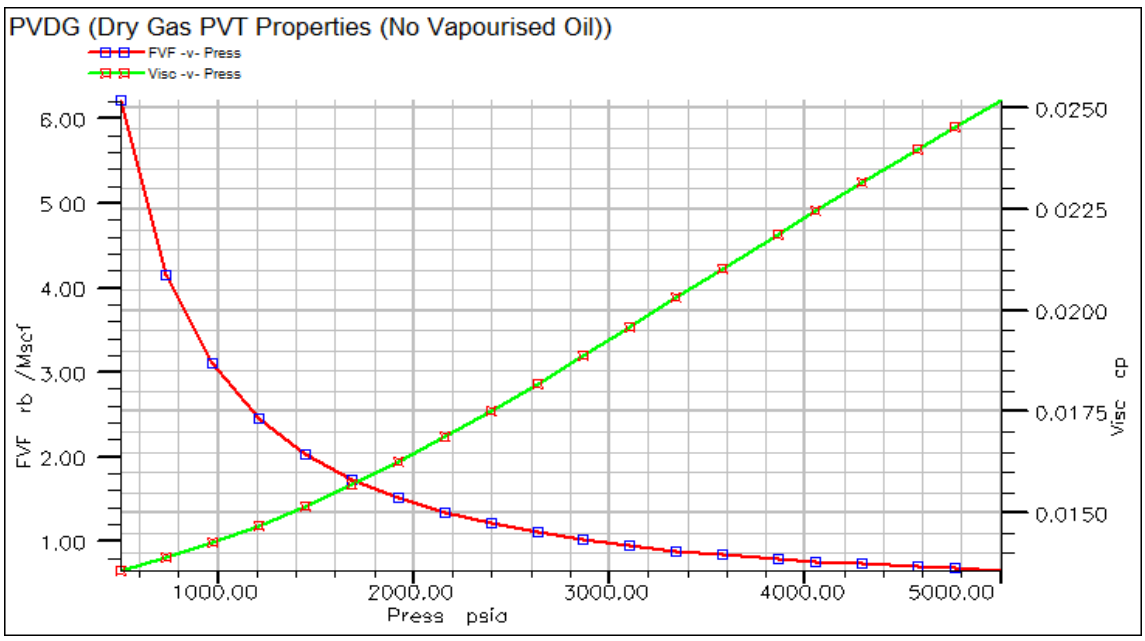

Figure 3.4: Dry gas PVT properties

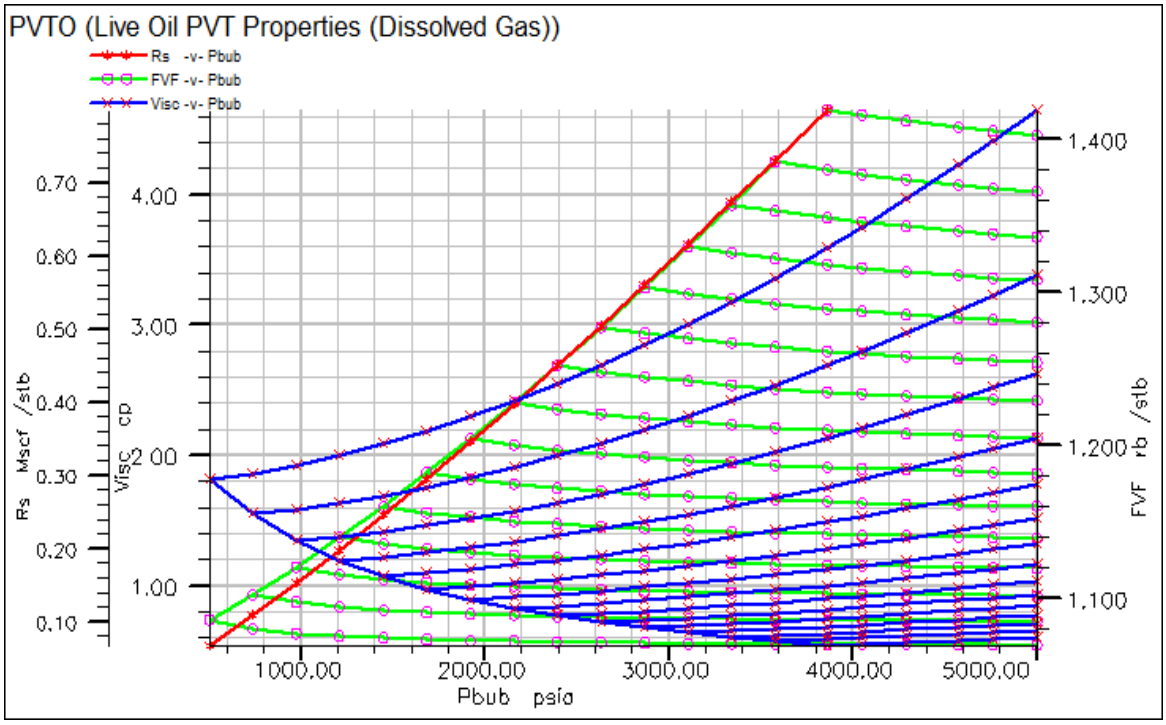

Figure 3.5: Live oil PVT properties

3.2 DYNAMIC RESERVOIR SIMULATION

3.2.1 OIL-THEN-GAS DEVELOPMENT (OTG) SCENARIO

All experiments designed in Table 3.2 were carried out as specified for each run, with production only made from the oil column for a maximum simulation run time of 20years. This operation simulates production in oil-rim reservoirs in which oil is withdrawn from the oil column with negligible or no deliberate production from the gas cap. The well trajectory, under this development scenario, is shown in Figure 3.6.

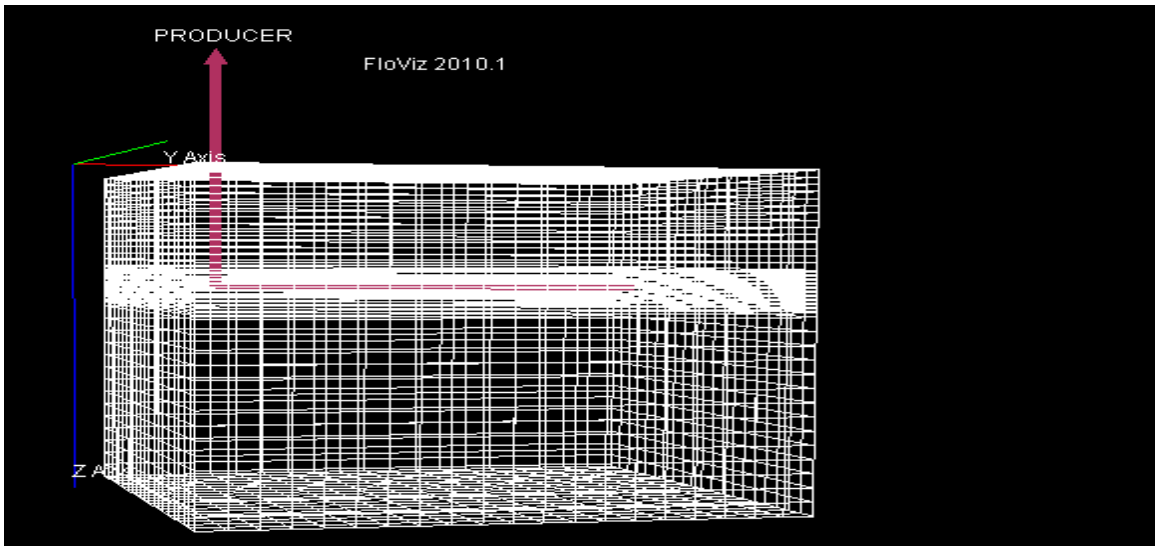

Figure 3.6: Grid block showing well trajectory for the oil-then-gas development scenario

3.2.2 CONCURRENT OIL AND GAS (COG) DEVELOPMENT SCENARIO

For this development option, the experiments of Table 3.2 were repeated with production from both the gas cap and oil column simultaneously for a period of 20years. To minimize coning, the vertical gas well was completed at a depth of 10101ft, far away from the GOC**.** To ensure proper control of the numerical experiments, this depth of completion of the vertical gas well was kept constant for all simulation runs. Figure 3.7 shows the well trajectory for this development option.

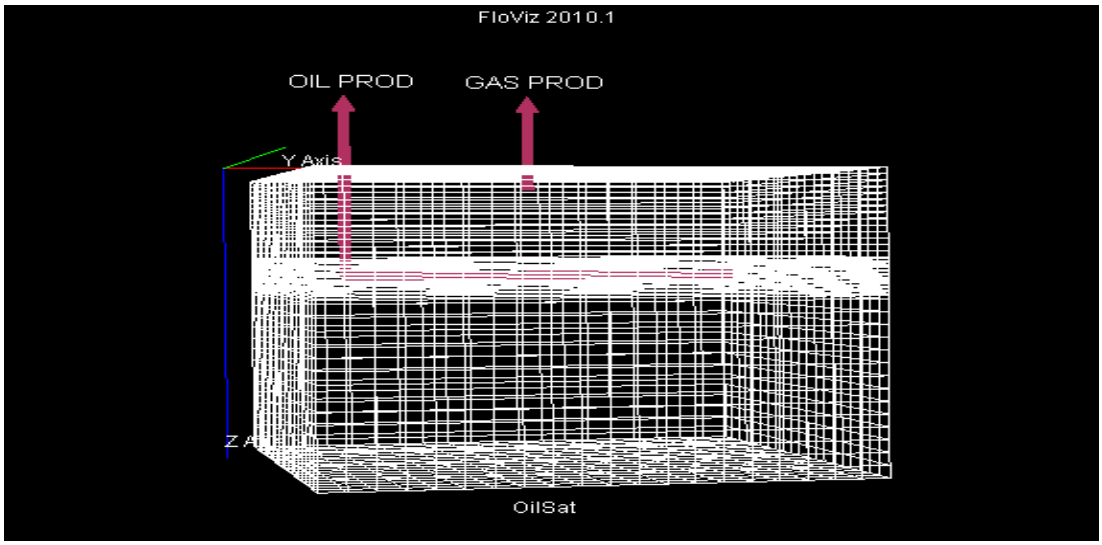

Figure 3.7: Well Trajectory and Status under Concurrent Oil and Gas Production

3.2.3 GAS-ONLY DEVELOPMENT (GOD) SCENARIO

In this section, the experiments of Table 3.2 were conducted with only gas production from the gas cap. To accomplish this scenario, the oil producer in Figure 3.7 was shut-in and gas production was carried out for the 20years simulation run time. Again, the vertical gas well was completed at a fixed depth of 10101ft in all the simulation cases.

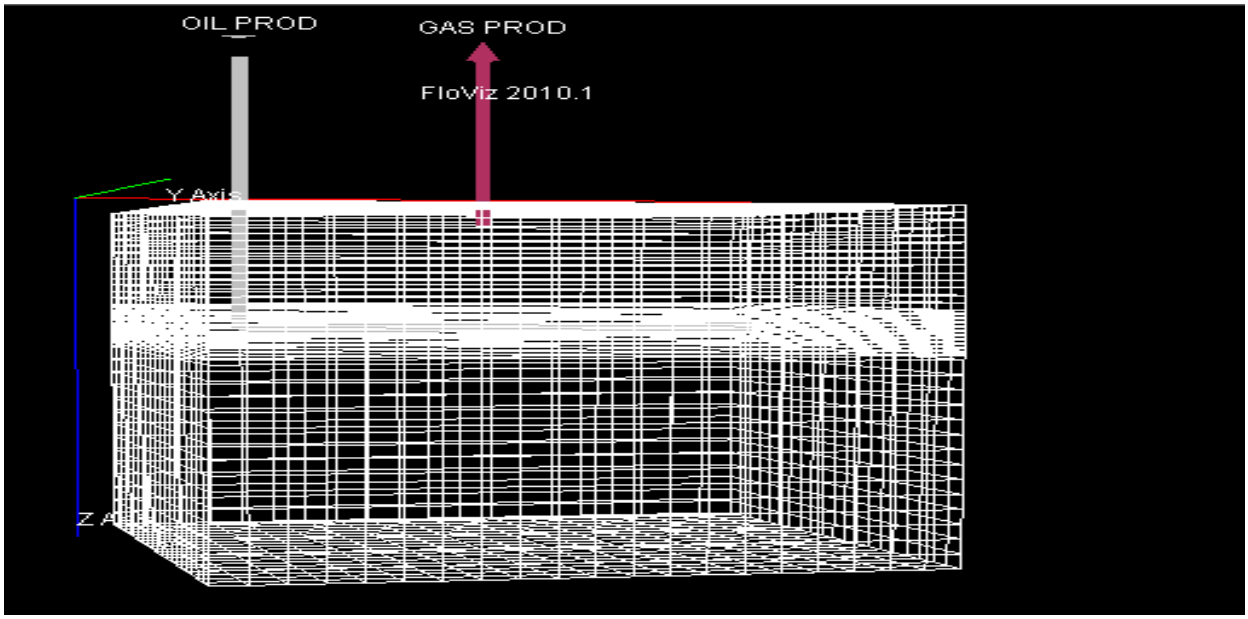

Figure 3.8: Well Trajectory and Status under Gas-Only Development Scenario.

3.3 PARAMETER SCREENING AND GENERATION OF SURROGATE MODELS

To ascertain the most significant parameters, or combinations of parameters, that affect recovery in oil-rim reservoirs, parameter screening was carried out using 2-level Factorial Design Analysis.

As earlier mentioned, the eight parameters screened are oil-rim thickness (H_o), oil API, reservoir anisotropy (Kv/Kh), rock relative permeabilities (Krg, Kro, Krw), and liquid and gas withdrawal rates.

Again, after conducting the experiments through dynamic reservoir simulation, the responses (RF) were populated in the design which was analyzed to generate surrogate models for predicting the response (recovery factor) and screened to identify the most significant factors or heavy hitters among the variables by comparing the relative

contribution of each variable and their aliases to recovery factor or oil-rim reservoirs performance. These experiments were carried out for three different development approaches for thin oil reservoirs with large gas cap and active aquifer of varying strength and size.

CHAPTER FOUR

RESULTS, ANALYSIS, AND DISCUSSION

4.1 OIL-THEN-GAS DEVELOPMENT SCENARIO

4.1.1 RESERVOIR SIMULATION RESULTS (OTG SCENARIO)

Table 4.1: Simulated Recovery Factors for OTG development scenario

RUN	Ho (ft.)	Oil API	Kv/Kh (fraction)	Krg (fraction)	Krw (fraction)	Kro (fraction)	Ql (5%STOIIP/yr) (STB/d)	FGIIP (BSCF)	STOIP (MM STB)	UR (MMSTB)	Oil RF (%)
1	20	40	0.5	0.7	0.3	0.9	442	43.90	3.23	0.55	17.09
2	60	24	0.5	0.7	0.7	0.5	1654	48.77	12.07	1.47	12.17
3	60	40	0.01	1	0.3	0.5	1328	52.11	9.70	2.32	23.92
4	20	24	0.5	1	0.3	0.5	551	42.79	4.02	0.34	8.35
5	20	24	0.01	1	0.7	0.9	551	42.79	4.02	0.67	16.53
6	20	40	0.01	0.7	0.7	0.5	442	43.90	3.23	0.68	21.15
7	60	24	0.01	0.7	0.3	0.9	1654	48.77	12.07	2.49	20.62
8	20	24	0.01	0.7	0.3	0.5	551	42.79	4.02	0.53	13.12
9	40	32	0.1	0.85	0.5	0.7	1007	46.97	7.35	1.23	16.74
10	60	40	0.5	1	0.7	0.9	1328	52.12	9.70	1.75	18.05
11	60	24	0.5	0.7	0.3	0.9	1654	48.77	12.07	2.02	16.76
12	60	24	0.01	0.7	0.7	0.5	1654	48.77	12.07	1.89	15.61
13	20	24	0.5	0.7	0.7	0.9	551	42.79	4.02	0.45	11.11
14	20	24	0.5	1	0.7	0.5	551	42.79	4.02	0.33	8.08
15	60	24	0.01	1	0.7	0.9	1654	48.77	12.07	2.28	18.89
16	20	40	0.5	1	0.3	0.9	442	43.90	3.23	0.54	16.78
17	60	40	0.01	0.7	0.3	0.9	1328	52.12	9.70	2.30	28.67

4.1.2 DESIGN ANALYSIS FOR THE OTG DEVELOPMENT SCENARIO

4.1.2.1 PARAMETER SCREENING

ANOVA for Selected Factorial Model

Table 4.2 shows the ANOVA table for the OTG development scenario design analysis/parameter screening. Equation 4.1 presents the surrogate model for predicting recovery factor for oil-rim reservoirs, under this depletion scenario, within the range of parameters used to generate the responses (RF) in Table 4.1.

The **Model F-value** of 72.74 implies the model is significant. There is only a 0.01% chance as indicated by the model's p-value (Row 3 of Table 4.2) that an F-value this large could occur due to noise.

Table 4.2: ANOVA table for the OTG Case Design Analysis

Response 1: OIL RF						
Source	**Sum of Squares**	**df**	**Mean Square**	**F-value**	**p-value**	
Model	434.07	5	86.81	72.74	< 0.0001	significant
B-Oil API	156.58	1	156.58	131.20	< 0.0001	
C-Kv/Kh	134.11	1	134.11	112.37	< 0.0001	
F-Kro	46.56	1	46.56	39.01	< 0.0001	
G-Ql (5%STOIIP/yr)	38.46	1	38.46	32.23	0.0001	
BC	16.82	1	16.82	14.10	0.0032	
Residual	13.13	11	1.19			
Cor Total	447.20	16				

P-values less than 0.0500 indicate model terms are significant. In this case, B, C, F, G, and BC are significant model terms. Their order or rank of significance can be inferred from Figure 4.1 and Equation 4.1.

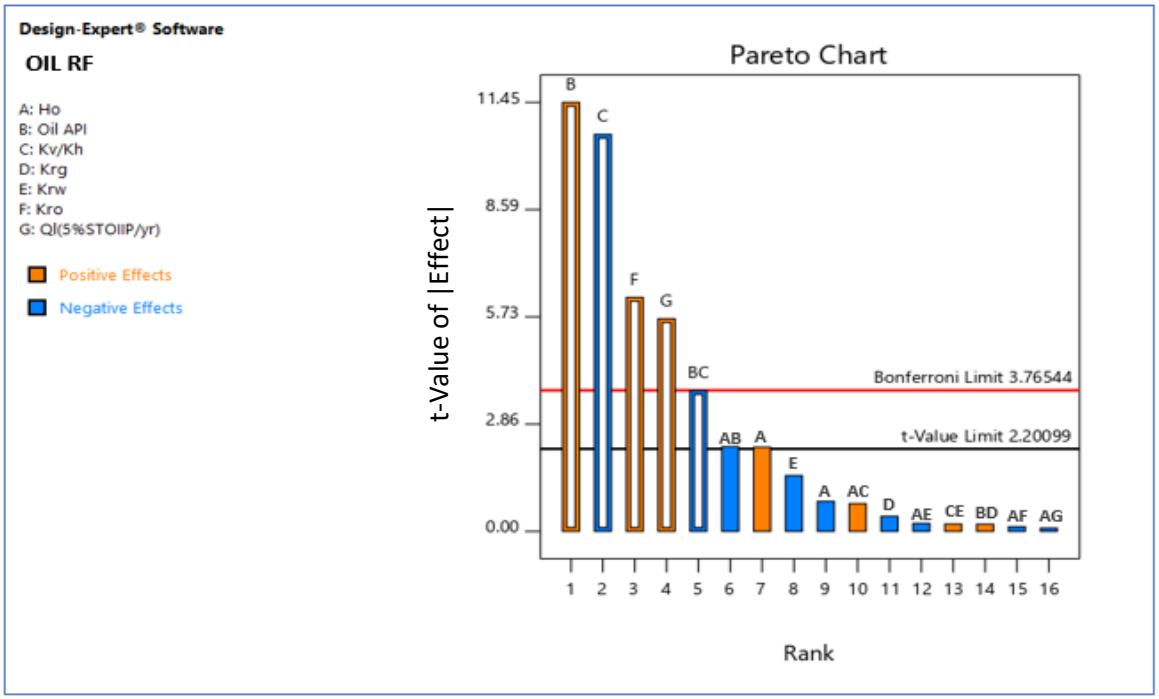

Figure 4.1: Pareto Chart Showing the Order of Significance of Parameters Affecting Oil-Rim Performance under the Scenario of OTG Development.

4.1.2.2 SURROGATE MODEL FOR OTG DEVELOPMENT SCENARIO

Equation 4.1 presents the surrogate equation generated from the analysis of the individual and interactions effects of the parameters in Table 4.1 on the response (RF). Figure 4.2 compares the simulated Oil RF values of Table 4.1 with the model predictions.

$$R_f = 17.21 + 3.38B - 3.19C + 1.99F + 1.93G - 1.18BC \quad \textbf{(4.1)}$$

Where:

$B = -7.5287 + 0.170651\ (API)$ **(4.1a)**

$C = 1.975141\left(\frac{k_V}{k_h}\right)$ **(4.1b)**

$F = 5.00794\ K_{ro}$ **(4.1c)**

$G = 0.001658 Q_l$ **(4.1d)**

$BC = 0.511525\left[(API)\left(\frac{k_V}{k_h}\right)\right]$ **(4.1e)**

API: $Oil\ API\ (degree)$

$\frac{K_v}{K_h}$: $Vertical\ anisotropy\ or\ ratio\ of\ vertical\ to\ horizontal\ permeability\ (fraction)$

K_{rw}: $Rock\ relative\ permeability\ to\ water\ at\ s_{orw}\ \ (fraction)$

K_{ro}: $Rock\ relative\ permeability\ to\ oil\ at\ s_{wmin}\ (fraction)$

Ho : $Oil\ rim\ thickness\ (ft)$

Q_l: $Liquid\ flow\ rate, 5\%STOIIP/yr\ (stb/day)$

Substituting Equations 4.1a, 4.1b, 4.1c, 4.1d and 4.1e into Equation 4.1 gives the surrogate equation in terms of the actual factor as shown in Equation A1 of Appendix AII. Table 4.3 presents the model fit statistics.

The **Predicted R^2** of 0.9405 (Table 4.3) is in reasonable agreement with the **Adjusted R^2** of 0.9573; i.e., the difference is less than 0.2.

Table 4.3: OTG Surrogate Model Fit Statistics

Std. Dev.	1.09
Mean	16.68
C.V. %	6.55
R^2	0.9706
Adjusted R^2	0.9573
Predicted R^2	0.9405
Adeq. Precision	30.2047

Adeq. Precision measures the signal to noise ratio. A ratio greater than 4 is desirable. The ratio of 30.2047 indicates an adequate signal. This model can be used to navigate the design space as shown in Figure 4.2.

Additional plots and parameters of this design analysis are presented in Appendix AII.

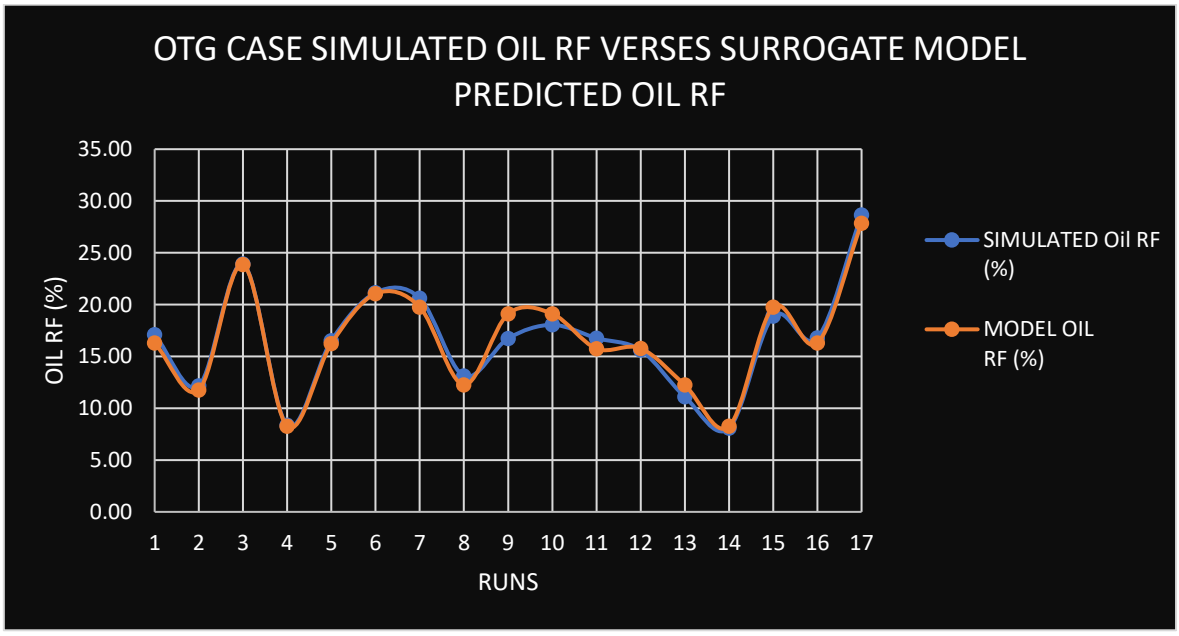

Figure 4.2: OTG Case Simulated Oil RF values Versus Model Predicted RF values.

4.1.3 INDIVIDUAL RUNS RESULTS ANALYSIS

OTGR1

Figure A(i), in Appendix A, shows the production forecast plots of this model and the fluid saturation distribution along the trajectory of the horizontal oil producer can be inferred from Figure A(ii) which shows that of the middle cell along the well trajectory. This $20ft$ pay zone reservoir has oil of 40°API, high vertical connectivity ($Kv/Kh = 0.5$) and was produced at an offtake rate of 442 stb/d (Row 1 of Table 4.1).

Early water and gas breakthrough were observed. Pressure decline rate was minimal before water and gas breakthrough but became rapid, as a result, gas withdrawal from the system, after gas breakthrough occurred. Water influx rate was enormous until well BHP was only sufficient for gas production, after the 9th year of production. The well life ended at the 11th month as the well BHP fell below the minimum specified $1000psia$ economic value.

OTGR2

This $60ft$ oil-rim model has oil of 40 °API, high Kv/Kh value of 0.5 and was produced at an offtake rate of 1654 stb/d (Row 2 of Table 4.1).

As shown by Figures A (iii) and A (iv), early water and gas coning were observed with water breakthrough occurring earlier, 1 year into production, and gas breakthrough occurring in the second year of production. Again, **with continuous gas withdrawal at an increasing rate, rapid pressure decline was observed,** and the well liquid production ceased at the 8th year while gas production ended a year later.

High water cut (up to 90%) was observed in this run. A combination of a high rate of production and high communication between the aquifer and oil column is responsible for this behaviour.

OTGR3

High recovery factor of 24% was observed (Row 3 of Table 4.1). This is attributable to a combination of favourable properties of the reservoir as it has the high case oil-rim thickness of $60ft$, light oil of $40° API$ and low vertical communication between the fluid layers ($Kv/Kh\ of\ 0.01$). However, the peak production rate was only sustained up to the fifth year of production after which high BS&W (up to 0.76) was observed after water breakthrough occurred when production time approached the fifth year. Gas breakthrough followed shortly afterwards and GOR rose to 48MMSCF/STB by the end of the field's life at the 6th year of production.

OTGR4

This reservoir (Row 4 of Table 4.1) has a relatively small oil-rim thickness of $20ft$ and good vertical communication between the oil, gas and water zones ($K_v/K_h = 0.5$). These unfavourable combinations of properties explain the early water and gas breakthrough observed in the production forecast trends and saturation plots in Figures A (vii) and A (viii), causing the oil well to water-out and shut-in in the 8th year of production.

OTGR5

This reservoir (Row 5 of Table 4.1) has the same thickness and oil API of 24° as OTGR4 but has low $K_v/K_h =$ value of 0.01. Figures A (ix) and a(x) present the production forecast and saturation plots, respectively.

Unlike the OTGR4 model, gas breakthrough, in this model was almost at the start of production and GOR increase rate was very high. This is attributable to the high gas relative permeability of the rock. This behaviour caused a rapid pressure decline profile. Notwithstanding, **this model has an unusually high recovery value for its low thickness as a result of the high relative permeability to oil of the rock.**

OTGR6

The OTGR6 (Row 6 of Table 4.1) reservoir model possesses the same reservoir pay thickness of 20ft and oil API of 40^{o} as OTGR1, it is also characterized by early water and gas breakthrough and high water cut. However, its low vertical permeability value and low offtake rate reduced gas coning rate and hence, the well BHP was at and above the minimum value of 1000psia for longer production time, causing a higher recovery than OTGR1. Figures A (xi) and A (xii) present the production forecast and saturation plots, respectively.

OTGR7

This 60ft oil-rim model has oil of 24 ^{o}API, low Kv/Kh value of 0.01 and was produced at an offtake rate of 1654stb/d (Row 7 of Table 4.1).

Peak production period was maintained for 4years, and water breakthrough did not occur until the same period. This is attributable to the low vertical communication between the fluid columns. However, gas breakthrough was observed earlier, as this phase is highly mobile. Figures A (xiii) and A (xiv) present the production forecast and saturation plots, respectively.

OTGR8 (LOW CASE RUN)

This model consists of all low case values of the model properties or parameters being investigated (Row 8 of Table 4.1). Production commenced at a liquid rate of 551stb/d.

Gas production was almost instantaneous with oil production, and although water breakthrough took a little longer, it occurred within year 1 of production. Figures A (xv) and A (xvi) present the production forecast and saturation plots, respectively.

OTGR9 (MID-CASE RUN)

This model consists of all mid-case values of the model properties/parameters being investigated. (Row 9 of Table 4.1). Production started at an offtake rate of 1007stb/d.

Early water breakthrough was observed with the rate of water cut and the rate of GOR increase both hiking after breakthrough which occurred just before the second year of production for both water and gas. Pressure decline rate was very rapid, as a result of the high gas withdrawal rate. Figures A (xvii) and A (xviii) presents the production forecast and saturation plots, respectively.

OTGR10 (HIGH CASE RUN)

This model consists of all high case values of the model properties/reservoir parameters being investigated. (Row 10 of Table 4.1). Production started at an offtake rate of 1328stb/d. A peak production rate of 1328stb/d was sustained for about 3years, longer than the low case and medium case runs. Also, water and gas breakthrough took longer to occur, and the recovery factor was higher, in this case, compared to the previous two runs.

Like the OTGR3 run, **this good performance is attributable to a combination of favourable properties of the reservoir as it has the high case oil-rim thickness of 60ft and light oil of 40º API.** However, the Kv/Kh is high and this caused earlier water and gas breakthrough than the OTGR3 reservoir in which peak production was sustained a little longer.

OTGR11

Similar to the OTGR2 model, this 60ft oil-rim model had oil of 24º API, high Kv/Kh value of 0.5 and was produced at an offtake rate of 1654stb/d (Row 11 of Table 4.1). The two models, however, differ in the rock relative permeability properties.

As shown by Figures A (xxi) and A (xxii), early water and gas coning were observed with water breakthrough occurring earlier, one year into production and gas breakthrough occurring towards the third year of production.

OTGR12

Like the OTGR7 model, this 60ft oil-rim model had oil of 24^{o} API, low Kv/Kh value of 0.01 and was produced at an offtake rate of 1654stb/d (Row 12 of Table 4.1). The two reservoirs, however, differ in the relative permeability properties of the rock. Specifically, endpoint relative permeabilities to water and oil.

Production trends of the two models are similar, and GOR curves exhibit the same pattern. However, with a lower value of relative permeability to oil (0.5) for the OTGR12 model, and a higher value of relative permeability to water (0.7) compared to the OTGR7 model (Kro = 0.9, Krw = 0.3), water breakthrough occurred earlier in the OTGR12 model as shown in Figures A(xxiii) and A(xxiv).

OTGR13

This model is akin to the OTGR4 model in reservoir thickness (20ft), oil API (24^{o}) and Kv/Kh (0.5) and the liquid offtake rate for it is also 551stb/d. The two models, however, differ in the rock relative permeability properties.

With lower relative permeability to gas in this case (Krg = 0.7) compared to the Krg of 1 in the OTGR4 model, the gas breakthrough was delayed till the 10th year of production in the OTGR13 model. Water production trends were similar for both models. However, while the oil well of the OTGR4 model watered out in the 8th year, the OTGR13 well was shut-in by BHP constraint when the BHP fell below 1000psia in the 12th year of production.

OTGR14 (MOST PESSIMISTIC CASE)

This 20ft oil-rim reservoir had oil of 24^{o} API, Kv/Kh value of 0.5 and was operated at an offtake rate of 551stb/d.

The delayed gas breakthrough was observed, and the GOR increase rate was moderate afterwards. Consequently, well BHP depletion rate was moderate within the simulation run time. However, **the well quickly watered out after the 7th year of production. This can**

be traced to the combination of high Krw, high vertical communication between the aquifer and pay zone coupled with high offtake rate in a small oil-rim reservoir.

OTGR15

This model has a pay zone thickness of 60ft, oil API of 24^{o} and a low Kv/Kh of 0.01, while the liquid offtake rate was 1654stb/d (Row 15 of Table 4.1).

Figure A (xxix) and A (xxx) reveal that early gas breakthrough occurred in the horizontal oil producer of this model and GOR increase has a steep slope, signifying huge gas withdrawal from the system. This is attributable to the high offtake rate used in the simulation. Consequently, pressure decline was also at a steep rate such that the minimum well BHP economic limit was reached within four years of production.

Water breakthrough, on the other hand, was delayed past the third year of production and as a result of the low Kv/Kh value. Again, once broken through, water cut increased at a vertical slope. This is attributable to the high production rate of 1640stb/d at the time of water breakthrough.

OTGR16

Figure A (xxxi) show the production forecast of this model and the fluid saturation distribution along the trajectory of the horizontal oil producer can be inferred from Figure A (xxxii) which shows that of the middle cell along the well trajectory. This 20ft pay zone reservoir has oil of 40^{o} API, high vertical connectivity and was produced at an offtake rate of 442 stb/d (Row 16 of Table 4.1).

Early water and gas breakthrough were observed, and pressure decline was rapid as a result of rapid gas withdrawal after gas breakthrough occurred. Water influx rate was enormous until well BHP was only sufficient for gas production after the 8th year of production which

ended at the 11th month as the well BHP fell below the minimum specified 1000psia economic value.

OTGR17 (MOST OPTIMISTIC CASE)

This model has parameters as given in Row 17 of Table 4.1 and its performance plots are presented in Figure A (xxxiii). It depicts the most optimistic scenario, as it presents the most favourable combination of parameters for a good oil-rim reservoir performance (high RF).

Production was at a peak rate of 1328stb/d for 4.5years during which water cut was zero and GOR was less than 40MSCF/STB. This desired performance was sustained for about 50% of the entire field life. Beyond this point, the model exhibited similar behaviour with other runs after water breakthrough. That is, water cut rose by 15 percentage points, and oil rate plummeted within 3months.

A recovery factor of 23.71% recorded by this run indicates that **good recovery can be achieved in a high API oil reservoir with up to 60ft pay zone thickness, low vertical permeability and relative permeability properties with a high preference for oil flow relative to the flow of the water and gas phases.**

4.2 CONCURRENT OIL AND GAS DEVELOPMENT SCENARIO

4.2.1 RESERVOIR SIMULATION RESULTS (COG DEVELOPMENT SCENARIO)

Table 4.4: Simulated Recovery Factors for the COG Development Scenario

RUN	Ho (ft.)	Oil API	Kv/Kh (fraction)	Krg (frac tion)	Krw (fraction)	Kro (frac tion)	Ql (5%STOIIP/yr) (STB/day)	Qg (5%FGIIP/yr) (MSCF/day)	FGIIP (BSCF)	STOIP (MMSTB)	UR (MMSTB)	Oil RF (%)
1	20	40	0.5	0.7	0.3	0.9	442	6014	43.90	3.23	0.49	15.16
2	60	24	0.5	0.7	0.7	0.5	1654	6681	48.77	12.07	1.48	12.24

3	60	40	0.01	1	0.3	0.5	1328	7139	52.11	9.70	1.93	19.88
4	20	24	0.5	1	0.3	0.5	551	5861	42.79	4.02	0.32	7.85
5	20	24	0.01	1	0.7	0.9	551	5861	42.79	4.02	0.54	13.49
6	20	40	0.01	0.7	0.7	0.5	442	6013	43.90	3.23	0.57	17.65
7	60	24	0.01	0.7	0.3	0.9	1654	6681	48.77	12.07	2.14	17.71
8	20	24	0.01	0.7	0.3	0.5	551	5861	42.79	4.02	0.43	10.79
9	40	32	0.1	0.85	0.5	0.7	1007	6435	46.97	7.35	1.04	14.10
10	60	40	0.5	1	0.7	0.9	1328	7139	52.12	9.70	1.56	16.04
11	60	24	0.5	0.7	0.3	0.9	1654	6681	48.77	12.07	1.68	13.87
12	60	24	0.01	0.7	0.7	0.5	1654	6681	48.77	12.07	1.63	13.50
13	20	24	0.5	0.7	0.7	0.9	551	5861	42.79	4.02	0.44	10.91
14	20	24	0.5	1	0.7	0.5	551	5861	42.79	4.02	0.30	7.36
15	60	24	0.01	1	0.7	0.9	1654	6681	42.94	4.23	2.03	16.78
16	20	40	0.5	1	0.3	0.9	442	6013	43.90	3.23	0.49	15.08
17	60	40	0.01	0.7	0.3	0.9	1328	7139	52.12	9.70	1.92	23.399

4.1.2 DESIGN ANALYSIS FOR COG DEVELOPMENT SCENARIO

4.2.2.1 PARAMETER SCREENING

ANOVA for Selected Factorial Model

Table 4.5 shows the ANOVA table for the COG development scenario design analysis/parameter screening. Equation 4.2 presents the surrogate model for predicting recovery factor for oil-rim reservoirs, under this depletion scenario, within the range of parameters used to generate the responses (RF) in Table 4.4.

The Model F-value of 44.12 implies the model is significant. There is only a 0.01% chance, as indicated by the model's p-value (Row 3, Column 6 of Table 4.5) that an F-value this large could occur due to noise.

Table 4.5: ANOVA Table for the COG Case Design Analysis

Response 1: RF						
Source	**Sum of Squares**	**df**	**Mean Square**	**F-value**	**p-value**	
Model	249.26	4	62.32	44.12	< 0.0001	significant
B-Oil API	109.93	1	109.93	77.84	< 0.0001	
C-Kv/Kh	51.30	1	51.30	36.33	< 0.0001	
F-Kro	20.22	1	20.22	14.32	0.0026	
G-Ql(5%STOIIP/yr)	37.34	1	37.34	26.44	0.0002	
Residual	16.95	12	1.41			

As explained in the oil-then-gas case, P-values less than 0.0500 indicate model terms are significant. In this case **B (Oil API), C (Kv/Kh), F (Kro), and G (Ql)** are the most significant model terms. Values greater than 0.1000 indicate the model terms are not significant. Alternatively, the terms or factors with the most effect on recovery can be read from Figure 4.3 and/or the surrogate equation.

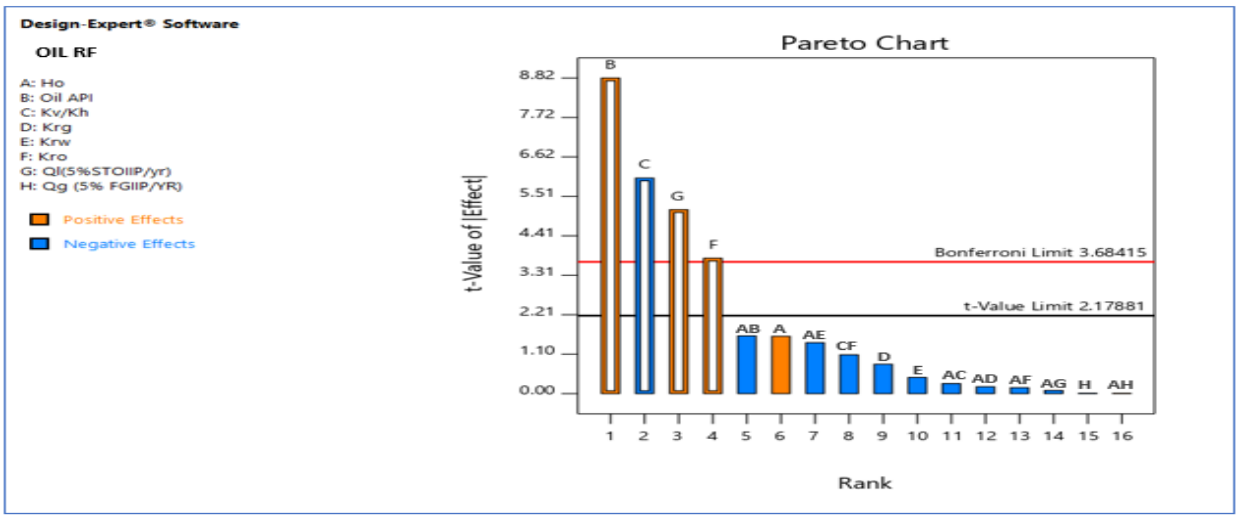

Figure 4.3: Pareto Chart showing the order of significance of Parameters affecting Oil-Rim Performance under COG production

4.2.2.2 SURROGATE MODEL FOR THE COG DEVELOPMENT SCENARIO

Equation 4.2 presents the surrogate model for this scenario from the analysis of the individual and interactions effects of the parameters in Table 4.4 on the response (RF). Figure 4.4 compares its predictions with the simulated RF values of Table 4.4.

$$R_f = 15.00 + 2.28B - 1.85C + 1.18F + 1.89G \quad \text{(4.2)}$$

Where:

$B = -7.33465 + 0.154518\ (API)$ (4.2a)

$C = 4.083676\left(\frac{K_V}{K_h}\right)$ (4.2b)

$F = 4.982034\ K_{ro}$ (4.2c)

$G = 0.00164\ Q_l$ (4.2d)

API: $Oil\ API\ (degree)$

$\frac{K_v}{K_h}$: $Vertical\ anisotropy\ or\ ratio\ of\ vertical\ to\ horizontal\ permeability\ (fraction)$

K_{ro}: $Rock\ relative\ permeability\ to\ oil\ at\ s_{wmin}\ (fraction)$

Q_l: $Liquid\ flow\ rate, 5\%STOIIP/yr\ (stb/d)$

Substituting Equations 4.2a, 4.2b, 4.2c, and 4.2d into Equation 4.2 gives the surrogate equation in terms of the actual factor as shown in Equation B1 of Appendix BII. Table 5.4 presents the model fit statistics.

Table 4.6: COG Case Surrogate Model Fit Statistics

Std. Dev.	1.19
Mean	14.46
C.V. %	8.22

R^2	0.9363
Adjusted R^2	0.9151
Predicted R^2	0.8774
Adeq Precision	21.8919

The **Predicted R^2** of 0.8774 is in reasonable agreement with the **Adjusted R^2** of 0.9151; i.e. the difference is less than 0.2.

Adeq Precision measures the signal to noise ratio. A ratio greater than 4 is desirable. This ratio of 21.892 indicated an adequate signal. This model can be used to navigate the design space.

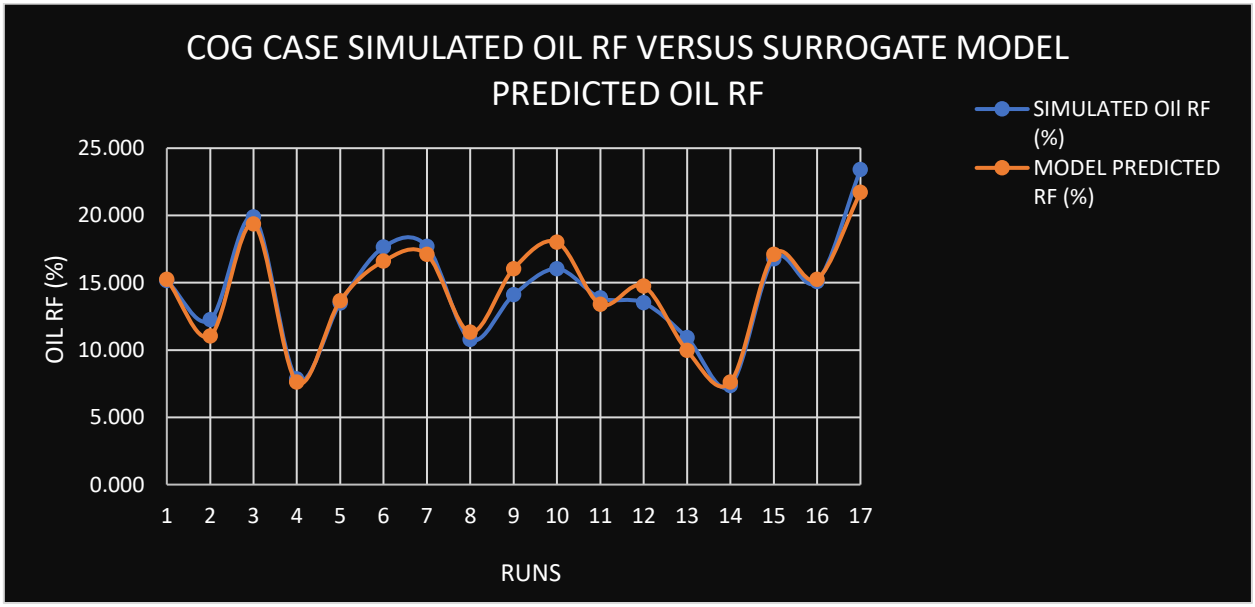

Figure 4.4: COG Case Simulated Oil RF versus Model Predicted RF

4.2.3 INDIVIDUAL RUNS RESULTS ANALYSIS

All models under this depletion scenario, differ from the OTG case models by the presence of a functional gas producer. One will expect these COG case reservoir models to reach their technical limits, in terms of minimum allowable BHP, faster than their counterparts in the previous development option considered. This is as a result of the free gas withdrawal from the gas cap and subsequent faster depletion of reservoir energy.

COGR1

The model dimensions are as given in Row 1 of Table 4.3 and its performance plots are shown in Figures B (i) and B (ii) of Appendix B.

A peak production rate was maintained at 442stb/d for 1.5years after which production started to decline. At this point, water breakthrough was observed, the GOR increased from about 20Mscf/stb to 56Mscf/stb, and the production rate fell by about 36% within 2.5 months. Afterwards, production continued to decline at the rate of circa 50stb/d/month until the end of the well life at the 8^{th} year of production.

Relative to the case of only oil production, as depicted by the OTGR1 model, the well life was shorter and recovery was less by 11.2% in the COGR1 model. However, water cut and GOR trends are similar in both scenarios – Figures A (i) and B (i). However, in this case**, production started with a GOR of 19Mscf/stb**, which reflects the conscious simultaneous production of oil and gas from inception.

COGR2

The model dimensions are as given in Row 2 of Table 4.3 and its performance plots are shown in Figures B (iii) and B (iv) of Appendix B.

Although the pay thickness is 60ft, the high case value for thickness, production decline started within the first year of production, coinciding with water breakthrough. At this point, production rate fell by 38% within 2.5months and GOR rose by about 2Mscf/stb and water cut rose sharply from zero to 40%. This relatively early and aggressive water breakthrough is attributed to the increased K_{rw} and reduced K_{ro} in this run.

Comparing this COGR2 model with the OTGR2 model, where production was only made from the oil column, we observe similar water cut and GOR profiles – Figures A (iii) and B (iii).

The early plummeting of production rate and hiking of water cut can be traced to the high rate at which production commenced and the good communication between the gas aquifer and oil zone (Kv/Kh = 0.5).

From the above observations in the model behaviour, we can conclude **that high offtake rates are therefore undesired and that the COG development approach may yield higher recovery factor than corresponding sequential development scenario when the pay thickness is much bigger**. Row 2 of Table 4.3 reveals a 0.54% increase in the Oil RF under this development approach relative to the OTG case (Row 2 of Table 4.1).

COGR3

The model dimensions are as given in Row 3 of Table 4.3 and its performance plots are shown in Figures B (v) and B (vi) of Appendix B.

Figure B (v) shows that the production decline did not occur until production approached the 4^{th} year and water cut was 0% until the same time. Although production commenced with a GOR of 6.64Mscf/stb, GOR increase was mild until the 4^{th} year of production. After water breakthrough, production rate nosedived while GOR and water cut hiked.

We can relate the longer length of peak production in this model, relative to the previous two; the delay in water breakthrough and low GOR before water breakthrough to a combination of high oil column thickness (60ft) with low vertical connectivity (Kv/Kh = 0.01).

Relative to the OTGR3 model, the sequential oil-then-gas development counterpart of the COGR3 model, the well life was longer in the former because **the reservoir energy was depleted faster with gas production from the gas cap as oil is been withdrawn from the oil column**.

COGR4

The model dimensions are as given in Row 4 of Table 4.3 and its performance plots are shown in Figures B (vii) and B (viii) of Appendix B.

The production forecast plots of this model show a decline from the plateau production rate at about 6months into the commencement of production. Similar to the previous models, **the start of this steep descent in flow rate coincides with the time in which water breakthrough occurs and usually, gas breakthrough either occurs the same time or an increase in GOR is observed at this point.**

Similar to the sequential development counterpart (OTGR4), this model run shows that **low thickness oil-rim reservoirs with high Kv/Kh values are associated with low recovery factor and prone to early termination of field life.**

COGR5

This model depicts a similar scenario with the previous model (COGR4) but with low communication between the fluid columns (Kv/Kh = 0.01) and the rock oil/water relative permeability properties (Row 5 of Table 4.3). Figures B (ix) and B(x) are the corresponding production performance plots.

Similar to the previous models, **the time of water breakthrough coincides with the start of the descent of the plateau production rate**. However, relative to the COGR4 model, **the low vertical communication between the fluid layers caused an extension of the plateau production period due to delayed water breakthrough.**

COGR6

Row 6 in Table 4.3 presents the set of parameters that describe this model. This is a case of low pay thickness reservoir with a high recovery factor, which can be attributed to the relatively high oil API (favourable oil properties). Its production forecast plots are given in Figures B (xi) and B (xii).

While it exhibits a few similar behaviours with other models, such as the sharp decline in production rate at water breakthrough, the COGR6 model shows that **a combination of low vertical permeability value and low production rate is favourable for production in thin oil columns** as this condition creates a delay in water breakthrough, reduction in pressure decline rate and subsequent conservation of reservoir energy or increase in field life. However, the impact of the relatively low oil offtake rates on project economics would have to be evaluated on a case-by-case basis.

COGR7

This model further underscores the effect of vertical permeability in the performance of oil-rim reservoirs. Even with a high offtake rate of 1654stb/d (but still within the imposed 5%STOIIP annual production rate), Figure B(xiii) reveals that plateau production was sustained for longer relative to previous models with higher Kv/Kh values, including other models with the same high case 60ft oil-rim thickness.

Production rate decline for The COGR7 model, unlike others, did not coincide with the commencement of water breakthrough – Figure B (xiii). Despite its relatively low oil API, the good performance of this run is partly explained by the favourable combination of high k_{ro} and low K_{rw}.

Compared with the sequential development counterpart (OTGR7), this model's peak production was sustained about three times longer and water coning was significantly delayed. **It can thus be deduced that a combination of low Krw and high Kro help to delay water coning in oil-rim reservoirs production.**

COGR8 (LOW CASE RUN)

This model consists of all low case values of the model properties or parameters being investigated. Its dimensions are as given in Row 8 of Table 4.3 and its performance plots are shown in Figures B (xv) and B (xvi) of Appendix B.

As observed in the other models, except for the COGR7, the fall of the production rate from the specified peak offtake value coincides with the time of water breakthrough. In this case, this occurred at the end of year 1 of production. Additionally, gas production was instantaneous with oil production as production commenced with a GOR of 14Mscf/stb.

Compared with its sequential development counterpart (OTGR8), recovery efficiency was less by 17.8% and the field life was longer in that case as gas withdrawal from the system reduced the field life of the COGR8 to 8 years.

COGR9 (MID-CASE RUN)

This model consists of all mid-case values of the model properties or parameters being investigated. Its dimensions are as given in Row 9 of Table 4.3 and its performance plots are shown in Figures B (xvii) and B (xviii) of Appendix B.

Peak production period was sustained in this model for over 1.5years, after which production rate nosedived at water breakthrough. As usual, the water cut increased sharply after breakthrough and pressure decline rate was very high. These trends can be explained by the high offtake rate of 1007stb/d in combination with the small thickness of the pay zone.

COGR10 (HIGH CASE RUN)

This model consists of several high case values of the reservoir properties being investigated. Its dimensions are as given in Row 10 of Table 4.3 and its performance plots are shown in Figures B (xix) and (B (xx) of Appendix B.

An oil recovery factor of 16% was recorded, which is about 11% less than the RF obtained in the sequential development counterpart model (OTGR10). This is because the field life was shorter in this scenario due to free gas withdrawal from the gas cap – comparing Figure B (xix) against Figure A (xix).

COGR 11

This model has parameters as given in Row 11 of Table 4.3 and its performance plots are presented in Figures B (xxi) and B (xxii).

The production profile shows that the peak production period was sustained for 1year after which water breakthrough occurred and production decline started simultaneously with a steady, then sharp GOR increase. After this point, production rate decline was at about 40stb/d/yr till the end of the well life. Water cut rose by 40% within 2.5months, continued to increase at circa 0.1%/yr until a few months to the 6^{th} year beyond which a continuous decline in GOR and water cut was observed till the end of oil production and end of field life as the gas well BHP went below the stipulated minimum limit of 1000psia.

COGR12

This model has parameters as given in Row 12 of Table 4.3 and its performance plots are presented in Figures B (xxiii) and B (xxiv).

The COGR12 model has production trend, water cut profile and GOR curve similar to those of the earlier described COGR11 model. However, relative to the latter, this model witnessed a delay in water breakthrough – Figure B (xxiii). This is attributable to the lower Kv/Kh value of 0.01 (Row 12, Table 4.3).

COGR13

This model has parameters as given in Row 13 of Table 4.3 and its performance plots are presented in Figures B (xxv) and B (xxvi).

Its performance plots are similar to those of the previous models, and it further shows the early water and gas breakthrough tendencies of low pay thickness reservoirs, as the 20ft reservoir witness water breakthrough within the first year of production.

Relative to the sequential development scenario counterpart (OTGR13), this model also highlights the fact that gas withdrawal from the gas cap during oil production shortens the field life and lowers the recovery factor of the oil-rim reservoir. This observation can partly be explained by the rapid depletion of reservoir energy, resulting in well quitting on BHP constraint.

COGR14 (MOST PESSIMISTIC CASE RUN)

This model has parameters as given in Row 14 of Table 4.3 and its performance plots are presented in Figures B (xxvii) and B (xxviii). It depicts the less pessimistic scenario, as it presents the most unfavourable combination of parameters for a good performance (high RF). As expected, Table 4.3 shows that it has the lowest oil recovery factor among all runs.

Plateau production was sustained for about 7months. As usual, **the end of peak production is usually associated with water breakthrough and a short interim of slight rise in GOR, hike in water cut and a huge descent in production rate.**

In this case, at water breakthrough, production rate fell by 438stb/d within 3months. Within the same interim, both water cut and GOR exhibited sharp and steady increases.

Apart from the relatively poor oil flow properties (low API), this behaviour is traceable to the high vertical communication between the oil, water and gas columns as signified by the high Kv/Kh value of 0.5 as well as the less favourable K_{ro} in comparison to the relative permeabilities (k_{rg} and k_{rw}) of the unwanted gas and water.

Between the 10th month, the end of the short period described above, and the end of the field life in the 8th year, there was stability in the rate of increase of water cut and the rate of decline of the production rate. However, a hike in the gas cut was experienced from the 6th to the end of the field's life due to a continuous influx of gas from the gas cap into the oil well.

COGR15

This model has parameters as given in Row 15 of Table 4.3 and its performance plots are presented in Figures B (xxix) and B (xxxx).

As a 60ft thick oil-rim with very low communication (due to relatively low kv/kh) between the gas, oil and water columns, water breakthrough and subsequent dropping of the production rate was delayed till the beginning of the 10th month. Similar to the COGR14 model, **the progressive increase in pressure decline rate is attributable to massive gas withdrawal from the system as gas cap influx into the oil well**, in the 7th year, **adds to the gas production through the gas well.**

COGR16

This model has parameters as given in Row 16 of Table 4.3 and its performance plots are presented in Figures B (xxxi) and B (xxxii).

Peak production was sustained till the mid of the second year at which water breakthrough coincided with the usual slight increase in GOR and plummeting of production rate, again, within a space of 0.2years.

Relative to the sequential development counterpart (OTGR16), this model also shows that gas withdrawal from the gas cap reduces the field's life and recovery factor, in this case, by 10.15%.

COGR17 (MOST OPTIMISTIC CASE RUN)

This model has parameters as given in Row 17 of Table 4.3 and its performance plots are presented in Figures B (xxxiii). It depicts the most optimistic scenario, as it presents the most favourable combination of parameters for a good performance (high RF).

Table 4.3 shows that it has an oil recovery factor of approximately 20% while the performance plots reveal desirable production rate, water cut, and GOR profiles.

A plateau production rate of 1328stb/d was sustained for up to 76% of the field's life (3.8years), within the same period, water cut was controlled, and GOR minimal increase. However, beyond this period, at water breakthrough, this model also witnessed a high ascent in water cut, gas cut and sharp fall in production.

It follows that, so long as there is sufficient reservoir energy for production, a combination of high pay zone thickness, low vertical permeability, high oil API and relative permeability functions that preferentially favour the oil phase are essential for excellent oil-rim reservoirs performance. COGR14 proves the reverse to be true.

4.3 GAS-ONLY DEVELOPMENT SCENARIO

4.3.1 RESERVOIR SIMULATION RESULTS (GOD SCENARIO)

Table 4.7: Simulated Recovery Factors for the GOD Scenario

RUN	Ho (ft.)	Oil API	Kv/Kh (fraction)	Krg (fraction)	Krw (fraction)	Kro (fraction)	Qg (5%FGIIP/yr) (MSCF/day)	FGIIP (BSCF)	STOIP (MMSTB)	Gp (BSCF)	Gas RF (%)
1	20	40	0.5	0.7	0.3	0.9	6013	43.90	3.23	33.678	76.72
2	60	24	0.5	0.7	0.7	0.5	6681	48.77	12.07	37.272	76.42
3	60	40	0.01	1	0.3	0.5	7139	52.11	9.70	39.308	75.43
4	20	24	0.5	1	0.3	0.5	5861	42.79	4.02	33.020	77.17
5	20	24	0.01	1	0.7	0.9	5861	42.79	4.02	32.992	77.11
6	20	40	0.01	0.7	0.7	0.5	6013	43.90	3.23	33.687	76.74
7	60	24	0.01	0.7	0.3	0.9	6681	48.77	12.07	37.272	76.42
8	20	24	0.01	0.7	0.3	0.5	5861	42.79	4.02	32.990	77.10
9	40	32	0.1	0.85	0.5	0.7	6434	46.97	7.35	35.917	76.47
10	60	40	0.5	1	0.7	0.9	7139	52.12	9.70	39.299	75.40
11	60	24	0.5	0.7	0.3	0.9	6681	48.77	12.07	37.270	76.42
12	60	24	0.01	0.7	0.7	0.5	6681	48.77	12.07	37.271	76.42
13	20	24	0.5	0.7	0.7	0.9	5861	42.79	4.02	33.018	77.17
14	20	24	0.5	1	0.7	0.5	5861	42.79	4.02	32.990	77.10
15	60	24	0.01	1	0.7	0.9	6681	48.77	12.07	33.149	67.97
16	20	40	0.5	1	0.3	0.9	6013	43.90	3.23	33.658	76.68
17	60	40	0.01	0.7	0.3	0.9	7139	52.12	9.70	39.300	75.41

4.3.2 DESIGN ANALYSIS FOR THE GOD SCENARIO

4.3.2.1 PARAMETER SCREENING

ANOVA for Selected Factorial Model

Table 4.8 shows the ANOVA table for the gas-only development scenario Design analysis/Parameter screening. Equation 4.3 presents the surrogate model for predicting recovery factor for oil-rim reservoirs, under this depletion scenario, within the range of parameters used to generate the responses (RF) in Table 4.7.

The **Model F-value** of 103102.73 (Table 4.8) implies the model is significant and that there is only a 0.01% chance (as indicated by the p-value) that an F-value this large could occur due to noise.

Table 4.8: ANOVA Table for the GOD Case Design Analysis

Response 1: Gas RF						
Source	**Sum of Squares**	**df**	**Mean Square**	**F-value**	**p-value**	
Model	73.99	10	7.40	1.031E+05	< 0.0001	significant
A-Ho	0.0224	1	0.0224	312.31	< 0.0001	
D-Krg	3.38	1	3.38	47061.28	< 0.0001	
E-Krw	0.0015	1	0.0015	20.58	0.0062	
F-Kro	0.0011	1	0.0011	15.27	0.0113	
G-Qg	1.44	1	1.44	20131.17	< 0.0001	
AD	6.26	1	6.26	87251.82	< 0.0001	
AG	2.95	1	2.95	41065.13	< 0.0001	
BD	4.26	1	4.26	59364.89	< 0.0001	
DE	0.0061	1	0.0061	84.59	0.0003	
DG	5.35	1	5.35	74503.40	< 0.0001	
Residual	0.0004	5	0.0001			
Cor Total	73.99	15				

Again, P-values less than 0.0500 indicate model terms are significant. In this case, **A, D, E, F, G, AD, AG, BD, DE, DG** are the significant model terms. Values greater than 0.1000 indicate the model terms are not significant. Figure 4.5 further shows the dominance of the gas relative permeability (Krg) over other factors affecting gas production in oil-rim reservoirs.

4.2.2.2 SURROGATE MODEL FOR THE GOD SCENARIO

Equation 4.3 presents the surrogate equation from the analysis of the individual and interactions effects of the parameters in Table 4.6 on the response (Gas RF).

$$R_f = 75.66 + 0.4564A + 6.55D - 0.0113E + 0.0115F - 7.87G - 25.35AD - 5.93AG - 4.34BD - 0.0280DE + 36.24DG \quad \textbf{(4.3)}$$

Where:

$$A = -11.1267 + 0.800962H_O \quad \text{(4.3a)}$$

$D = -0.05091\ K_{rg}$ _ ____ ___ __ _ (4.3b)

$E = -0.0156\ K_{rw}$ _ ____ ___ __ _ (4.3c)

$F = 0.195651\ K_{ro}$ _ ____ ___ __ _ (4.3d)

$G = 11796.29 Q_g$ _ ____ ___ __ _ (4.3e)

$AD = 20.01527(H_o \times K_{rg})$ _ ____ ___ __ _ (4.3f)

$AG = 513049(H_o \times Q_g)$ _ ____ ___ __ _ (4.3g)

$BD = 15.21879(API \times K_{rg})$ _ ____ ___ __ _ (4.3h)

$DE = 0.030695(K_{rg} \times K_{rw})$ _ ____ ___ __ _ (4.3i)

$DG = 1317.555(K_{rg} \times Q_g)$ _ ____ ___ __ _ (4.3j)

Substituting equations 4.3a through 4.3j in equation 4.3 presents the surrogate equation in terms of the actual factor as shown in Equation C1 of Appendix CII. Table 4.9 presents the model fit statistics, while Figure 4.6 highlights the agreement between simulations and surrogate model.

Table 4.9: GOD Surrogate Model Fit Statistics

Std. Dev.	0.0085		**R^2**	1.0000
Mean	76.05		**Adjusted R^2**	1.0000
C.V. %	0.0111		**Predicted R^2**	0.9930
			Adeq Precision	1310.1674

The **Predicted R^2** of 0.9930 is in reasonable agreement with the **Adjusted R^2** of 1.0000; i.e. the difference is less than 0.2. **Adeq Precision** measures the signal to noise ratio. A ratio greater than 4 is desirable. This ratio of 1310.167 indicates an adequate signal. This model can be used to navigate the design space.

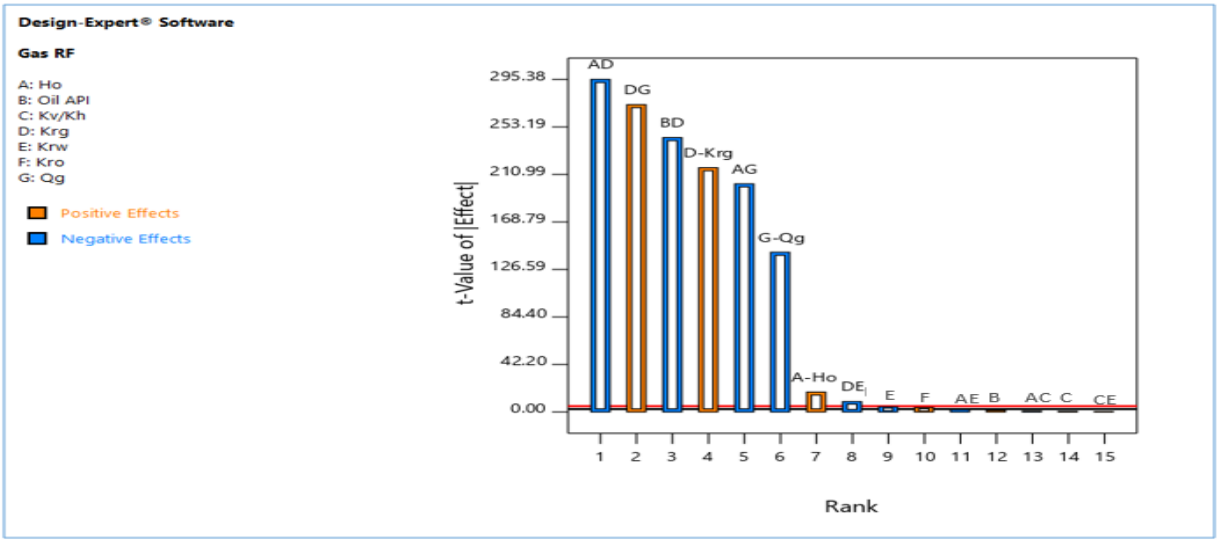

Figure 4.5: Pareto Chart showing the order of significance of Parameters affecting Oil-Rim Performance during only gas production

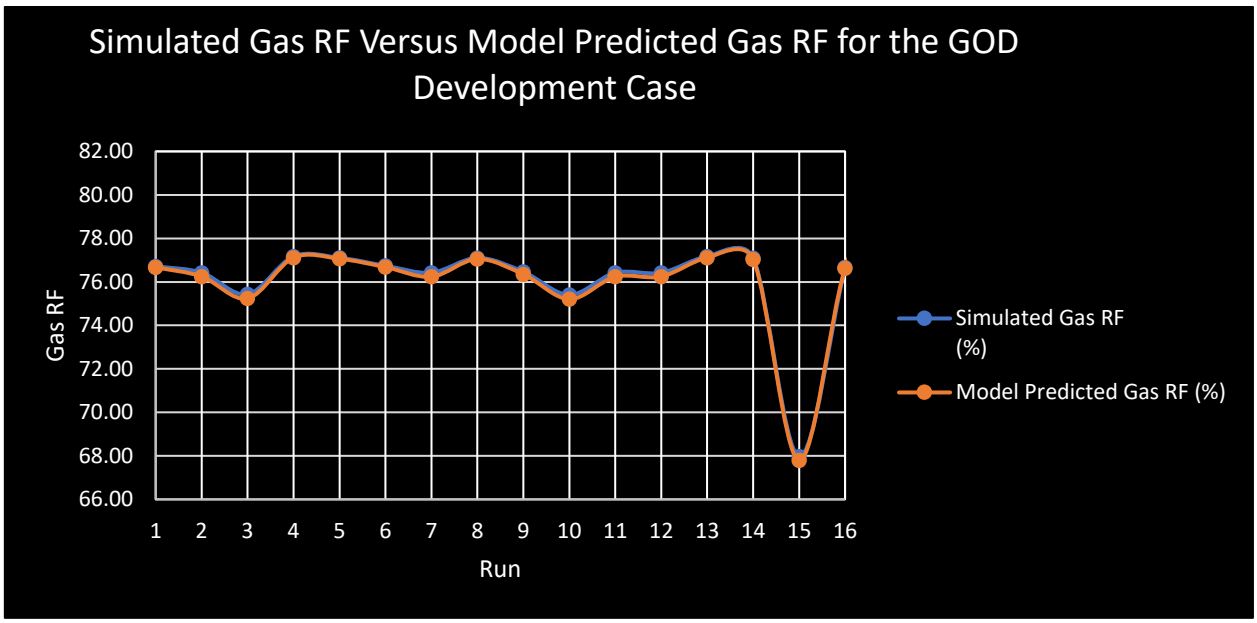

Figure 4.6: GOD Case Simulated RF versus Model Predicted Gas RF.

4.4 PERFORMANCE COMPARISON OF DIFFERENT OIL-RIM DEVELOPMENT OPTIONS

Figure 4.7 compares the ultimate oil and gas recoveries in terms of the BOE for the three development options under the different reservoir conditions depicted by each run. To compute the BOE of the produced gas in each case, one STB had been set at 5800scf.

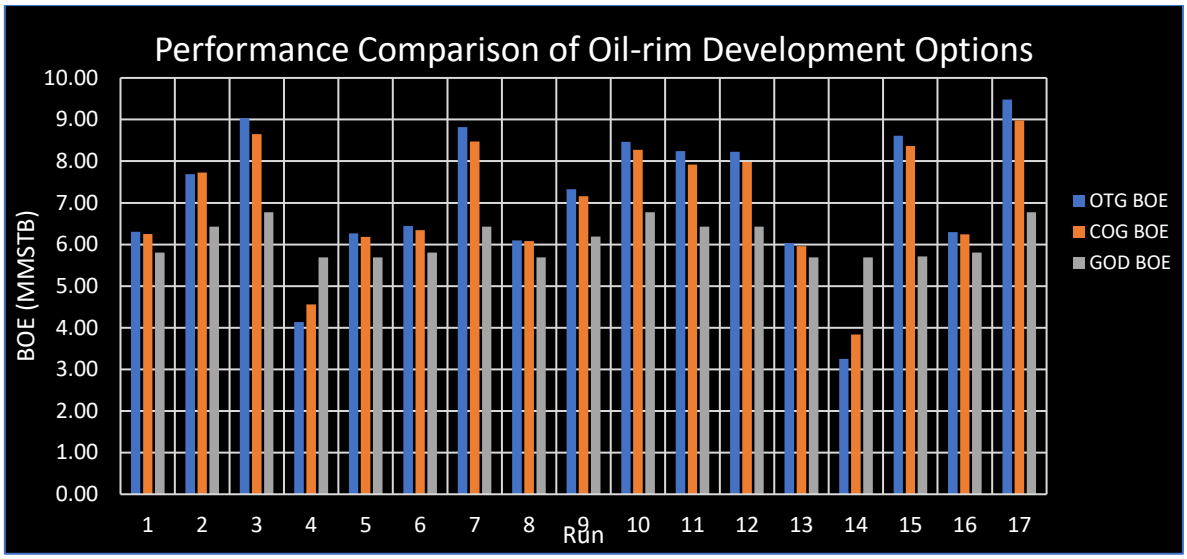

Figure 4.7: Performance Comparison of Different Oil-rim Development Options

In the majority of the runs, the OTG development option yielded significant BOE than the COG ad GOD options. This is shown in runs 3, 7, 9, 10, 11, 12, 15 and 17. These reservoirs have high pay zone thickness (60ft), with the exception being run 9, which has the base (mid) case oil column thickness of 40ft. Also, these reservoirs are associated with low vertical anisotropy values of 0.01, but for runs 9 (Base case), 10 and 11. With run 17 representing the most optimistic reservoir conditions and the rest having good BOE values, it is safe to conclude that the sequential oil-then-gas option is the preferred choice when reservoir conditions are promising.

Also, some of the reservoirs demonstrated that, in terms of the BOE, there is not much difference between the sequential oil-then-gas development option and the concurrent oil-and-gas development case. However, there may be differences if discounted BOE had been used for the comparison.

Runs 1, 2, 5, 6, 8, 13 and 16 demonstrate that while the GOD yields far less BOE than others, any of OTG and GOD options can be adopted for the development of these reservoirs, at least from the technical standpoint of competitive BOE recovery. They are all characterized by relatively low oil-rim thickness, but for run 2.

The GOD option yielded the best performance only in runs 4 and 14. These reservoirs are both characterized by the low oil-rim thickness (20ft), low oil API (24^o API) and high vertical communication. In addition to these undesirable properties, run 14, with good water and gas mobility properties (K_{rw} = 0.7; K_{rg} = 1) presented the 'most pessimistic' reservoir conditions as discussed in section 4.1.3, for the OTG development scenario and section 4.2.3, for the COG development option. It, therefore, follows that when a reservoir is characterized by this relatively unfavourable combination of properties, the GOD option is the most promising.

CHAPTER 5

CONCLUSIONS AND RECOMMENDATIONS

5.1 Oil-rim Reservoirs flow behaviours and effect of Subsurface Properties on RF under Sequential OTG Development.

5.1.1 Conclusions and Recommendations drawn from the OTG Development Approach Simulation Results and Design Screening Analysis.

- Of the seven static and dynamic properties investigated under this scenario, it was observed that the heavy individual hitters, in order of significance are the oil API, vertical anisotropy, oil relative permeability, and liquid offtake rate. In addition to the above, the interaction of oil API and anisotropy makes the pair substantial in deciding the performance of oil-rim reservoirs.
- Water and gas coning were observed to be prevalent when oil-rim reservoirs are produced using oil-then-gas development approach with water and gas cut skyrocketing after water and gas breakthrough respectively. In addition to the other causes discussed below, this behaviour is traceable to the fundamental problem of oil-rim reservoirs: low pay thickness sandwiched between large gas cap and aquifer. Effort should, therefore, be made to minimize and handle water and gas production when planning the development of reservoirs of this nature.
- All models/reservoirs under this development approach exhibited accelerated pressure decline after gas breakthrough. This was attributed to the reservoir energy loss associated with gas cap depletion. Also, high gas cuts were observed in models with the high case K_{rg} value. Oil-rim reservoirs with a preference for a gas flow should, therefore, be flagged for high gas cut and consequent quick reservoir energy depletion.
- Reservoirs with low pay thickness and high vertical permeability suffered earlier water and gas coning relative to those with high pay thickness and low vertical

permeability values. In addition to the above properties, coning was observed to occur earlier in models with higher liquid offtake rates. Since the reservoir properties are difficult to modify on a large scale, efforts should be made to reduce liquid production rate during sequential oil-then-gas development of oil-rim reservoirs.

- Similar to the above bullet, good reservoir performance or high recovery factors were observed in models with a combination of high pay zone thickness, high oil API, low vertical permeability and rock relative permeability properties that give preference to oil flow over the flow of water and gas. This combination of reservoir conditions was identified as the most optimistic case in oil-rim reservoir development under sequential oil-then-gas production development approach.
- Converse to the above point, low recovery factors were observed in models/reservoirs with low pay thickness, low API and high vertical communication between the different fluid zones. This combination of reservoir conditions was marked as the most pessimistic case in oil-rim reservoir development. Development of fields with such properties should be done after a thorough economic feasibility analysis.

5.2 Oil-rim Reservoirs flow behaviours and effect of Subsurface Properties on RF under Concurrent Oil and Gas Development.

5.2.1 Conclusions and Recommendations drawn from the COG Development Approach Simulation Results and Design Screening Analysis.

- The effect of eight factors, including operational parameters and reservoir static and dynamic properties, on oil-rim recovery factor, under concurrent oil and gas production, was investigated in this scenario. The factors are liquid and gas offtake rates, rock relative permeability to water, gas and oil, oil-rim reservoir thickness, oil API and vertical anisotropy. Of these, it was observed that **Oil API, vertical**

anisotropy (Kv/Kh), liquid offtake rate and oil relative permeabilities are the most influential. Figure 4.3 showed the relative contributions of the other factors to recovery up to second-order alliances of them.

- All models/reservoirs under this production scenario reached their economic limits, in terms of the minimum well BHP, earlier than their counterparts for the oil-then-gas scenario because of the direct gas production from the gas cap.
- Most models also showed that production of oil-rim reservoirs using concurrent oil and gas production approach was associated with gas production from the onset. Operators are therefore advised to have adequate gas handling facilities in place.
- It was also observed that the end of peak production is associated with water breakthrough and a short interim of a slight rise in GOR, a hike in water cut and a huge descent in the production rate. It is, therefore, safe to predict the occurrence of any of the above behaviours and stipulate them as the economic limit for the field during the field development plans of oil-rim reservoirs that will be produced using the COG approach.
- Before the above economic limit occurs, during which there is sufficient reservoir energy for production, a combination of high pay zone thickness, low vertical permeability, high oil API and relative permeability functions that preferentially favour the oil phase were confirmed to be the most desired and essential for excellent oil-rim reservoirs performance. The converse of the above statement was also proved to be true.

5.3 Oil-rim Reservoirs flow behaviours and effect of Subsurface Properties on RF under GOD Scenario

5.2.1 Conclusions and Recommendations drawn from the GOD Approach Simulation Results and Design Screening Analysis.

- Several factors were observed to be very influential in the development of oil-rim reservoirs when the approach of producing the gas cap and when the oil column is neglected. Seven factors were investigated and the following factors were found to have a significant impact on oil-rim performance under gas-only development. They are **oil-rim thickness (H_o), the rock relative permeability properties (K_{rg}, K_{rw} and K_{ro}), gas offtake (Q_g)** rate and the following **2**-level interactions: **(H_o and K_{rg}), (H_o and K_{rg}), (Oil API and K_{rg}), (K_{rg} and K_{rw}), (K_{rg} and Q_g).**
- Dominating in the above list of heavy hitters is the gas relative permeability of the rock.

5.4 Overall conclusion and recommendations

- In the majority of reservoir options, and especially when reservoir properties are promising, the sequential oil-then-gas option is the preferred oil-rim development option.
- It has been demonstrated that while the GOD yields far less BOE, any of the OTG and GOD options with the preferred cost, economic, operational and logistics advantages, can be adopted for the development of some low thickness oil-rim reservoirs without incurring too much opportunity cost.
- For reservoirs with the most pessimistic combination of reservoir properties (low oil-rim thickness, high vertical communication, low API oil, and high water and gas cuts); it is best to develop only the gas cap, while largely neglecting the oil column.

This is the only condition in which the Gas-only development option performs better than the others.

5.5 Recommendations for further works

- A fourth development approach, the gas cap blowdown, can be investigated to make this work more robust. This option places the production well in the gas cap but very close to the GOC such that the oil producer kicks off with 100% gas cut and commences oil production at a later stage when the GOC has moved upward. This approach should be very effective in checking excessive water cut and early water breakthrough.
- Economic analysis of the different oil-rim development options should be performed to ascertain economic feasibility before they are adopted as the choice option for any particular oil-rim reservoir.
- Additional static and dynamic properties such as full PVT and SCAL functions as well as abandonment pressure regimes should be considered in discriminating the various development options for oil-rim reservoirs.
- More sophisticated surrogate models, with a more robust reflection of complex non-linear relationships, should be investigated.
- As an improvement to the current use of idealized box reservoir simulation models, more realistic reservoir simulations that reflect both rock and fluid heterogeneities are worth considering.

REFERENCES

1. Abdulkarim, M. A. (2014), "Development of Coning Correlations for Oil-rim Reservoirs Using Experimental Design and Response Surface Methodology", MSc. thesis, African University of Science and Technology, Abuja.
2. Behrenbruch P. and Mason L. T. (1993), "Optimal Oilfield Development of Fields with a Small Gas Cap and Strong Aquifer". SPE paper 25353, presented at SPE Asia Pacific Oil and Gas Conference and Exhibition, Singapore, 8-10 Feb.
3. Claudio C. and Oluwaseyi F. (2004), "Challenges of Gas Development: Soku Field Oil-rim Reservoirs" SPE paper 88894, presented at the 28th Annual SPE International Technical Conference and Exhibition, Abuja, Nigeria, August 2-4.
4. Damsleth, E., Hage, A., and Volden, R. (1982), "Maximum Information at Minimum Cost: A North Sea Field Development Study with an Experimental Design," Journal of Petroleum Technology, (December 1992), 1350-1356.
5. Hoang, V., Alamsyah, O., and Roberts, J. (2005), "Darajat Geothermal Field Performance-A Probabilistic Forecast," Proceedings, World Geothermal Congress, Antalya, Turkey, 24-29 April 2005.
6. Kabir C.S., Agamini M. and Holguin R. A. (2008), "Production Strategy for Thin-Oil Columns in Saturated Reservoirs." SPE Reservoir Evaluation & Engineering 11 (1): 73–82.
7. Lawal A.K., Wells I.A. and Adenuga A. (2010), "Preliminary Assessment of Oil-Rim Reservoirs: A Review of Current Practices and Formulation of New Concepts." SPE paper 136955, presented at the 34th SPE Nigeria Annual International Conference and Exhibition, Calabar Nigeria, July 31-Aug. 7.
8. Masoudi R. (2011), "How to Get the Most out of Your Oil-rim Reservoirs - Reservoir Management and Hydrocarbon Recovery Enhancement Initiatives." SPE Distinguished Lecturer Program Technical Paper, presented at the SPE-Iran Section

Technical Workshop, 22 Oct.

9. Obah B., Livinus A. and Ezugwu C.M. (2012), "Simplified Models for Forecasting Oil Production: Niger Delta Oil-rim Reservoirs Case." Petroleum Technology Development Journal 2 (2): 1–12.
10. Olamigoke O. and Peacock A. (2009), "First-Pass Screening of Reservoirs with Large Gas Caps for Oil-rim Development", SPE paper 128603, presented at the 33rd Annual SPE International Conference and Exhibition in Abuja, Nigeria, 3 – 5 August.
11. Olatunde A. A, Aladeitan Y., Ogbe D. O. (2015), Integration of structural uncertainty and experimental design for uncertainty quantification, Journal of Petroleum and Gas Engineering, Vol. 6(7), pp. 74-89, July 2015.
12. Omeke J. E., Livinus A., Uche I. N., Obah B., Ekeoma E. (2010), "A proposed cone breakthrough time model for horizontal wells in thin oil-rim reservoirs" SPE paper 140743, presented in the 34th Annual SPE International Conference and Exhibition in Tinapa Calabar, Nigeria, 31st Jul-7th Aug. 2010.
13. Putten S. and Naus M. (2008), "Concurrent Oil and Gas Development Wells: A Smart Well Solution to Thin Oil-rim Presence in Gas Reservoirs," IPTC paper 12344, presented at International Petroleum Technology Conference, Kuala Lumpur.3-5 Dec. 2008.
14. Quinao J. J. and Zarrouk S. J. (2014), "Applications of Experimental Design and Response Surface Method in Probabilistic Geothermal Resource Assessment – Preliminary Results," Proceedings, 39th Workshop on Geothermal Reservoir Engineering, Stanford University, Stanford, California, February 24-26, 2014 SGP-TR-202
15. Razak E. A., Chan K. S. and Darman N. (2010), "Breaking Oil Recovery Limit in

Malaysian Thin Oil-rim Reservoirs: Force Balance Revisited." SPE paper 130388, Presented at the SPE EUROPE/EAGE Annual Conference and Exhibition held in Barcelona, Spain, 14 – 17 June.

16. Shari K. (2013), "How to Get Started with Design Expert® Software"; Software User Guide/Slide Presentation available at www.statease.com/webinar.html
17. Shrivastava V. K., Singha A. K. and Wang J. J. (1998), "Strategy for Control of Water and Gas Cresting in a Thin Oil Column Using Horizontal Wells," SPE paper ***39549, presented at*** SPE India Oil and Gas Conference and Exhibition held in New Delhi, India, 17 -19 February.
18. Silva, J.M., and Dawe, R.A. (2010), "The Challenge of Producing Thin Oil-rims in Trinidad." The West Indian Journal of Engineering 32 (January): 36–41.
19. Uwaga A. O. and Lawal A. K. (2006), "Concurrent Gas cap and Oil-Rim Production: The Swing Gas Option." SPE paper 105985, presented at the 30th Annual SPE International Technical Conference and Exhibition held in Abuja Nigeria, 1- 2 August.
20. Vo D. T., Waryan S, Dharmawan A., Susilo R. and Wicaksana R. (2000), "Lookback on Performance of 50 Horizontal Wells Targeting Thin Oil Columns, Mahakam Delta, East Kalimantan." SPE paper 64385, presented at the SPE Asia Pacific Oil and Gas Conference and Exhibition held in Brisbane, Australia, 16–18 October.
21. Yao, Y., Yunting L, Yuangang W., Zemin J. (2013), "A New Model for Evaluation of Horizontal Well in Bottom Water Reservoirs," *Journal of Applied Mechanics and Materials Vols. 411-414 (2013), pp 486-491.*
22. Yeoh, X. Q. (2014). "Thin Oil-rim Reservoir Development." MSc. Thesis, Imperial College London.

APPENDIX A

PRODUCTION FORECAST PLOTS AND SATURATION PLOTS FOR THE OIL-THEN-GAS (OTG) PRODUCTION SCENARIO RUNS

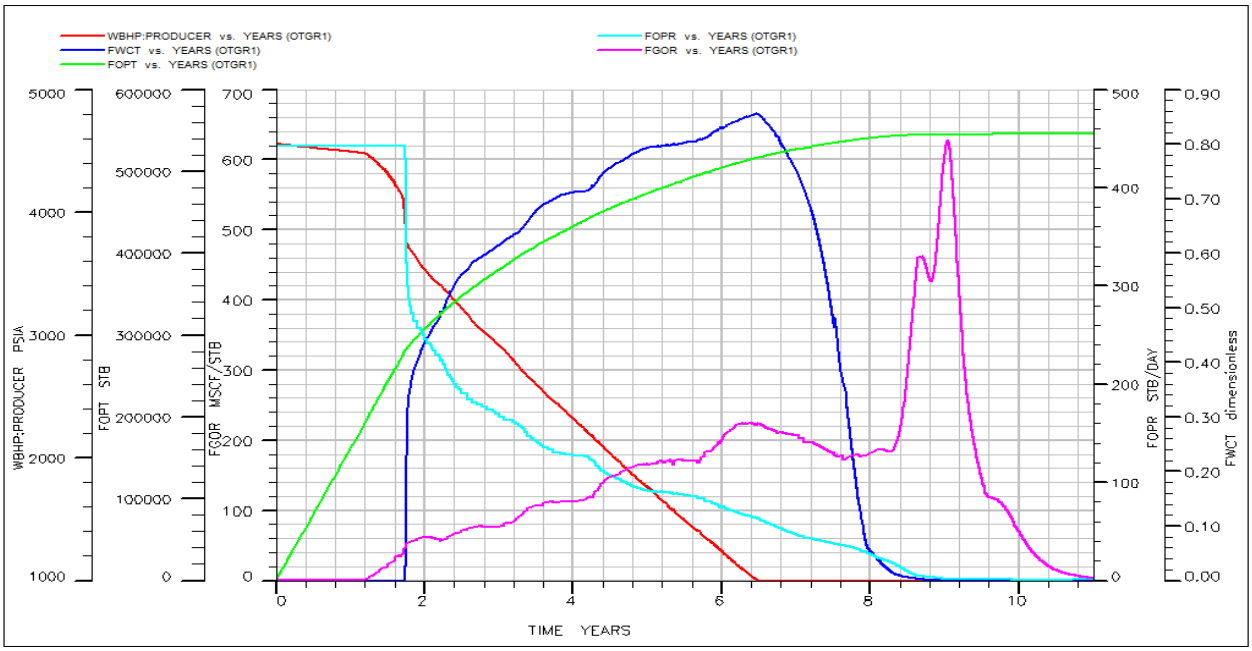

Figure A (i): OTGR1 production forecast plots

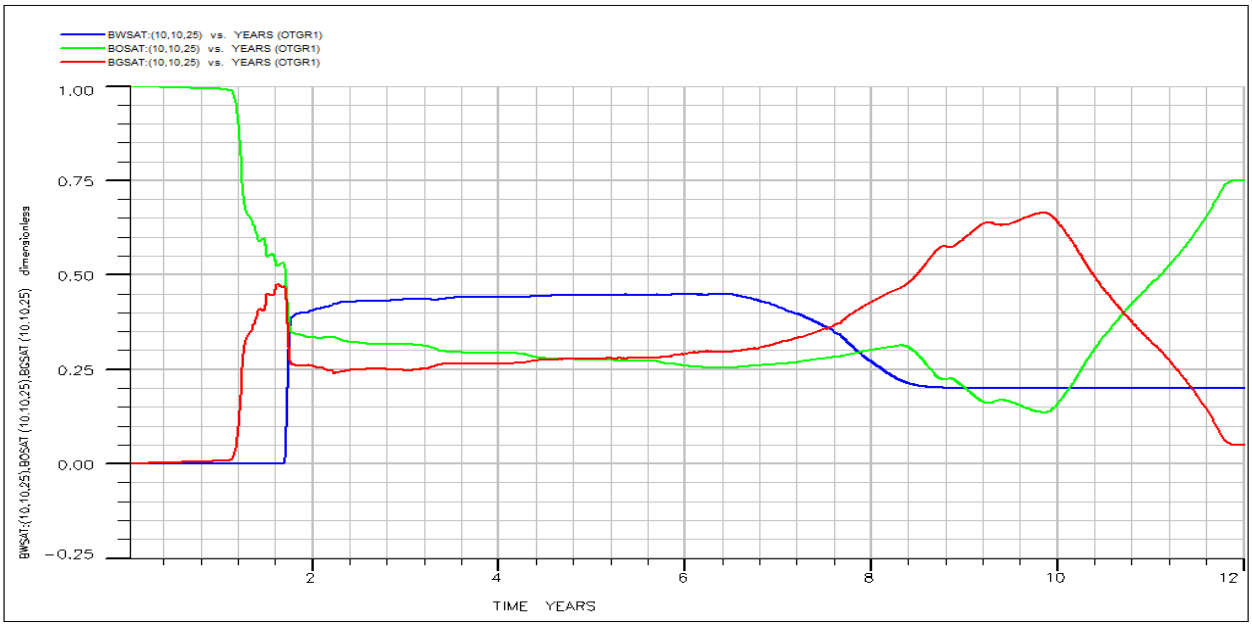

Figure A (ii): OTGR1 fluid saturation plots of the mid-oil-well-trajectory cell.

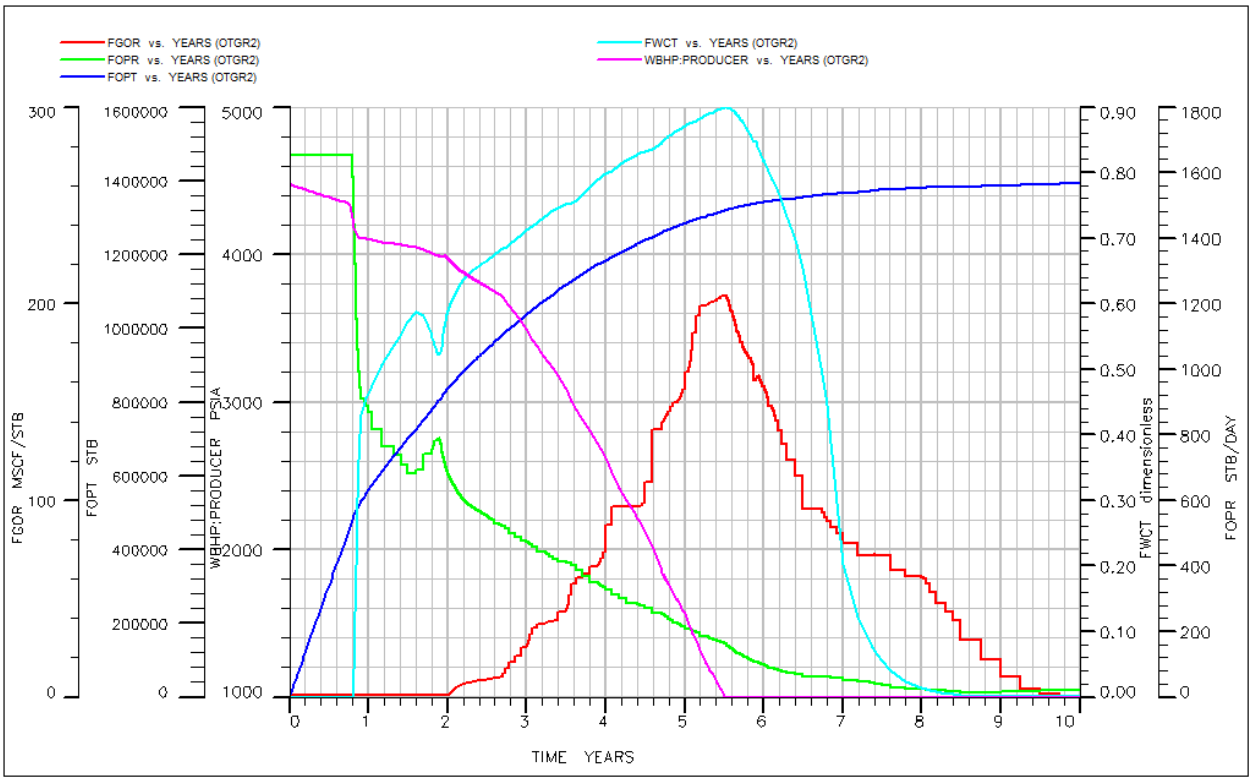

Figure A (iii): OTGR2 production forecast plots

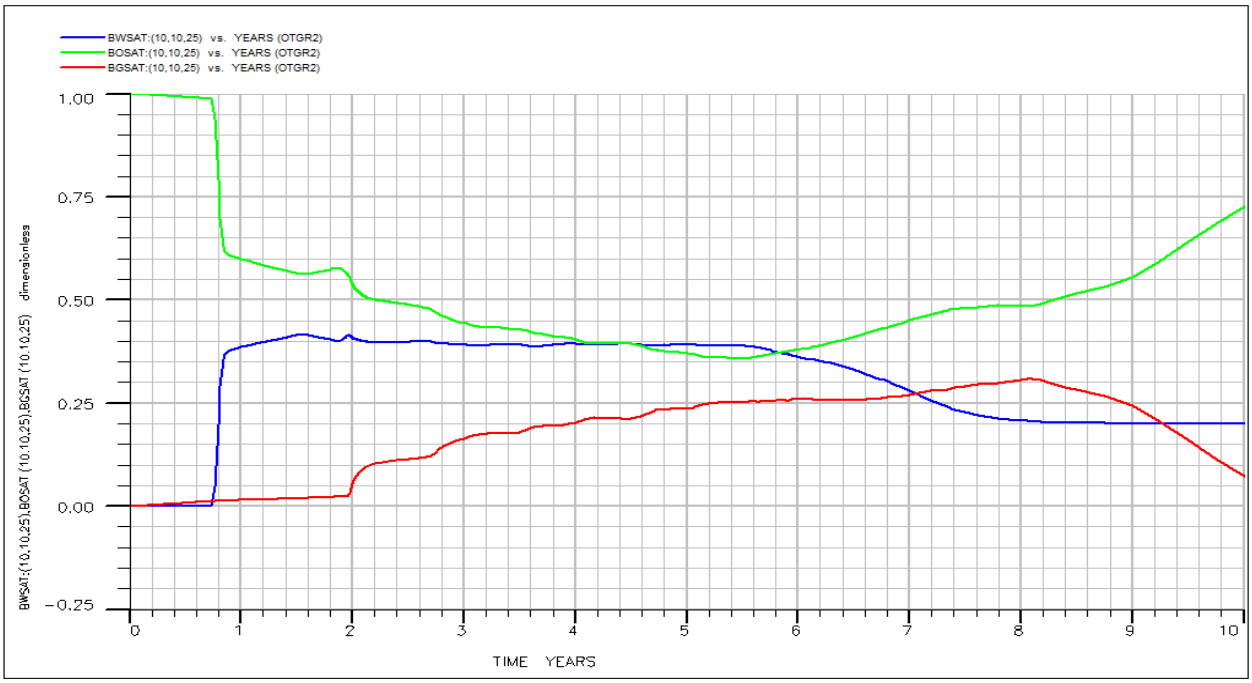

Figure A (iv): OTGR2 fluid saturation plots of the mid-oil-well-trajectory cell.

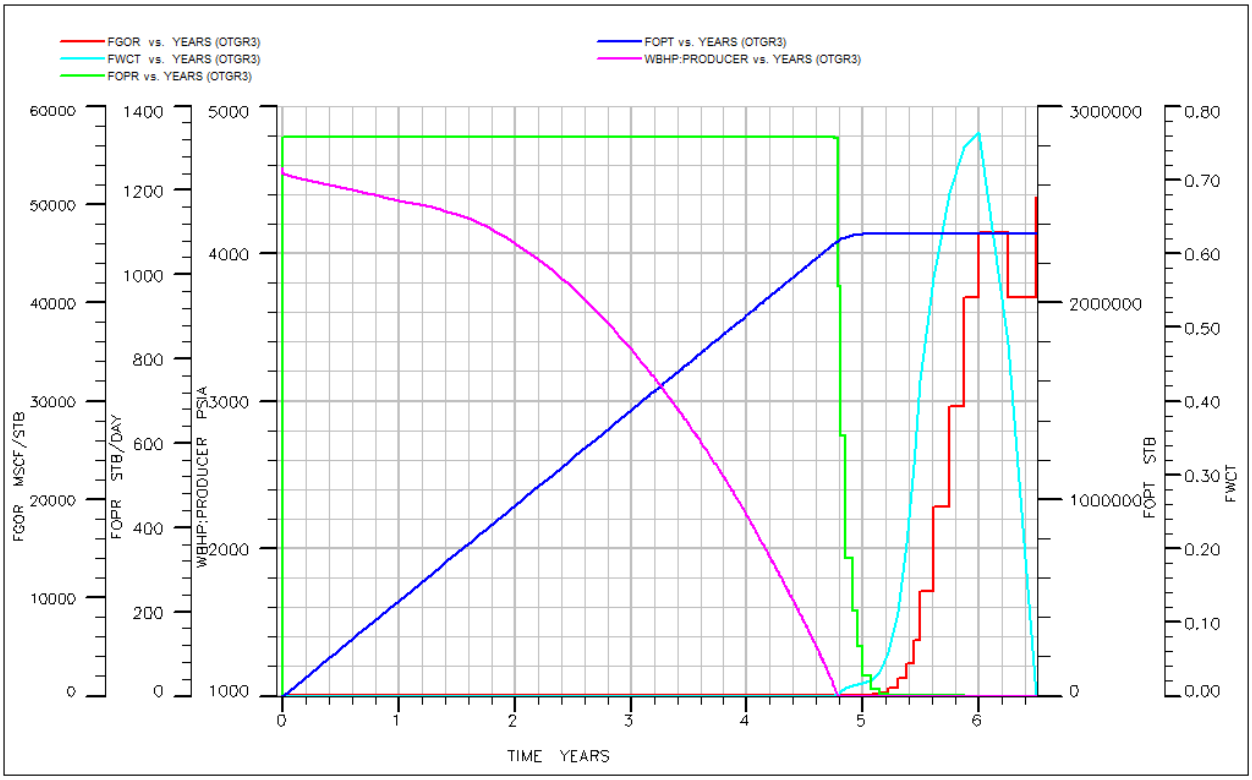

Figure A (v): OTGR3 production forecast plots

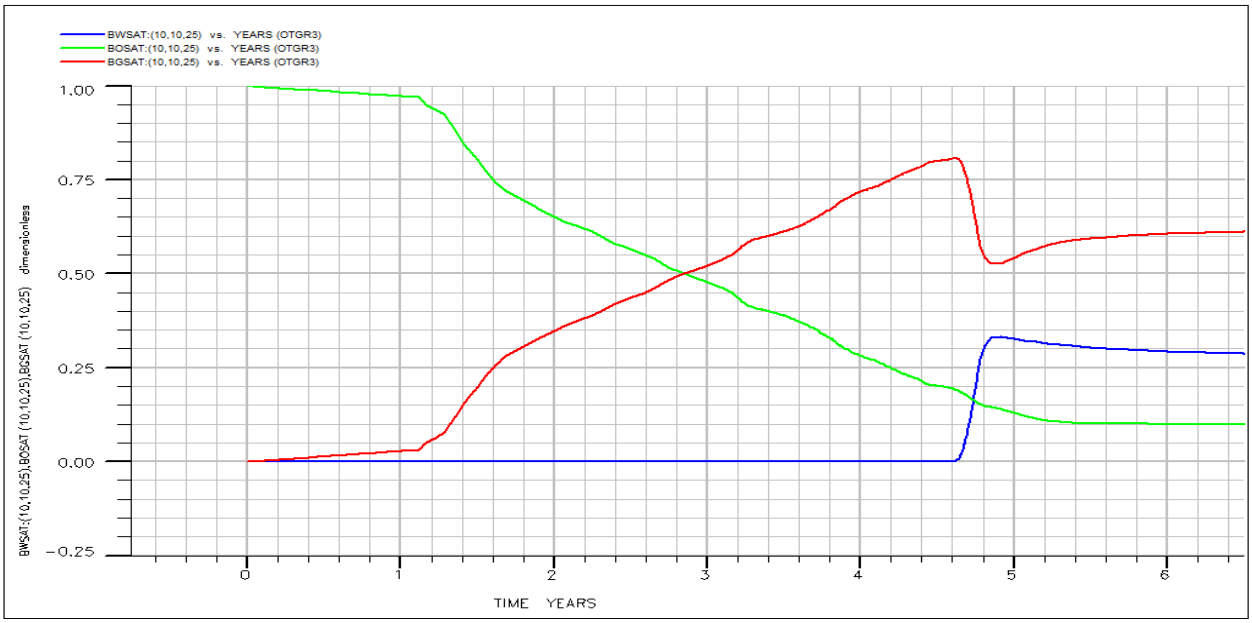

Figure A (vi): OTGR3 fluid saturation plots of the mid-oil-well-trajectory cell.

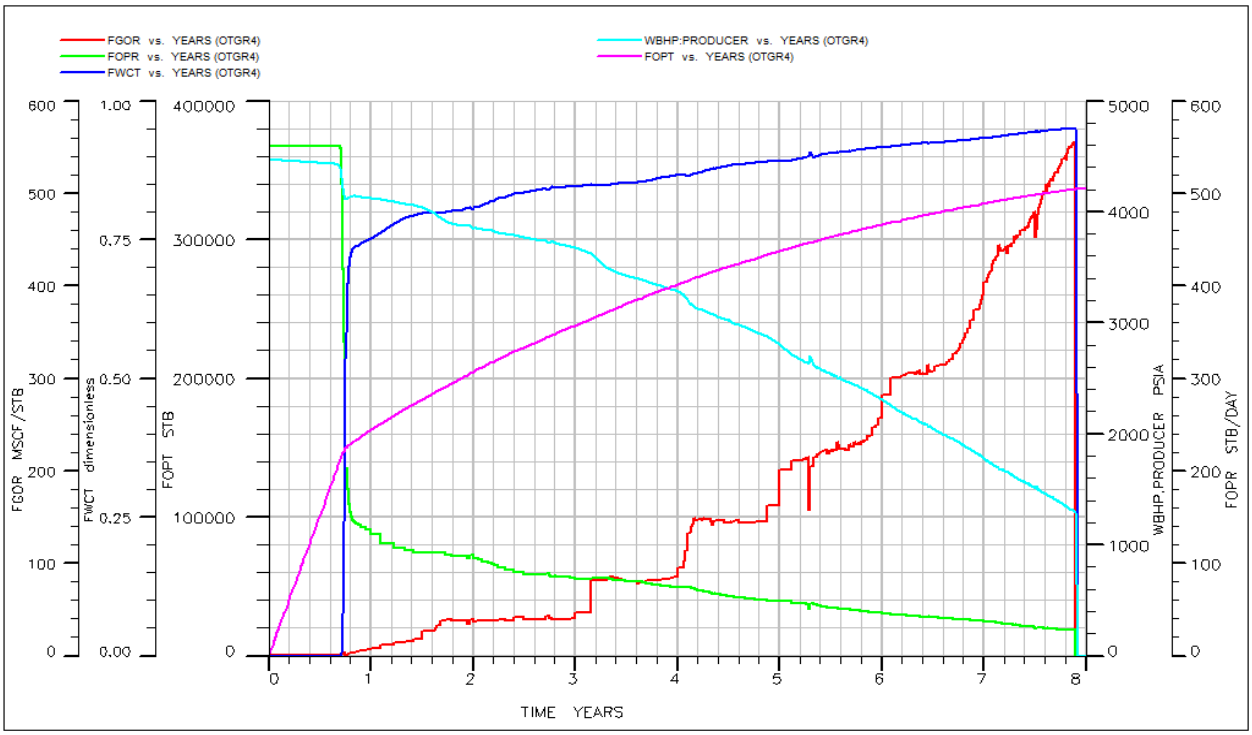

Figure A (vii): OTGR4 production forecast plots

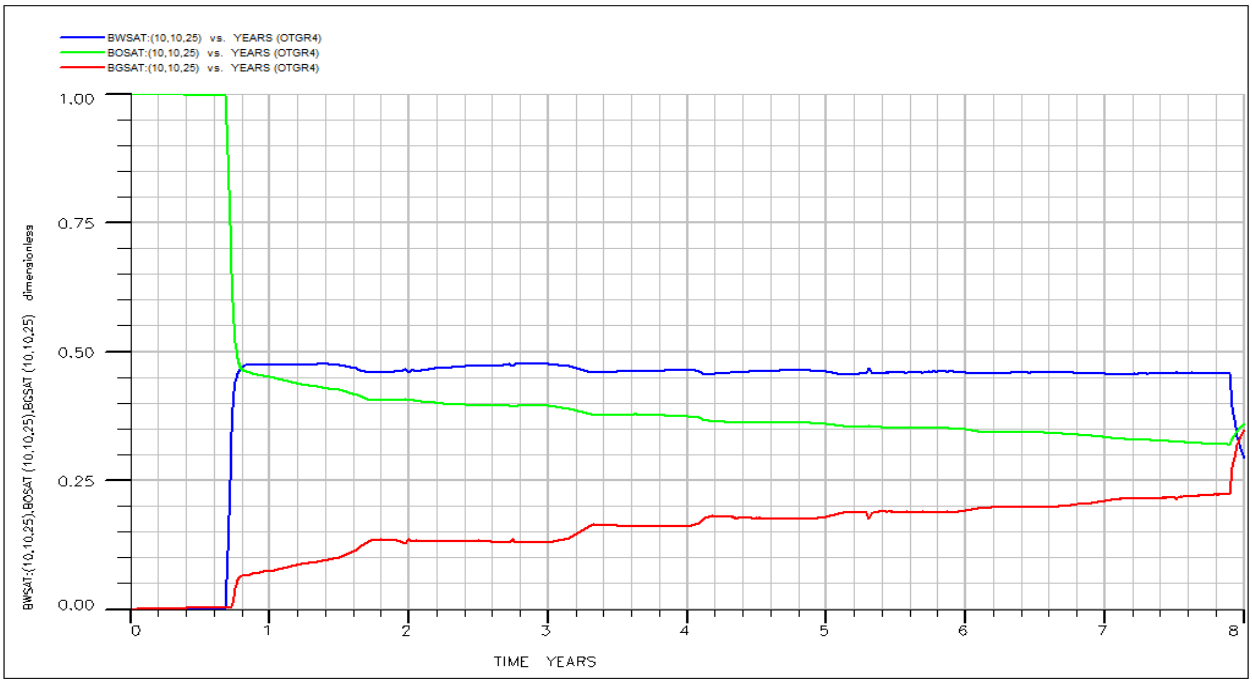

Figure A (viii): OTGR4 fluid saturation plots of the mid-oil-well-trajectory cell.

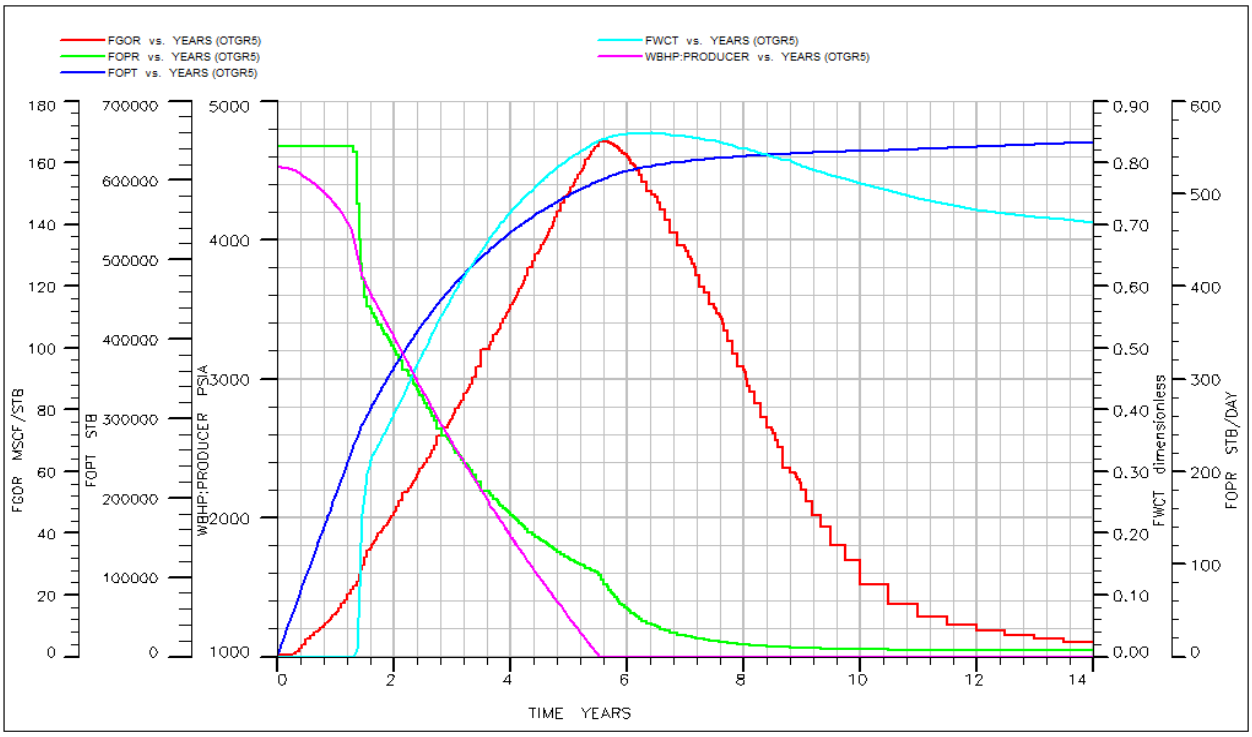

Figure A (ix): OTGR5 production forecast plots

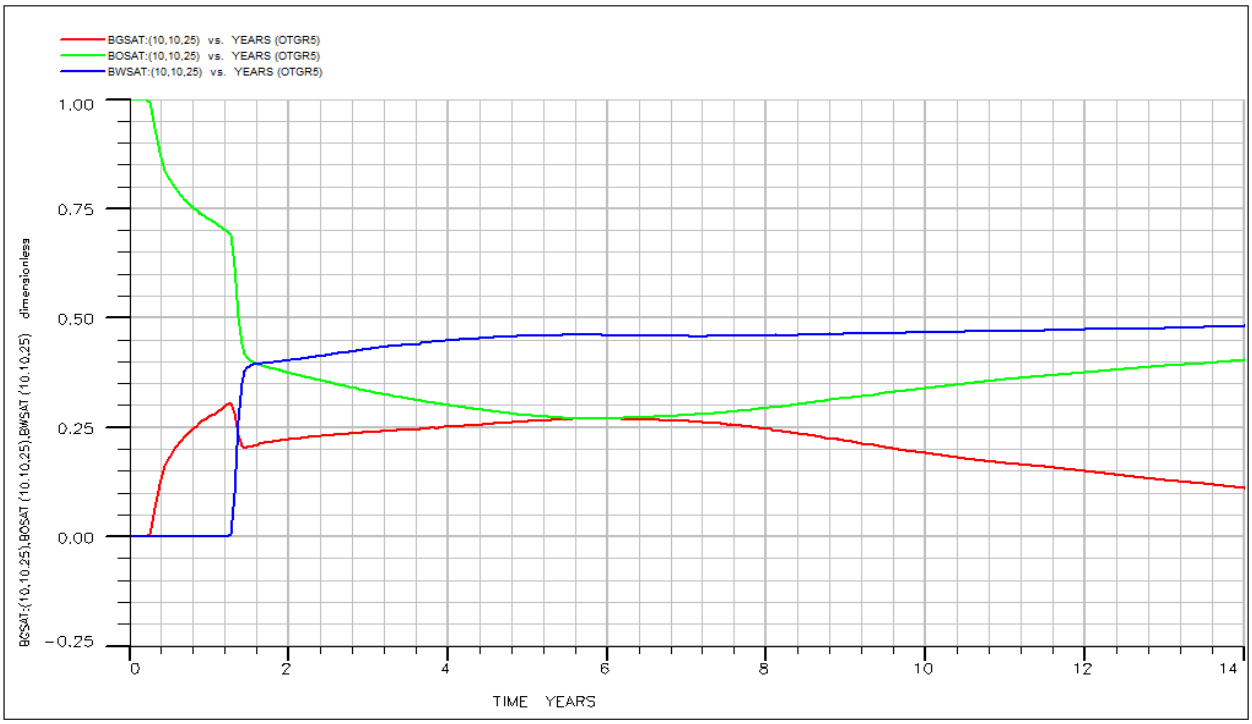

Figure A(x): OTGR5 fluid saturation plots of the mid-oil-well-trajectory cell.

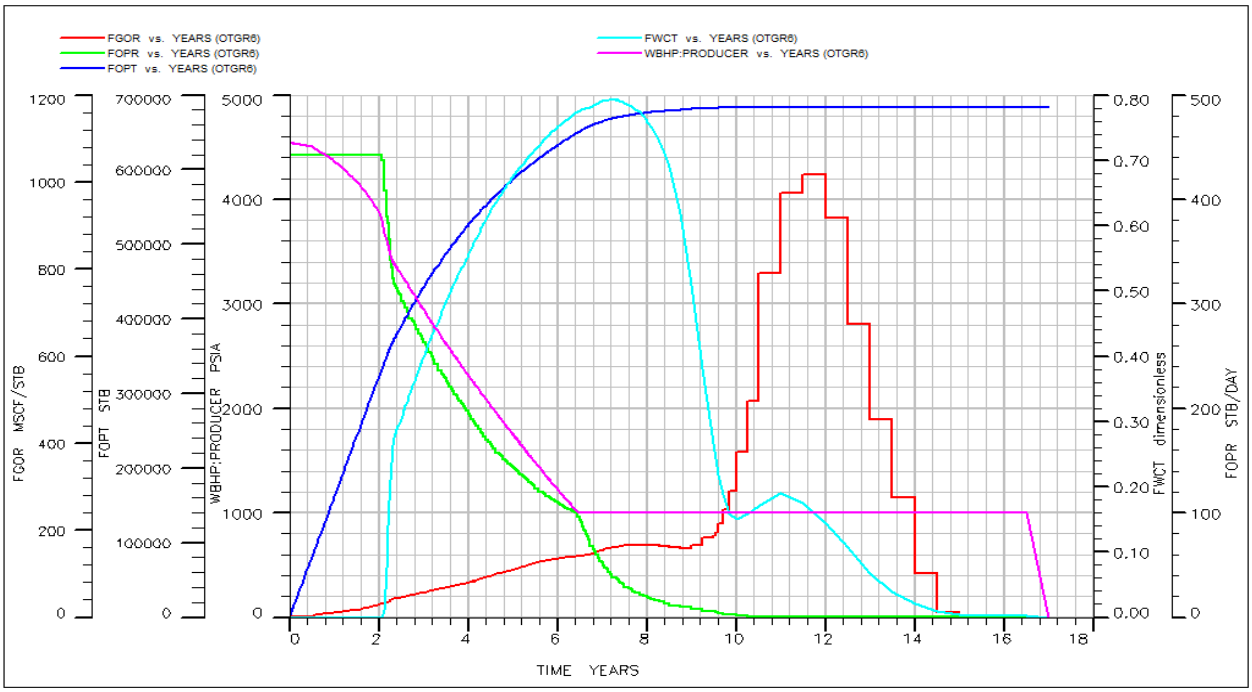

Figure A (xi): OTGR6 production forecast plots

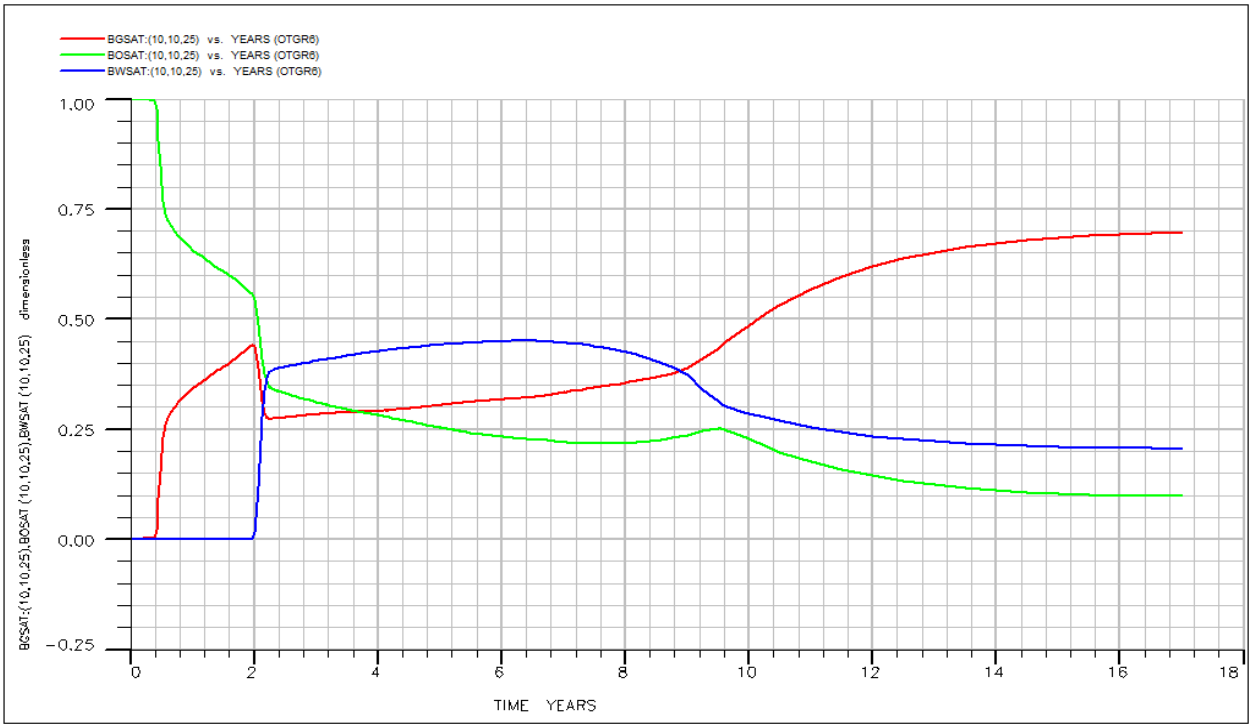

Figure A (xii): OTGR6 fluid saturation plots of the mid-oil-well-trajectory cell.

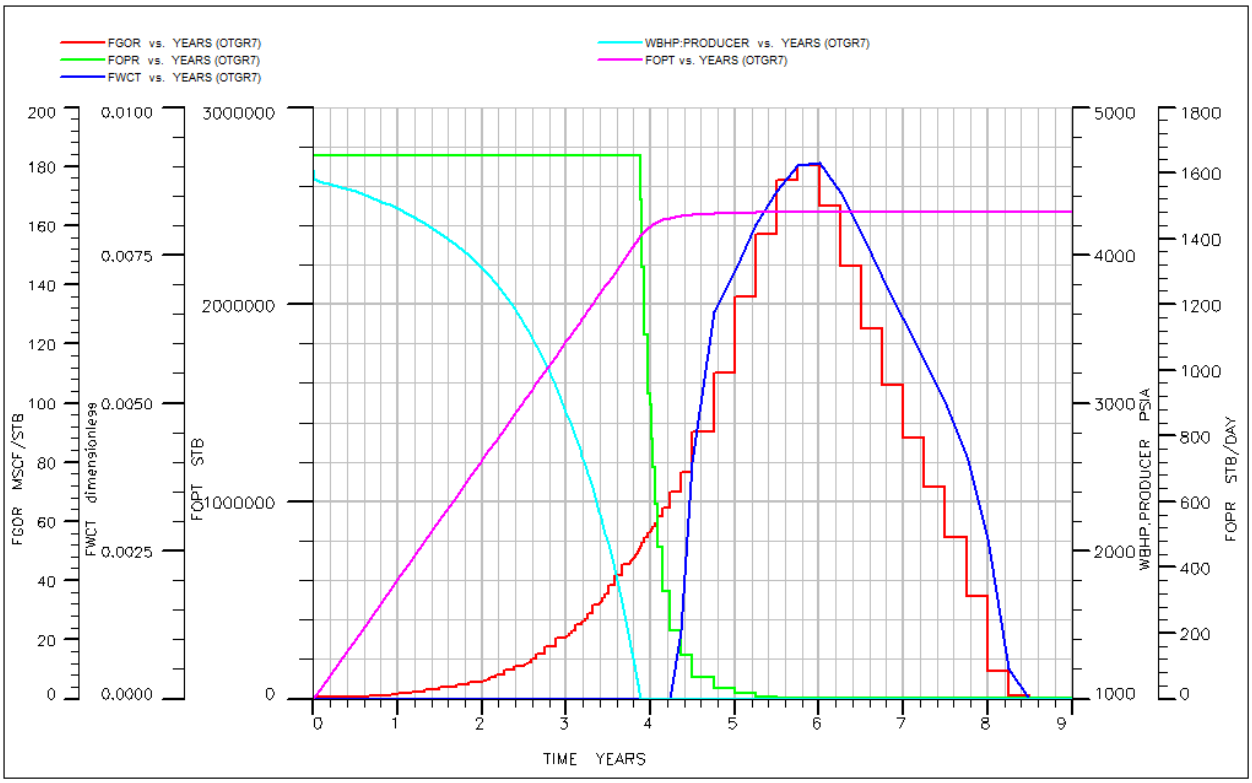

Figure A (xiii): OTGR7 production forecast plots

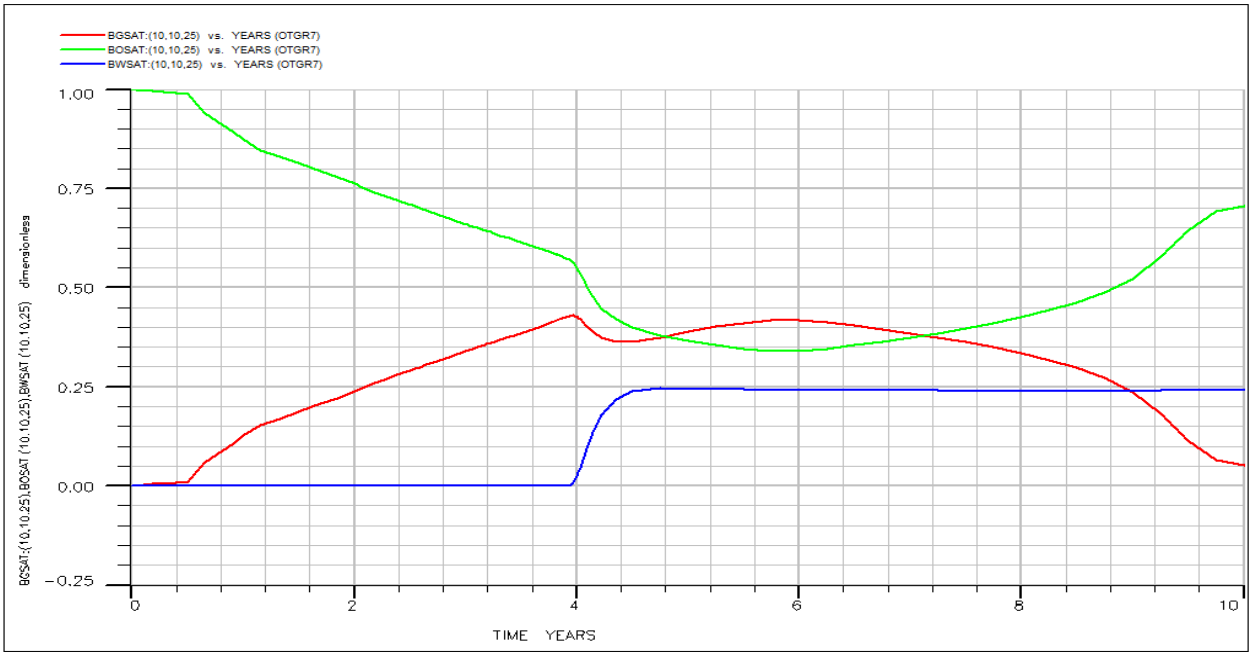

Figure A (xiv): OTGR7 fluid saturation plots of the mid-oil-well-trajectory cell.

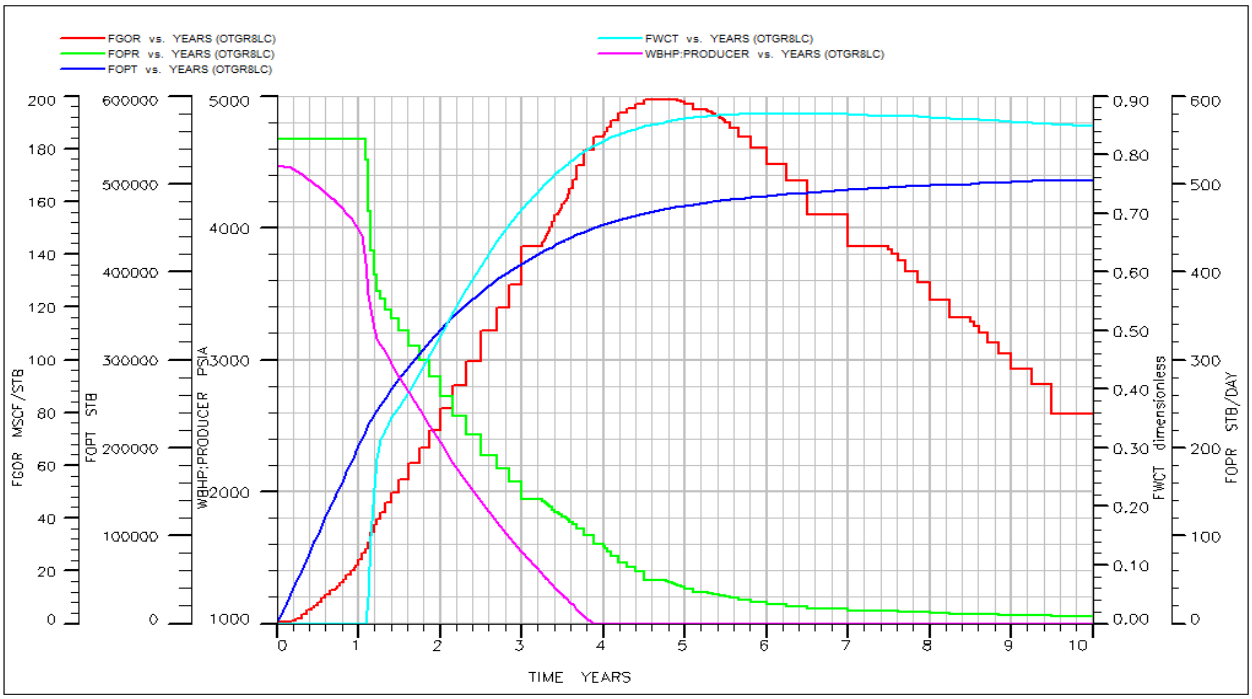

Figure A (xv): OTGR8 production forecast plots

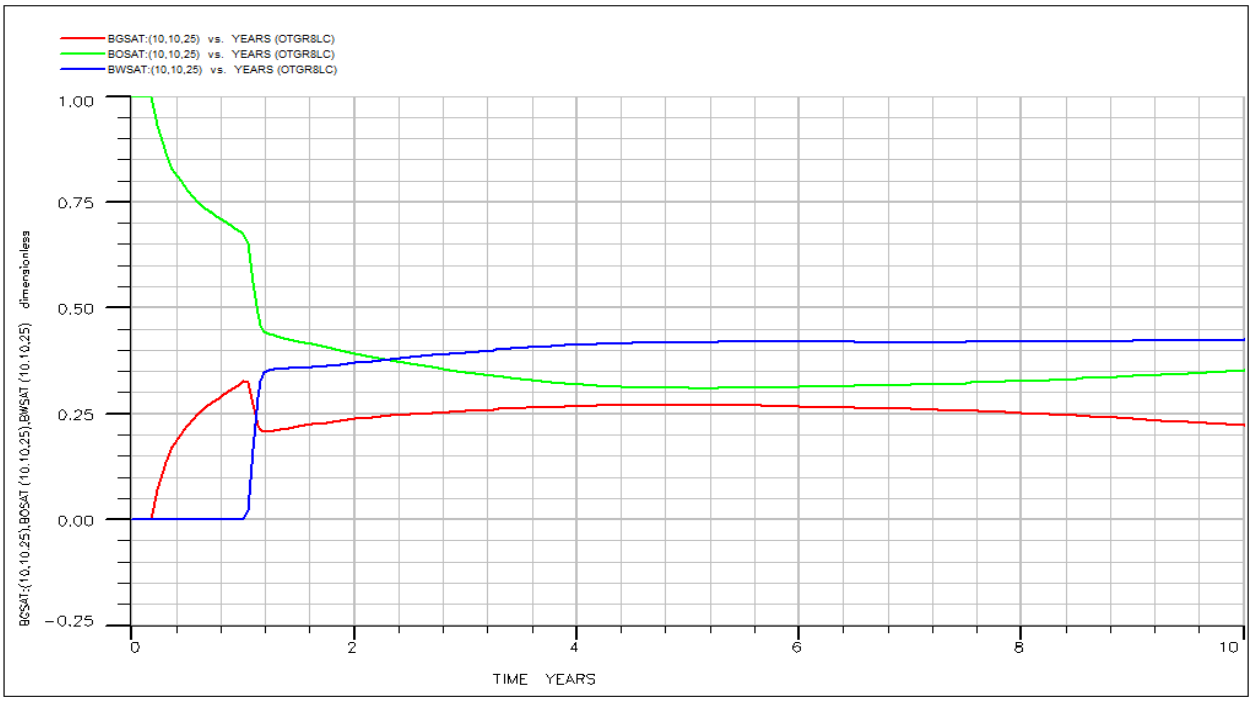

Figure A (xvi): OTGR8 fluid saturation plots of the mid-oil-well-trajectory cell.

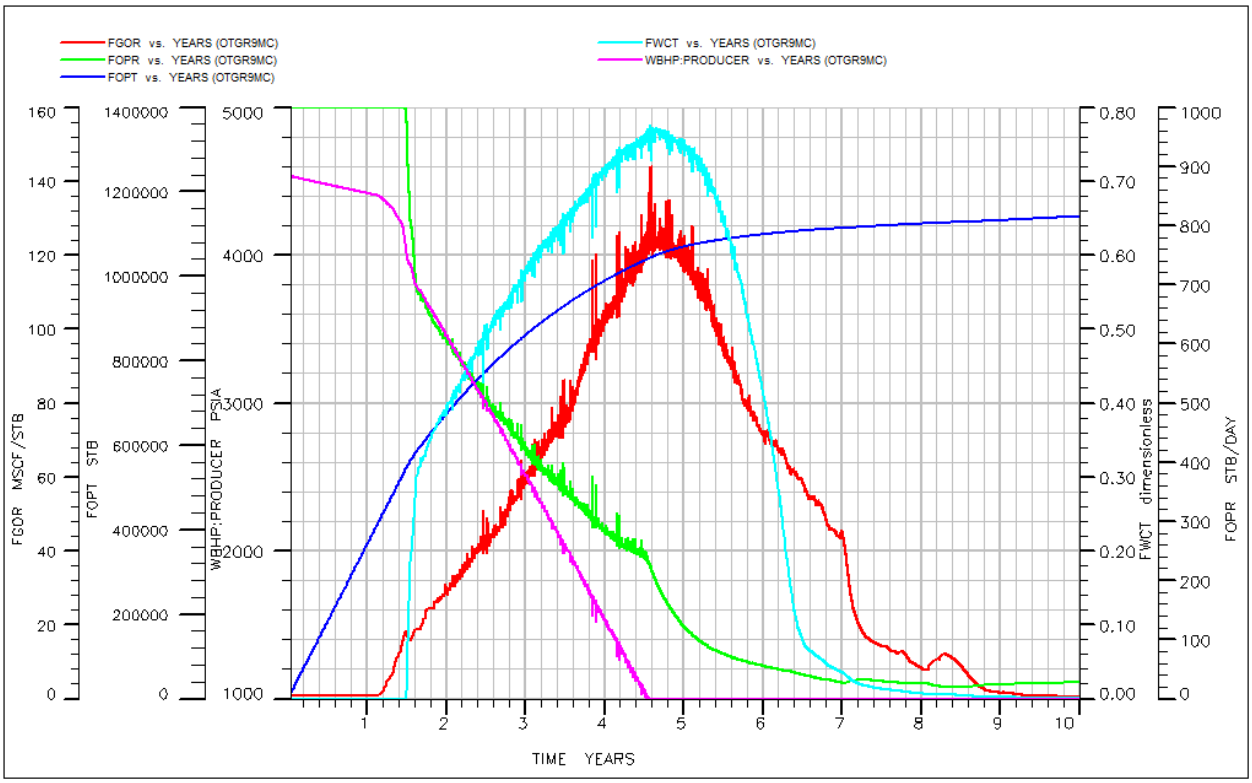

Figure A (xvii): OTGR9 production forecast plots

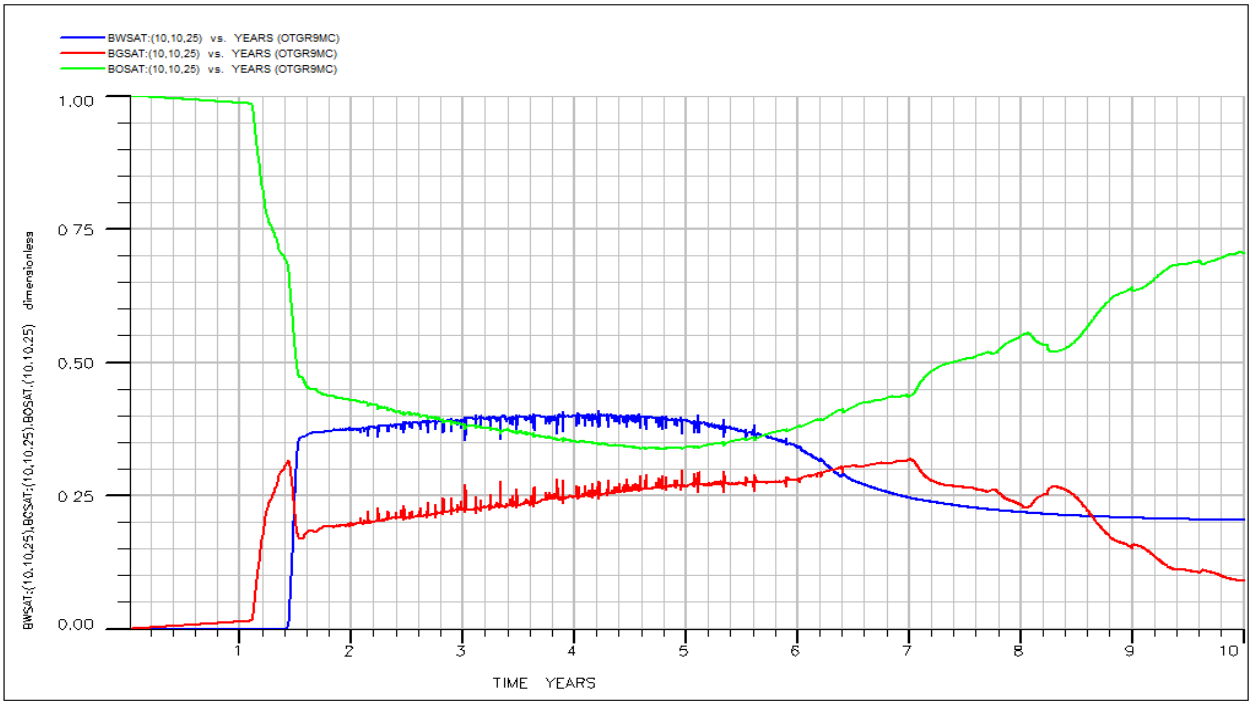

Figure A (xviii): OTGR9 fluid saturation plots of the mid-oil-well-trajectory cell.

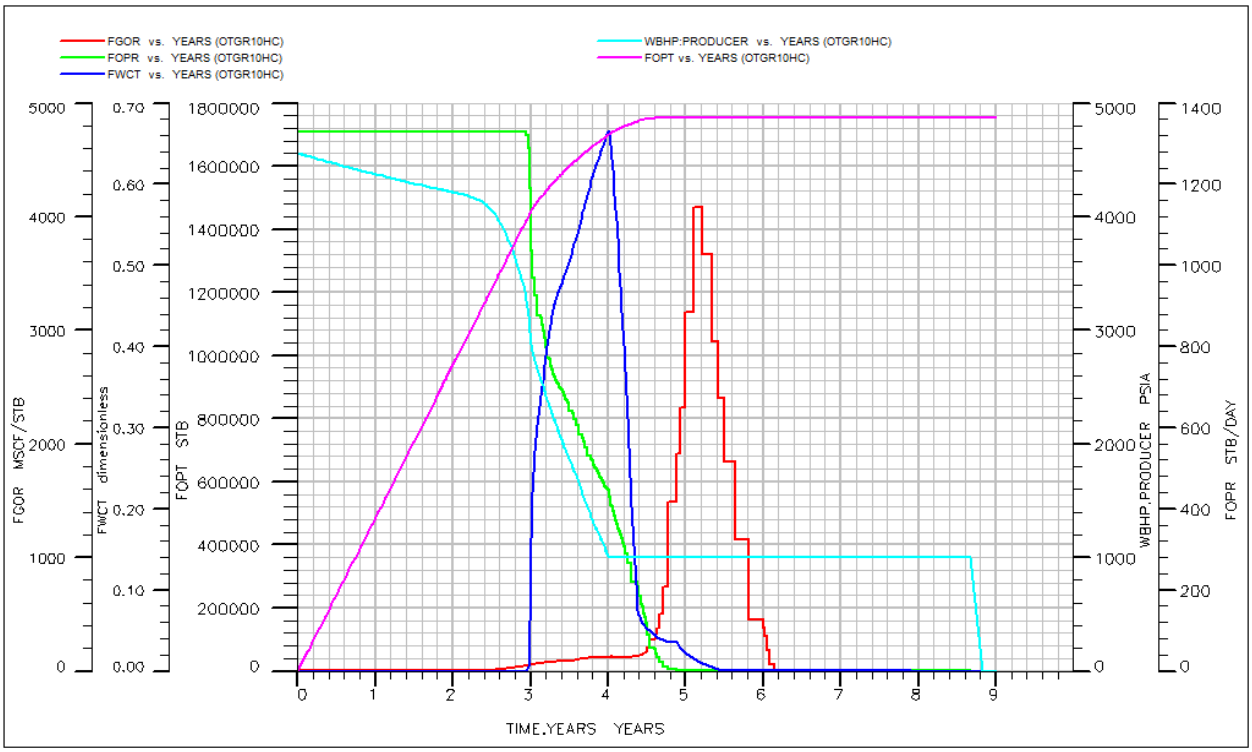

Figure A (xix): OTGR10 production forecast plots

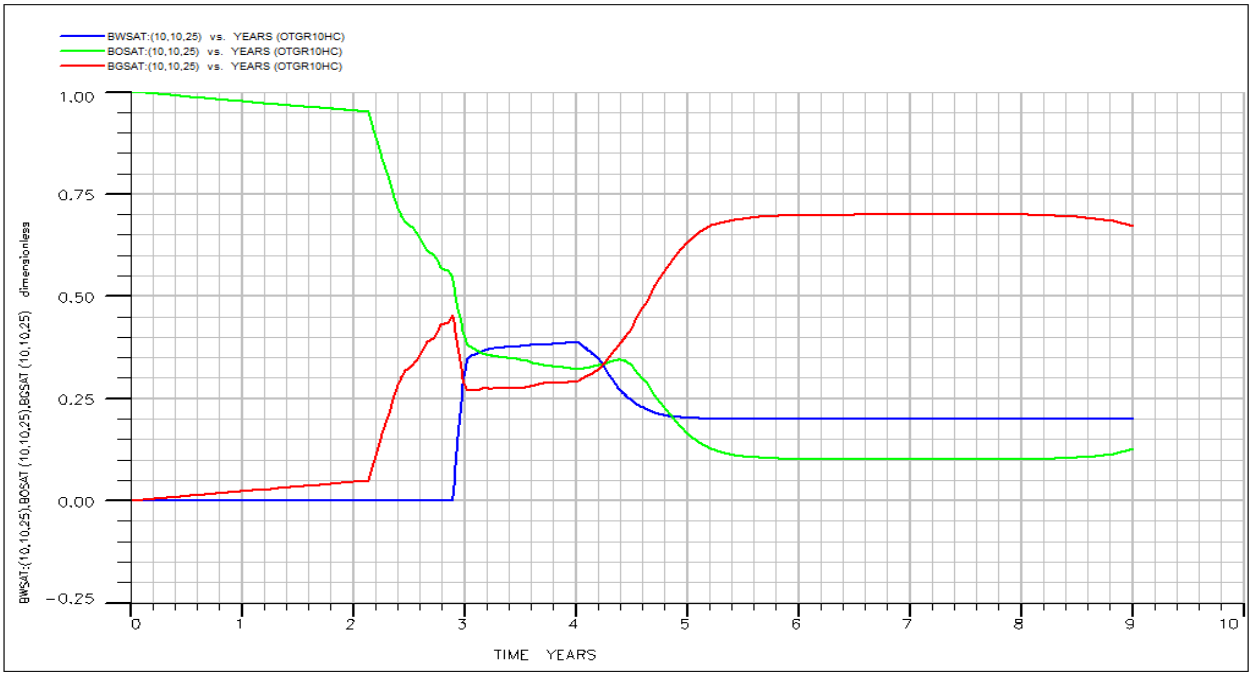

Figure A (xx): OTGR10 fluid saturation plots of the mid-oil-well-trajectory cell.

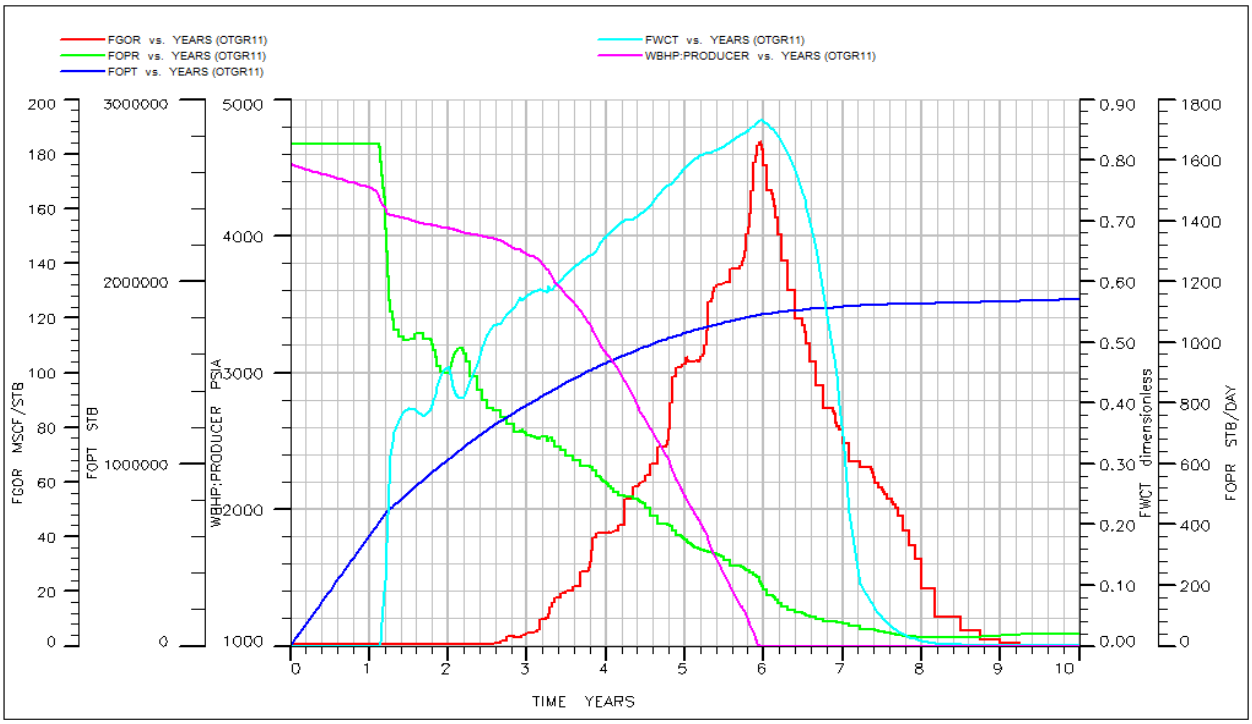

Figure A (xxi): OTGR11 production forecast plots

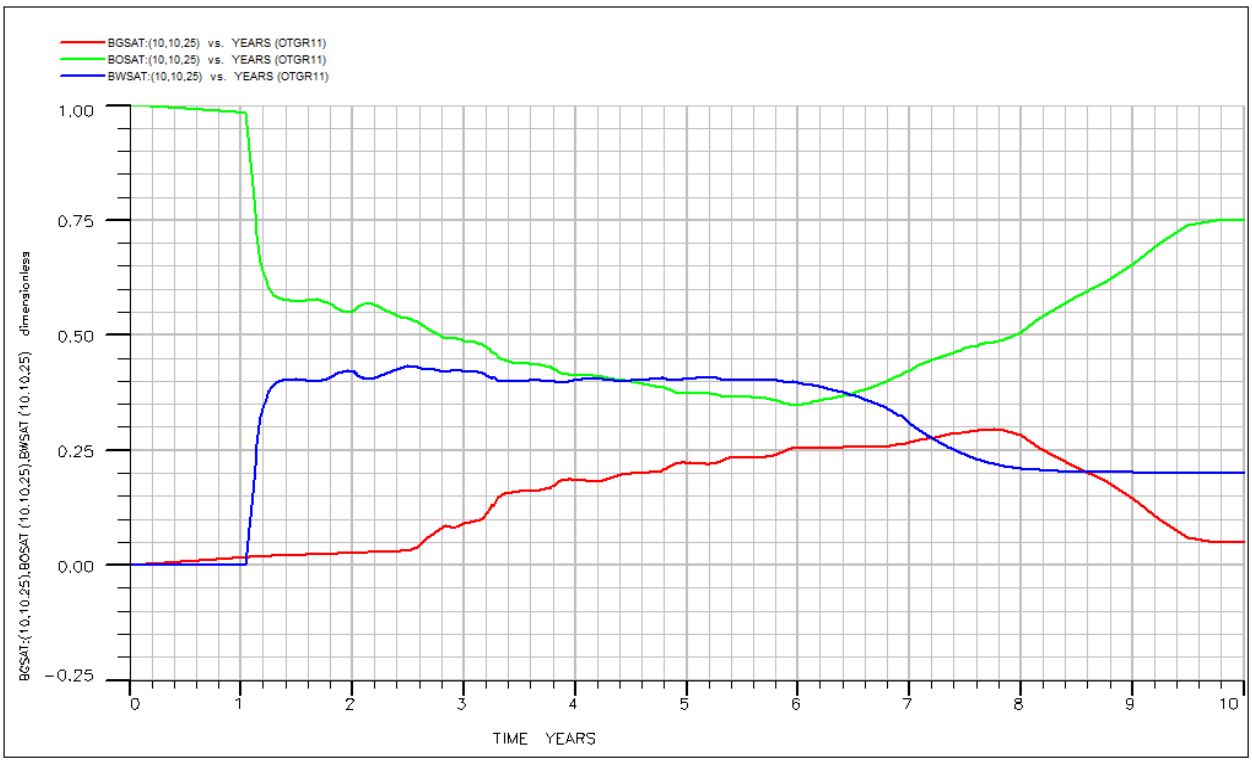

Figure A (xxii): OTGR11 fluid saturation plots of the mid-oil-well-trajectory cell.

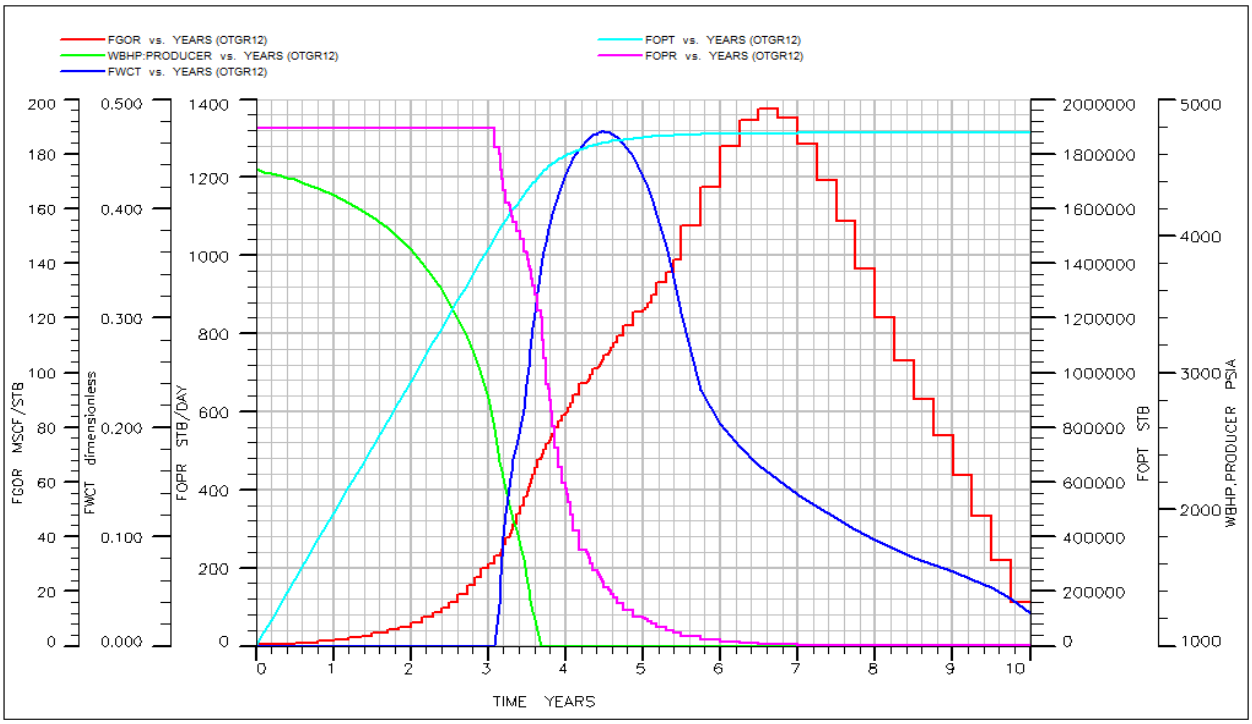

Figure A (xxiii): OTGR12 production forecast plots

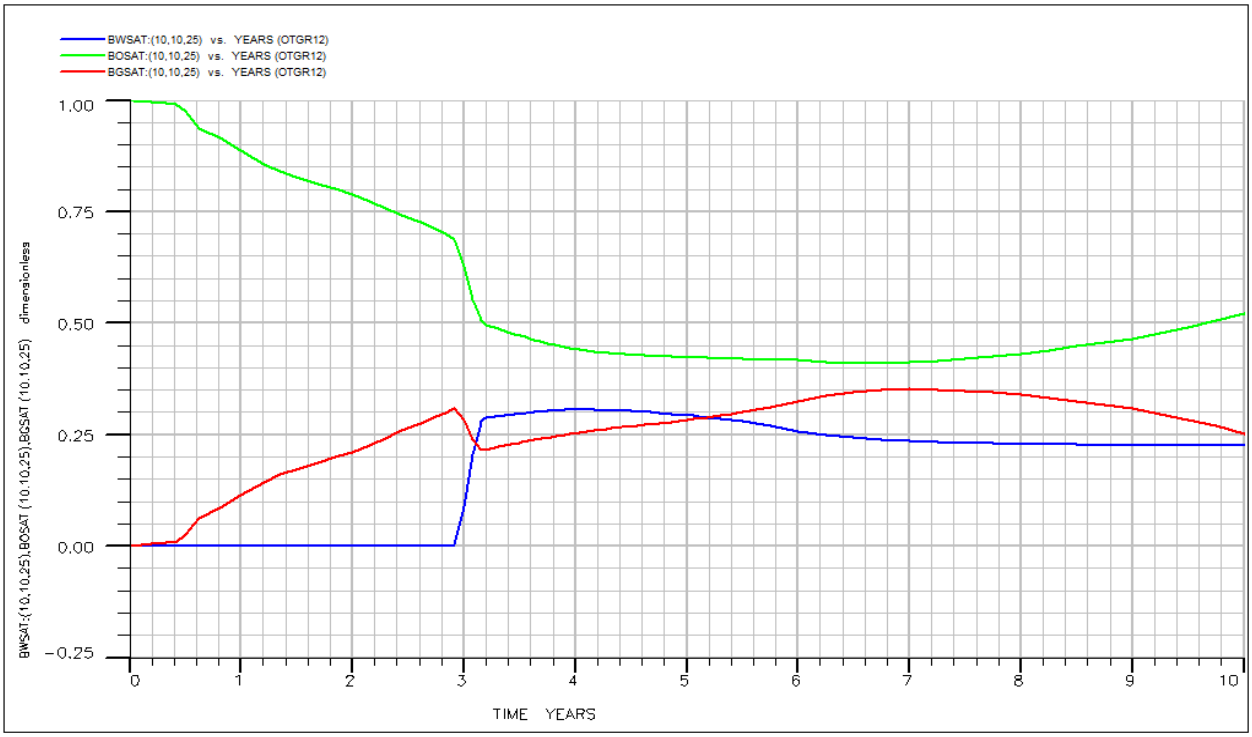

Figure A (xxiv): OTGR12 fluid saturation plots of the mid-oil-well-trajectory cell.

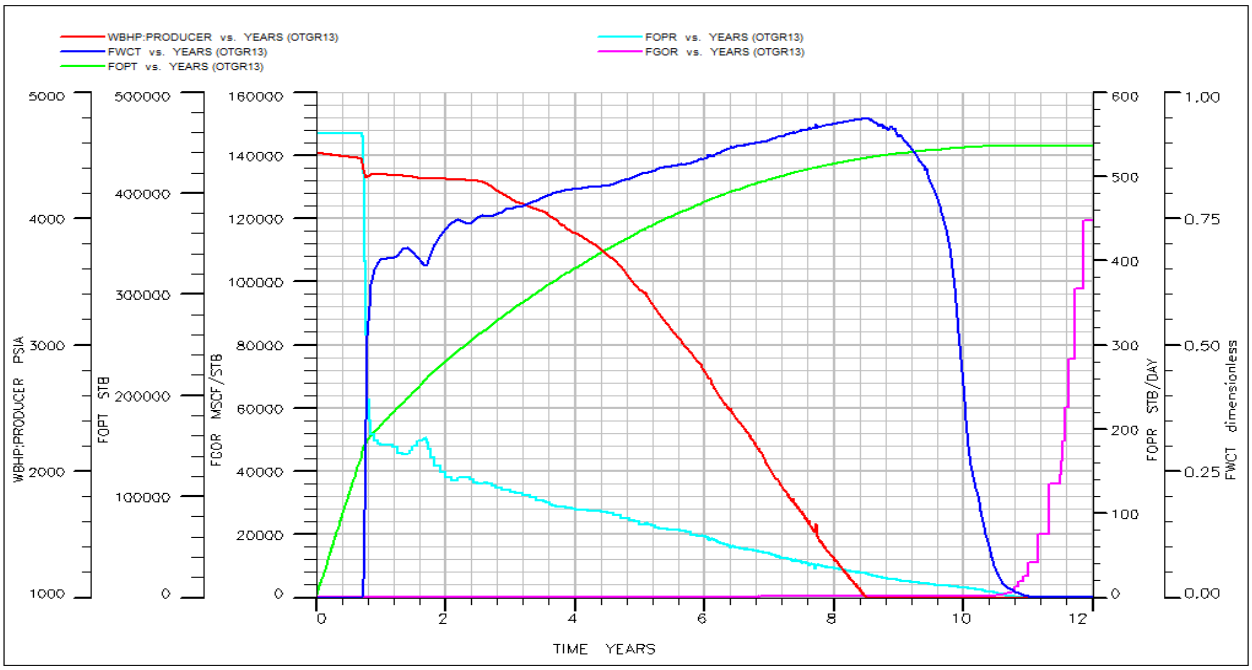

Figure A (xxv): OTGR13 production forecast plots

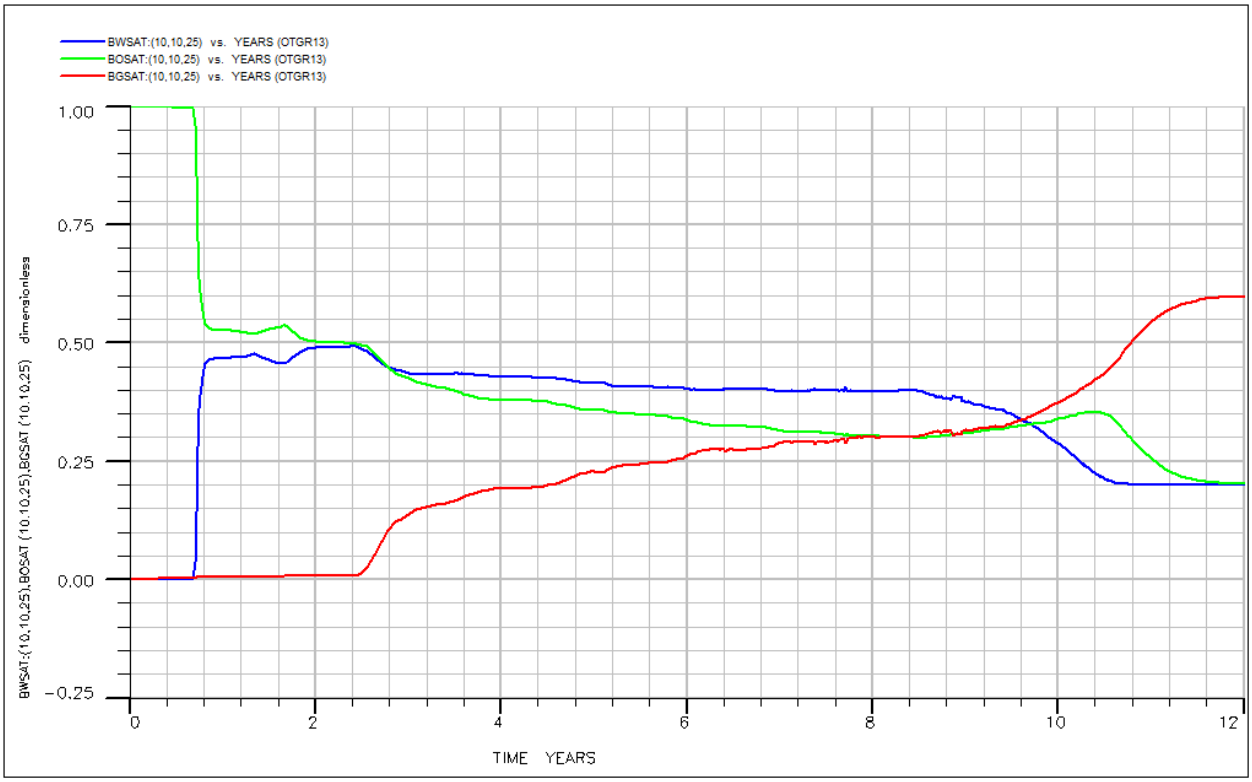

Figure A (xxvi): OTGR13 fluid saturation plots of the mid-oil-well-trajectory cell.

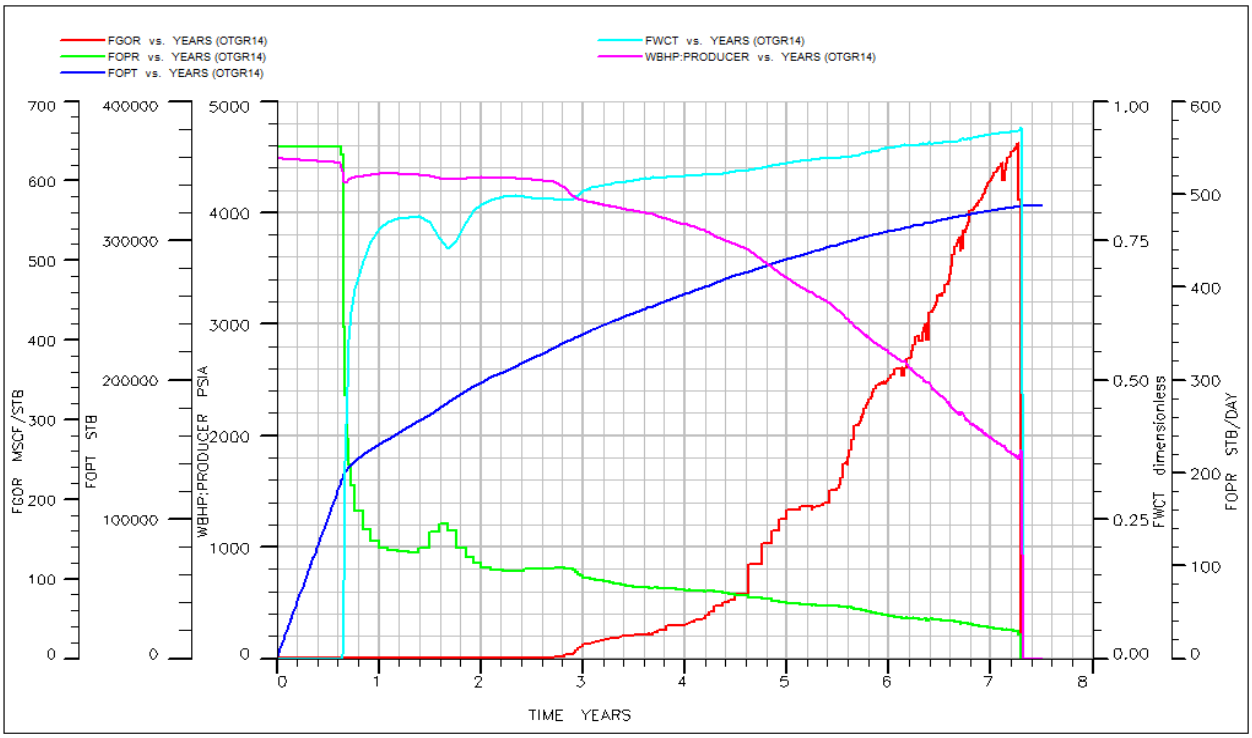

Figure A (xxvii): OTGR14 production forecast plots

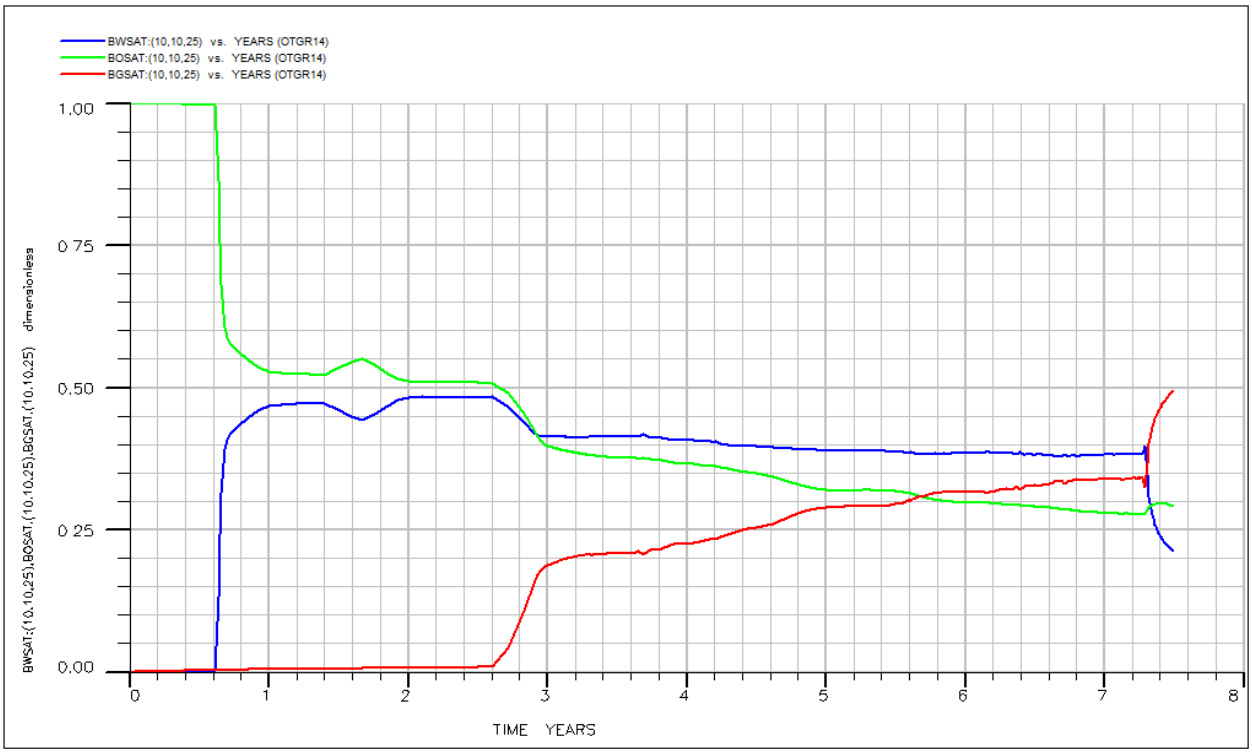

Figure A (xxviii): OTGR14 fluid saturation plots of the mid-oil-well-trajectory cell.

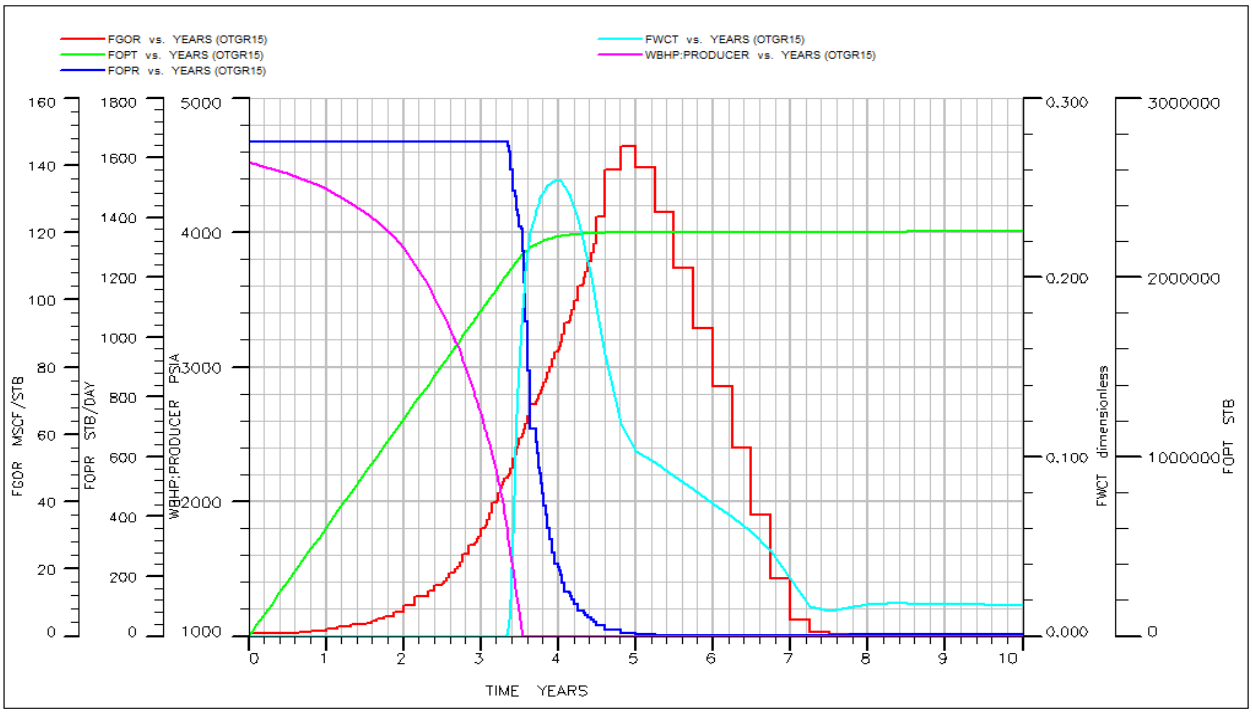

Figure A (xxix): OTGR15 production forecast plots

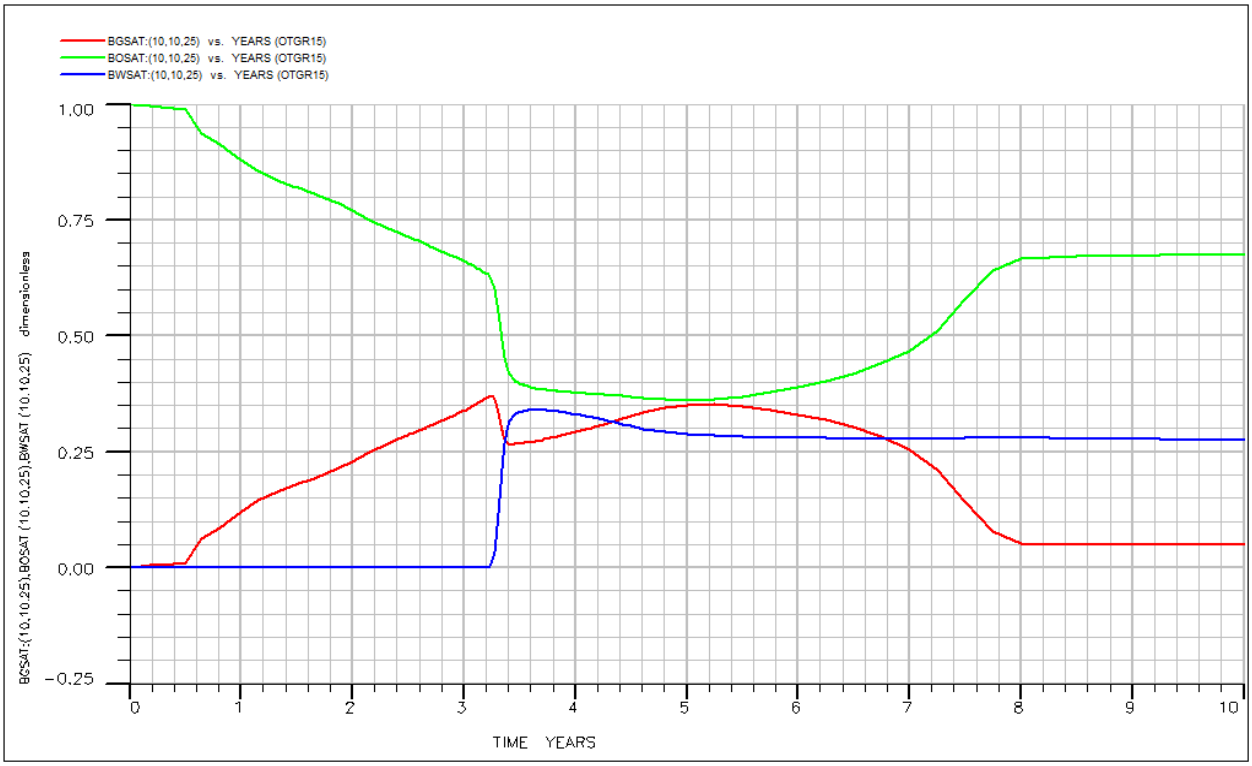

Figure A (xxx): OTGR15 fluid saturation plots of the mid-oil-well-trajectory cell.

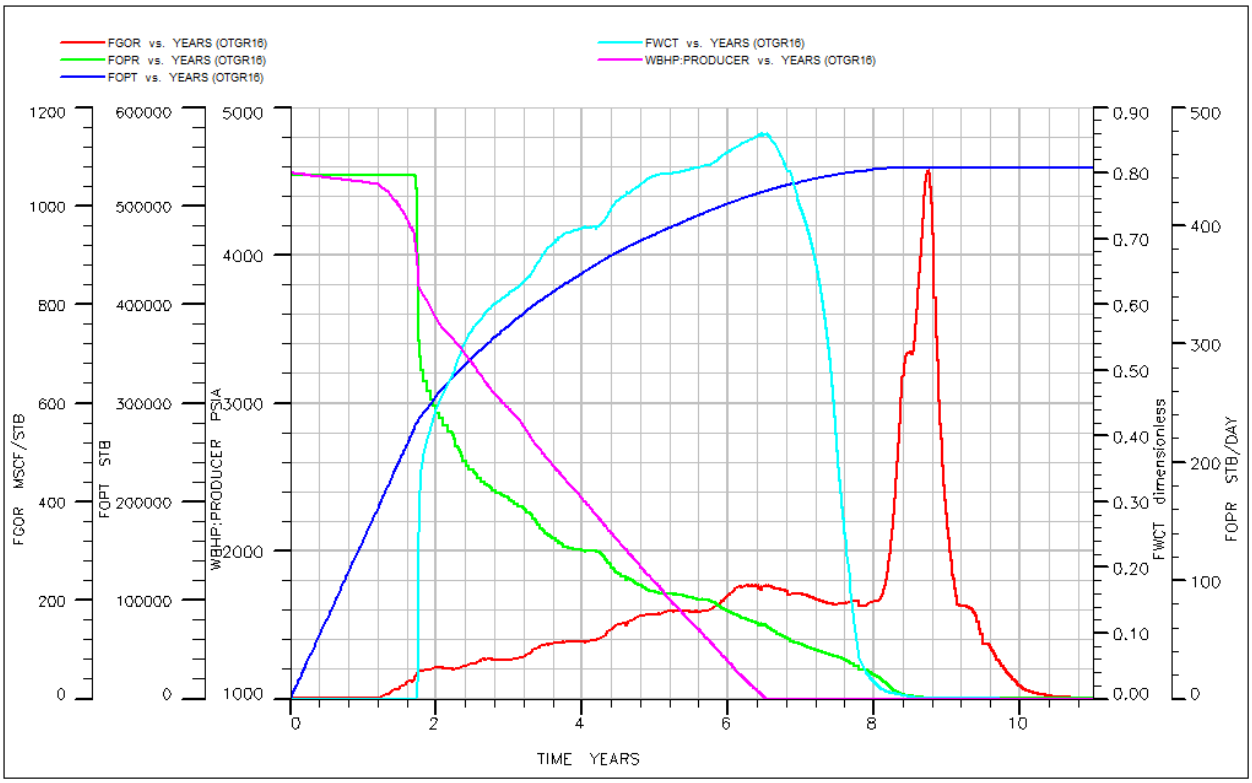

Figure A (xxxi): OTGR16 production forecast plots

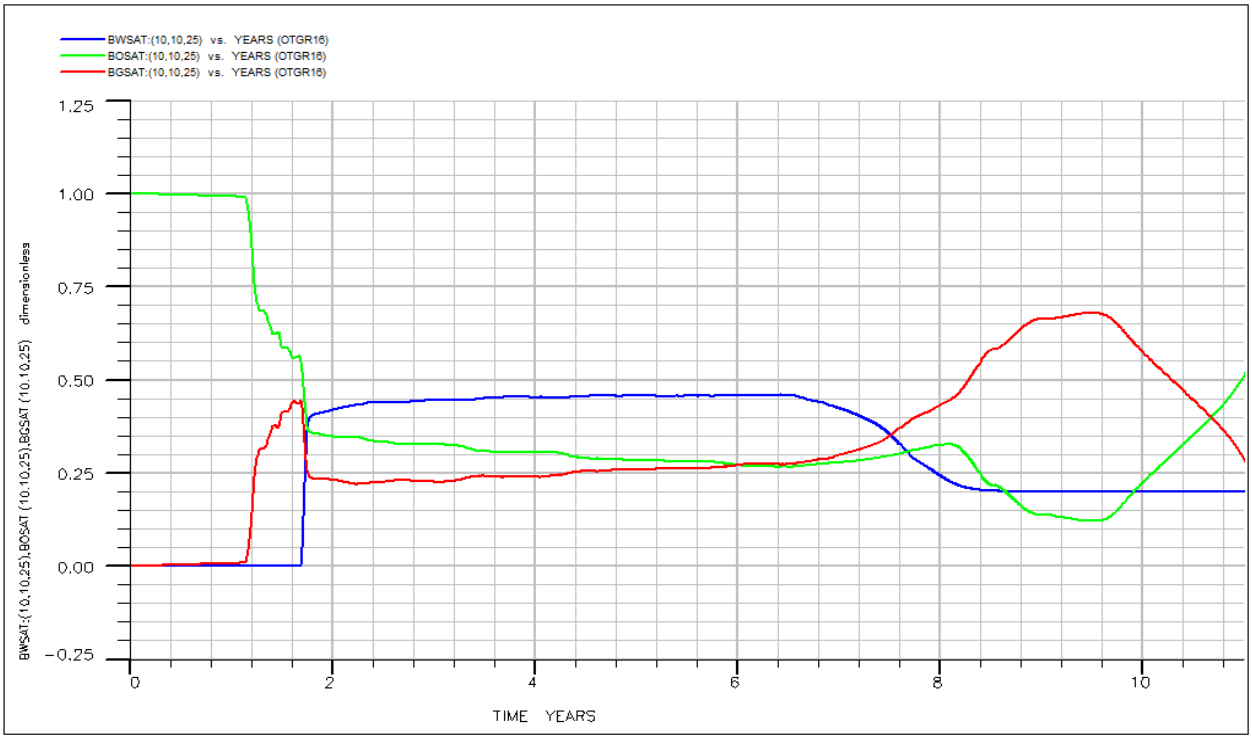

Figure A (xxxii): OTGR16 fluid saturation plots of the mid-oil-well-trajectory cell.

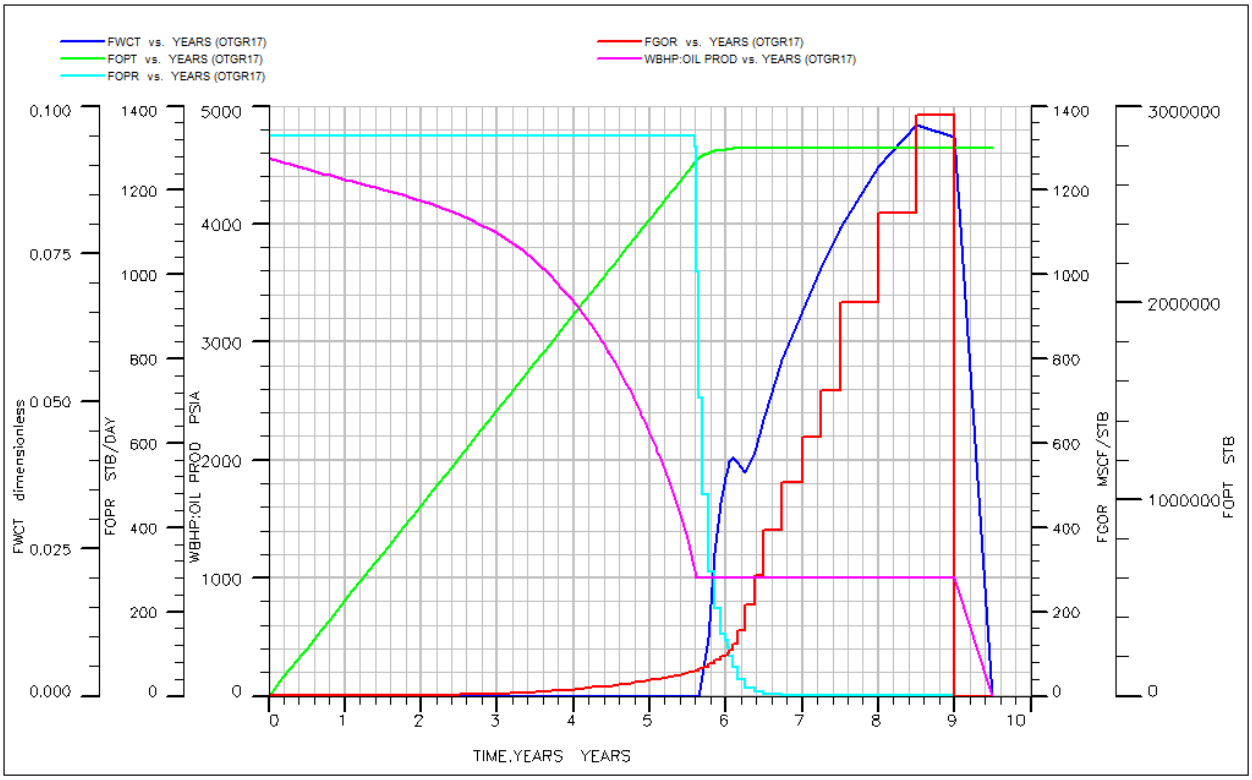

Figure A (xxxiii): OTGR17 production forecast plots

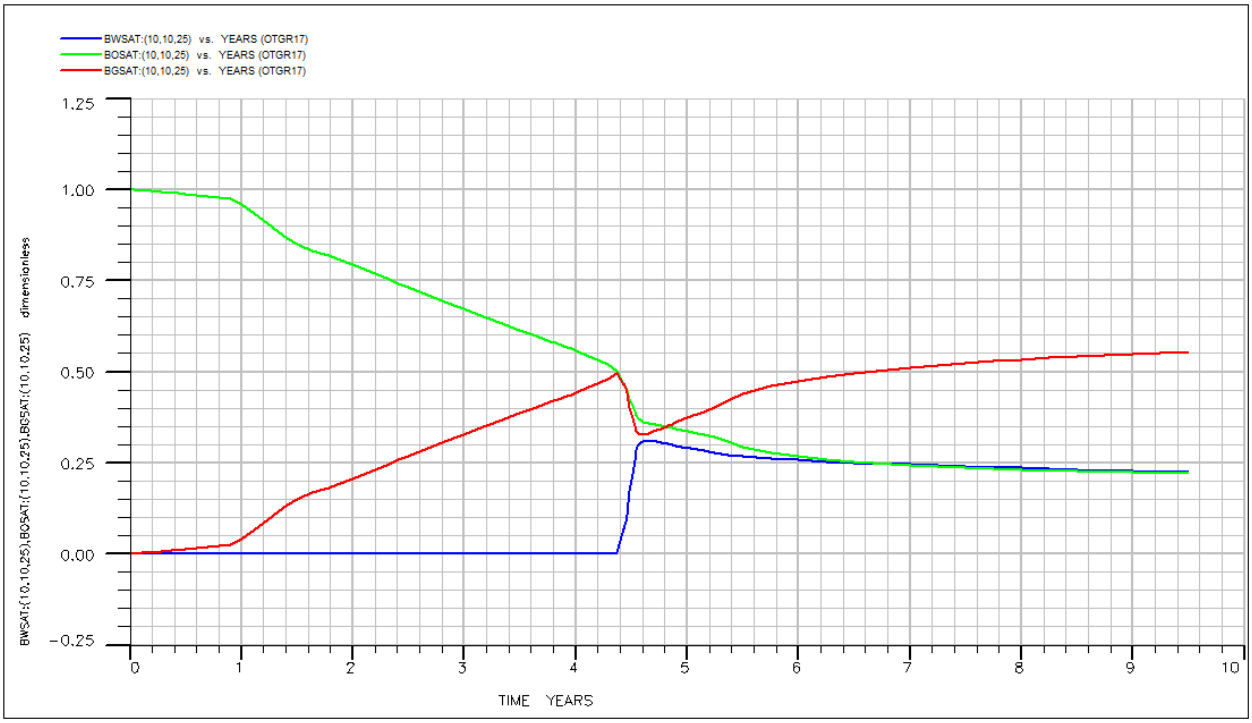

Figure A (xxxiv): OTGR17 fluid saturation plots of the mid-oil-well-trajectory cell.

APPENDIX AII

ADDITIONAL PARAMETERS OF THE DESIGN ANALYSIS OF THE OIL-THEN-GAS CASE.

Surrogate Equation in Terms of Actual Factors

Substituting Equations 4.1a, 4.1b, 4.1c, 4.1d and 4.1e into Equation 4.1 gives the surrogate equation in terms of the actual factor as:

$$\text{Oil } R_f = -8.2370 + 0.5768(API) - 6.3007\left(\frac{k_V}{k_h}\right) + 9.9658\,k_{ro} + 0.0032\,Q_l - 0.6036\left[(API)\left(\frac{k_V}{k_h}\right)\right] \quad \text{A1}$$

Model Diagnostic Plots

1. **Normal Plot of Residuals**

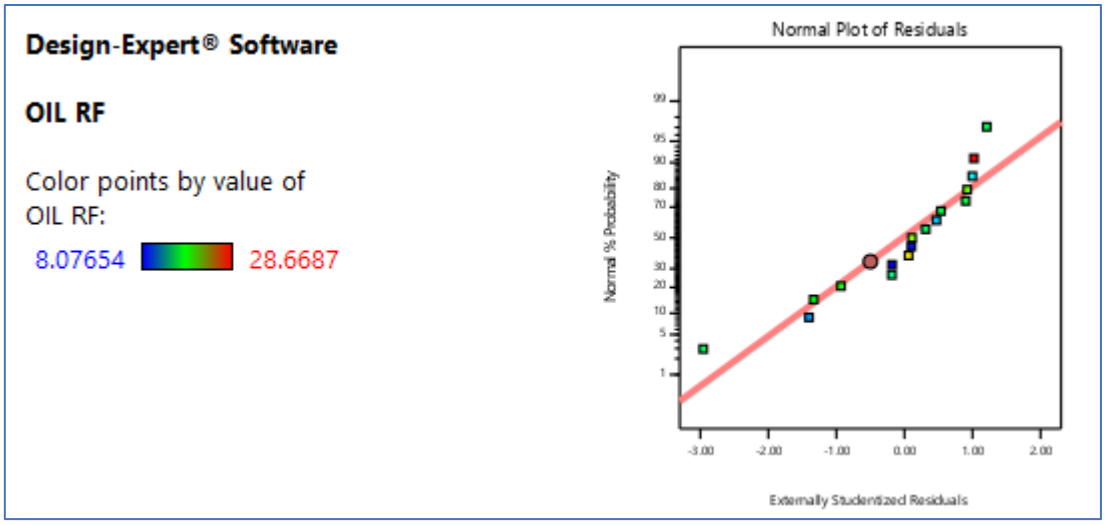

Figure A (xxxv): Normal Plot of Residuals for the OTG Design Analysis

The normality plot of residuals is used to confirm the normality assumption. Most parametric tests require that the **assumption** of **normality** be met. **Normality** means that the data is normally distributed (or bell-shaped), i.e. it has a 0 mean, with one standard deviation and a symmetric bell-shaped curve. For a perfectly normal distribution, residuals

follow a straight line. In real-life cases and most experiments, some scatter or the definite "S," like the one shown in Figure (Axxxv), patterns are expected (Shari K. 2013).

2. The Box-Cox Plot

The Box-Cox plot shows whether a transformation of the data may help to improve the model (Shari K. 2013). Notice that Figure (Axxxvi) says “none” for recommended transformation.

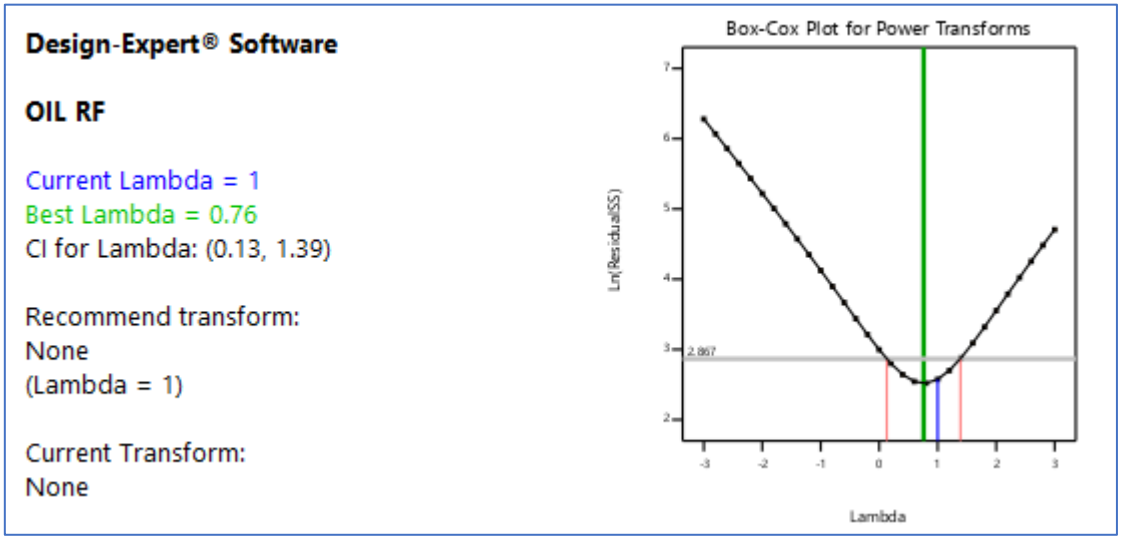

Figure (Axxxvi): Box-Cox Plot for the OTG Design Analysis

3. Predicted versus Actual Plot

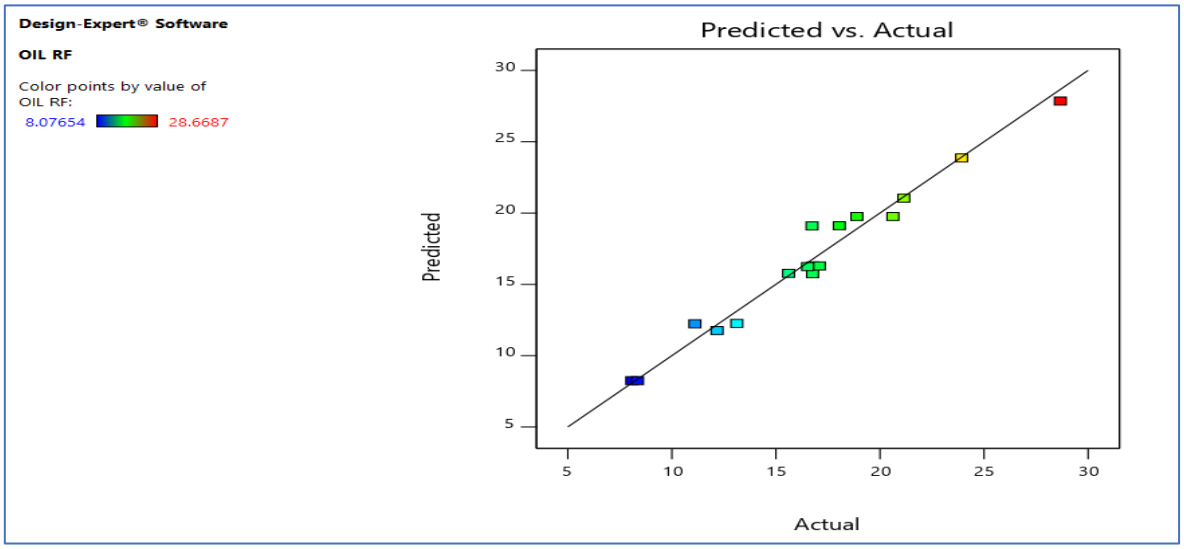

Figure A (xxxvii): Predicted versus Actual Plot of the OTG Design Analysis

The predicted vs. actual plot is used to see how the model predicts over the range of data. For a perfect case, the plot should exhibit random scatter about the 450 degrees line. Clusters of points above or below the line indicate problems of over or under predicting. Figure A (xxxvii) indicates that equation 4.1 is reliable not to under predict or over predict the design responses. Figure 4.2 further buttresses that.

APPENDIX B

PRODUCTION FORECAST PLOTS AND SATURATION PLOTS FOR THE COG PRODUCTION SCENARIO RUNS

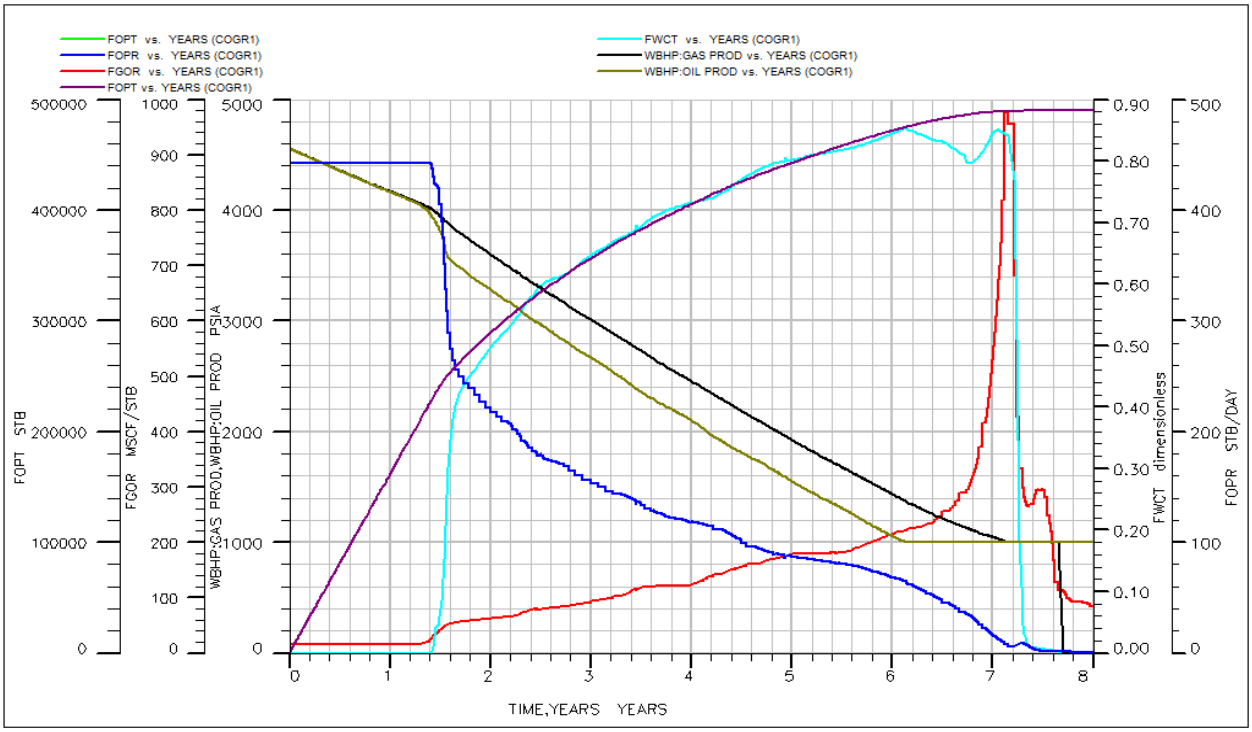

Figure B(i): COGR1 production forecast plots

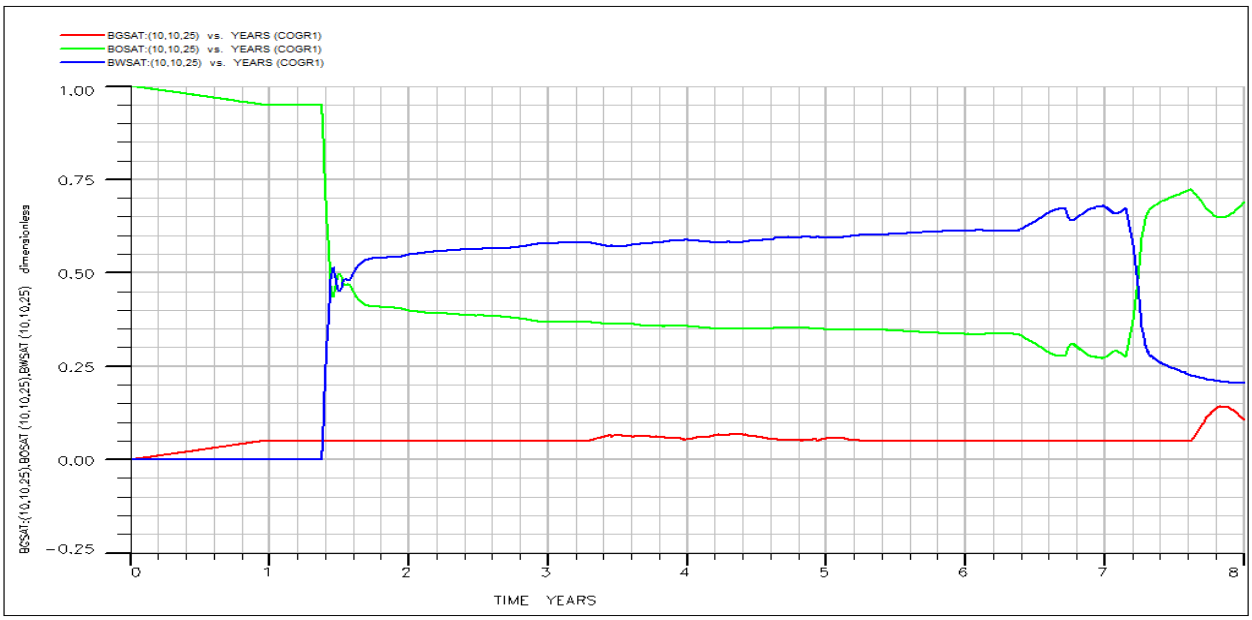

Figure B(ii): COGR1 fluid saturation plots of the mid-oil-well-trajectory cell.

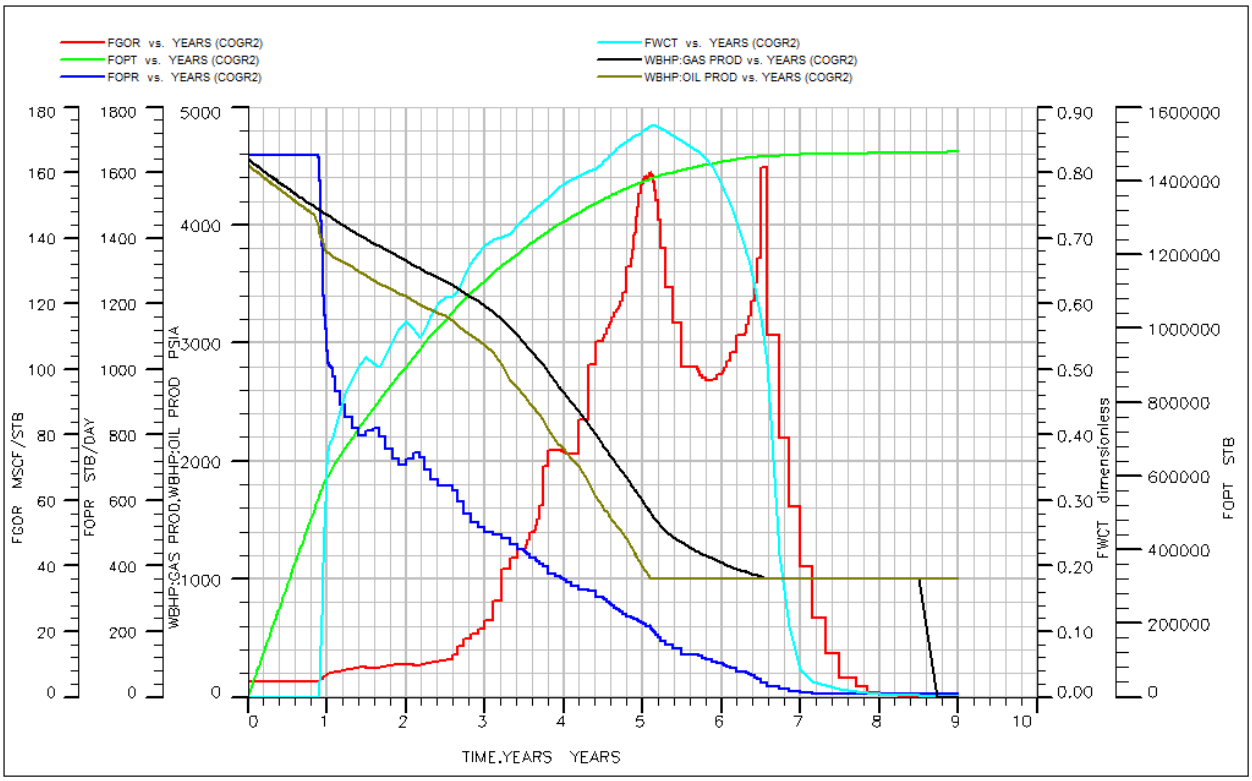

Figure B(iii): COGR2 production forecast plots

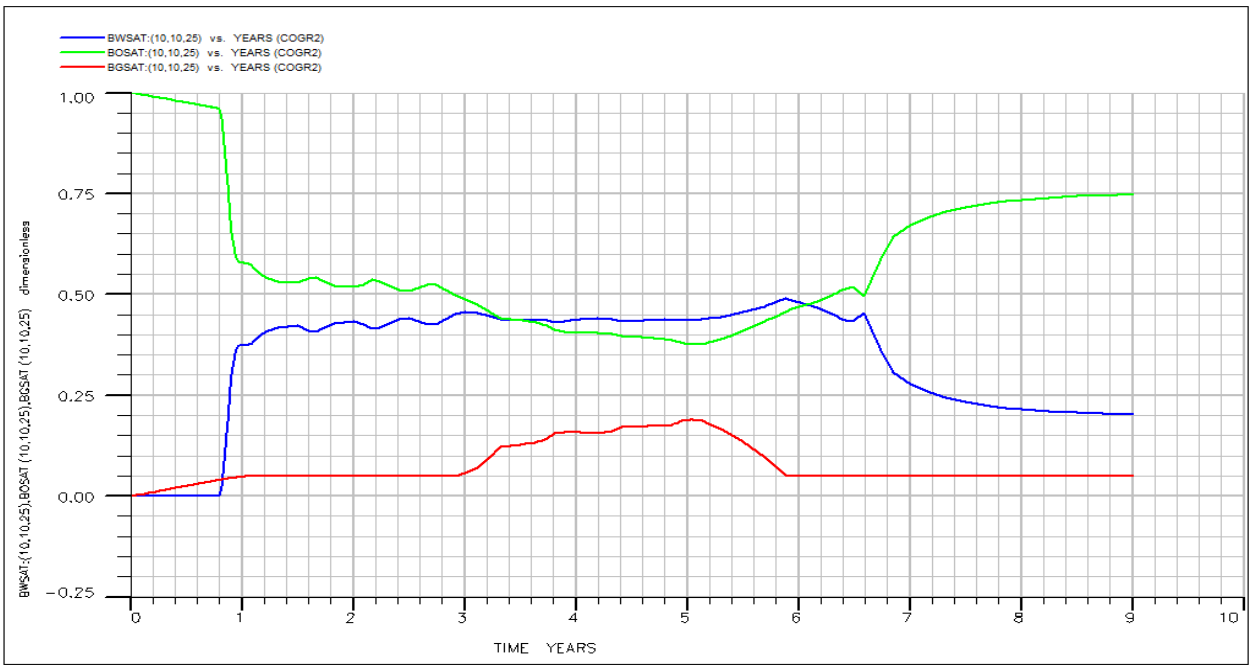

Figure B(iv): COGR2 fluid saturation plots of the mid-oil-well-trajectory cell.

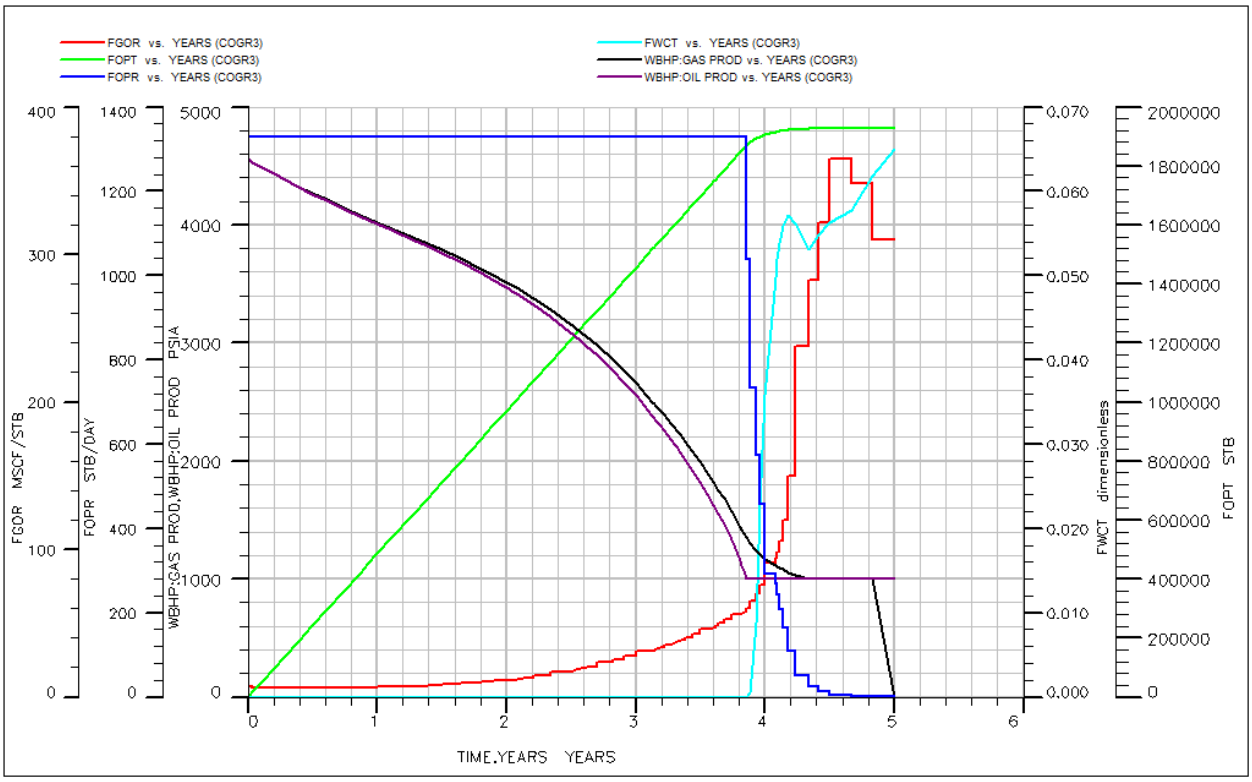

Figure B(v): COGR3 production forecast plots

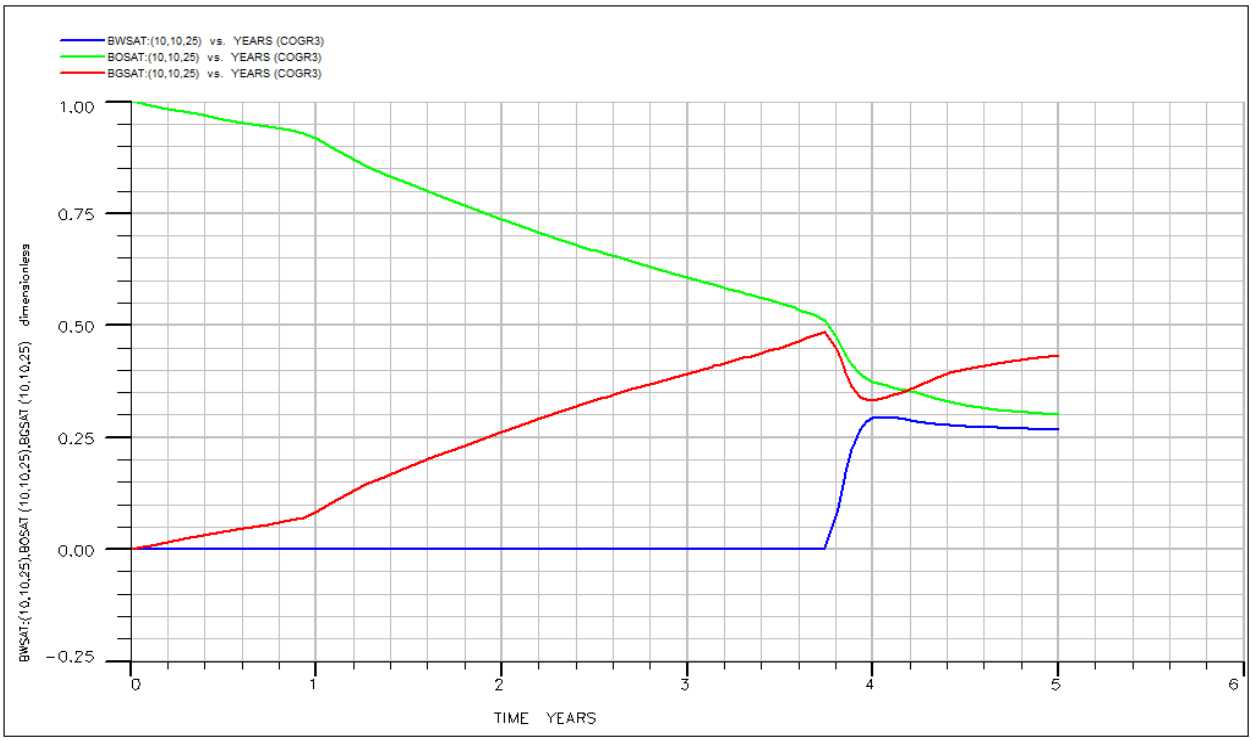

Figure B(vi): COGR3 fluid saturation plots of the mid-oil-well-trajectory cell.

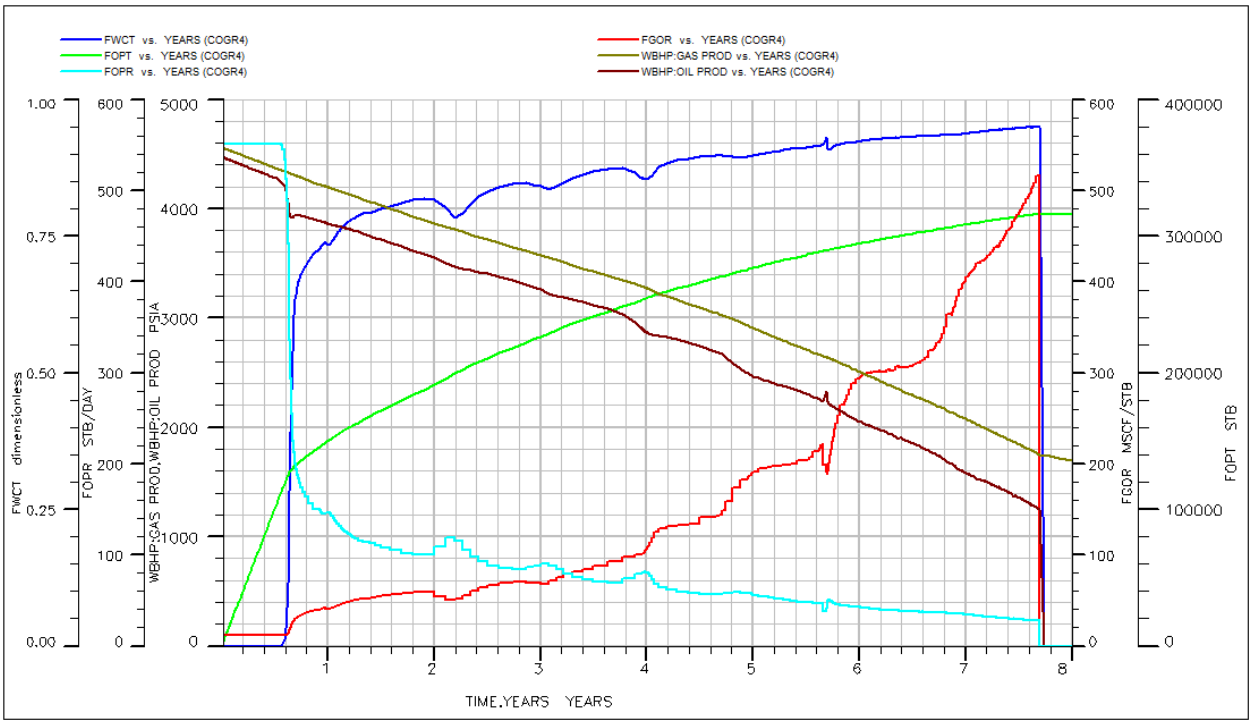

Figure B(vii): COGR4 production forecast plots

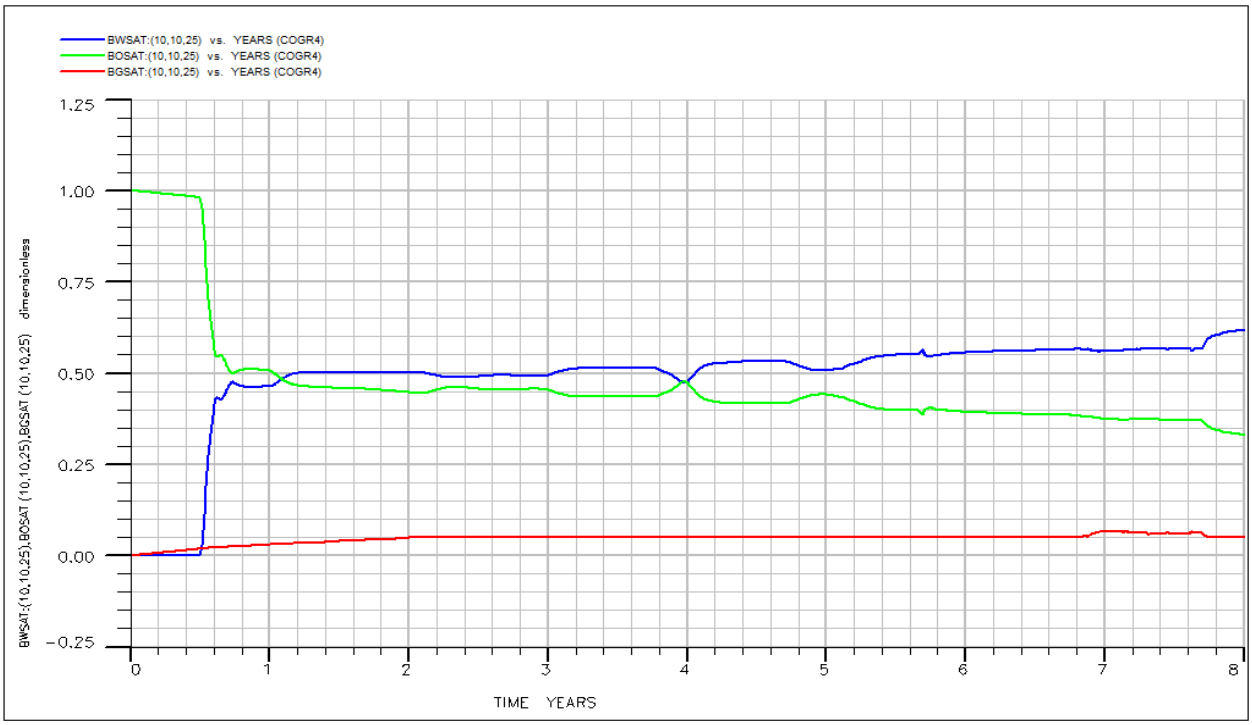

Figure B(viii): COGR4 fluid saturation plots of the mid-oil-well-trajectory cell.

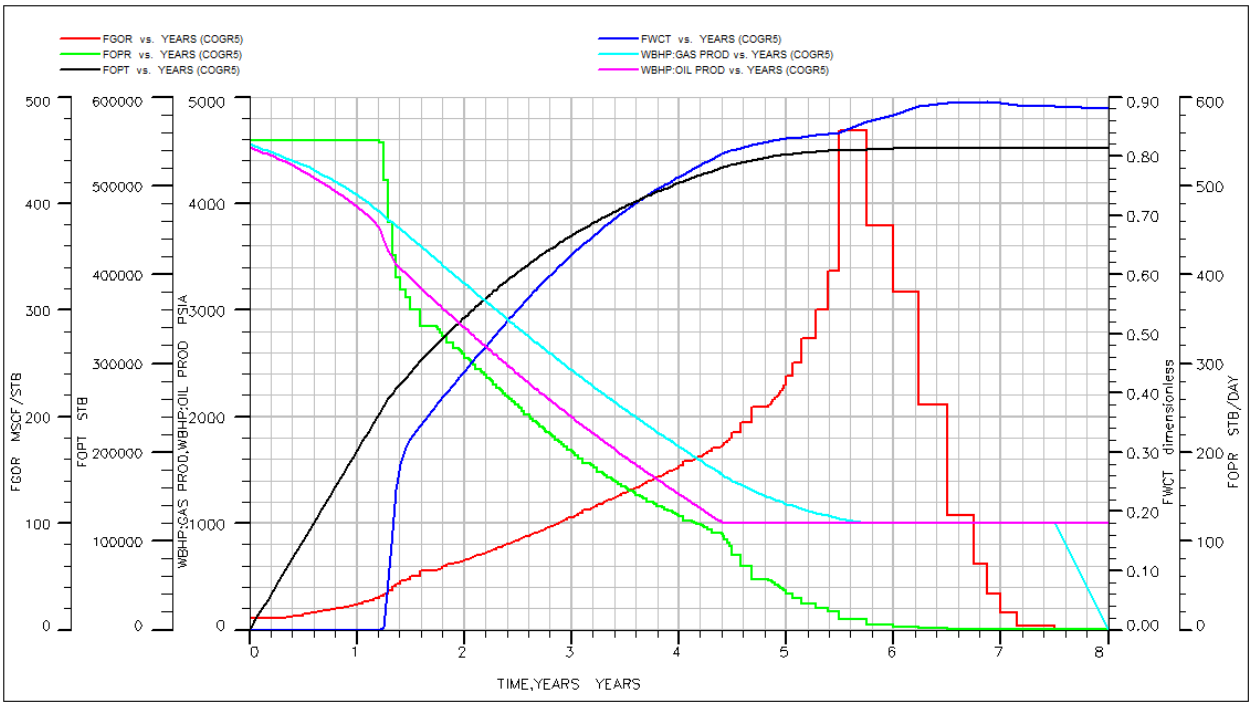

Figure B(ix): COGR5 production forecast plots

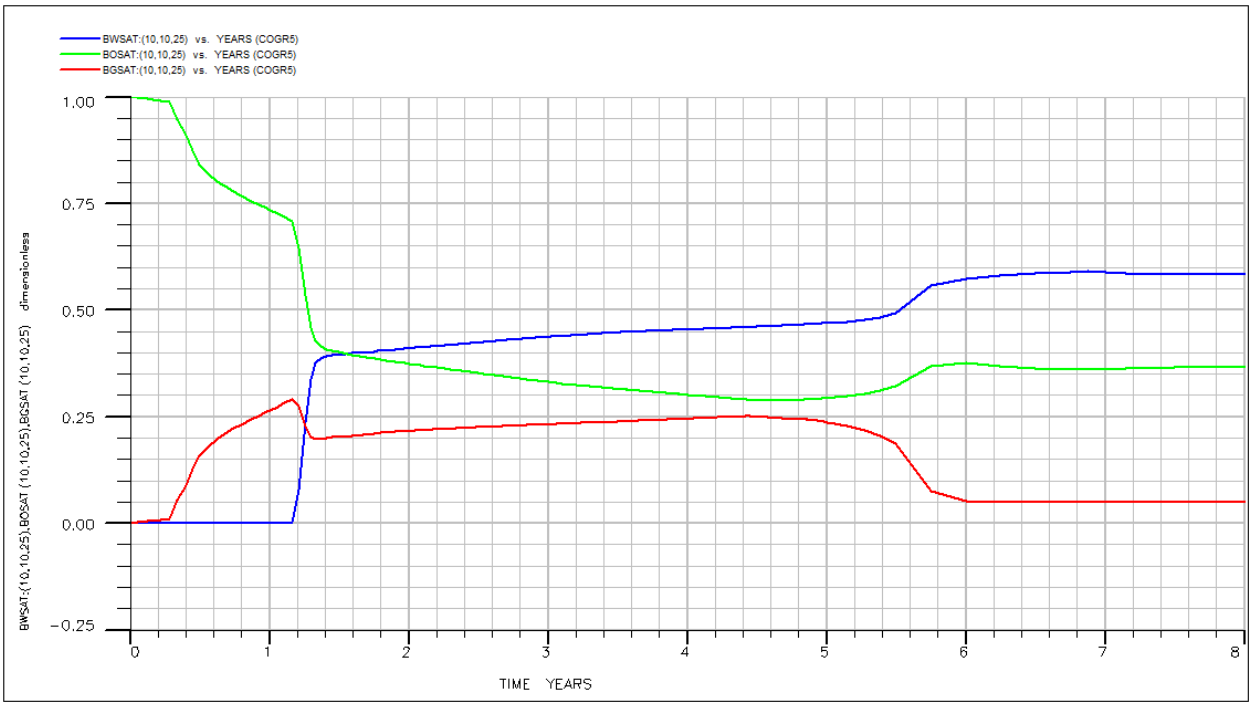

Figure B(x): COGR5 fluid saturation plots of the mid-oil-well-trajectory cell.

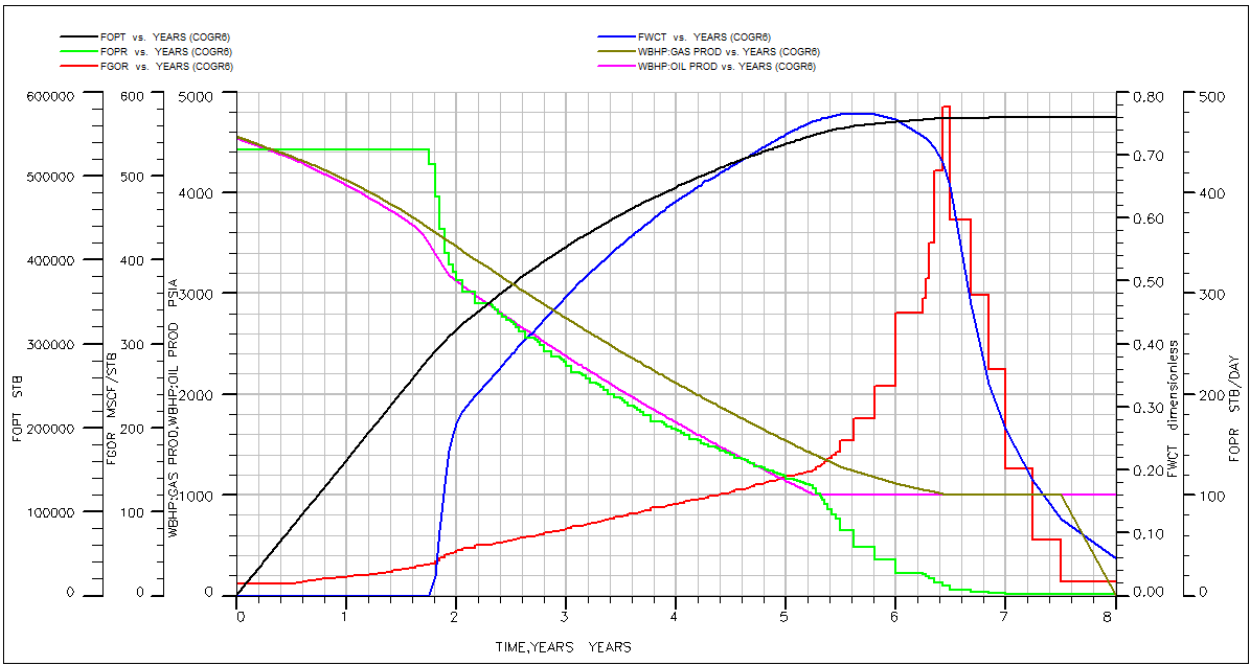

Figure B(xi): COGR6 production forecast plots

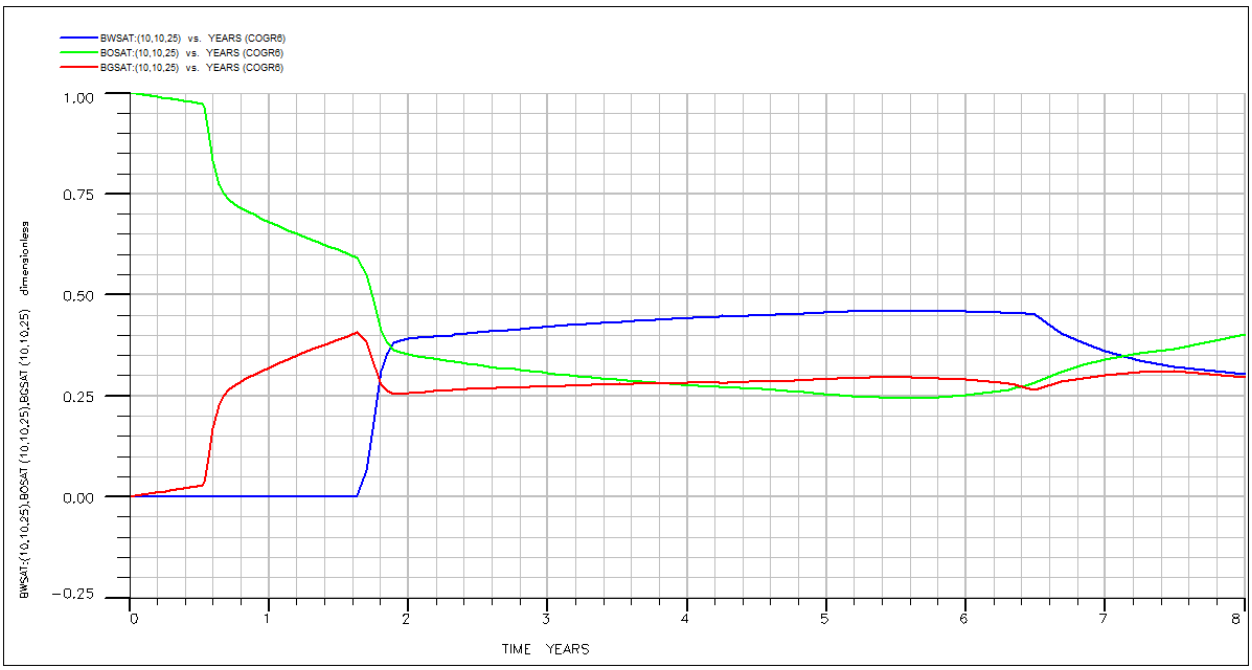

Figure B(xii): COGR6 fluid saturation plots of the mid-oil-well-trajectory cell.

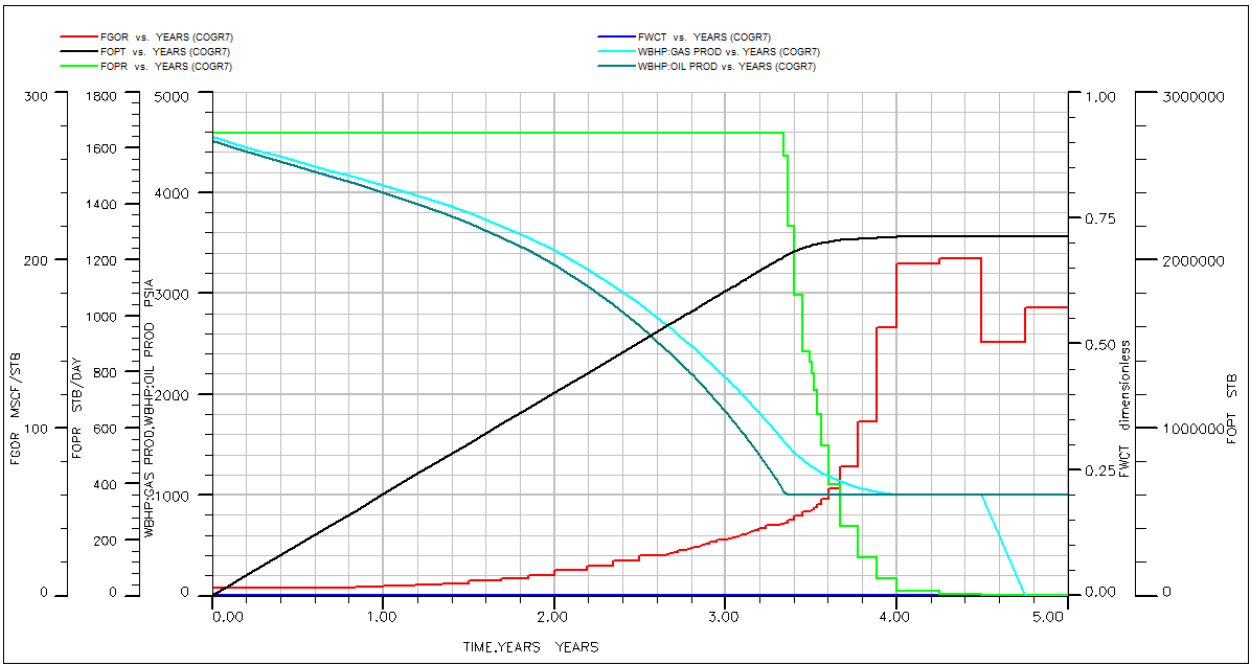

Figure B (xiii): COGR7 production forecast plots

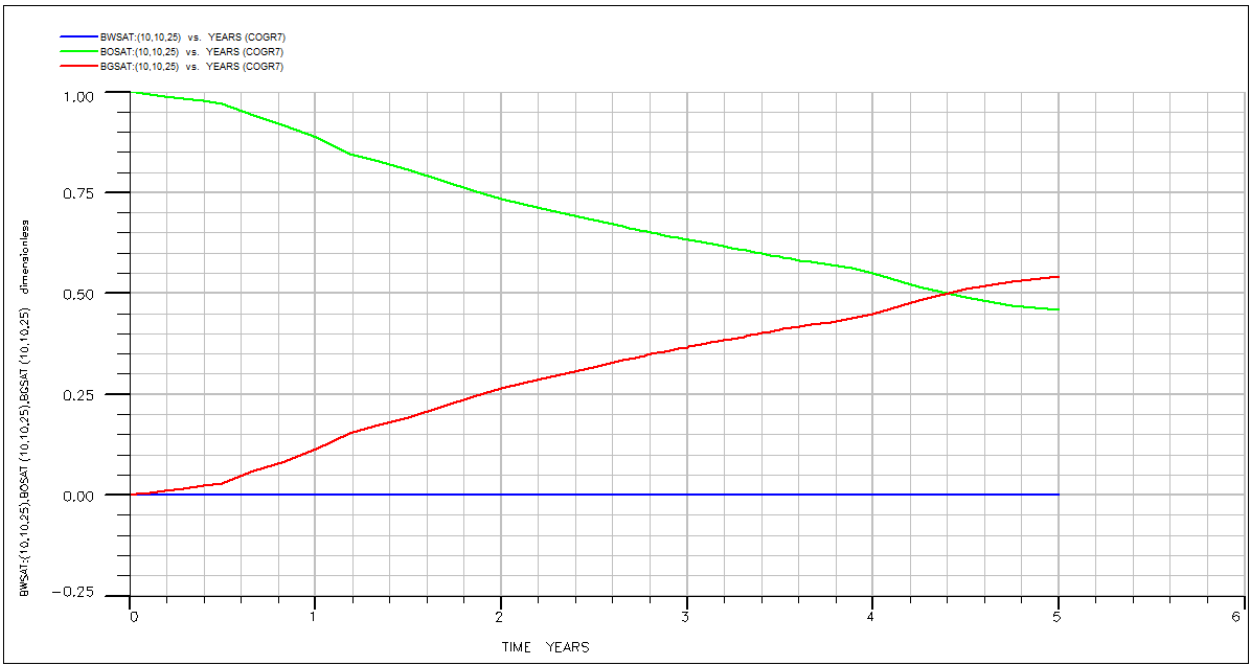

Figure B (xiv): COGR7 fluid saturation plots of the mid-oil-well-trajectory cell.

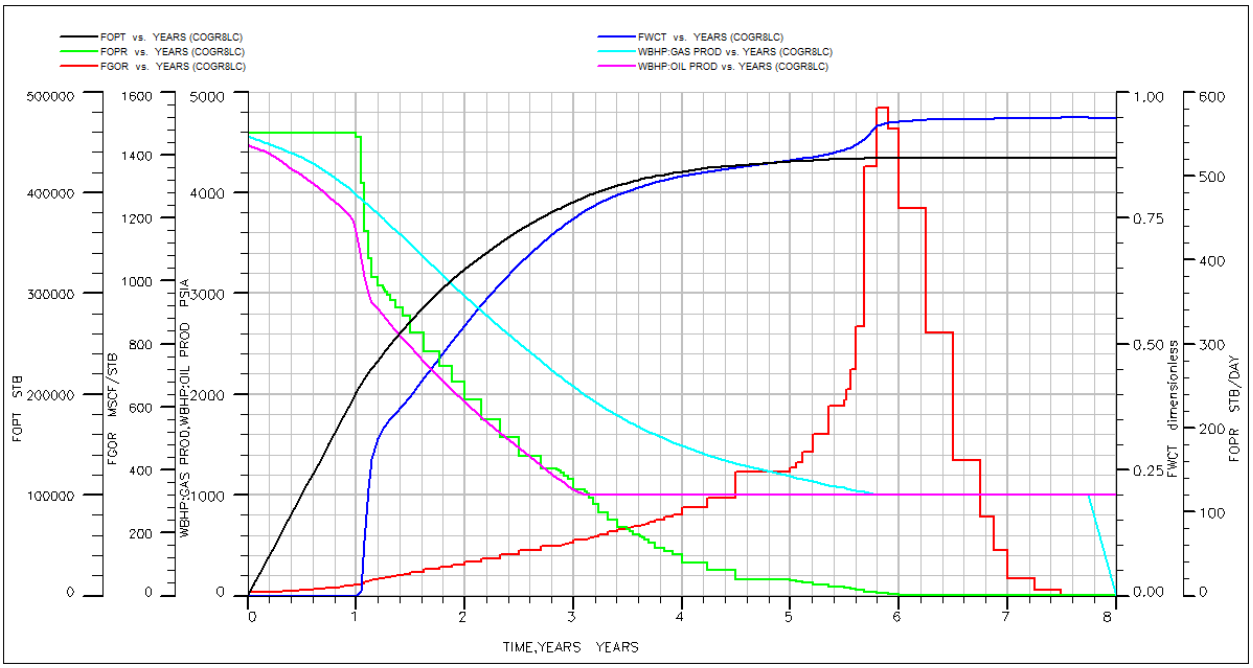

Figure B (xv): COGR8 production forecast plots

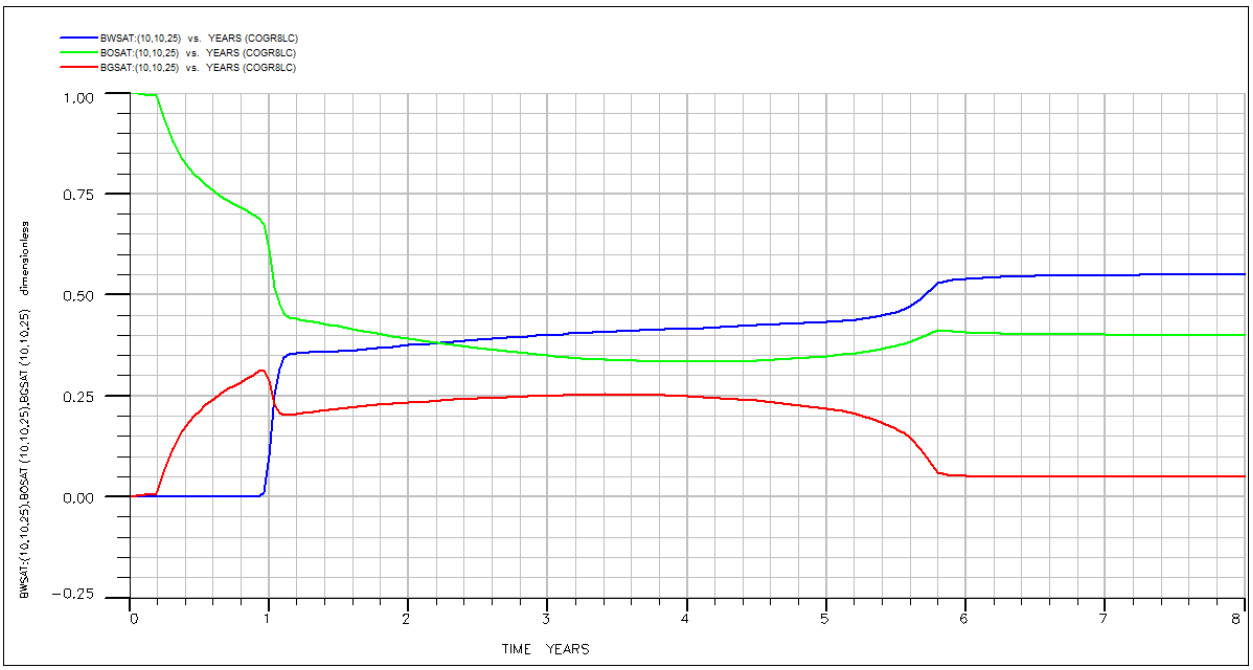

Figure B (xvi): COGR8 fluid saturation plots of the mid-oil-well-trajectory cell.

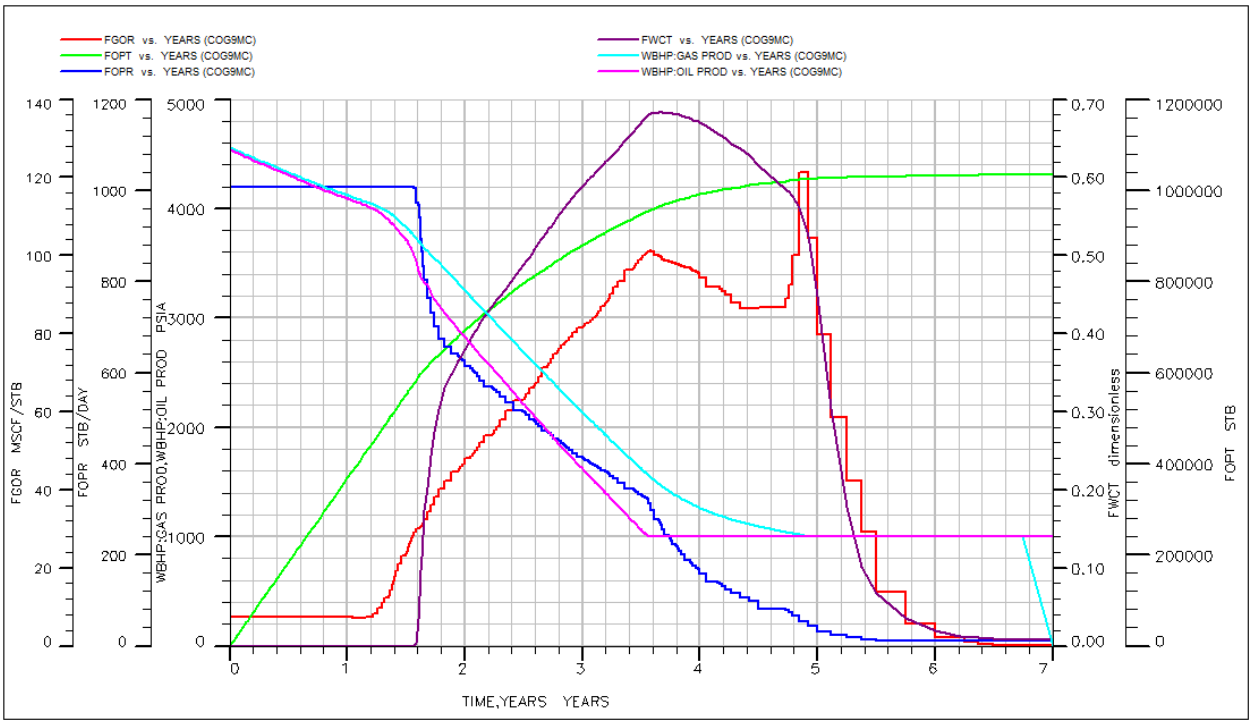

Figure B (xvii): COGR9 production forecast plots

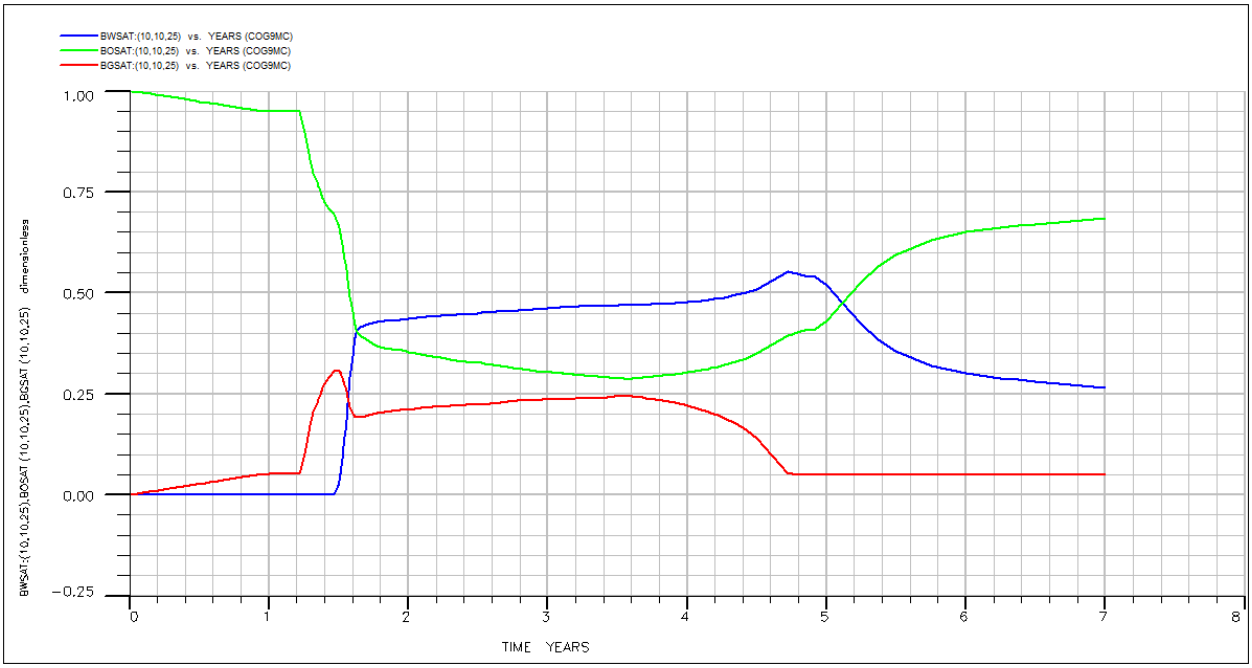

Figure B (xviii): COGR9 fluid saturation plots of the mid-oil-well-trajectory cell.

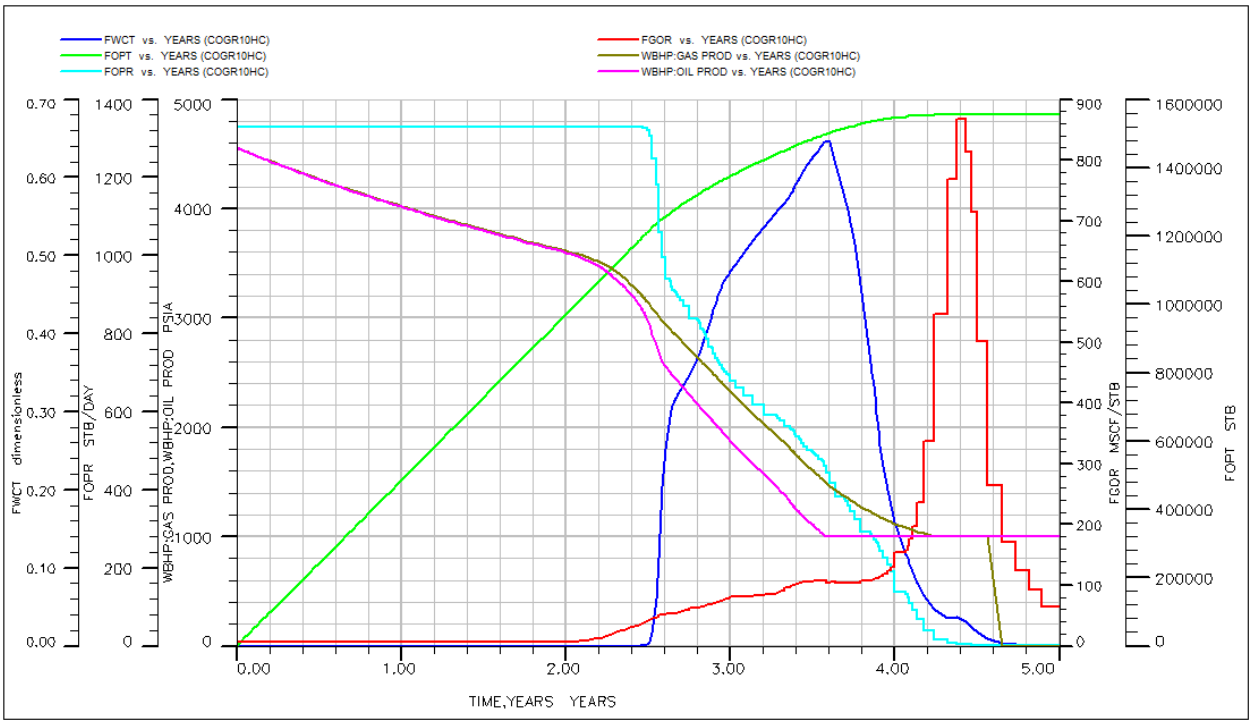

Figure B (xix): COGR10 production forecast plots

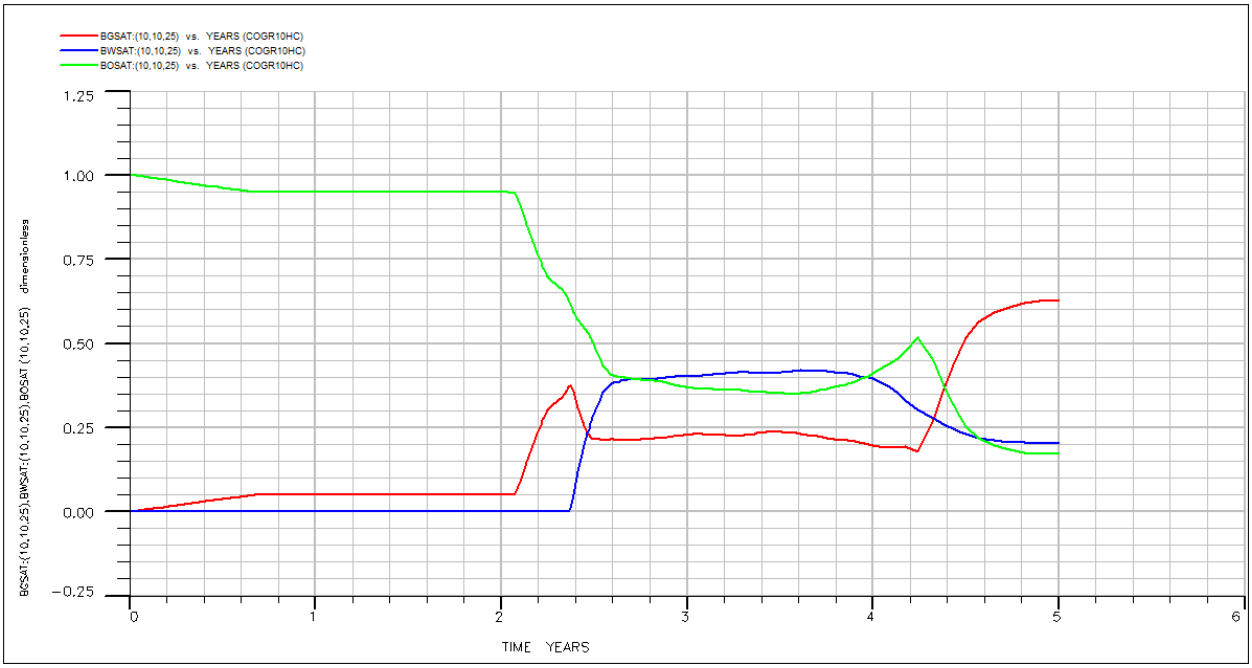

Figure B (xx): COGR10 fluid saturation plots of the mid-oil-well-trajectory cell.

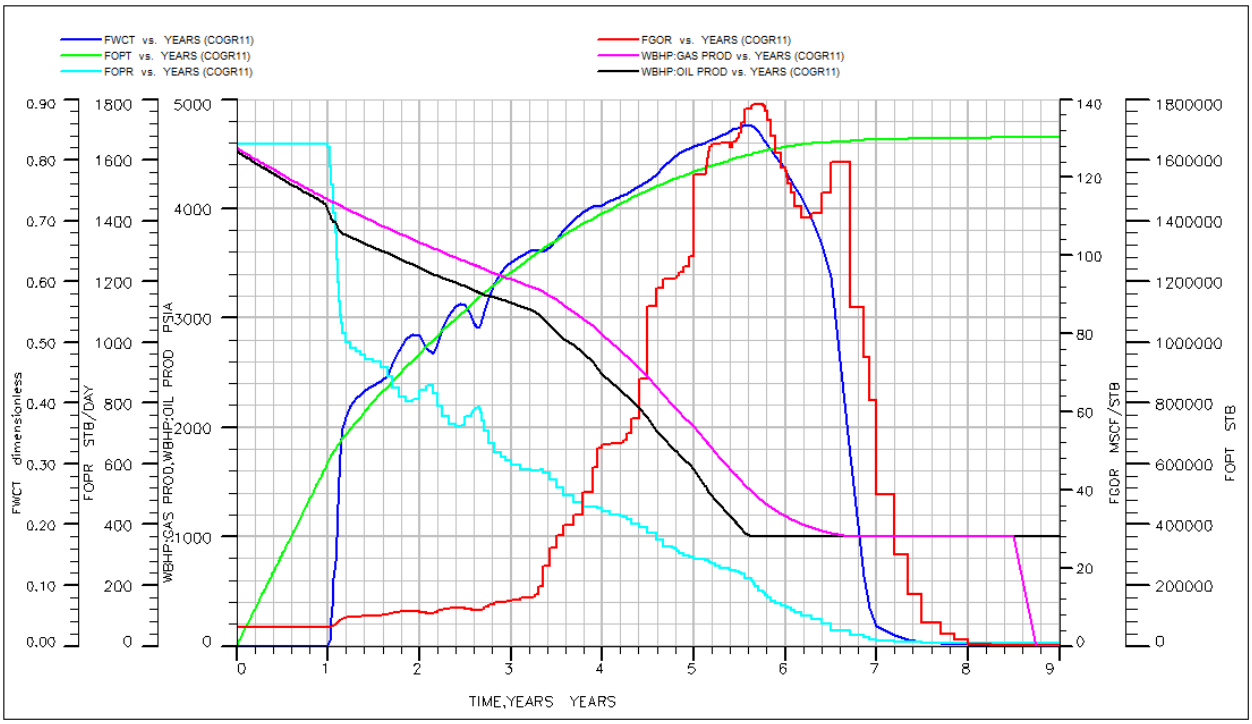

Figure B (xxi): COGR11 production forecast plots

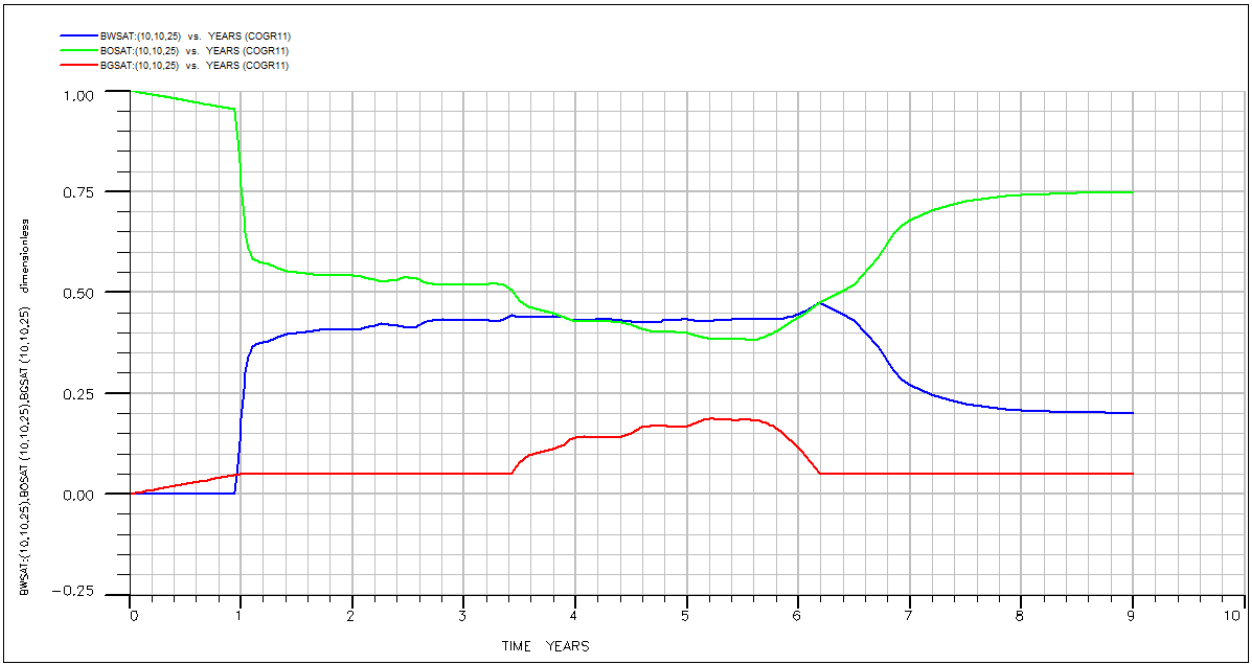

Figure B (xxii): COGR11 fluid saturation plots of the mid-oil-well-trajectory cell.

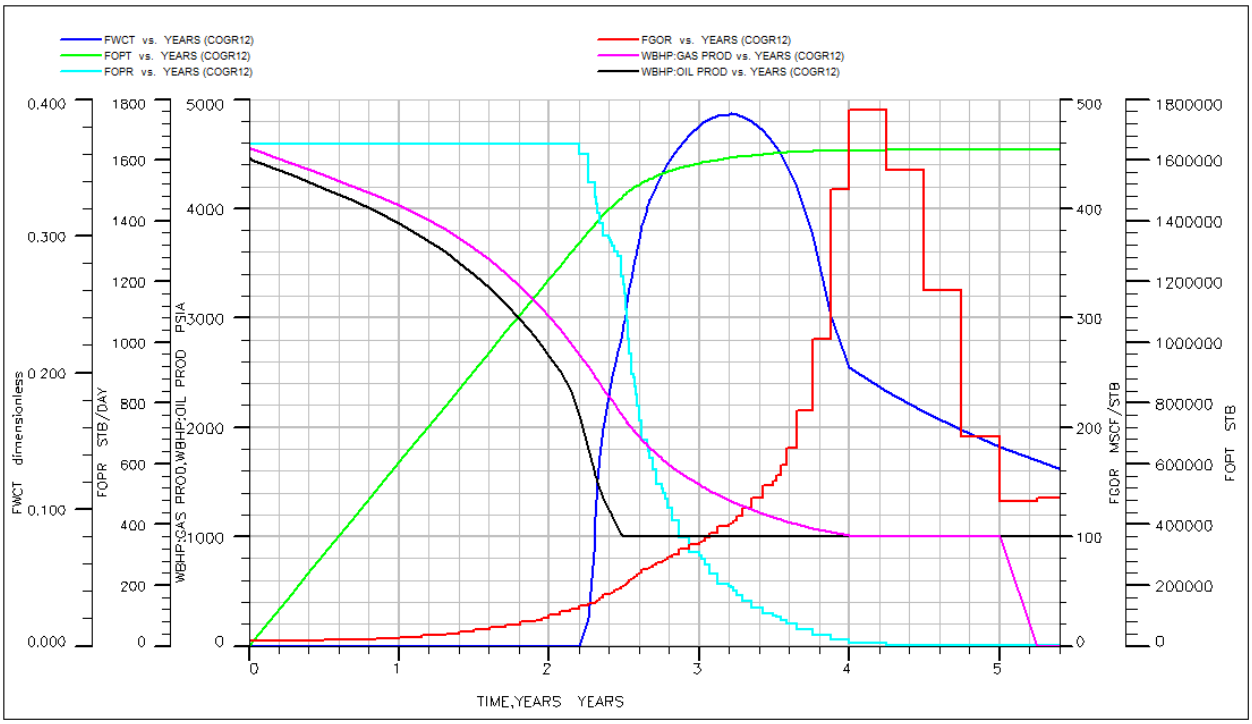

Figure B (xxiii): COGR12 production forecast plots

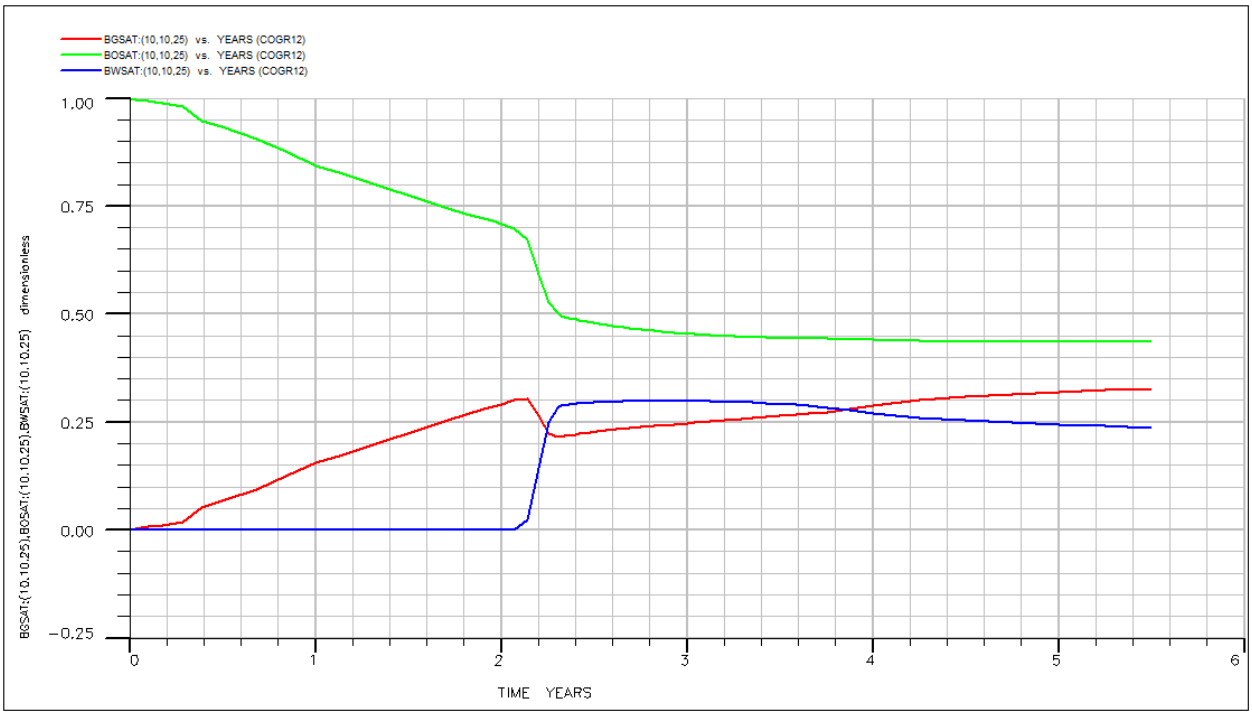

Figure B (xxiv): COGR12 fluid saturation plots of the mid-oil-well-trajectory cell.

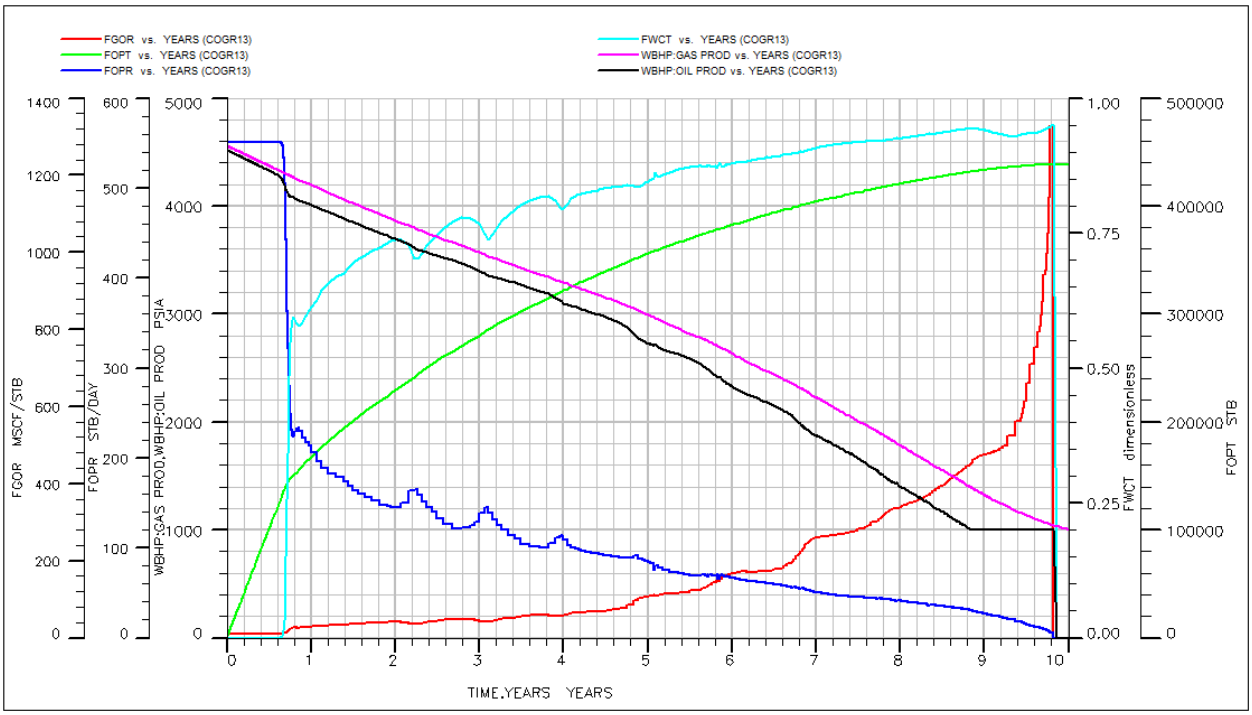

Figure B (xxv): COGR13 production forecast plots

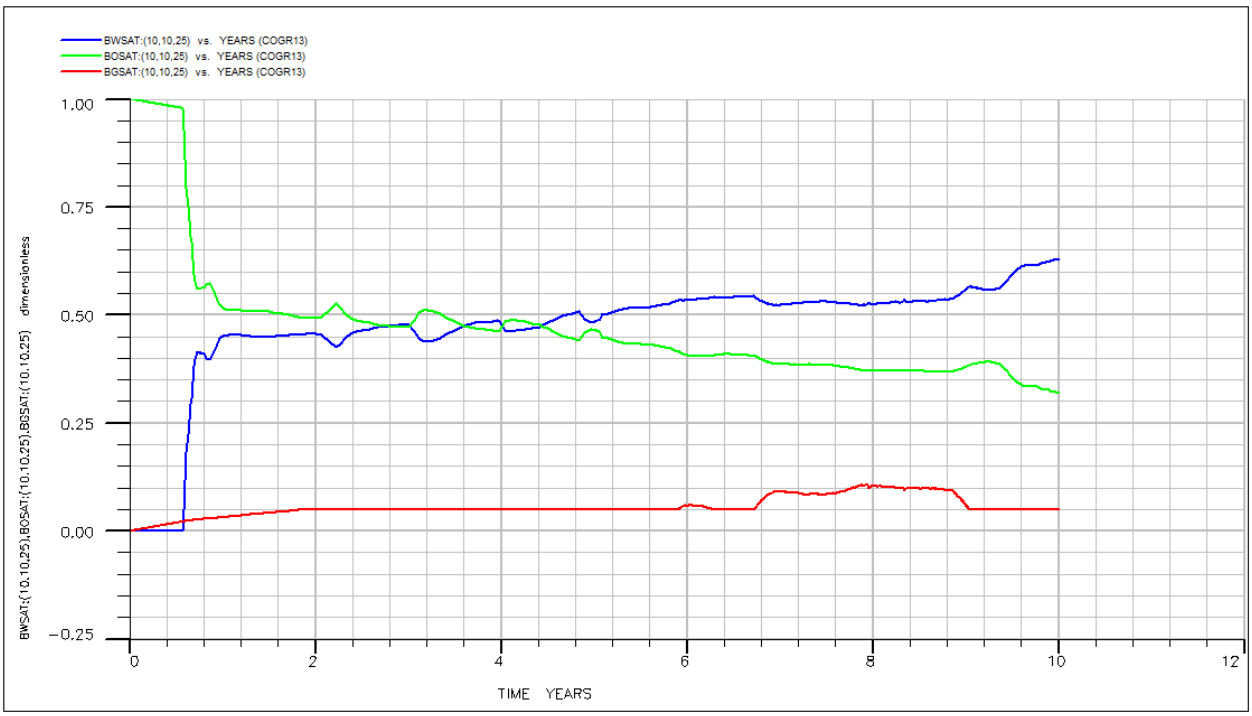

Figure B (xxvi): COGR13 fluid saturation plots of the mid-oil-well-trajectory cell.

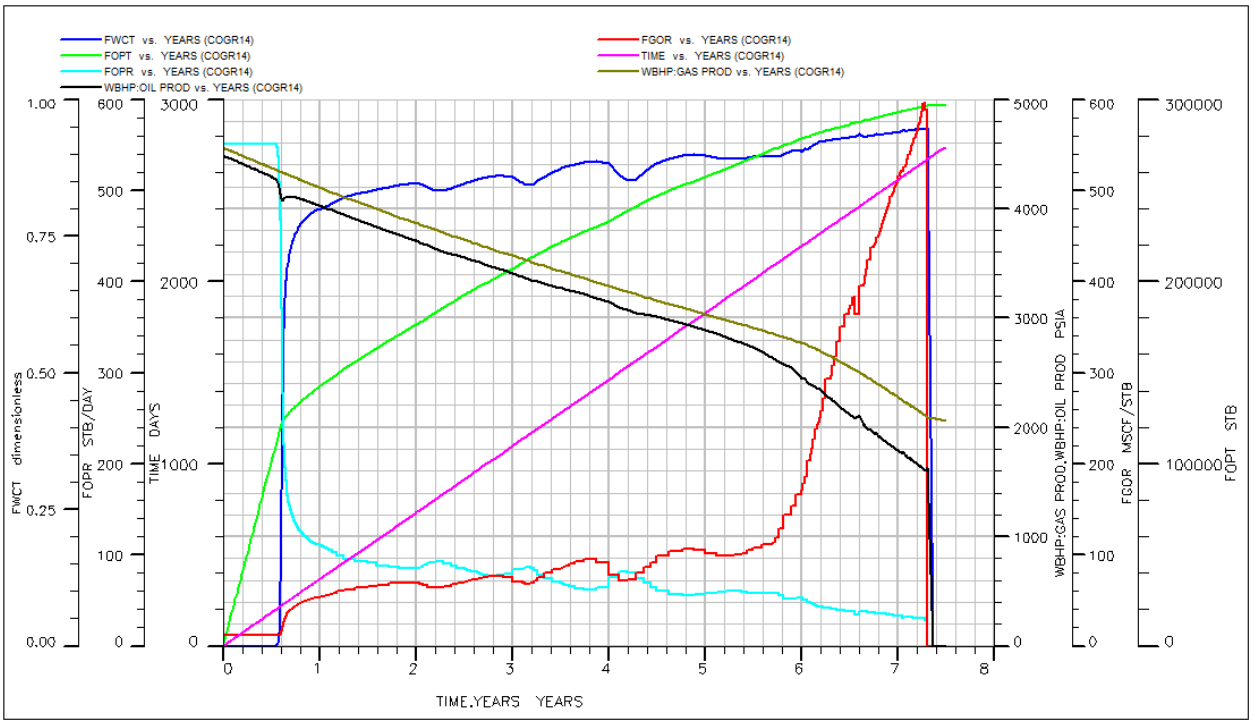

Figure B (xxvii): COGR14 production forecast plots

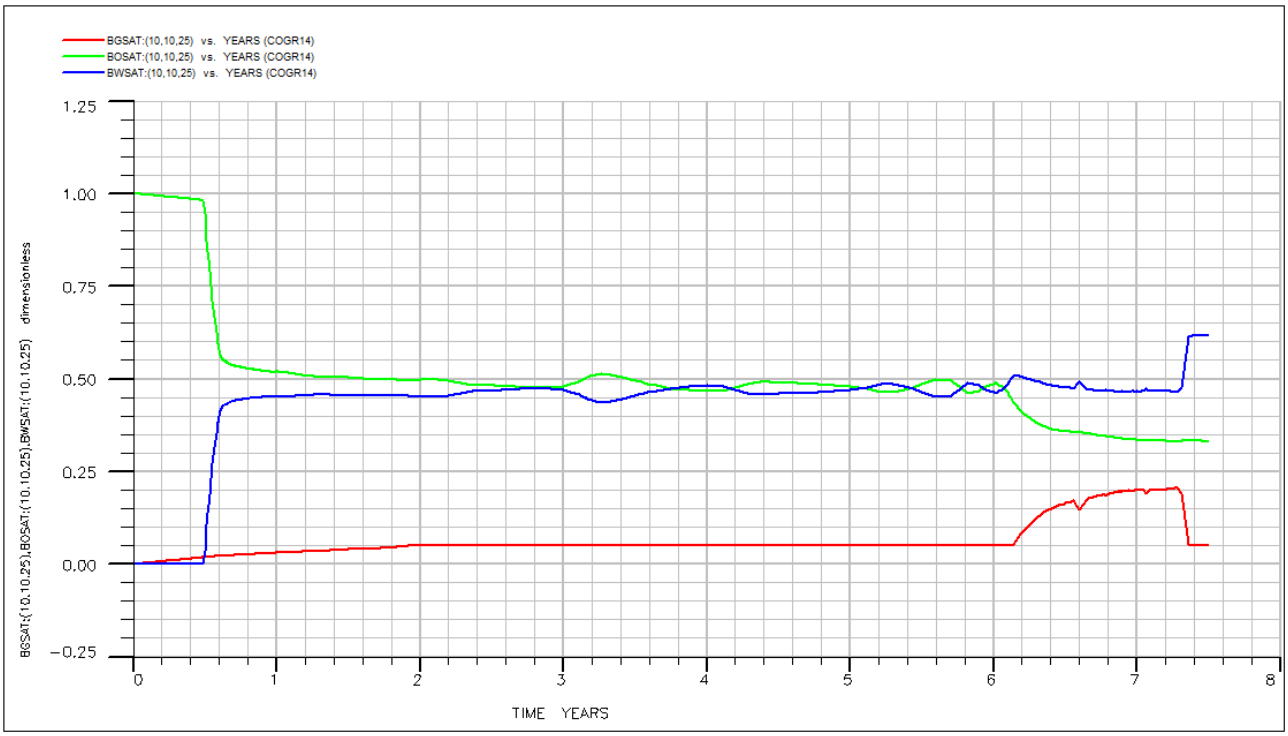

Figure B (xxviii): COGR14 fluid saturation plots of the mid-oil-well-trajectory cell.

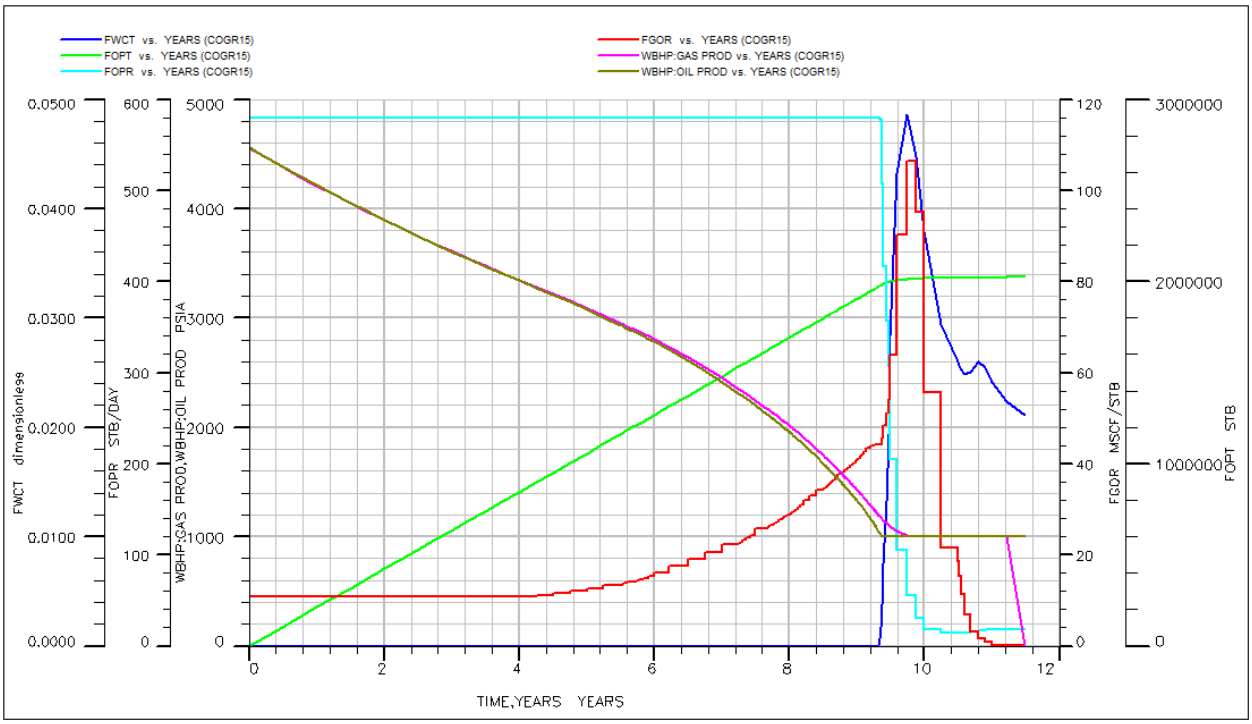

Figure B (xxix): COGR15 production forecast plots

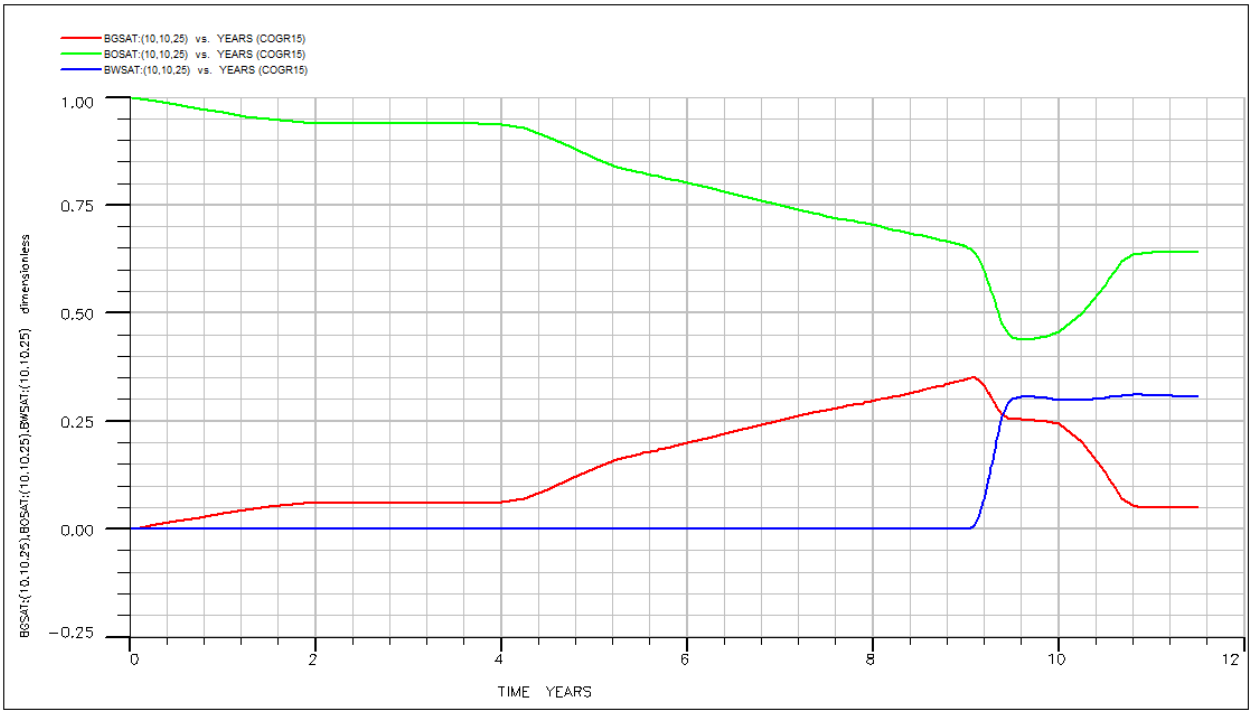

Figure B (xxx): COGR15 fluid saturation plots of the mid-oil-well-trajectory cell.

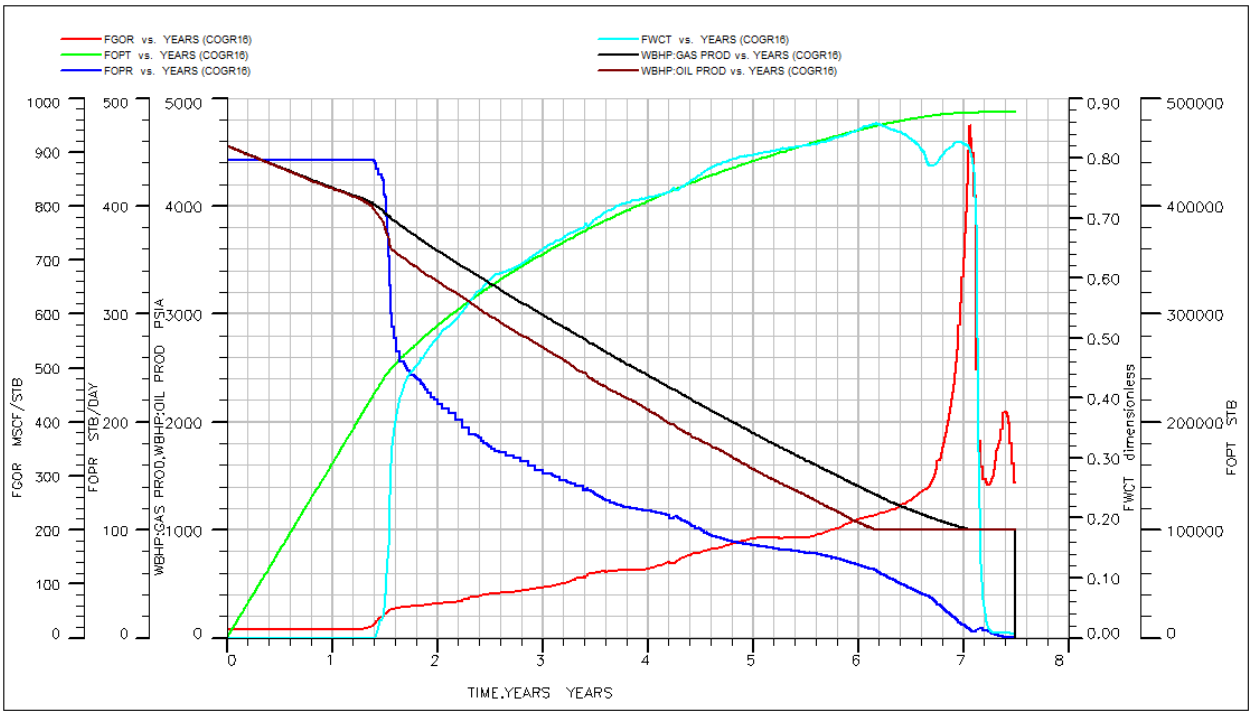

Figure B (xxxi): COGR16 production forecast plots

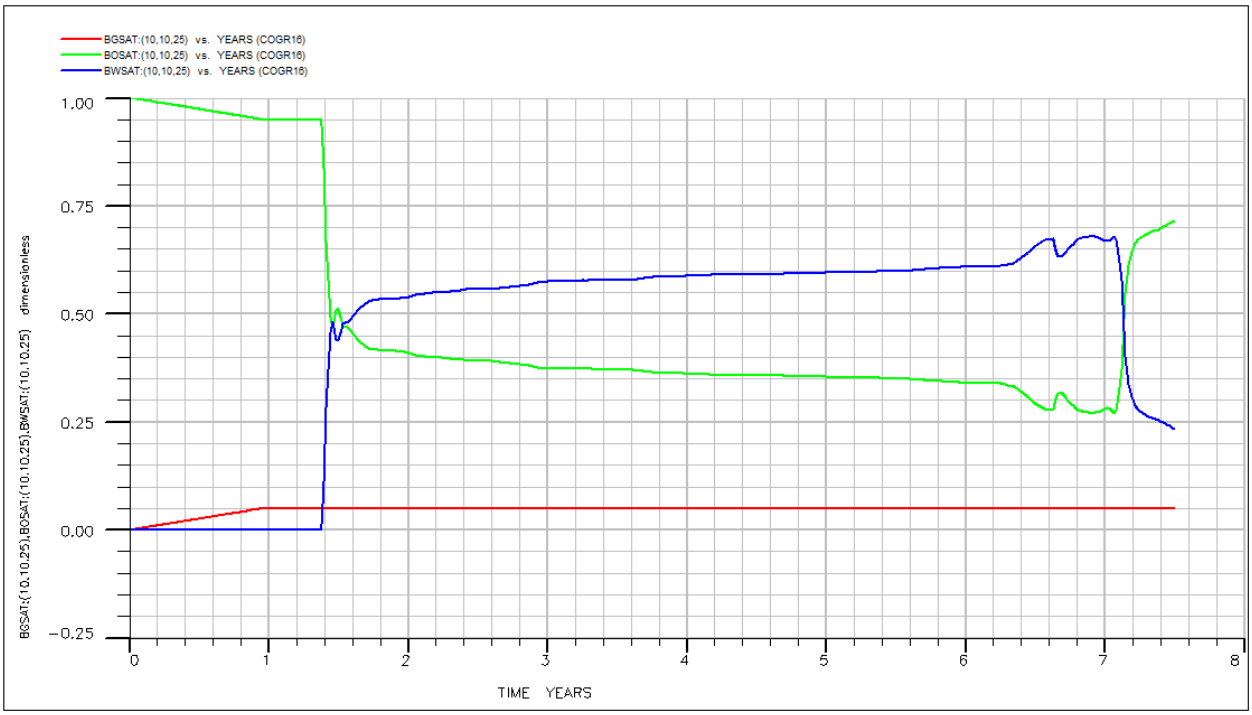

Figure B (xxxii): COGR16 fluid saturation plots of the mid-oil-well-trajectory cell.

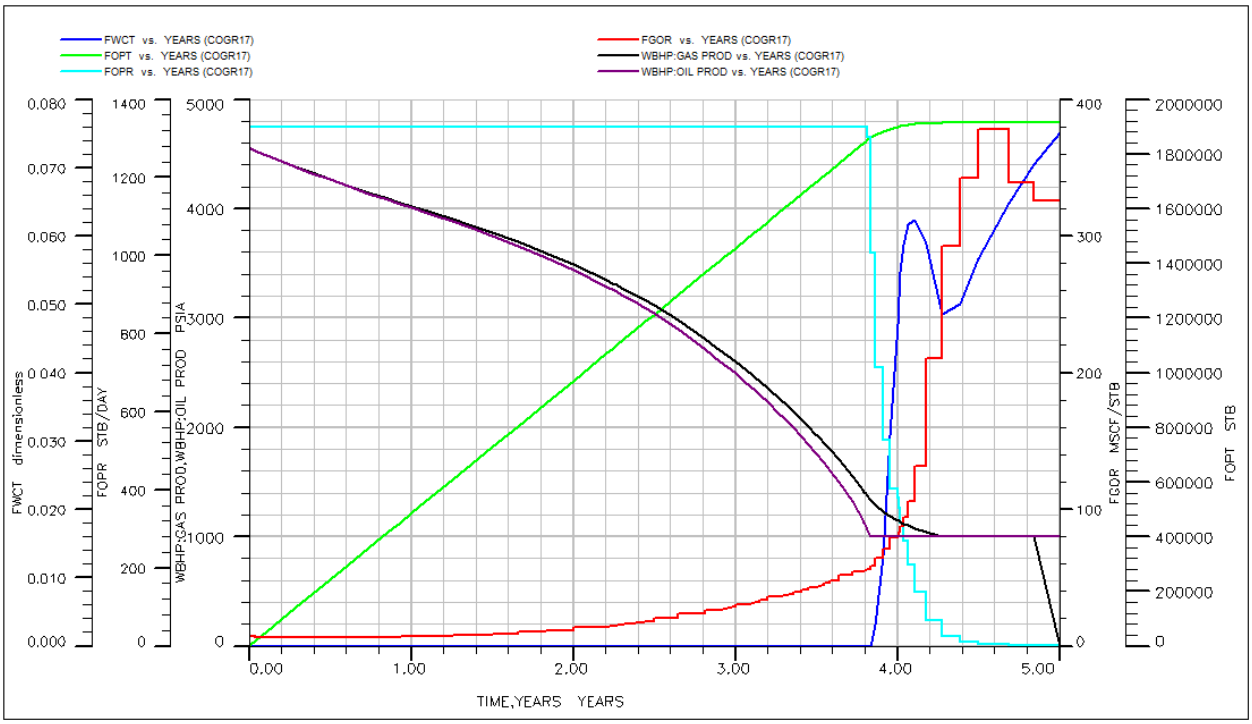

Figure B (xxxiii): COGR17 production forecast plots

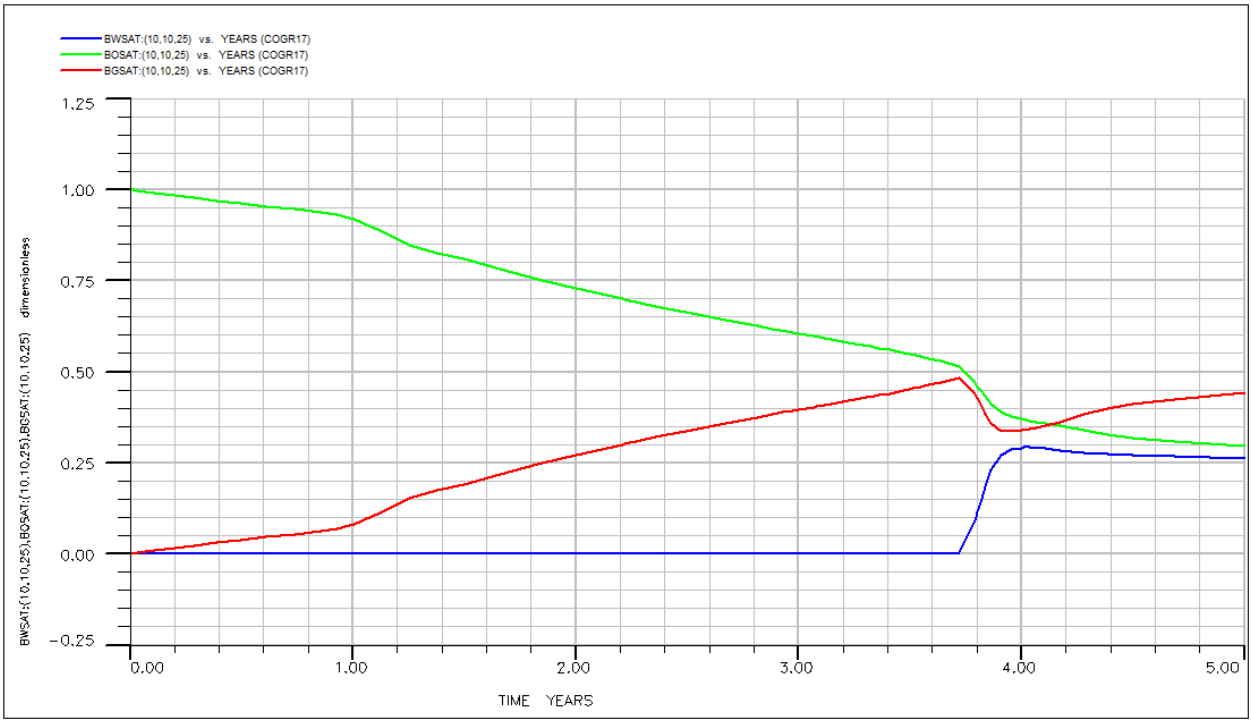

Figure B (xxxiv): COGR17 fluid saturation plots of the mid-oil-well-trajectory cell.

APPENDIX BII

ADDITIONAL RESULTS OF THE COG SCENARIO DESIGN ANALYSIS

FINAL EQUATION IN TERMS OF CODED FACTORS

Substituting Equations 4.2a, 4.2b, 4.2c and 4.2d into Equation 4.2 gives the surrogate equation in terms of the actual factor as shown in Equation B1 of Appendix BII

$$R_f = -1.7230 + 0.3523\,API - 7.5548\frac{k_v}{k_h} + 5.8788k_{ro} + 0.0031Q_l \qquad \textbf{Eq. B1}$$

MODEL DIAGNOSTIC PLOTS

1. **Normal Plot of Residuals**

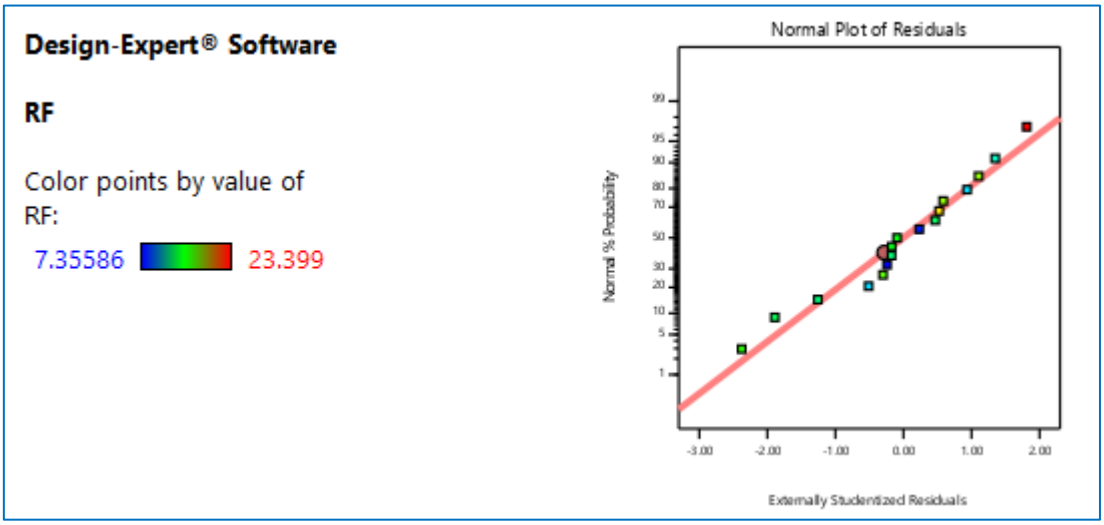

Figure B (xxxv): Normal Plot of Residuals for the COG Design Analysis

The significance of the normal plot of residuals has been explained in Appendix AII. Figure B (xxxv) shows the desired scatter or the definite "S", patterns.

2. **The Box-Cox Plot**

As mentioned in Appendix AII, the Box-Cox plot tells you whether a transformation of the data may help to improve the model (Shari K. 2013). In this case, also, Figure B (xxxvi) stipulates that no further transformations are necessary to improve our model.

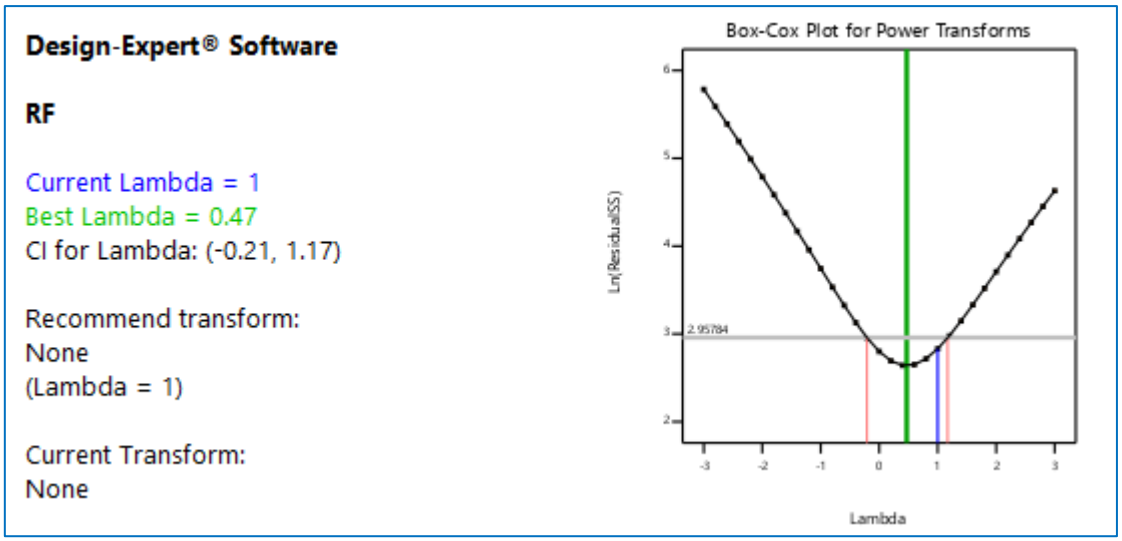

Figure (Axxxvi): Box-Cox Plot for the COG Design Analysis

3. Predicted versus Actual Plot

The predicted vs actual plot is used to see how the model predicts over the range of data. For a perfect case, the plot should exhibit random scatter about the 45^{o}line. Clusters of points above or below the line indicate problems of over or under predicting. Figure B (xxxvii) indicates that equation 4.2 is reliable not to under predict or over predict the design responses. Figure 4.4 further buttresses that.

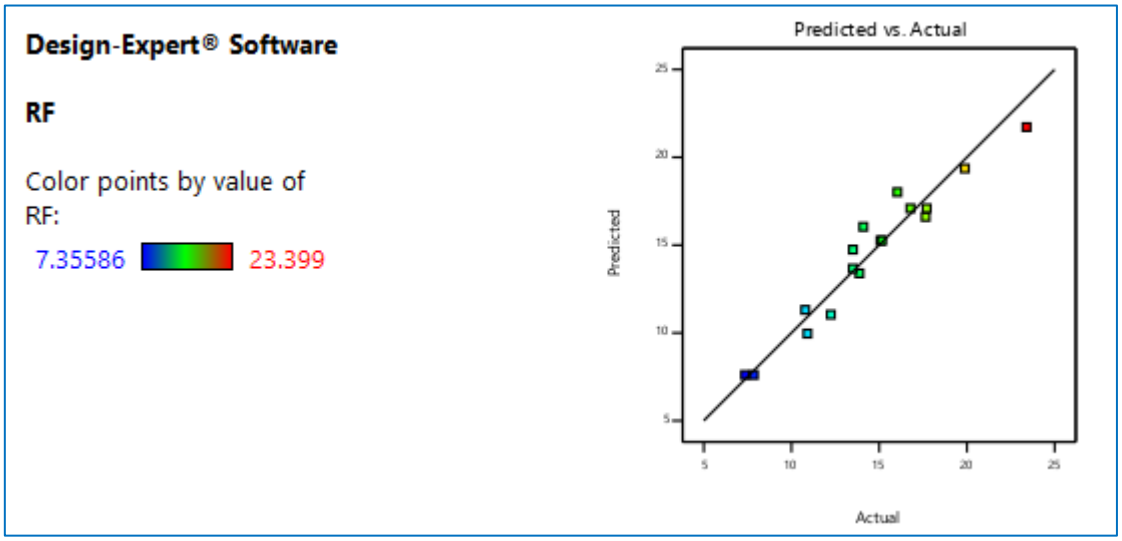

Figure A (xxxvii): Predicted versus Actual Plot of the COG Design Analysis

APPENDIX C

PRODUCTION FORECAST PLOTS AND SATURATION PLOTS FOR THE GOD PRODUCTION SCENARIO RUNS

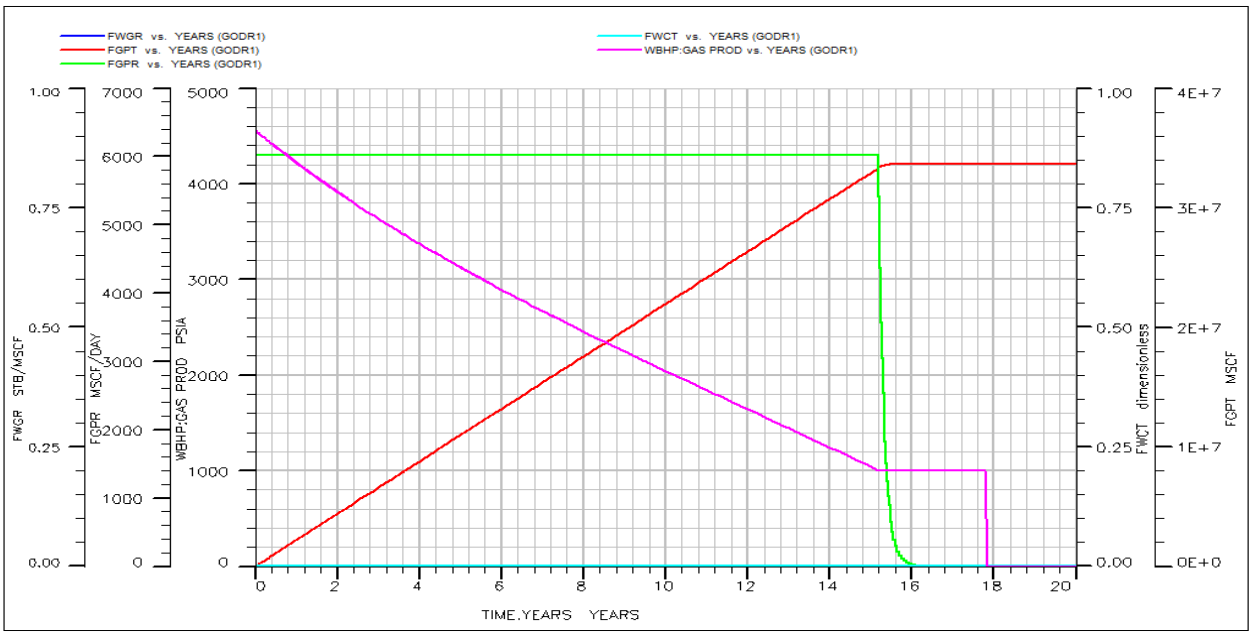

Figure C (i): GODR1 production forecast plots

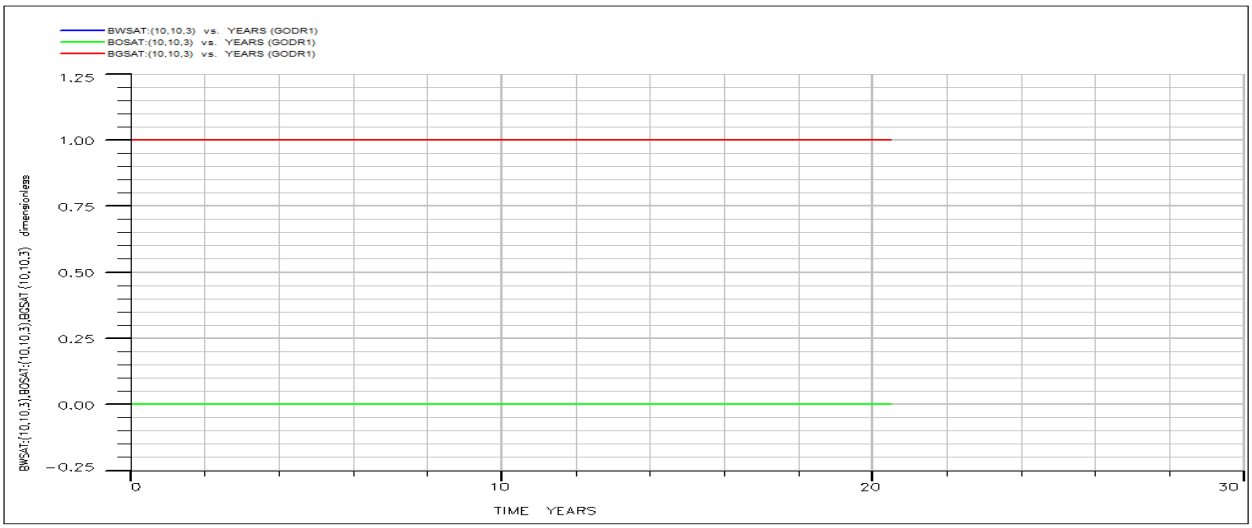

Figure C (ii): GODR1 fluid saturation plots of deepest gas well perforation cell.

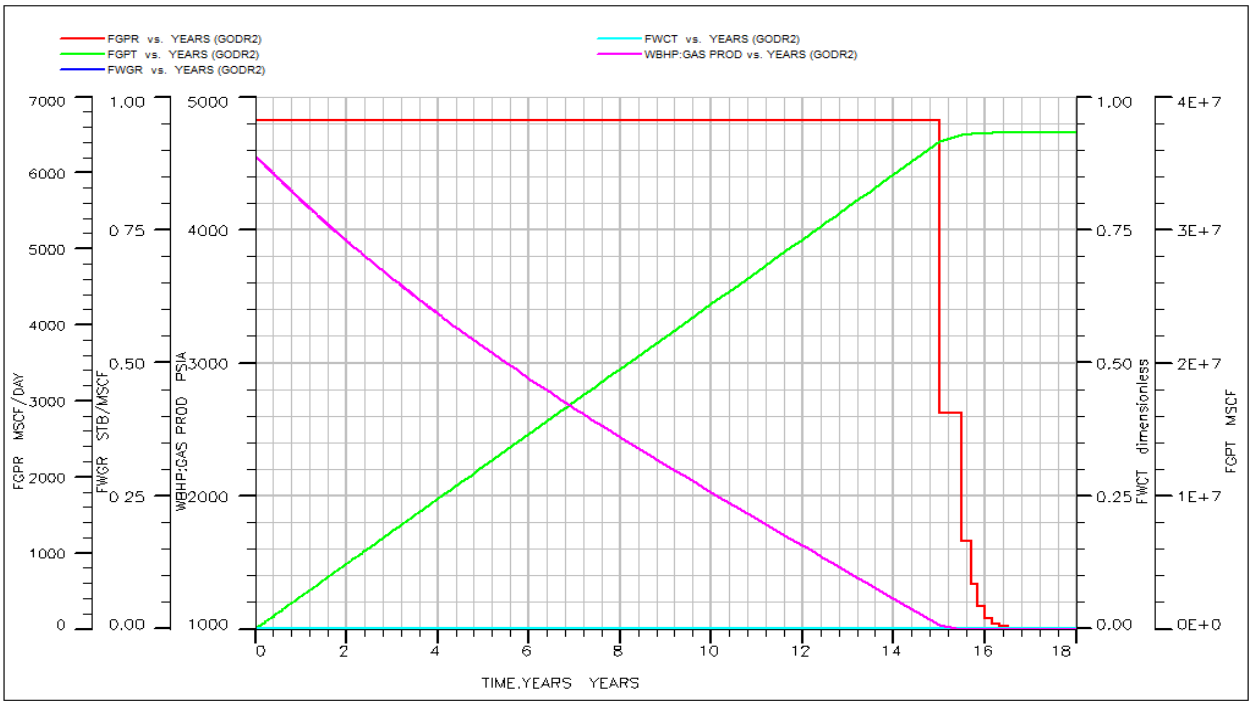

Figure C (iii): GODR2 production forecast plots

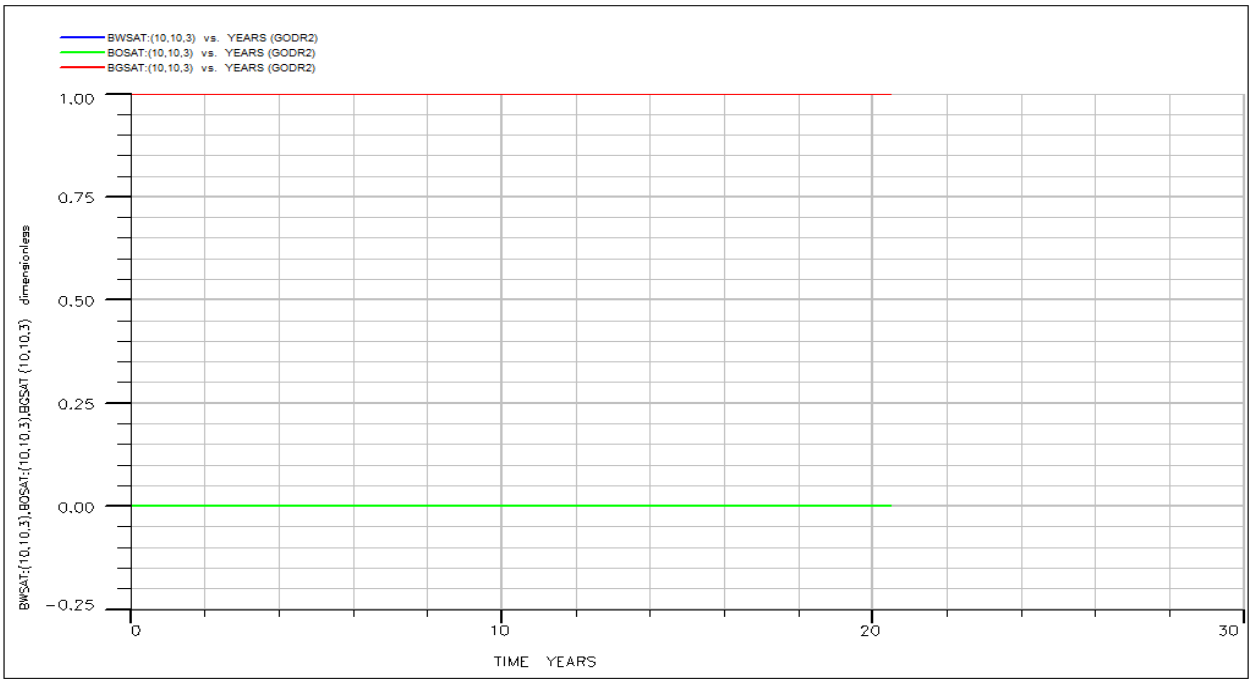

Figure C (IV): GODR2 fluid saturation plots of deepest gas well perforation cell.

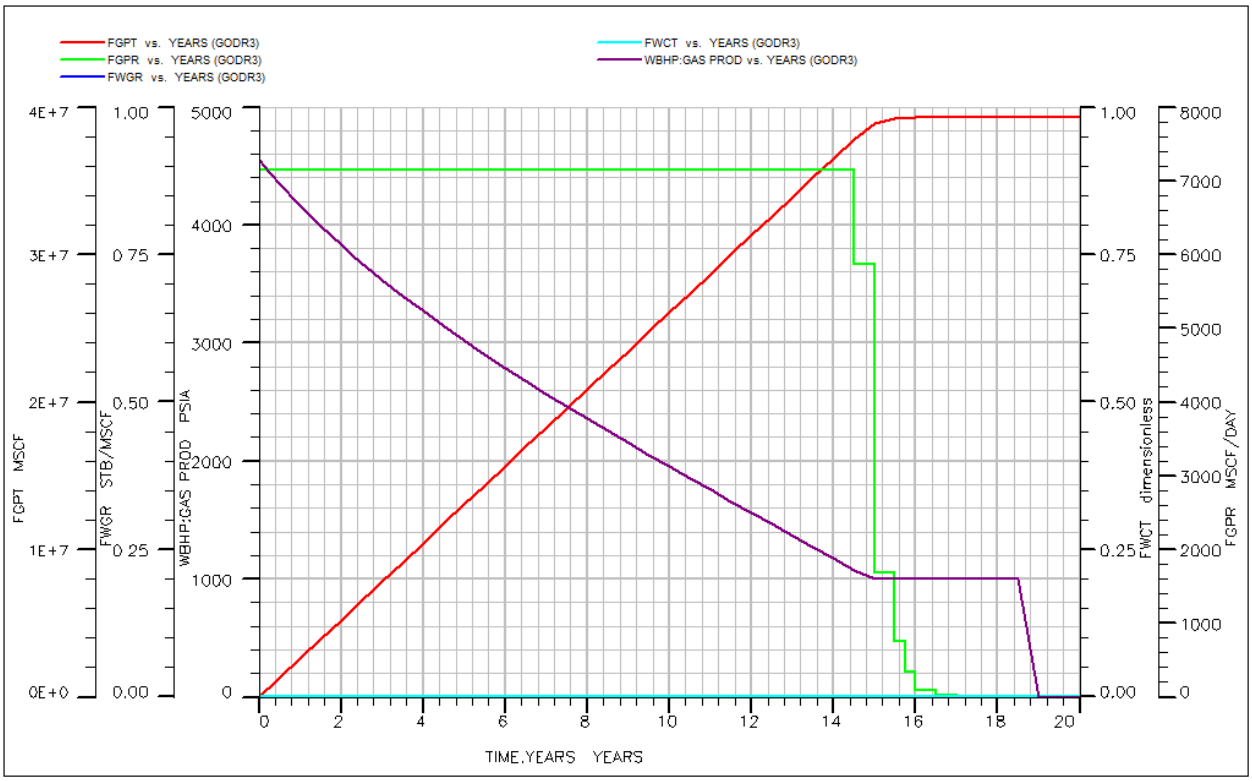

Figure C (v): GODR3 production forecast plots

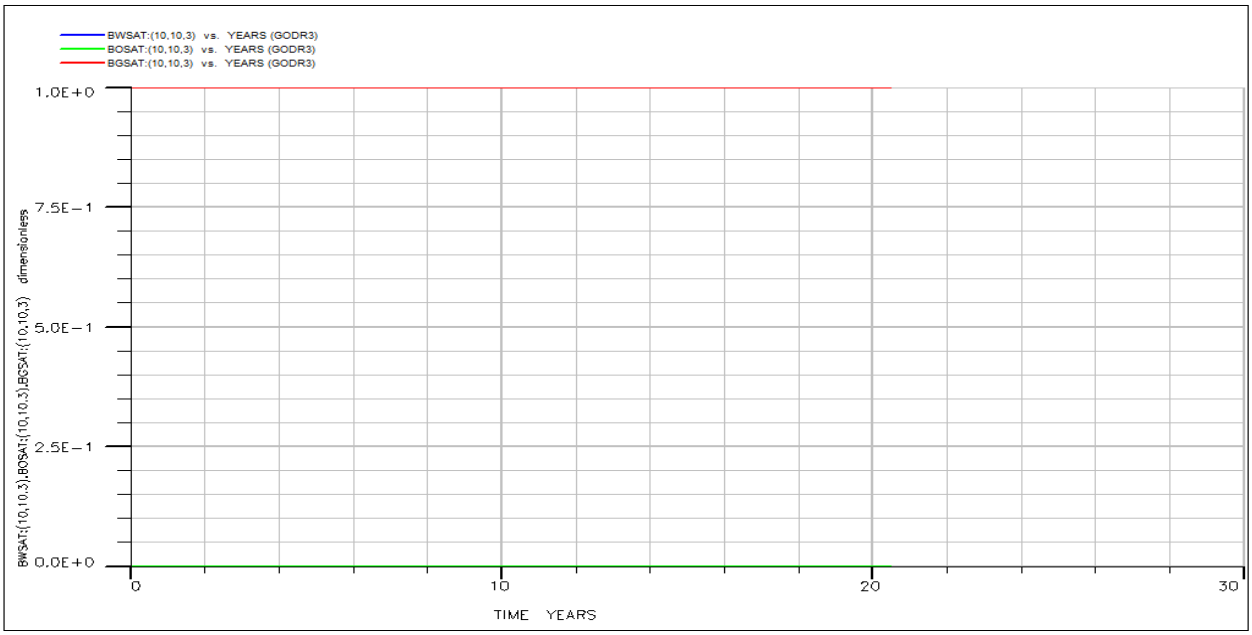

Figure C (vi): GODR3 fluid saturation plots of deepest gas well perforation cell.

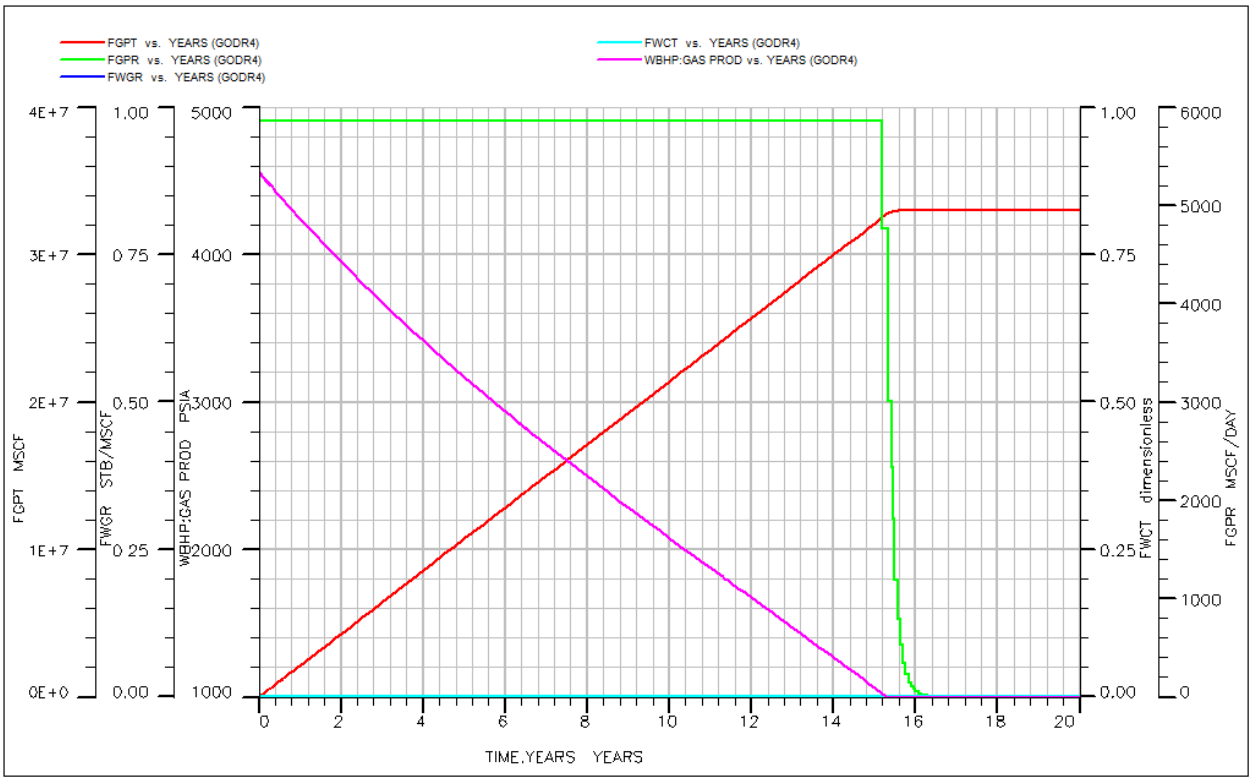

Figure C (vii): GODR4 production forecast plots

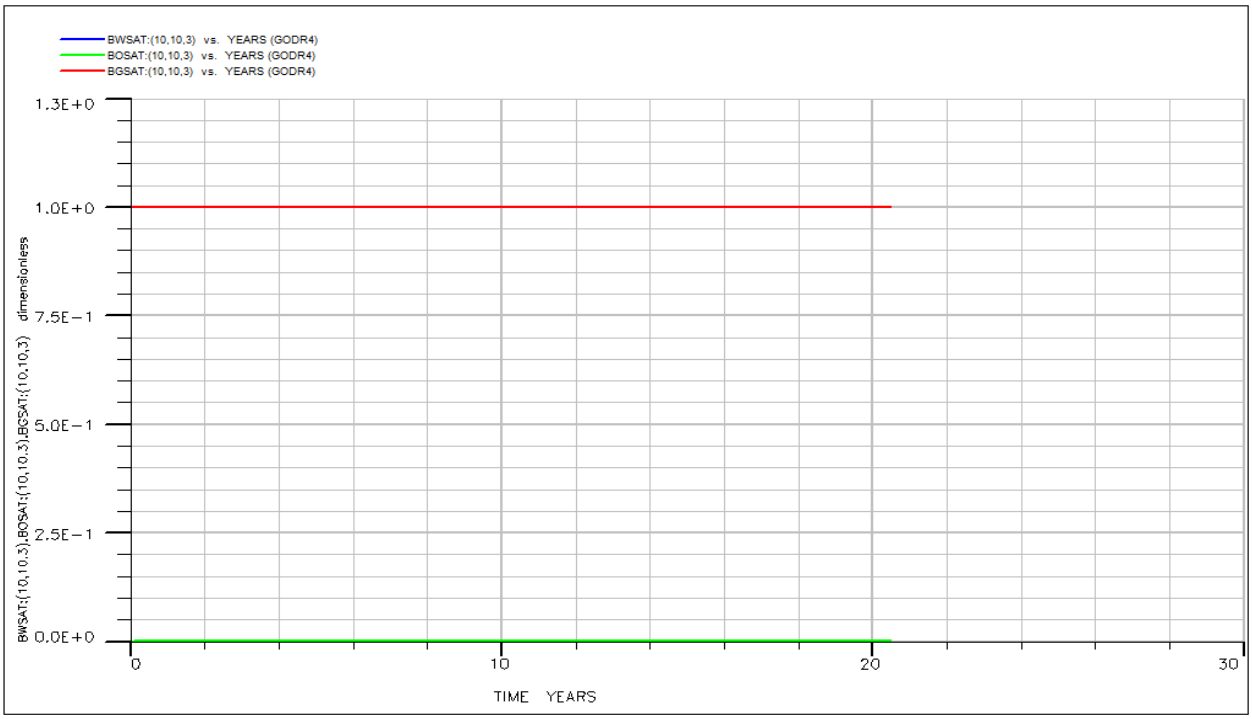

Figure C (viii): GODR4 fluid saturation plots of deepest gas well perforation cell.

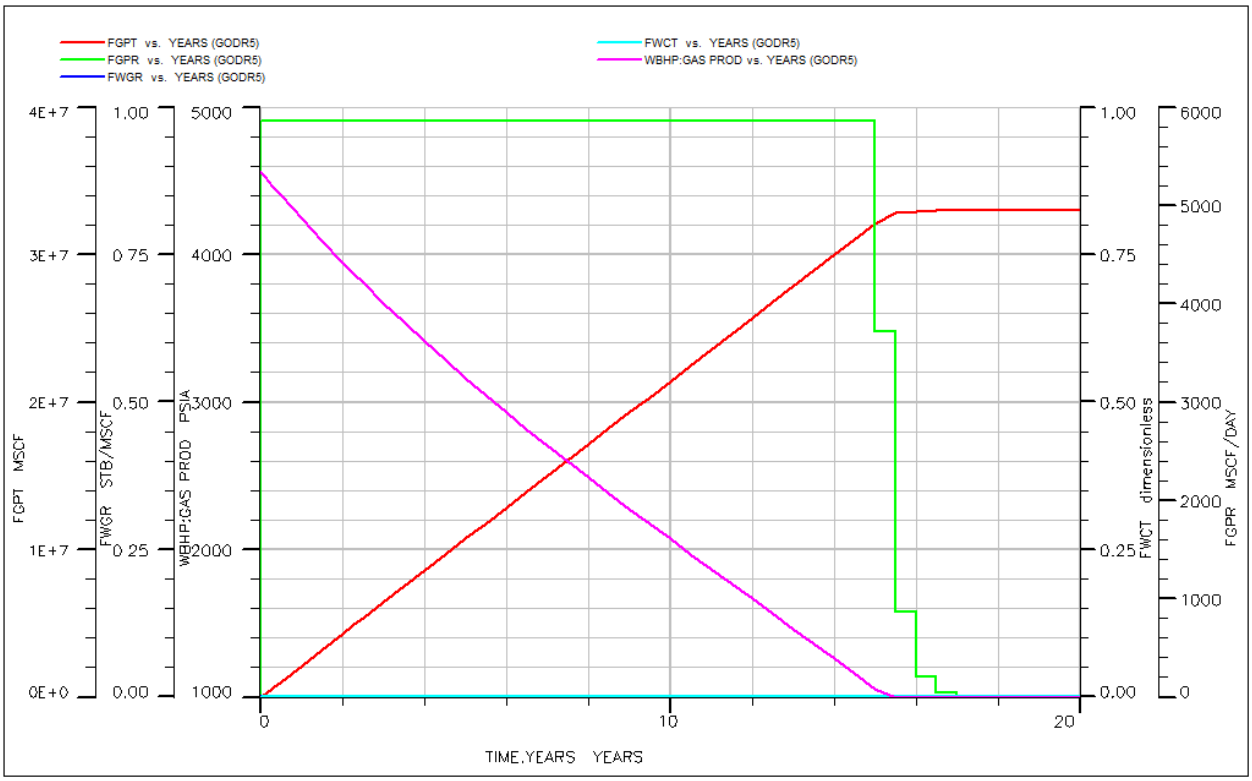

Figure C (ix): GODR5 production forecast plots

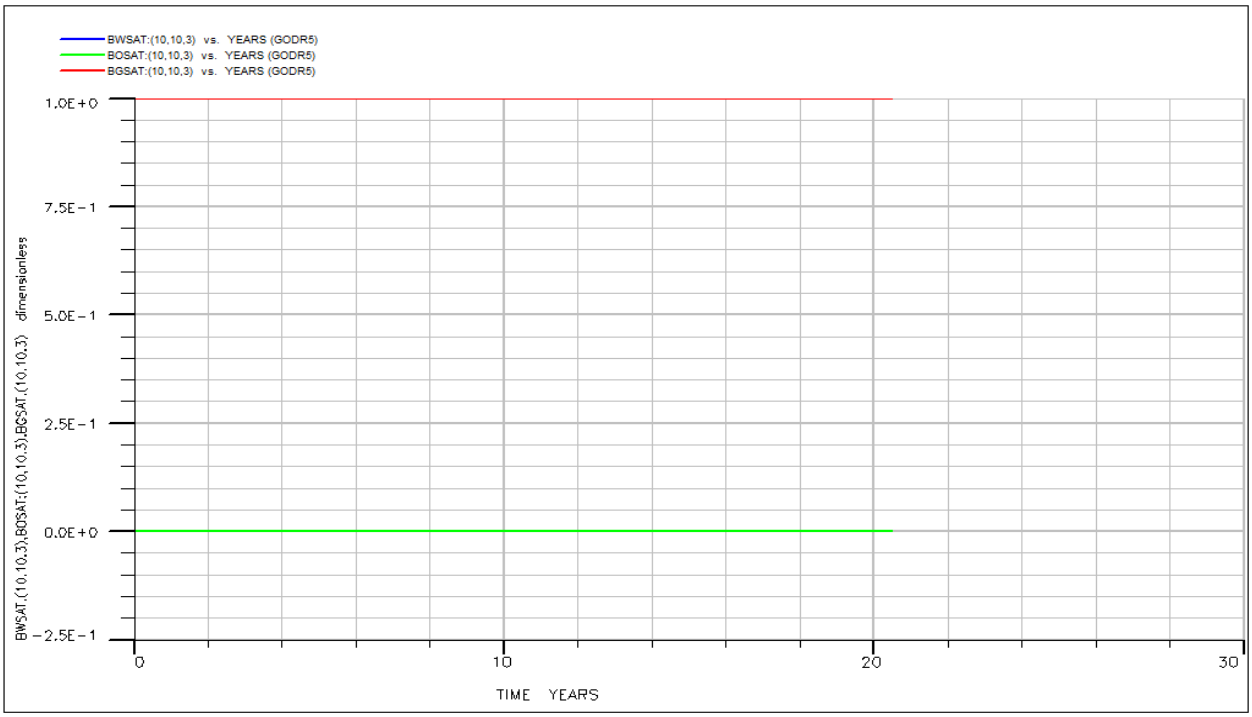

Figure C(x): GODR5 fluid saturation plots of deepest gas well perforation cell.

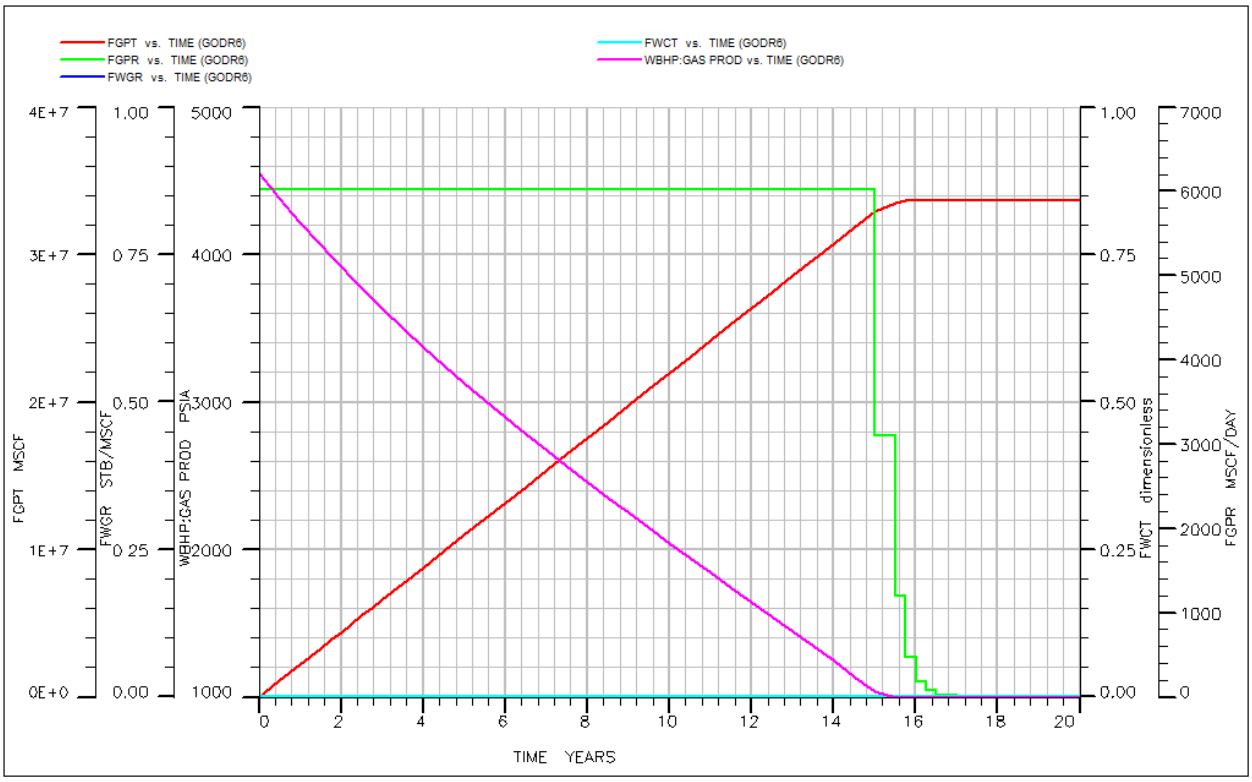

Figure C (xi): GODR6 production forecast plots

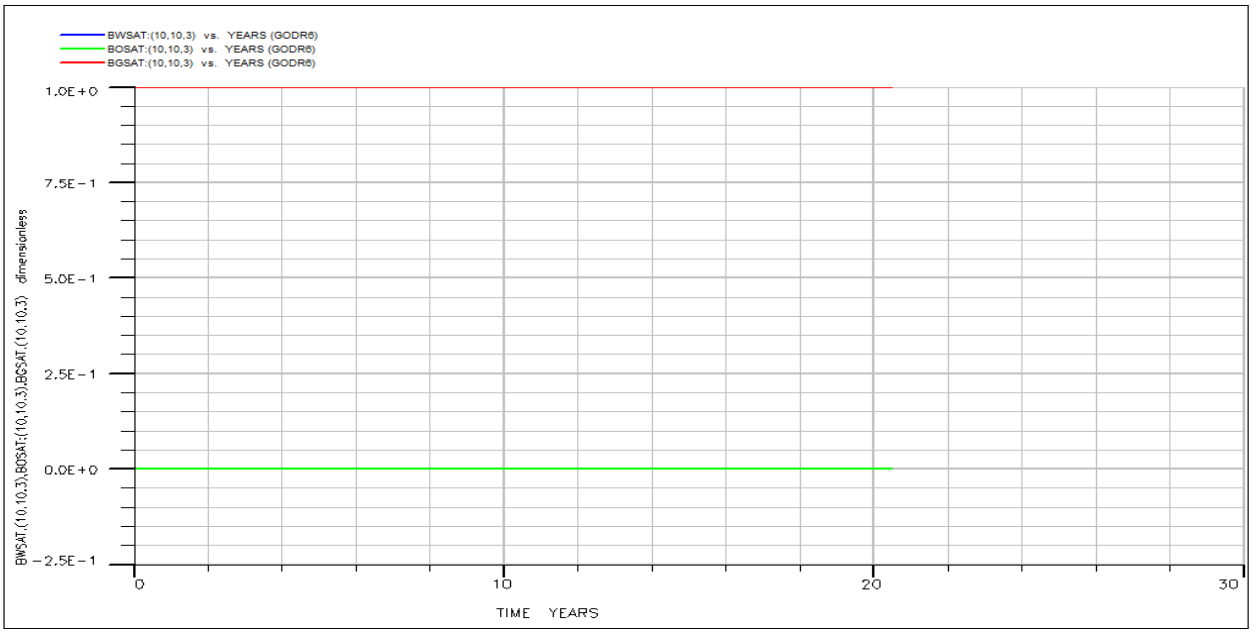

Figure C (xii): GODR6 fluid saturation plots of deepest gas well perforation cell.

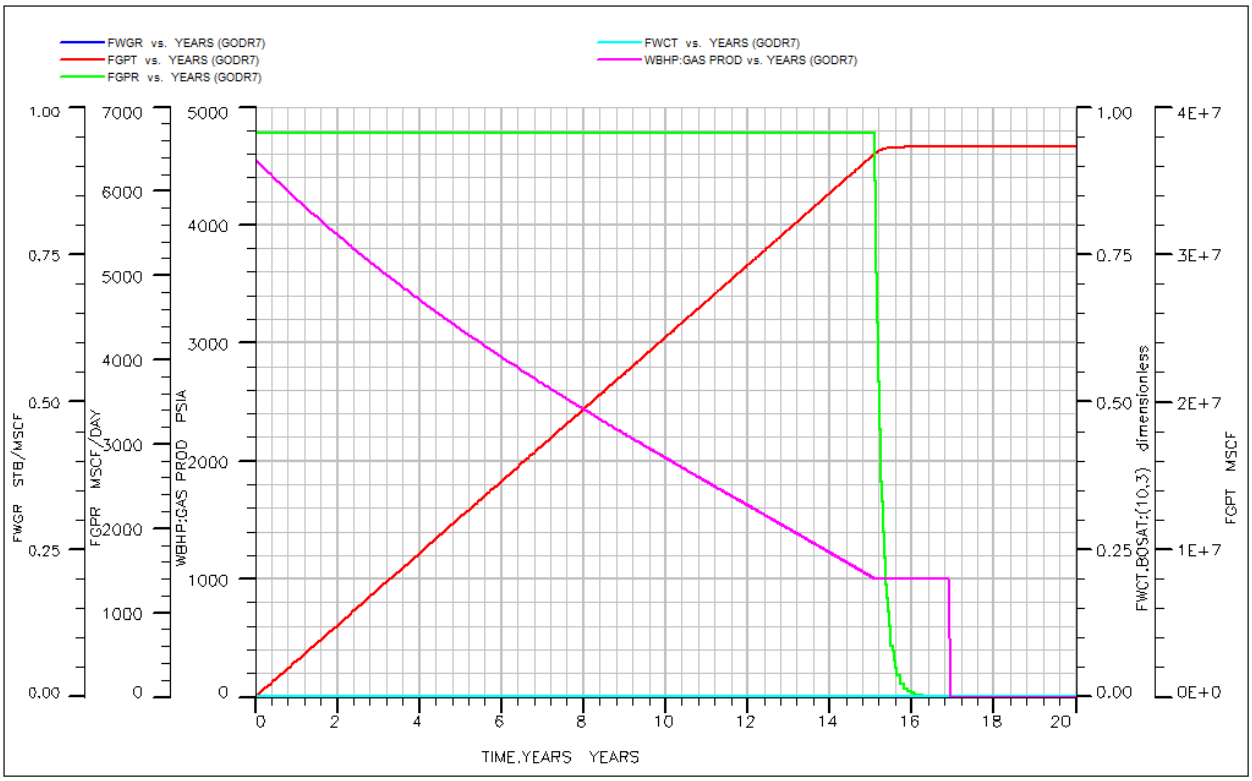

Figure C (xiii): GODR7 production forecast plots

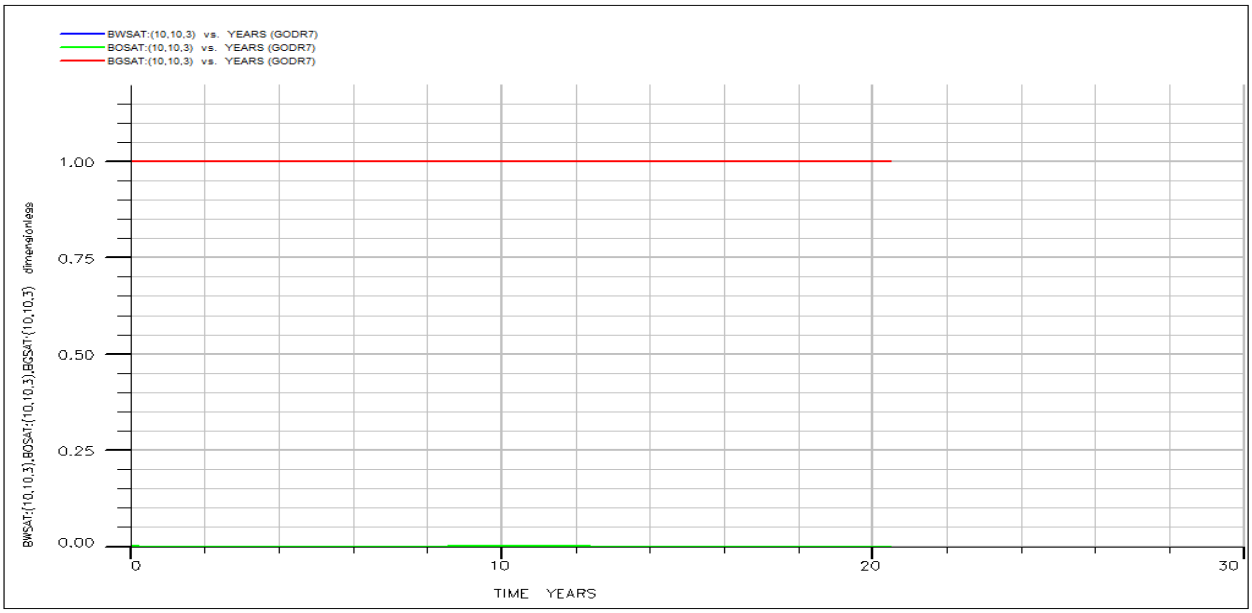

Figure C (xiv): GODR7 fluid saturation plots of deepest gas well perforation cell.

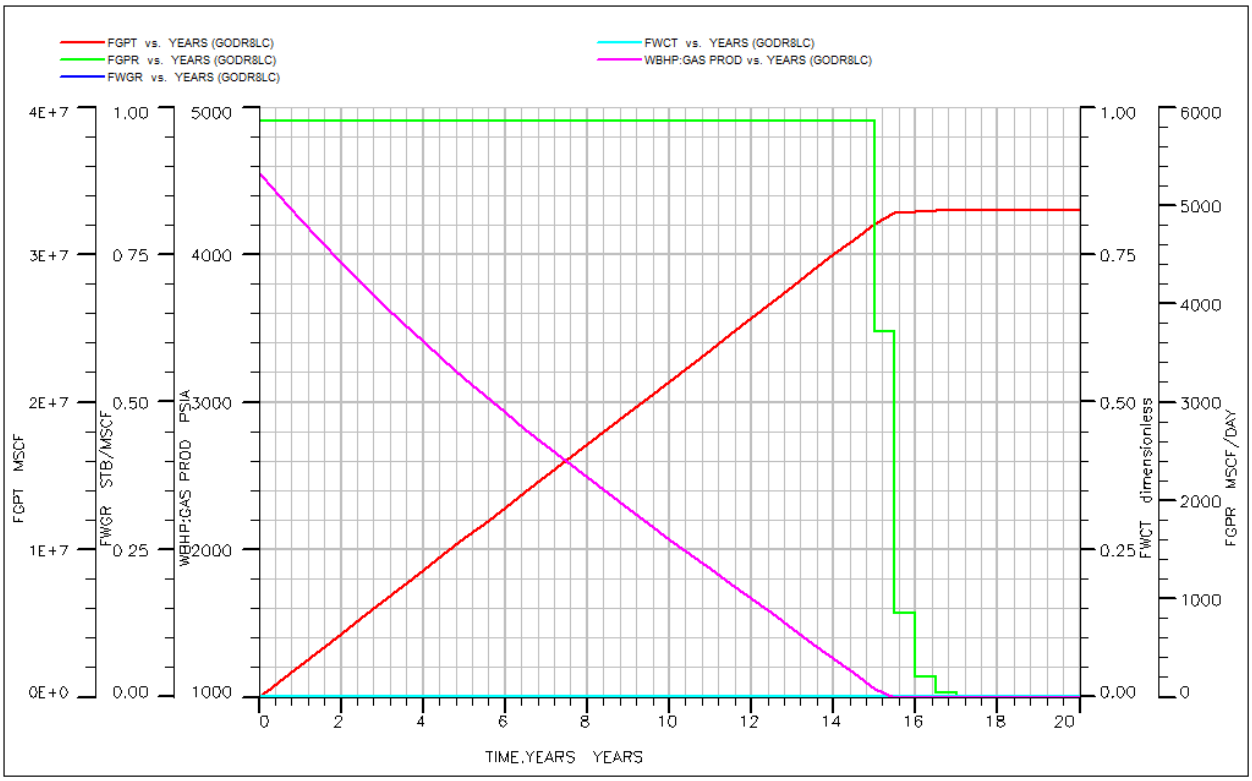

Figure C (xv): GODR8 production forecast plots

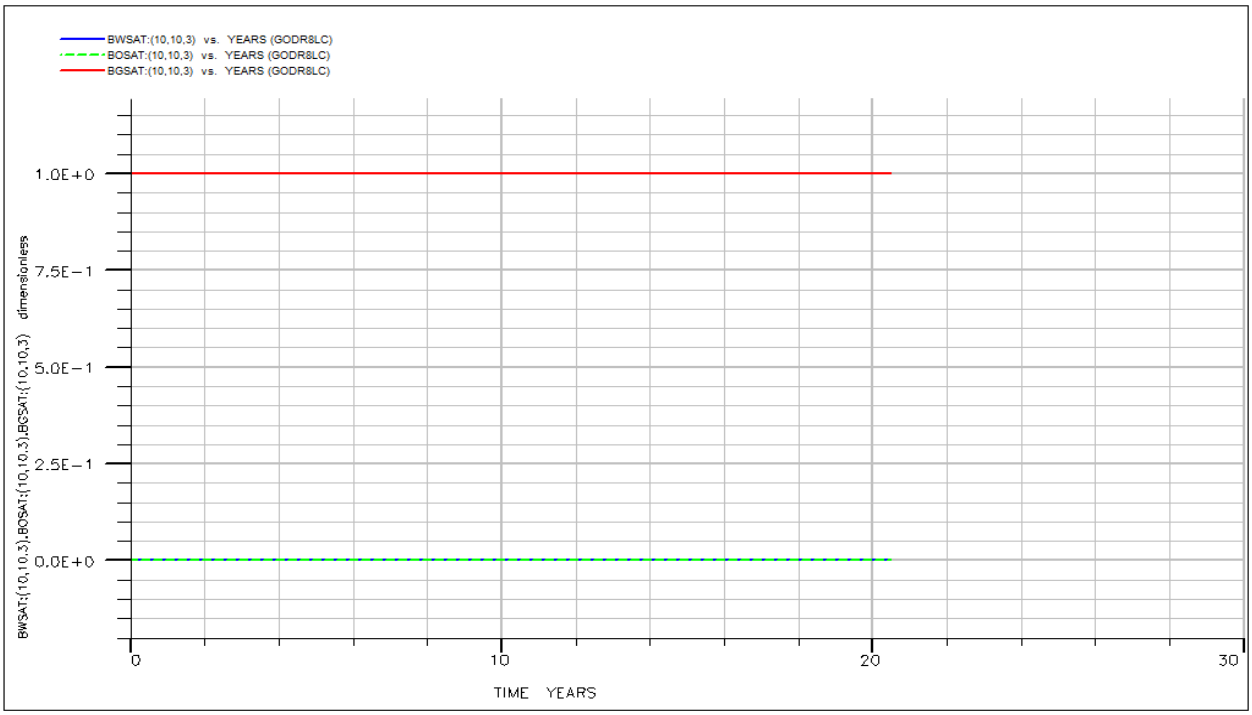

Figure C (xvi): GODR8 fluid saturation plots of deepest gas well perforation cell.

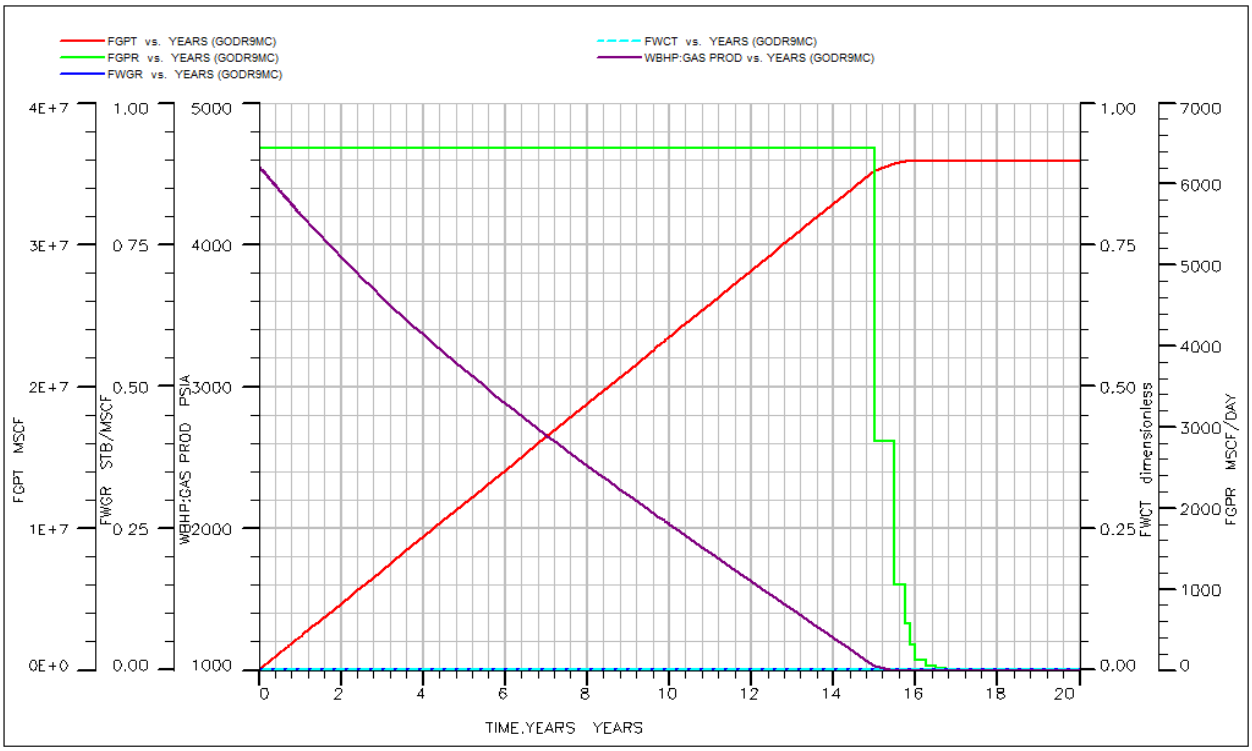

Figure C (xvii): GODR9 production forecast plots

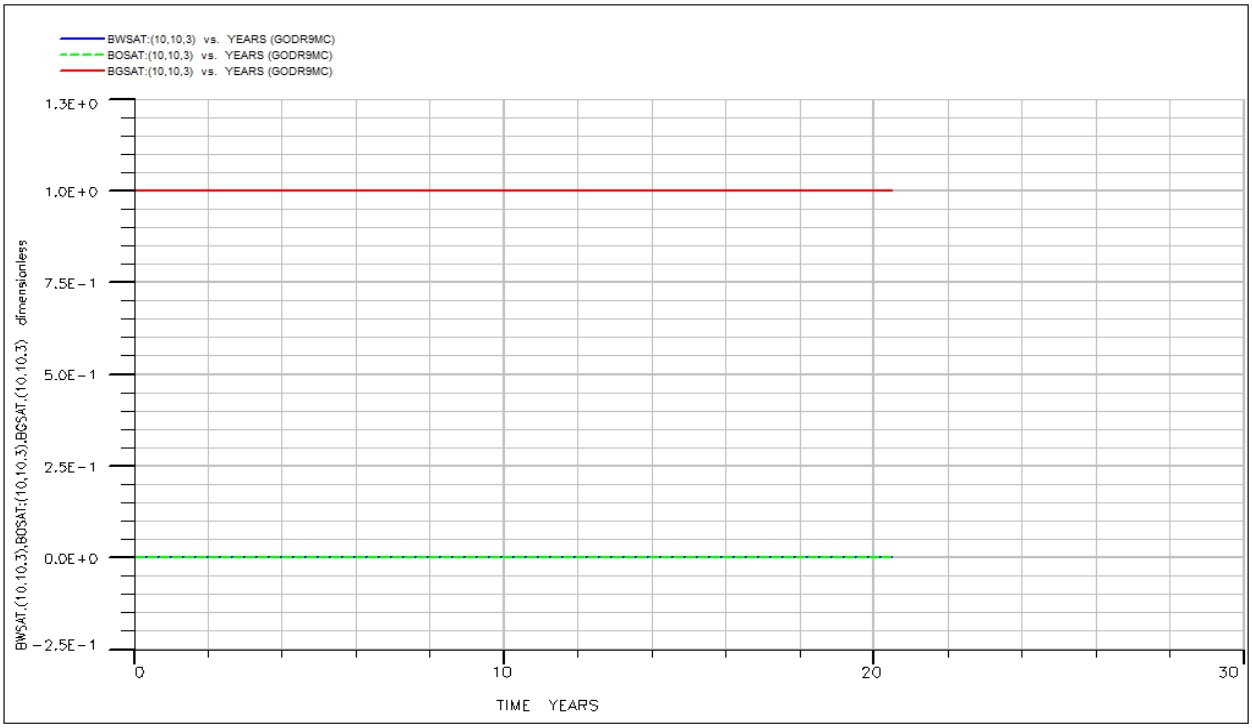

Figure C (xviii): GODR9 fluid saturation plots of deepest gas well perforation cell.

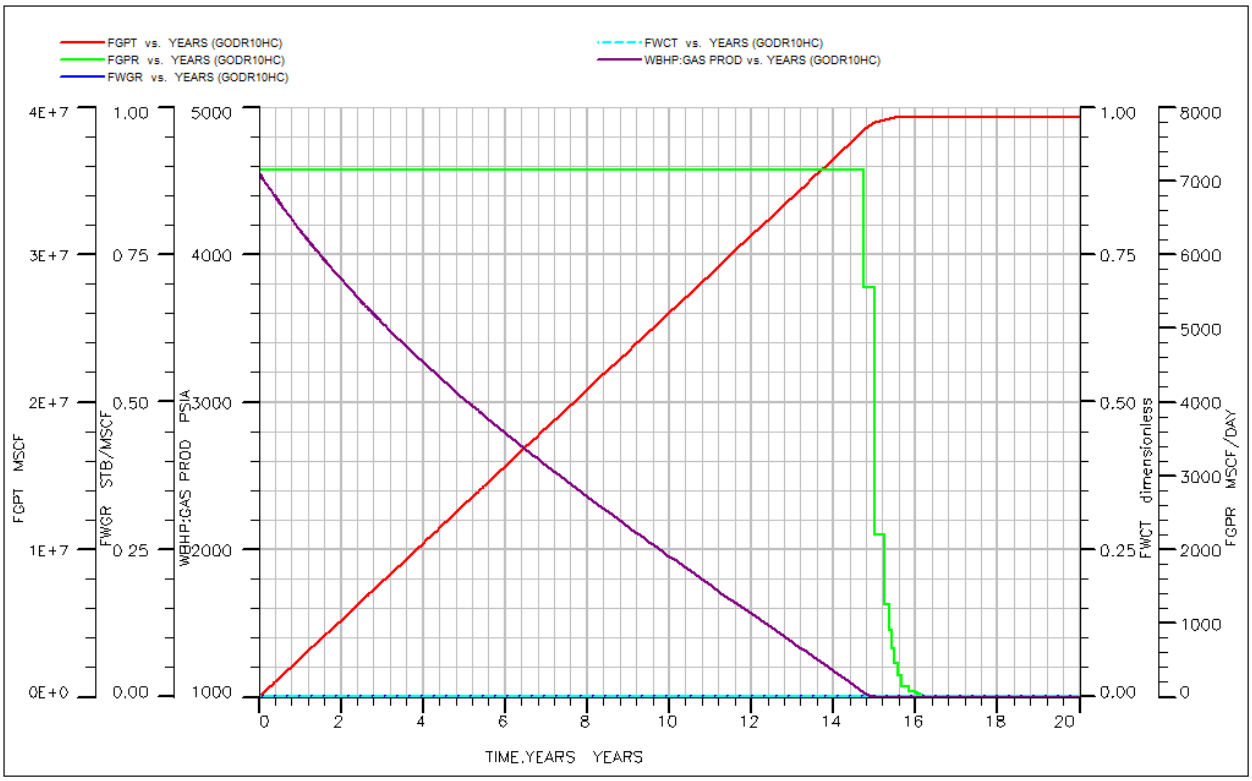

Figure C (xiv): GODR10 production forecast plots

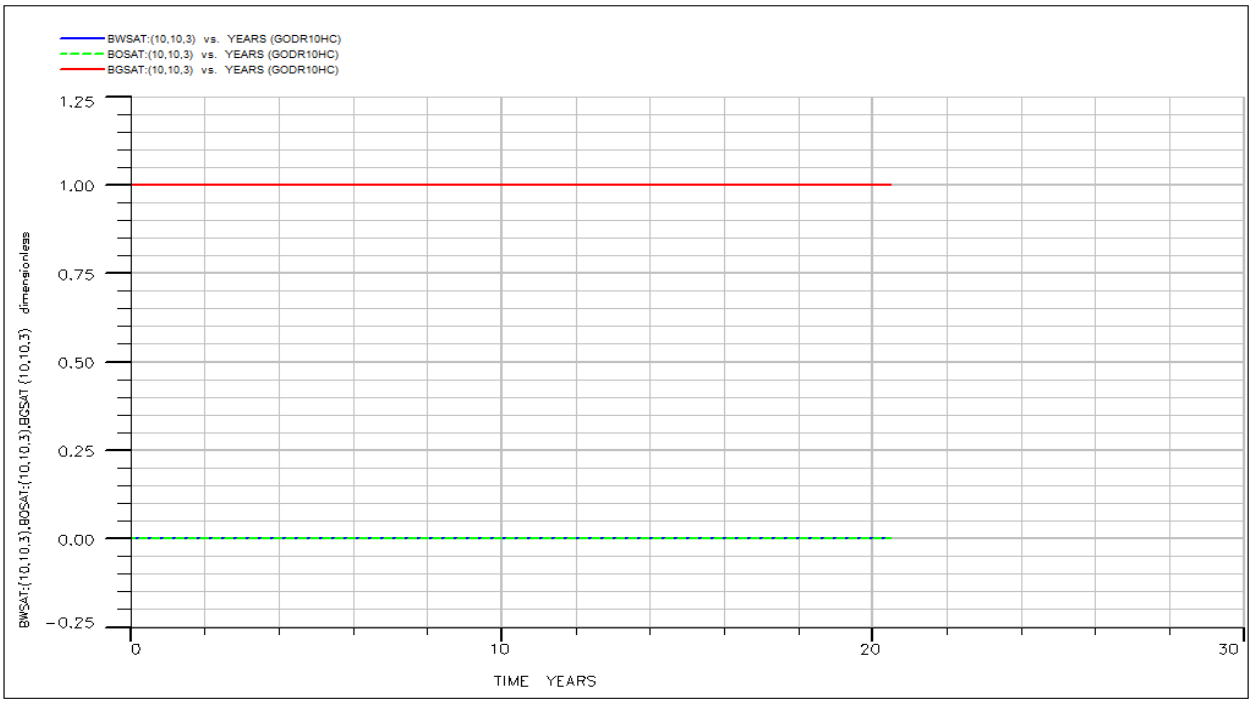

Figure C (xx): GODR10 fluid saturation plots of deepest gas well perforation cell.

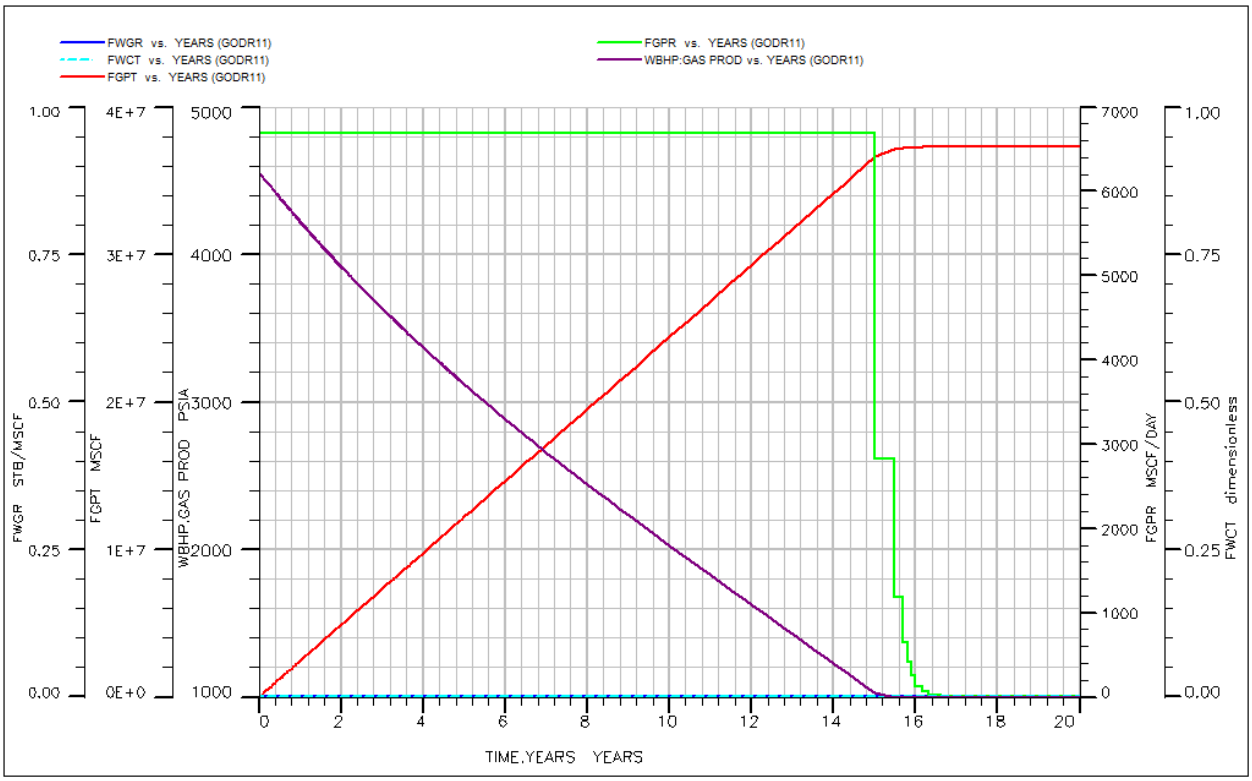

Figure C (xxi): GODR11 production forecast plots

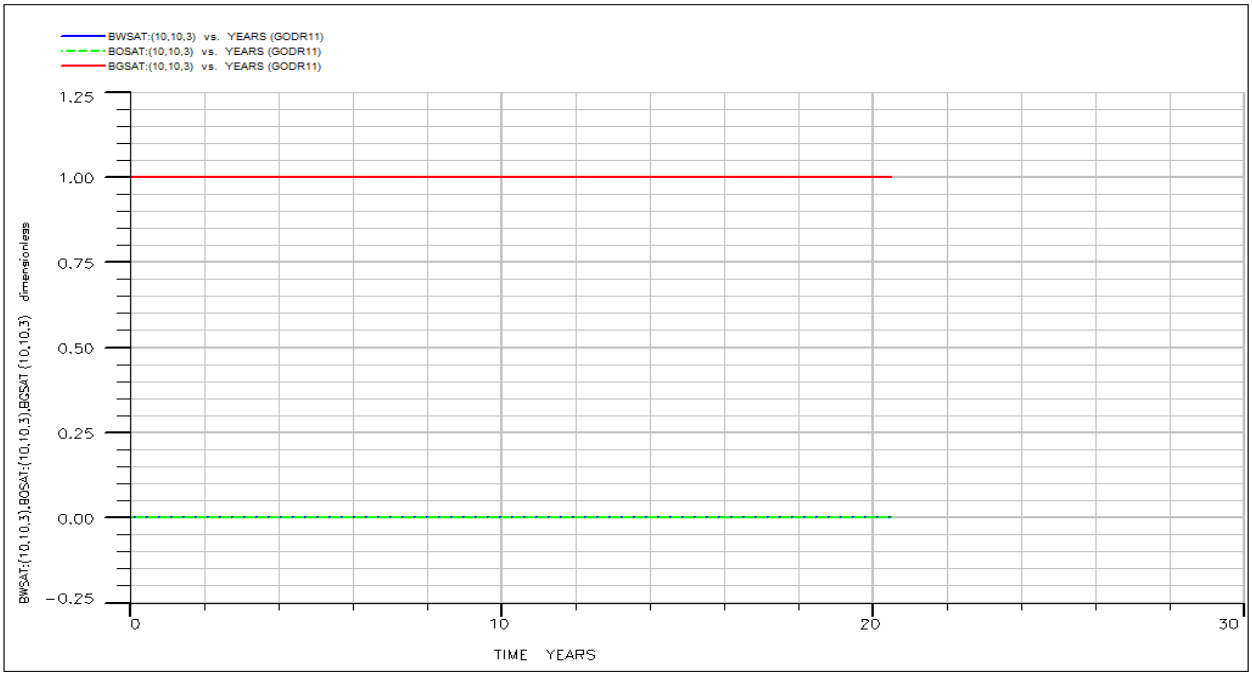

Figure C (xxiii): GODR11 fluid saturation plots of deepest gas well perforation cell.

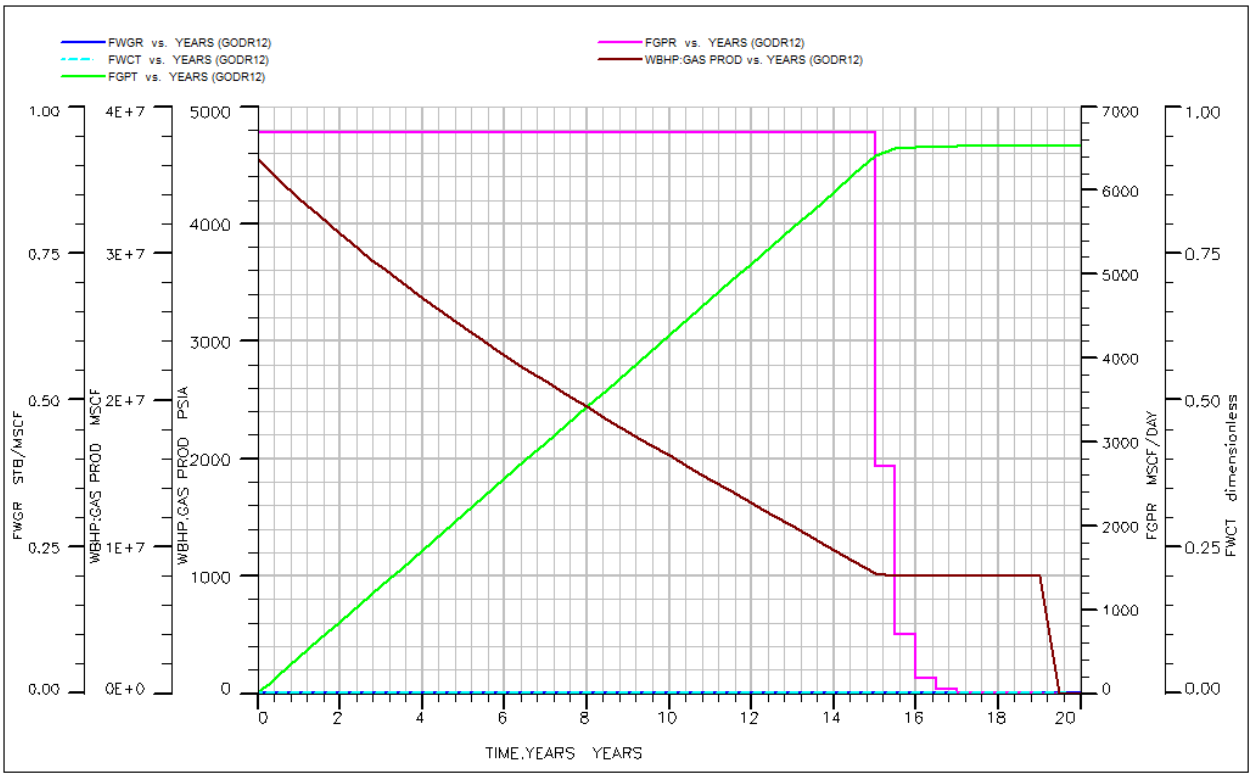

Figure C (xxiii): GODR12 production forecast plots

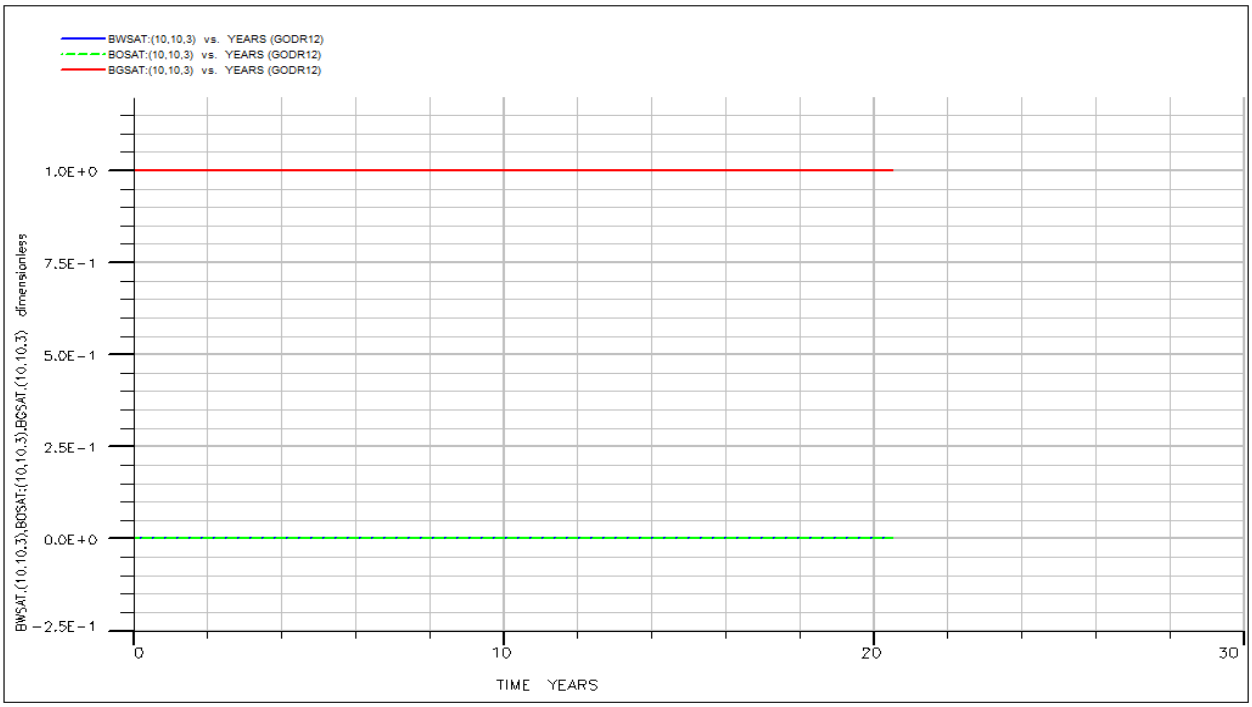

Figure C (xxiv): GODR 12 fluid saturation plots of deepest gas well perforation cell.

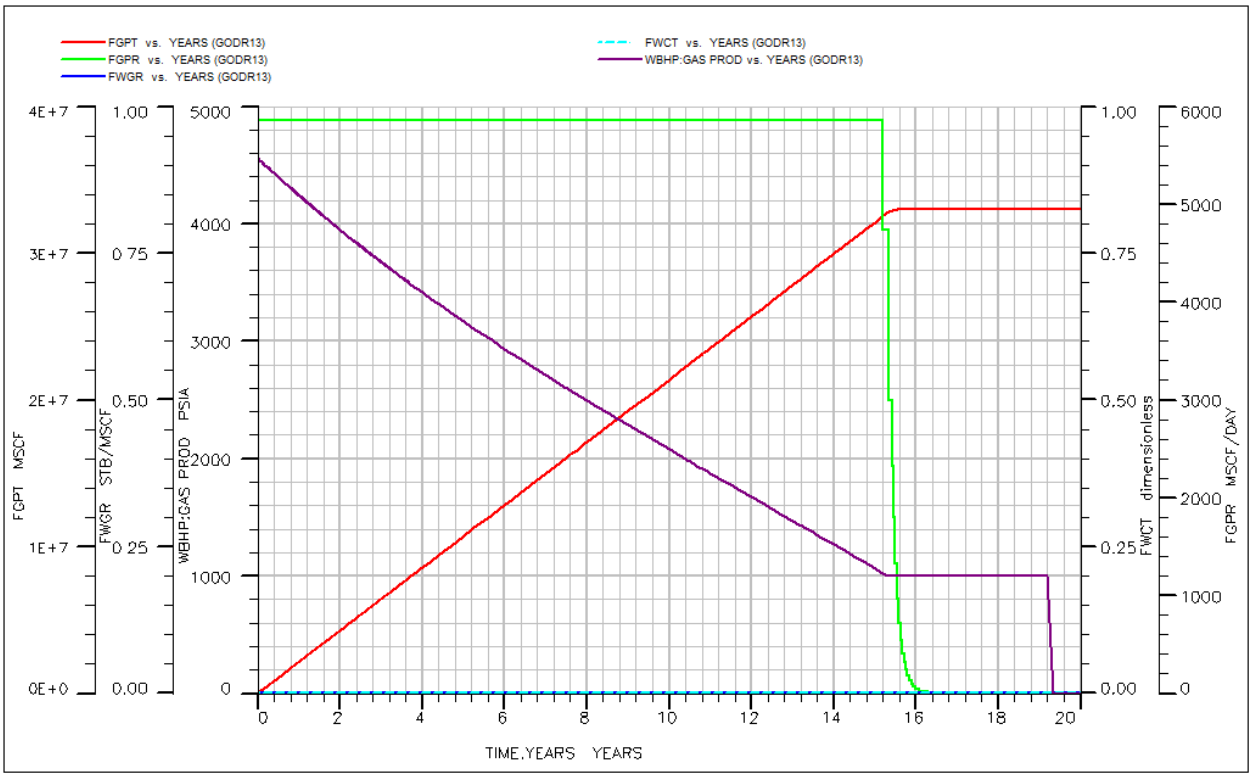

Figure C (xxv): GODR13 production forecast plots

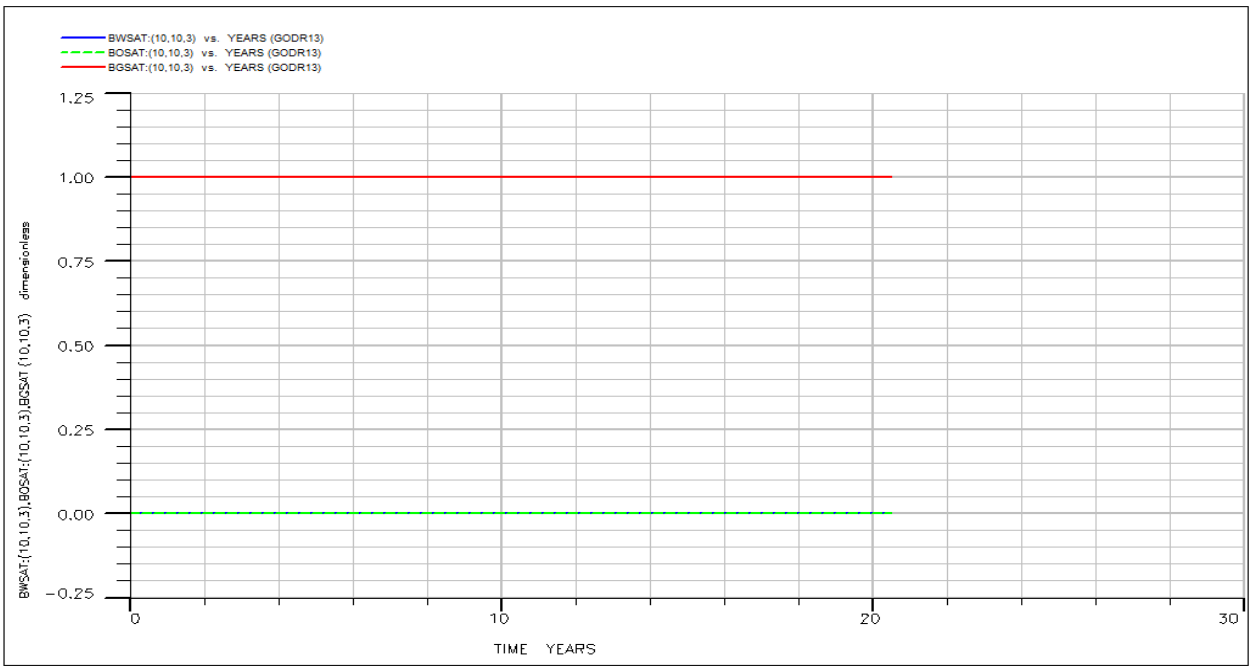

Figure C (xxvi): GODR13 fluid saturation plots of deepest gas well perforation cell.

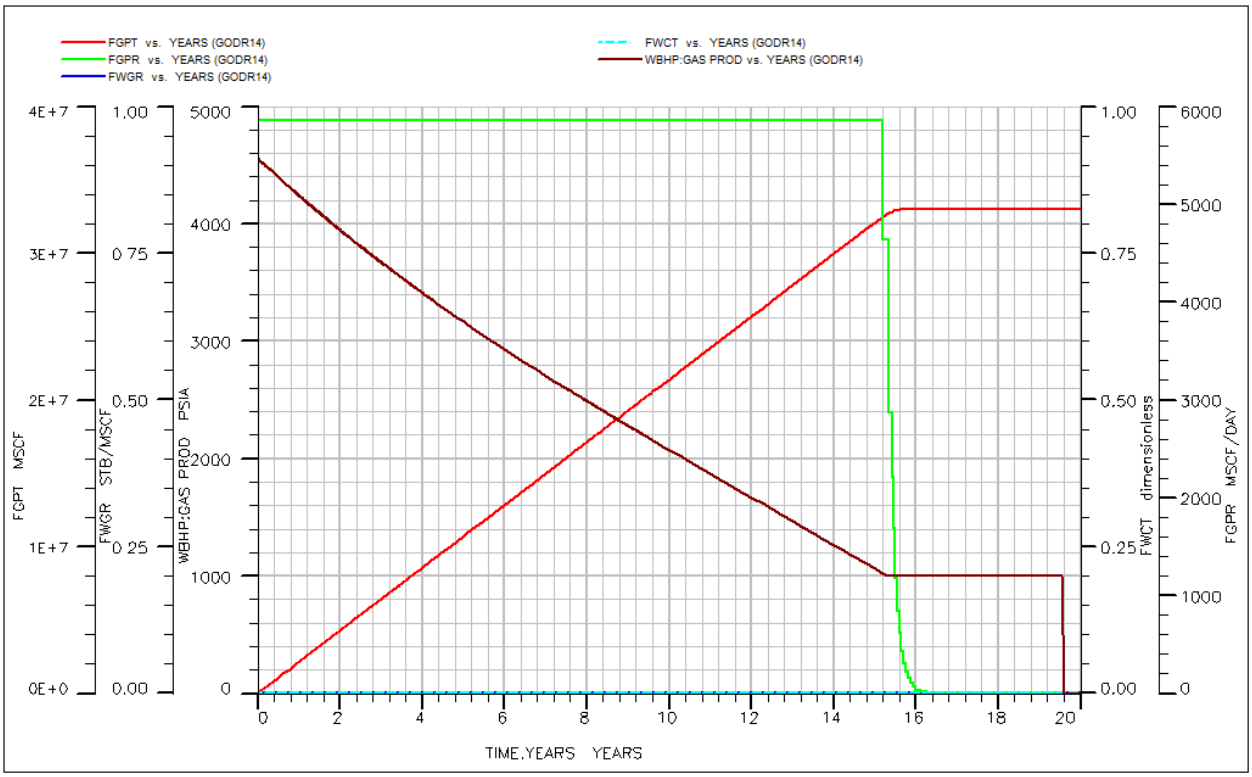

Figure C (xxvii): GODR14 production forecast plots

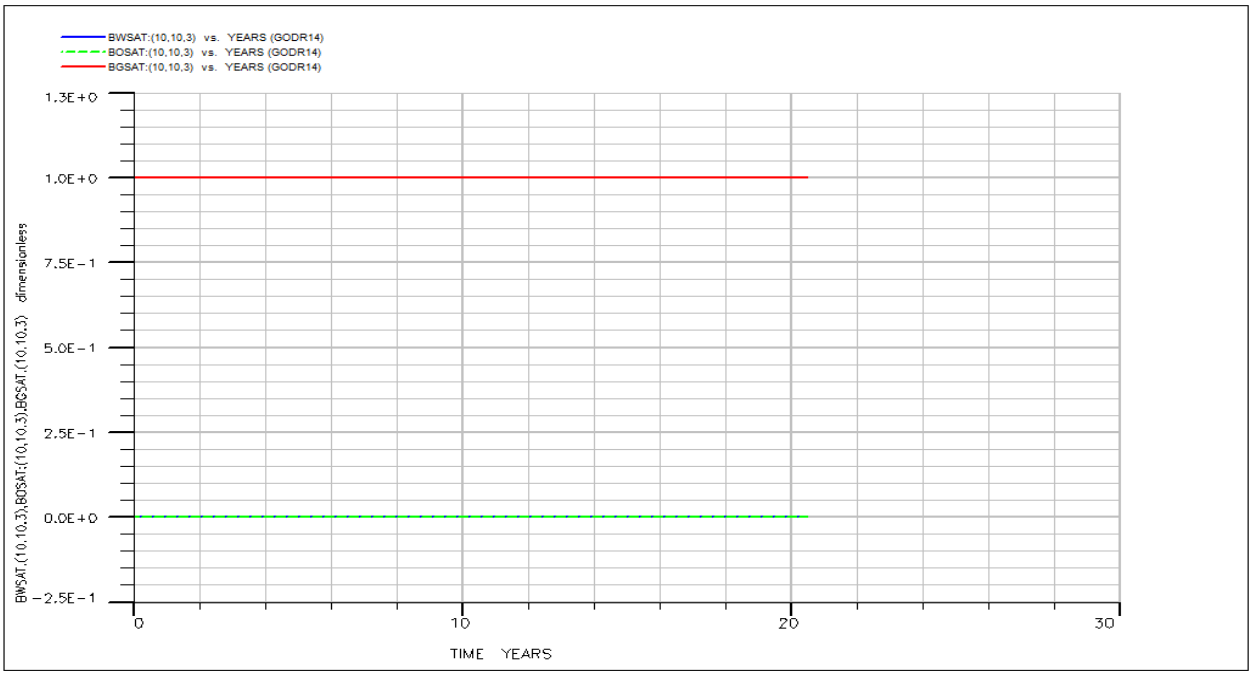

Figure C (xxviii): GODR14 fluid saturation plots of deepest gas well perforation cell.

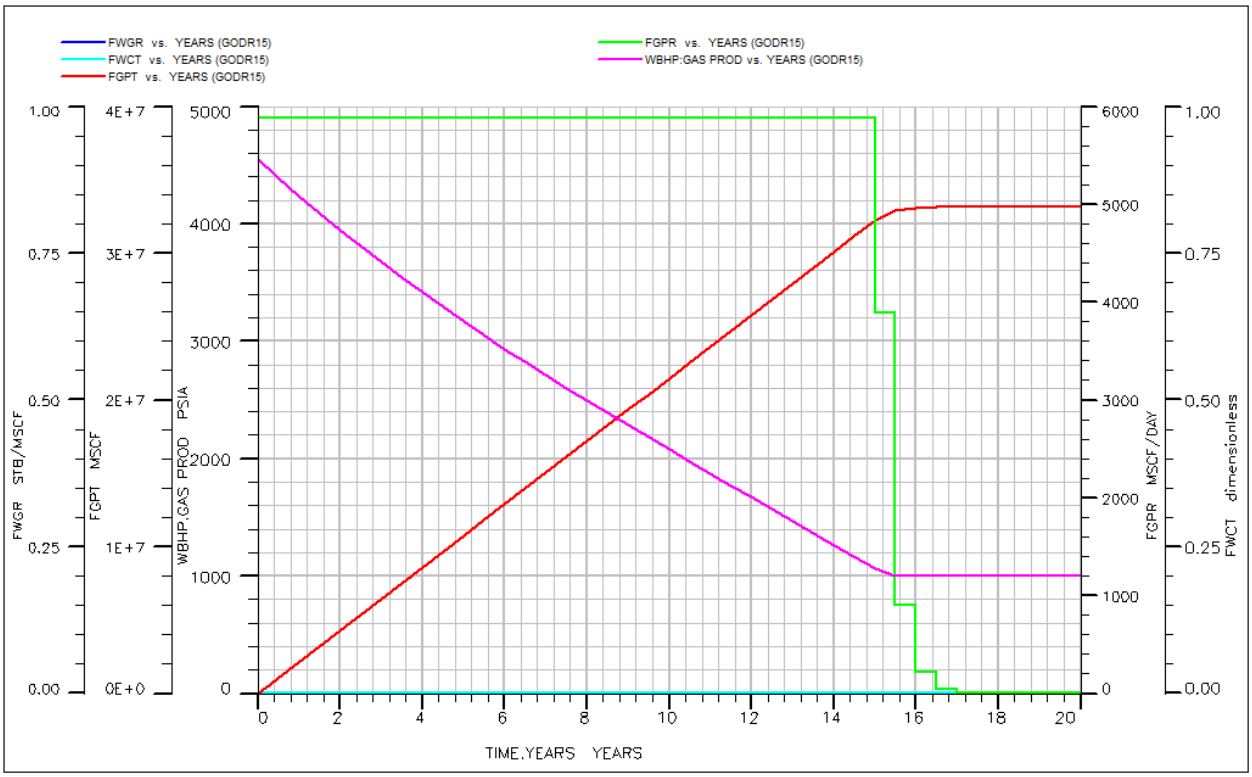

Figure C (xxix): GODR15 production forecast plots

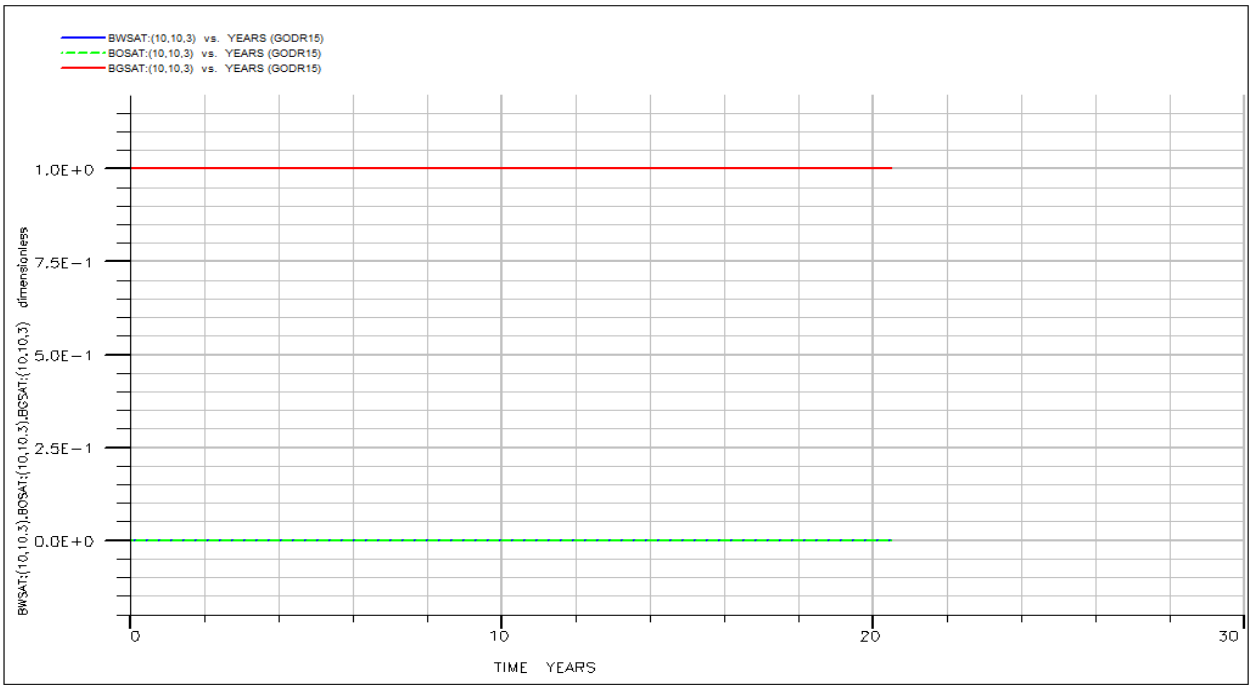

Figure C (xxx): GODR15 fluid saturation plots of deepest gas well perforation cell.

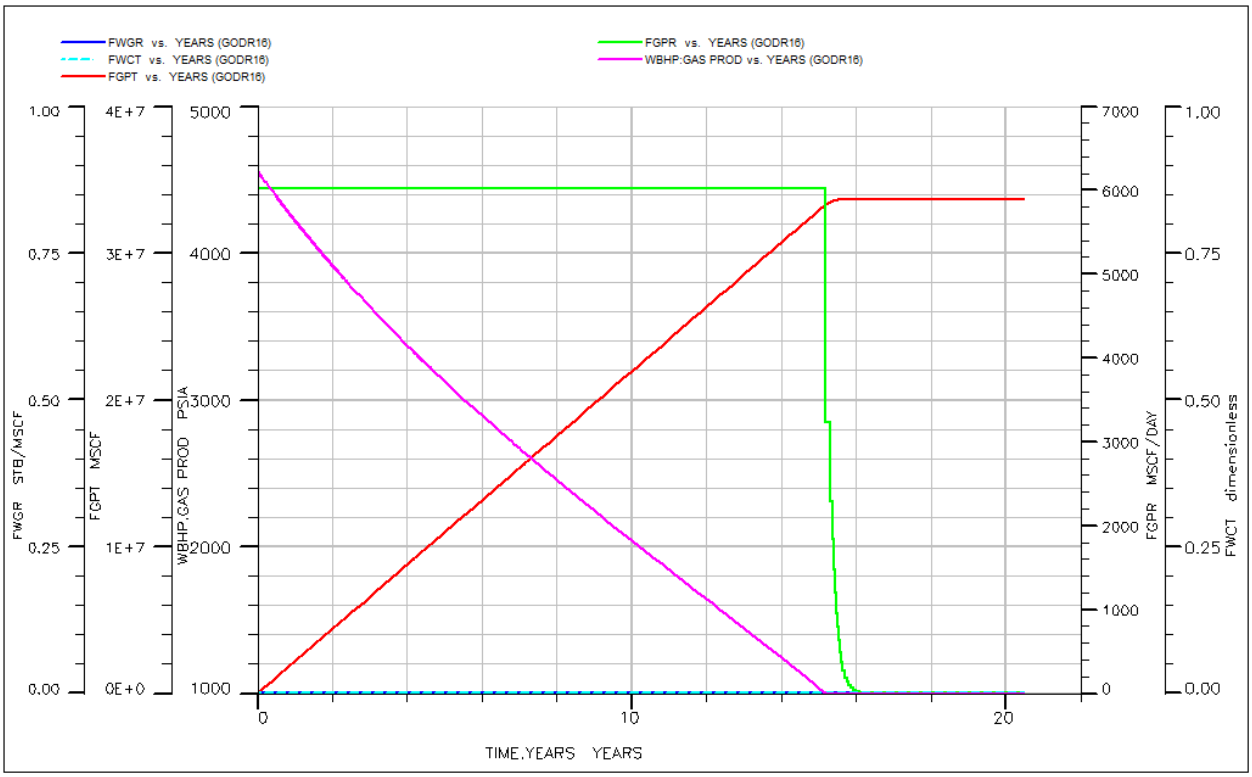

Figure C (xxxi): GODR16 production forecast plots

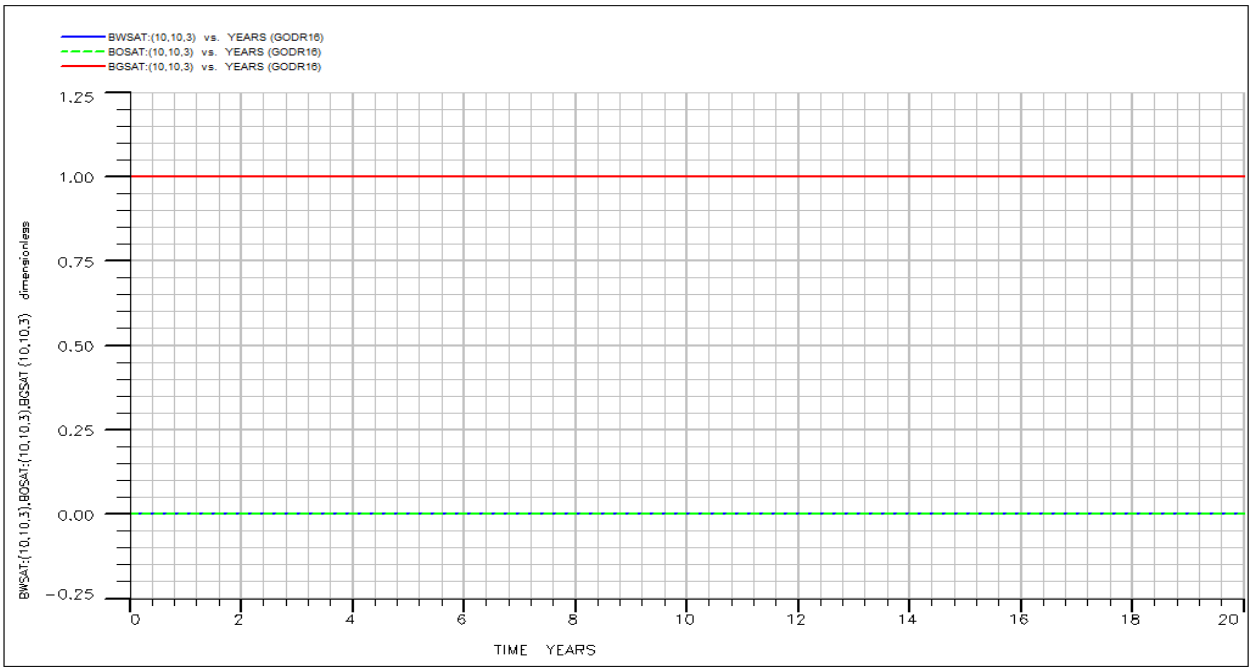

Figure C (xxxii): GODR16 fluid saturation plots of topmost gas well perforation cell.

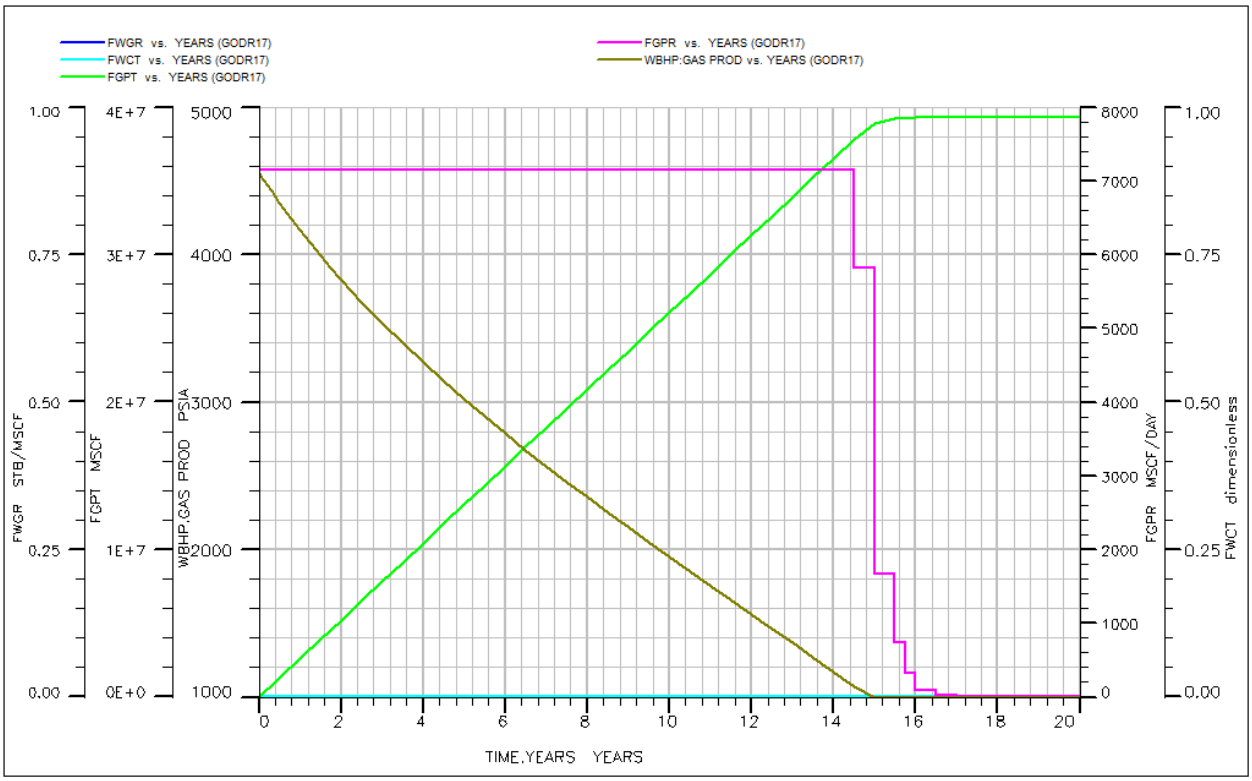

Figure C (xxxiii): GODR17 production forecast plots

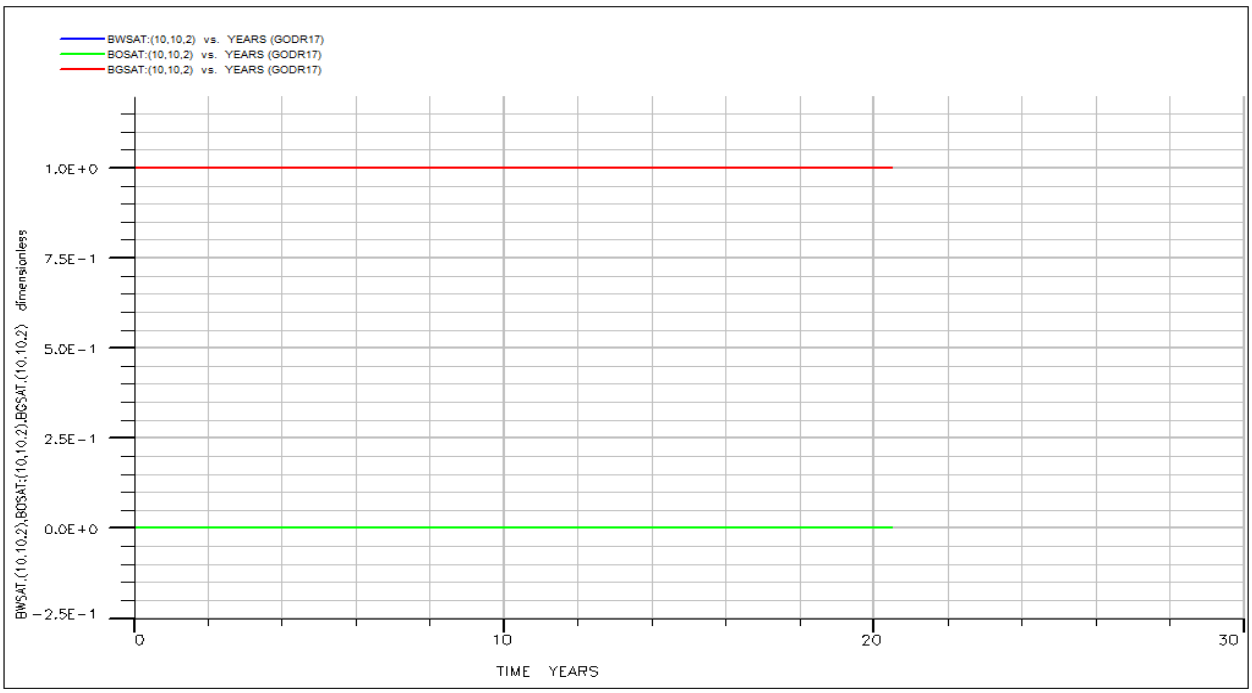

Figure C (xxxiv): GODR17 fluid saturation plots of topmost gas well perforation cell.

APPENDIX CII

ADDITIONAL RESULTS OF THE GOD CASE DESIGN ANALYSIS

SURROGATE EQUATION IN TERMS OF ACTUAL FACTORS

Substituting equations 4.3a through 4.3j in equation 4.3 gives the surrogate equation in terms of the actual factor as shown in Equation C1 of Appendix CII. Table 4.9 presents the model fit statistics.

$$R_f = 70.5800 + 0.5698H_o - 128.5604K_{rg} + 0.7237K_{rw} + 0.0588K_{ro} - 0.0007Q_g - 1.2665\left(H_o \times K_{rg}\right) - 0.000012\left(H_o \times Q_g\right) - 0.2850\left(API \times K_{rg}\right) - 0.9134\left(K_{rg} \times K_{rw}\right) + 0.0275\left(K_{rg} \times Q_g\right)$$

__ _C1

MODEL DIAGNOSTICS PLOTS

1. **A normal plot of residuals**

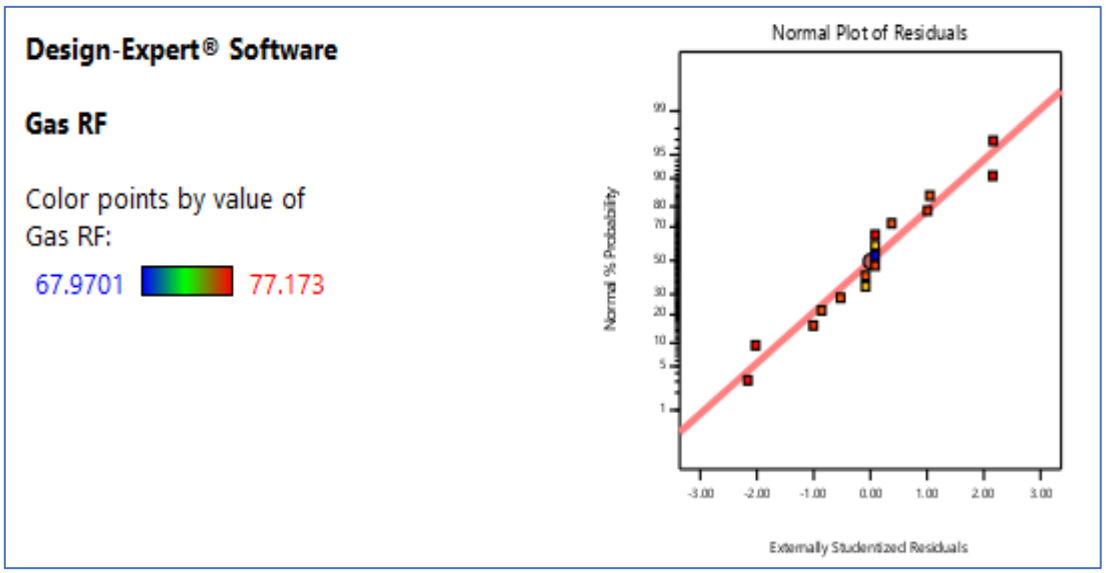

2. **Predicted versus actual plot**

Design-Expert® Software

Gas RF

Color points by value of
Gas RF:

67.9701 77.173

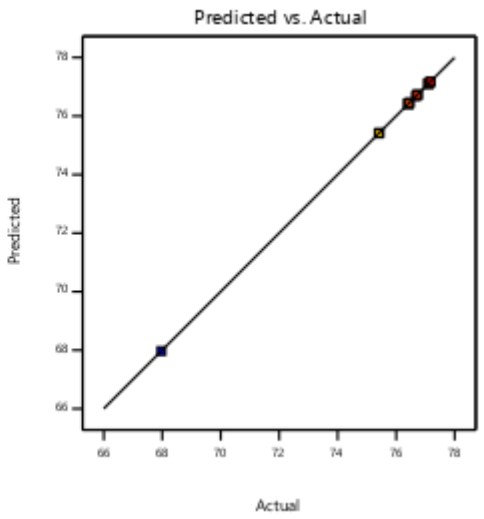

3. Box-Cox Plot for Power Transforms

Design-Expert® Software

Gas RF

Current Lambda = 1
Best Lambda = -1.63
CI for Lambda: (-11.77, 8.51)

Recommend transform:
None
(Lambda = 1)

Current Transform:
None